IDENTIFICATION OF BIOMARKERS FOR THE FRUITING BODY FORMATION IN *MYXOCOCCUS XANTHUS*

Dissertation

zur Erlangung des Doktorgrades

der Naturwissenschaften

vorgelegt beim Fachbereich für Biowissenschaften (15)

der Johann Wolfgang Goethe - Universität

in Frankfurt am Main

von

Wolfram Lorenzen

aus Berlin

Frankfurt 2014

D 30

vom Fachbereich für Biowissenschaften (15) der

Johann Wolfgang Goethe - Universität als Dissertation angenommen.

Dekanin: Prof. Dr. Anna Starzinski-Powitz
Gutachter: Prof. Dr. Helge B. Bode
Zweitgutachter: Prof. Dr. Dieter Steinhilber
Datum der Disputation: 16.12.2014

Danksagung

Meinem Doktorvater, Mentor und Chef Professor Dr. Helge B. Bode möchte ich besonderen Dank für die Betreuung und Unterstützung meiner Projekte aussprechen. Mit seinem aufrichtigen Interesse, seinen Beiträgen aus seinem schier unerschöpflich erscheinenden Schatz aus Wissen und Erfahrung, seinem permanenten Einsatz und Ideenreichtum stets Möglichkeiten zur Bewältigung neuer Herausforderungen zu schaffen hat er mehr als nur die Grundlage meiner Forschungsprojekte gesichert. Unvergessen bleibt auch sein in wenig aussichtsreichen Phasen unerschütterliches Vertrauen in den Erfolg meiner Projekte.

Meinen „Saarbrücker“ Mitstreitern Dr. Daniela Reimer, Dr. Michael W. Ring, Dr. Alexander O. Brachmann, Dr. Carsten Kegler und Gertrud Schwär danke ich für deren Unterstützung bei der Einarbeitung in die Mikrobiologie, Molekularbiologie und ersteren Beiden für die Unterstützung bei der HPLC-MS bzw. technische Einarbeitung in die GC-MS Analytik. Meinem einzigen „Myxo-“ Mitstreiter in Frankfurt Tilman Ahrendt möchte ich meine Verbundenheit dafür ausdrücken, dass er sich mutig und mit großem Einsatz in dieses Arbeitsfeld gewagt hat und stets für eine positive Stimmung im Labor gesorgt hat. Kenan A. J. Bozhüyük gebührt mein Dank für die erfolgreiche Lösung selbst spitzfindigster Bioinformatikherausforderungen und Dr. Dominic Bäumlisberger, Dr. Sebastian W. Fuchs und Dr. Marion Rohmer danke ich für ihre fundierte Hilfe bei meinen MALDI-MS Messungen.

Darüber hinaus danke ich allen aktuellen und ehemaligen Mitgliedern der Arbeitsgruppe Bode für die freundliche und produktive Atmosphäre während der vielen Jahre und wünsche ihnen, wie auch meinen ehemaligen Kooperationspartnern Dr. Silke Schmidt, Dr. Florian Hilbers, Dr. Frederik Barka und Dr. Dawid Brat eine glückliche und erfolgreiche Zukunft.

Herrn Professor Dr. Dieter Steinhilber danke ich ganz herzlich für die Übernahme der Zweitgutachterfunktion, sowie Alexander J. Perèz und Tilman Ahrendt für die produktiven Kommentare und das wachsame Auge bei der Überarbeitung dieses Manuskriptes.

All meinen Freunden möchte ich schließlich meine tiefe Verbundenheit für all die erhellenden Erlebnisse und vertrauensvollen Gespräche aussprechen.

Table of contents

Table of abbreviations

ACP	acyl carrier protein
AEPE	1-*O*-(13-methyltetradecyl)-2-*O*-(13-methyltetradecanoyl)glycero-3-phosphatidylethanolamine
a.k.a.	also known as
ATP	adenosine triphosphate
BCKAD	branched-chain-2-oxo-acid dehydrogenase complex
CDP	cytidine diphosphate
DMAA-CoA	3,3-dimethylacrylyl-Coenzyme A
DMAPP	dimethylallyl diphosphate
e.g.	exempli gratia
ELK	eukaryotic-like protein kinase
G protein	guanosine nucleotide-binding proteins
GC-MS	gas chromatography coupled with mass spectrometry
GPCR	G-protein-coupled receptor
3-HMG-CoA	3-hydroxymethylglutaryl-Coenzyme A
Ile	isoleucine
IP_3	inositol-1,4,5,-trisphosphate
IPP	isopentenyl pyrophosphate
IV-CoA	isovaleryl-Coenzyme A
(HP)LC-MS	(high performance) liquid chromatography coupled with mass spectrometry
Leu	leucine
MAPK	mitogen activated protein kinase
3-MG-CoA	3-methylglutaconyl-Coenzyme A
NAD+	nicotinamide adenine dinucleotide

NRPS	non-ribosomal peptide synthetase
PAF	platelet-activating factor
PCA	principal component analysis
PCD	programmed cell death
Phe	phenylalanine
PIP_2	glycerophosphoinositol-4,5-bisphosphate
PKA	protein kinase A
PKC	protein kinase C
PKS	polyketide synthase
ROS	reactive oxygen species
SCAD	short-chain dehydrogenase
SEM	scanning electron microscopy
TG-1	1,2-di-(13-methyltetradecanoyl)-3-(13-methyltetradecyl)glycerol
TMS	trimethylsilyl ether
Trp	tryptophan
Tyr	tyrosine
UPLC-ESI-MS	ultra performance liquid chromatography coupled with mass spectrometry after electrospray ionization
UPLC-MS	ultra performance liquid chromatography coupled with mass spectrometry
VEPE	1-*O*-(13-methyl-1-Z-tetradecenyl)-2-*O*-(13-methyltetradecanoyl)glycero-3-phosphatidylethanolamine

Summary

Bacteria are generally considered as more or less “simple” organisms due to their unicellular live style lacking the ability to form differentiated tissues that feature labor division. However, intercellular communication using specific signaling molecules, generally termed as “quorum sensing”, is known from several prokaryotic species. Additionally but to a limited extend, cell differentiation and tissue formation are known for example from actinomycetes (aerial mycelium formation) and cyanobacteria (heterocyst formation).

A remarkably sophisticated example for cell differentiation and complex intercellular communication can be found within the order of the myxobacteria. These Gram-negative, soil dwelling bacteria feature an impressive number of properties: they can glide on solid surfaces by using two different motility motors, subsist by preying on other microorganisms, are often producers of multiple natural products, and upon adverse environmental conditions, they are able to form multicellular structures called “fruiting bodies”. Their complexity ranges species-specifically from simple mounds to maddish, tree-like forms. The process, in which these macroscopically visible structures arise from independent single cells, has been the predominant subject of myxobacterial research for many decades. More precisely, researchers have strived for the discovery of genes, proteins and small molecules that act as signals, receivers or modulators of this complex process. In this regard, the species *Myxococcus xanthus* has evolved into the model organism due to its relatively simple and reliable handling in a laboratory environment. The research underlying this thesis focused on the identification and biosynthesis of lipids that may act as signaling molecules as part of the “E-signal” system. In general, lipids containing branched-chain fatty acids with an uneven number of carbon atoms were found to be important players in the process of fruiting body formation and sporulation. Nevertheless, their exact roles remain largely unknown.

The first publication that is part of this thesis deals with an aspect that even strengthened the importance of role of iso-branched compounds in myxobacteria: myxobacterial metabolism is able to transform precursors of iso-lipids to isoprenoids. It addresses the question whether isoprenoids in general are important for fruiting body formation. Phenotypic analysis of mutants impaired in the biosynthesis of the central isoprenoid precursor 3-hydroxymethylglutaryl-Coenzyme A (3-HMG-CoA) from acetate and/or

branched chain keto acids and their genetic and metabolic complementation clearly showed that isoprenoids are essential for fruiting body formation and confirmed that leucine derived isovalerate is an important source for isoprenoid precursors in myxobacteria.

The second, and by far and away most tedious and sophisticated study, addressed the question as to how myxobacteria form fatty acid derived iso-branched ether lipids and to what extent they are important for fruiting body formation and sporulation. In a previous study, those unusual lipids were identified as specific biomarkers for myxobacterial development. No biochemical pathways to ether lipids specific for prokaryotes were known by then. In this study, a putative candidate gene that may be in involved in ether lipid biosynthesis was investigated. A combination of gene disruption and complementation experiments, phenotypic analysis and monitoring of ether lipid formation by means of GC-MS demonstrated its involvement in myxobacterial ether lipid biosynthesis and the importance of these lipids for the developmental process. Heterologous expression and biochemical testing of this gene together with *in-silico* sequence analysis and docking experiments confirmed the functions of its predicted domains. The discussion section provides an additional suggestion on how the ether bond formation is performed. Furthermore and most importantly, iso-branched ether lipids were found to be essential for sporulation but not for fruiting body formation. In summary, one or several molecules derived from an iso-branched alkylglycerol seem to play a role during sporulation in *M. xanthus* and a multidomain enzyme unique for myxobacteria is involved in their biosynthesis.

The last manuscript addresses the complexity of lipid metabolism in myxobacteria. Prior to this work, there was limited knowledge about the exact composition of the myxobacterial lipidome and no method was available to monitor putative changes in the myxobacterial lipidome down to the single molecular species for studying lipid biosynthesis or regulation. An ultra-performance liquid chromatography coupled with mass spectrometry based method with electrospray ionization (UPLC-ESI-MS) utilizing standard equipment and a water/acetonitrile/isopropanol based eluent system proved to be geared for the construction of lipid profiles for wild type and mutant cells of *M. xanthus* and to show their differences. Fragmentation spectra based structure elucidation of lipid molecular species resulted in the identification of 99 molecular species comprising glycerophosphoethanolamines, glycerophosphoglycerols, glycerolipids, ceramides and ceramide phosphoinositols. The

latter have never been described for any prokaryotes before. Three dimensional plots were created from the relative intensity differences of the single molecular ion species between the different samples to provide an efficient and versatile visualization of the data and enable the researcher to quickly detect differences.

Zusammenfassung

Mit der Entdeckung des Lichtmikroskops erschloss sich Forschern zunehmend eine vollkommen neue, vorher unvorstellbare Welt von überwiegend einzellig lebenden Organismen. Im Laufe der Zeit stellte sich deren Einfluss auf das menschliche Leben als immens heraus, wenn man nur die Bedeutung von Bakterien und Pilzen in der Zubereitung von Lebensmitteln einerseits und deren Verantwortung für die Entstehung von zum Teil schwerster Infektionskrankheiten andererseits bedenkt. Die wahrscheinlich größte Vielfalt von Mikroorganismen lässt sich im Erdboden finden. Auf kleinsten Raum ringen hier hunderttausende von Arten um Ihr Fortkommen, wobei jede Ihre eigenen Strategien entwickelt hat, um sich einen ausreichenden Zugang zu Nahrung, Platz und Schutz vor Fraßfeinden zu verschaffen und das Überleben während der sich ständig ändernden Umweltbedingungen zu sichern. Dazu gehört die Produktion nieder- und hochmolekularer Substanzen, die als Toxine oder hormonähnliche Signale agieren können. Die Umwandlung von Zellen in stoffwechselinaktive, hitze-, kälte- und trockenheitsresistente Sporen, sowie begrenzte Zelldifferenzierung, wie zum Beispiel die stickstofffixierenden Heterozysten bei den Cyanobakterien und die luftmyzelbildenden Sporen bei den Streptomyzeten, gehören ebenso zu den Überlebensstrategien von Bakterien. Innerhalb der Klasse der Deltaproteobakterien finden sich in der Ordnung Myxococcales Bakterienarten, die eine ganz besonders faszinierende Kombination an Eigenschaften besitzen. Sie alle sind in der Lage unter Verwendung von zwei unterschiedlichen Fortbewegungsmaschinerien auf festen Oberflächen in koordinierten Schwärmen vorwärtszugleiten und neben einigen Arten welche Cellulose verdauen können ernähren sie sich von der „Jagd“ auf andere Mikroorganismen. Dazu überschwärmen sie deren Kolonien und verdauen jene mit Hilfe hydrolytischer Enzyme. Zudem finden sich unter den Myxobakterien Produzenten einer Vielfalt von Naturstoffen. Berühmt sind sie jedoch vor allem für ihre Art und Weise Dauerformen zu bilden: Gehen die verfügbaren Nährstoffe, insbesondere Aminosäuren für die Proteinbiosynthese, zur Neige, so schwärmen die einzelnen Individuen einer Kolonie in Richtung von Aggregationszentren in denen nach und nach „Fruchtkörper“ genannte Gebilde entstehen. Diese sind von einer gallertartigen Schutzschicht umhüllt, mit Sporen gefüllt und weisen eine Höhe von bis zu 100 µm auf. In Abhängigkeit von der Art haben diese eine einfache hügelförmige, bis hin zu einer sehr komplexen, baumförmigen Gestalt. Verständlicherweise wird seitens der Myxobakterienforschung der Frage wie Myxobakterien diesen für Prokaryoten sehr

komplexen Prozess koordinieren große Aufmerksamkeit gewidmet. So erkannte man bereits Ende der 70er Jahre in Untersuchungen an dem Modellorganismus *M. xanthus*, dass bestimmte Gruppen von Mutanten, welche nicht mehr zur Fruchtkörperbildung und Sporenbildung in der Lage sind, diese Fähigkeiten wiedererlangen können, wenn man sie mit dem Wildtypzellen oder Mutanten einer anderen Gruppe mischt. Daraufhin wurde die Hypothese aufgestellt, dass zwischen den Zellen für den Entwicklungsprozess notwendige Signale ausgetauscht werden, die bei der komplementierten Mutante fehlen. Somit definierte man fünf (A-E) Gruppen von „bedingt sporulationsunfähigen Mutanten", auch als „Komplementationsgruppen" bezeichnet und benannte die dazugehörigen Signale als A-E Signale, unbeachtete dessen, ob es sich um eines oder mehrere Signale, um Proteine, Peptide, kleine Moleküle oder Regulatoren handelt, welche bei den entsprechenden Mutanten nicht mehr zur Geltung kommen.

Die vorliegende Arbeit beschäftigt sich mit speziellen Aspekten des sogenannten „E-Signals" in *M. xanthus*. Mutanten mit einem Defekt in der Funktion dieses Signals sind nicht mehr in der Lage aus verzweigtkettigen Aminosäuren wie Leucin die korrespondierenden, um ein C-Atom verkürzten, verzweigtkettigen Carbonsäuren zu erzeugen. Da in *M. xanthus* diese wichtige Vorläuferverbindung für verzweigtkettige Fettsäuren, Naturstoffe und Isoprenoide sind, ist nicht ersichtlich, welches der betroffenen Verbindungen wichtig für die Fruchtkörperbildung und Sporulation sind. Erste Antworten geben die Resultate aus der Publikation „Isoprenoids Are Essential for Fruiting Body Formation in *Myxococcus xanthus"*. Für jene Untersuchungen standen im Vorfeld Mutanten zur Verfügung, welche eine verminderte Fähigkeit hatten, aus Acetat und/oder verzweigtkettigen Carbonsäuren den Isoprenoidvorläufer 3-Hydroxymethylglutaryl-Koenzym A (3-HMG-CoA) zu synthetisieren. Diese wurden mikroskopisch auf ihre Fähigkeit untersucht, zeitabhängig Fruchtkörper zu bilden und mit Hilfe der Gaschromatographie gekoppelt mit Massenspektrometrie (GC-MS) verzweigtkettige Fettsäuren zu synthetisieren. Anschließend wurden diese Ergebnisse verglichen mit jenen, die man erhielt, als die Mutanten genetisch durch das Gen für das Schlüsselenzym HMG-CoA Synthase (*mvaS*) oder die Zugabe von Mevalonolacton, einem Isoprenoidvorläufer, komplementiert wurden. Aus jenen Experimenten ergab sich, dass die Sicherstellung der Isoprenoidbiosynthese eine wichtige Voraussetzung für die Fruchtkörperbildung ist. Allerdings ist diese im Wildtyp erheblich auf die 3-HMG-CoA Biosynthese aus verzweigtkettigen Carbonsäuren angewiesen. Hier scheint die Aktivität der HMG-CoA

Synthase nicht auszureichen, um einen Verlust zu kompensieren. Erst das Einbringen einer zusätzlichen *mvaS* Kopie oder die Komplementation mit größeren Mengen von Mevalonolacton (1 mM) gleichen den Verlust an 3-HMG-CoA Synthese wieder aus.

Kann es also sein, dass der Phänotyp der E-Signal Mutanten eher auf eine Verminderung der Isoprenoidbiosynthese und weniger auf jene der verzweigtkettigen Lipide beruht, letzteres also lediglich ein Surrogat für ersteres darstellt? Im Kontext zu einer vorhergehenden Arbeit gibt die Publikation „A multifunctional enzyme is involved in a novel bacterial ether lipid biosynthesis pathway“ eine recht klare Antwort. Es konnte bereits vorher gezeigt werden, dass *M. xanthus* während der Fruchtkörperentwicklung Etherlipide mit verzweigtkettigen Alkyl- und Acylresten akkumuliert. Dazu gehören der Vinylether „VEPE“ (PE(P-i15:0/i15:0) (verwendete Nomenklatur gemäß „LIPID MAPS Lipid Classification System“, siehe http://www.lipidmaps.org/data/classification/LM_classification_exp.php) und die Alkylether „AEPE“ (PE(*O*-i15:0/i15:0) sowie das Alkyldiacylglycerol „TG-1“ (TG(*O*-i15:0/i15:0/i15:0). Alle getesteten Mutanten mit Defekten in dem Entwicklungsprogramm akkumulieren keine Etherlipide, sodass es sich bei Ihnen zunächst um Biomarker für die Fruchtkörperbildung handeln. Die Suche nach Biosynthesegenen für Etherlipide führte zu einem aus fünf Genen bestehenden Cluster (genannt *elbA-E* für ether lipid biosynthesis) in dem das Gen *elbD* für ein bis dato unbekanntes Multidomänenenzym kodiert. Wird dessen Transkription gestört, so kommt es zu einer sehr starken Abnahme der Etherlipidbiosynthese inklusive einem Totalverlust an der Synthese von TG-1. Der Entwicklungsphänotyp hingegen ist eher schwach, jedoch enthalten die Fruchtkörper keine keimungsfähigen Sporen. Genetische Komplementation mit *elbD* führt zu einer Wiederherstellung der Etherlipidbiosynthese und des Entwicklungsphänotyps sowie einer Zunahme von lebensfähigen Sporen. Analoge Untersuchungen an *Stigmatella aurantiaca*, einen nahen Verwandten von *M. xanthus*, bestätigten das Ergebnis hinsichtlich der Bedeutung von *elbD* für die Etherlipidbiosynthese. Außerdem wurden Gene mit einer starken Homologie zu *elbD* in allen bisher sequenzierten Genomen von Myxobakterien identifiziert. Ferner zeigte eine stichprobenartige Untersuchung an einer Reihe von anderen Myxobakterien, dass sie alle Etherlipide bilden. Weitere Untersuchungen beschäftigten sich mit der Funktionsweise von ElbD. Biochemische Tests an heterolog exprimierten und isoliertem ElbD bewiesen die Existenz einer Acyl-Carrier-Protein- und Acyl-CoA Synthetasedomäne. Phylogenetische Untersuchungen und *in-silico* Dockingexperimente

gaben deutlich Hinweise auf eine weitere Acylglycerolphosphat-Acyltransferase-Domäne, welche PE(0:0/i15:0) als Acylakzeptor verwendet. Dies stand zudem im Einklang mit der Beobachtung, dass eben jenes PE(0:0/i15:0) in *elbD* Mutanten während der Fruchtkörperbildung anstatt von TG-1 akkumulierte. Eine weitere Domäne, welche laut der Conserved Domain Database des National Centers of Bioinformatics Homologien zu Acyl-CoA-Reduktase-Domänen besitzt scheint in die Erzeugung von i15:0 Aldehyd involviert zu sein: Wildtypzellen erzeugen dieses, und nur dieses, langkettige Aldehyd, wobei *elbD* Mutanten diese Fähigkeit nicht mehr besitzen. Fasst man die Ergebnisse zusammen, so gelang es im Zuge der Untersuchungen das erste bakterielle Enzym zu identifizieren, welches in die Etherlipidbiosynthese involviert ist. Darüber hinaus kann man die *elbD* Mutante als erstes Beispiel ansehen, bei dem eine bestimmte Gruppe von verzweigtkettigen Etherlipiden identifiziert wurde, die ganz oder teilweise ein wichtiges Signal für die Ausdifferenzierung von vegetativen Zellen in Sporen darstellen. Demgegenüber kann der viel stärkere Phänotyp der *esg* Mutanten auf die Verarmung an mehreren Substanzklassen (Isoprenoide, sekundäre Naturstoffe, verzweigtkettige Lipide) in Verbindung gebracht werden und ist somit unspezifischer als der *elbD* Phänotyp.

Im Zuge der gesamten Arbeiten an der Etherlipidbiosynthese und deren Bedeutung für die Fruchtköperbildung stellte die Analytik der beteiligten Lipide aus den entsprechenden Extrakten eine große Herausforderung dar. Lipide der gesamten Polaritätsbreite von Lysophospholipiden über Glycerophospholipiden und Glycerolipiden bis hinunter zu einzelnen Molekülspezies mussten an der einen oder anderen Stelle identifiziert und deren relatives Vorkommen in unterschiedlichen Proben bestimmt werden. Hierzu mussten alle zur Verfügung stehenden Methoden angewendet und deren Ergebnisse kombiniert werden, um spezifische Aussagen treffen zu können. Um dies in Zukunft zu vermeiden wurde im Rahmen des dritten Manuskriptes eine einzige Methode entwickelt, die gleichzeitig in der Lage ist, das gesamte bekannte Lipidom von Myxobakterien bis zu einzelnen Molekülspezies darzustellen. Hierfür wurden Lipidextrakte aus Kulturen verschiedener Mutanten von *M. xanthus* mit Hilfe einer C18 Säule für die Ultrahochleistungsflüssigkeitschromatographie (UPLC) unter Verwendung eines Wasser/Acetonitril/Isopropanol Gradienten aufgetrennt und die eluierenden Lipide mit Hilfe eines Ionenfallenmassenspektrometers nach Elektrosprayionisation (ESI-MS) analysiert. Aus den Fragmentspektren der Molekülionen wurde die Klassen der Lipide und aus den Integralen der extrahierten Einzelionenchromatogramme deren relative Häufigkeit

ermittelt. Insgesamt 99 Molekülspezies konnten Lipiden zugeordnet werden. Identifiziert wurden Glycerophosphoethanolamine, 1-(1*Z*-alkenyl),2-acylglycerophosphoethanolamine, Glycerophosphoglycerole, Ceramide, Ceramidinositolphosphate, Diacyl- und Triaclyglycerole. In dem Extrakt der *elbD* Mutante war wie erwartet der Gehalt an 1-(1*Z*-alkenyl),2-acylglycerophosphoethanolaminen stark vermindert, in jenem einer α-Hydroxylasemutante (Δ*0191 (MXAN_0191)*) fehlten wie erwartet α-hydroxylierte Sphingolipide und eine solcher von einer Serin-Palmitoyl-CoA-Transferase (*spt (MXAN_3748))* ließen sich keinerlei Sphingolipide mehr nachweisen. Trotz der Vielzahl der Molekülspezies ließen sich die Resultate in 3D Streudiagrammen ohne weitere statistische Aufarbeitung darstellen, sodass auch relativ quantitative Unterschiede in einzelnen Molekülspezies und Lipidklassen zwischen den einzelnen Extrakten für den Betrachter sichtbar wurden. Es steht somit nun eine geeignete Methode zur Verfügung, die auch unterschwellige Verschiebungen im Lipidom von Mutanten zu Tage fördern kann, ohne dass mehr als eine Analyse herangezogen werden muss. Bei Verwendung eines geeigneten Versuchsdesigns sind quantitative Aussagen ebenfalls möglich. Eine tiefergehende molekularbiologische und metabolische Untersuchung der Lipidbiosynthese in Myxobakterien kann nun angegangen werden. Zudem steht das gesamte Lipidprofil von *M. xanthus* für Vergleiche zur Verfügung.

Alles in allem gelang es mit dieser Arbeit die molekulare Natur der *esg* Mutante zu konkretisieren. Die aus Leucin gewonnenen verzweigtkettigen Carbonsäuren stellen Vorläufermoleküle sowohl für Isoprenoide und sekundäre Naturstoffe als auch für Lipide mit verzweigtkettigen Fettsäuren, inklusiver der Etherlipide dar. Ein reichhaltiges Angebot an Isoprenoidvorläufermolekülen ist eine ausreichende Voraussetzung für die Fruchtkörperbildung. Die Etherlipide hingegen sind notwendig für die Differenzierung der Zellen in lebensfähige Sporen. Ferner spielt ein bisher unbekanntes Multidomänenenzym eine zentrale Rolle in der Etherlipidbiosynthese von Myxobakterien dar und ist somit auch das erste Beispiel für einen prokaryotspezischen Etherlipidbiosyntheseweg. Weitere Untersuchungen wären vonnöten, um festzustellen, ob spezifische Isoprenoide oder Etherlipide Signalcharakter haben. Darüber hinaus steht nun die exakte Erforschung der Lipidbiosynthesewege in *M. xanthus* mit den bereits vorhandenen molekularbiologischen und mit der neu entwickelten Lipidomtechnik offen.

1 Introduction

1.1 About myxobacteria: unicellular prokaryotes with strong social traits

The world of the smallest living beings remained inaccessible to early natural scientist until the invention of the light microscope. It was Antoine Philips van Leeuwenhoek, driven by his interest in lens making, to be the first to describe single-celled organisms in one of his numerous letters published by the British Royal Society in the 17th century[1,2]. Those organisms became of significant interest as bacteria were identified as originators of human diseases like tuberculosis, anthrax, and cholera by Robert Koch[3,4].

In 1892, the American mycologist and member of the Cryptogamic Laboratory of the Harvard University, Roland Thaxter, comprehensively described a harmless, but particularly intriguing order of bacteria named the "Myxobacteriaceae"[5]. For the first time, and with the acute eye of a skilled and talented natural scientist, he aptly recognized these intriguing species as "Schizomycetes", as prokaryotes (though by mistake regarded as "plants") were named these days. Using color plates of impressive richness of detail drawn from microscopic investigations, he precisely described nine myxobacterial species with all features for which myxobacteria are generally known today. This work was published in the Botanical Gazette in December 1892[5]. What he saw seemed to impress himself so much that he noted: "This life history (…) is so peculiar, (…) and is altogether so unique to the group of Schizomycetes, to which they should undoubtedly be referred, that their separation as a distinct order seems unavoidable"[5].

What makes myxobacteria special among the variety of prokaryotes? One of the most striking features of the myxobacteria was what Thaxter encountered first when his attention was drawn to these organisms. It was something visible by the naked eye that he described as "… a bright orange-colored growth occurring upon decaying wood (…) somewhat highly organized (…) to consist of apparently amorphous material, without signs of hyphae and spores of any kind. Its general appearance and the general character of the substance which composed it suggested an immature condition of some myxomycete (…) which, when artificially cultivated, yielded immature conditions that rendered already its true nature apparent"[5]. This "form" or "cyst", as Thaxter named it, is known today as "fruiting body"[6], a more or less structured, macroscopically visible, multicellular construction occupied by thousands of heat and drought resistant spores. **Figure 1.1** panel

a and **b** show original drawings of fruiting bodies by Thaxter at various stages from *Chondromyces crocatus* (**Figure 1.1 a**) and *Myxococcus rubescens* (**Figure 1.1 b**). At a first glance, these structures somewhat resemble the fruiting bodies of the eukaryotic, thus completely unrelated, slime molds. The close commonality of the myxobacterial fruiting bodies to those of the myxomycetes led to the misidentification of *Chondromyces crocatus* as a fungus before[5,7]. These fruiting bodies are formed by the individual vegetative rod-shaped cells (as exemplarily depicted in **Figure 1.1 c-g**) in a process known as "developmental process" or "fruiting body formation" already described in detail by Thaxter. The colors and structures of those fruiting bodies are used to describe individual taxonomic species and reach from simple "mounds" to complex "tree-like" structures with a vertical "stalk" and "branches" ending in rounded "cyst" which then contain, densely packed, mature spores referred to as "reproductive bodies"[6,8,9].

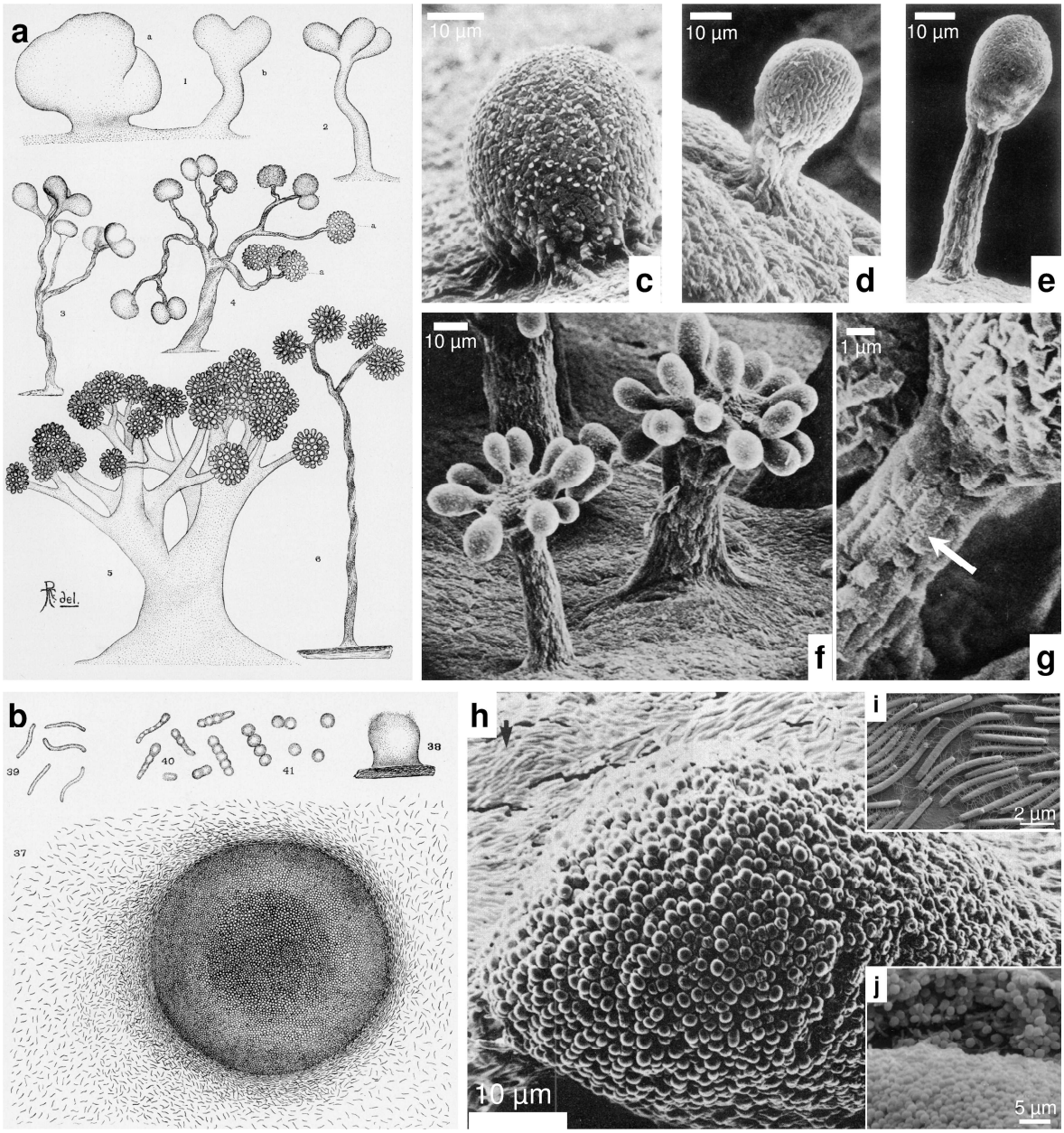

Figure 1.1 | Phenotypical characterization of myxobacteria back then and today

Historical drawings from Thaxter (**a** and **b**) illustrating his observations by light microscopy and more recent images obtained by scanning electron microscopy (SEM) (**c-j**) from *Chondromyces crocatus* (**a**/**c-g**), *Myxococcus rubescens* (**b**) and *Myxococcus xanthus* (**h-j**) strains. Images **c-g** show different consecutive stages of fruiting body formation with a bulb formed first (**c**) which is gradually uplifted by a rising stalk (**d** and **e**) and finally separates into a couple of mature sporangia separated from the stalk by pedicels (**f**). The stalks as well as the pedicels are made of rods aligned in a parallel way (white arrow, **g**). **b**: Individual, slender, rod shaped vegetative cells as well as the sphere-shaped mature spores were well depicted by Thaxter (**39**-**41**) and identical to what a modern researcher perceives when investigating *Myxococcus* strains under a contemporary light microscope. Side view (**38**) and top view (**37**) of a mature fruiting body in its simple, mound-like form as characteristic of those from *Myxococcus* sp. surrounded by peripheral rods. **h**: A similar view acquired by SEM with peripheral rods visible in the background and the sphere-shaped spores that form the majority of the fruiting body. Images **i** and **j** are higher magnifications of vegetative rods and the spores visible in a fissure of a fruiting body. Note the extracellular fibrils surrounding the cells in **i**. Photo credits (each with permission): **a** and **b**: Thaxter[5] (Courtesy of JSTOR); **c-g**: Grilione and Pangborn[8]; **h**: O'Connor and Zusman[10]; **i**: Kearns and Shimkets[11]; **j**: Licking *et al.*[12].

1.1.1 Taxonomy and properties of myxobacteria

Although Thaxter described myxobacteria as “plants”, to which Schizomycetes were assigned in those days, myxobacteria are Gram-negative, rod-shaped prokaryotes belonging to the genus myxococcales, an order of the δ-subdivision of the proteobacteria, and are further subdivided into the three suborders Cystobacterineae, Sorangiineae and Nanocystaceae with an increasing number of families and species described as research progresses[13]. In general, myxobacteria can be isolated from, preferably pH neutral, soil samples all over the world with up to 450,000 individual cells per gram of soil. An extensive study, published in 2000, comprising 64 sample series with a total number of 1398 individual, globally collected samples, found only 9% free of myxobacteria[14]. Within a single soil sample, myxobacteria can account for between 0.4 - 4.5% of the bacterial community based on 16s rDNA gene sequencing[15]. As most myxobacteria are mesophilic, their highest variety of species occurs in the tropical climate, but psychrophilic (genera *Polyangium* and *Nannocystis*[16]), halo tolerant and halophilic (genera *Haliangium*[17], *Enhygromyxa*[18], *Plesiocystis*[19]) and microaerophilic (genus *Anaeromyxobacter*[20]) species were also isolated from Antarctic soil, marine coastal sediments and anaerobic environments respectively.

1.1.2 A huge genome for a unique lifestyle

The rather complex lifestyle of myxobacteria is also reflected in the size of their genomes. Several myxobacterial genomes were sequenced and that of *Sorangium cellulosum* So0157-2 exhibits with 14.78 Mb in size and an estimated number of 10,503 genes the largest genome of a prokaryote sequenced so far[21]. That is even bigger than the one of the eukaryotic yeasts from the genus *Saccharomyces* whose genome sizes range from 10-13 Mb[22]. The best studied myxobacterium *Myxococcus xanthus* has with 9.14 Mb (strain DK1622) a genome of intermediate size among the myxobacteria[23]. Interestingly, the species from the genus *Anaeromyxobacter* do only bear genomes of about 5 Mb[24] in size which is similar to *E. coli*[25]. Unlike all other known myxobacteria, *Anaeromyxobacter* do not form fruiting bodies which may indicate that the developmental process requires a large genome[24].

With respect to the abundance of certain genes there are two unique features that distinguish myxobacteria from other prokaryotes: a large number of gene clusters

dedicated to the biosynthesis of secondary metabolites[26] and an unusual number of genes encode proteins which are involved in regulatory pathways[23,27,28].

In general, myxobacteria were found to be potent producers of secondary metabolites quite early and more than 100 different basic structures with about 500 structural variants have been isolated since then[29]. A number of biological activities including inhibition of the respiratory chain (e.g. β-methoxyacrylates like myxothiazol, melithiazol and cyrmenins), antibiosis (e.g. myxovirescin) and cytotoxicity (e.g. tubulysins, chivosazols, epothilons)[26,30,31]were determined for some of these substances. The microtubule-stabilizing macrolactone epothilon has become the first and so far only myxobacterial natural product in clinical use against taxol-resistant breast tumor[32]. Most natural products from myxobacteria, for which data about their biosynthesis are available, have been identified as products of hybrids of non-ribosomal peptide synthetases (NRPS) and polyketide synthases (PKS), very often additionally modified by glycosylation, oxygenation, methylation etc[29].

The genome of *M. xanthus* encodes 18 putative NRPS/PKS gene clusters[26] being potentially involved in the biosynthesis of secondary metabolites, which represent about 8.6% of the whole genome. This is considerably more than in *Streptomyces coelicolor* (4.5 %)[33] and *Streptomyces avermitilis* (6.6%)[34,35], two actinomycetes which are likewise well-known for being rich sources of natural products. However, under standard laboratory conditions, only five compound classes (the antibiotic myxovirescins, the myxalamids, myxochromides, the myxochelin siderophores and the DKxanthene pigments) are found in cell culture extracts[36], even though almost all NRPS/PKS enzymes are detectible in transcriptomic and proteomic samples[37,38]. Finally, three more substances, myxoprincomide and two other entities with unknown structures, designated as c844 and c329, were identified after comparison of wild type and mutant extracts by means of ultra performance liquid chromatography coupled with mass spectrometry (UPLC-MS) and principal component analysis (PCA) of the resulting spectra[39]. Consequently, those biosynthetic genes are expressed and the resulting enzymes are active and do not represent "genetic waste"[39]. In addition to this, liquid chromatography coupled with mass spectrometry (LC-MS) based screening of 98 *M. xanthus* strains, isolated from all over the world, revealed that some of them produce other known secondary metabolites such as cittilin A and althiomycin[36]. The exact physiological and ecological meanings of the secondary metabolites are still largely unknown. With respect to its life cycle the

DKxanthenes are of significance for spore formation in *M. xanthus.* Mutants not producing DKxanthenes are defective in spore formation and act in the same way when pure substance is supplemented[40].

Apart from a remarkably high density of genes involved in secondary metabolism, those encoding regulatory proteins are of high abundance in myxobacterial genomes. Many of them belong to the group of eukaryotic-like protein kinases (ELKs)[27,41]. These enzymes catalyze the reversible phosphorylation of proteins in order to modify their activity and are important elements of eukaryotic signaling systems such as neuronal G protein-coupled receptor (GPCR) mediated signal transduction or hormone dependent mitogen activation[42,43]. In myxobacterial genomes, their abundance increases exponentially with genome size. As a result, in *Sorangium cellulosum* and *Plesiocystis pacifica* their density, determined by number of kinases per thousand of coding sequences, is even higher than that of eukaryotes like mice, fruit flies and sea urchins[27]. In total, there are 99 ELKs present in *M. xanthus* and 317 in *S. cellulosum*. It seems as if the myxobacteria acquired and accumulated this kind of signal transmission and regulation systems to enable multicellular behavior, a hypothesis that is in accordance with a similar high density of ELKs in other prokaryotes with comparably complex lifestyles, such as of phyla actinobacteria, cyanobacteria and Chloroflexi. The typically one- and two-component signal transduction systems are also present in myxobacteria. However, they are rather underrepresented in myxobacterial genomes compared to those of other bacteria[27]. In short, most myxobacteria possess the largest genomes among known prokaryotes which feature an unusually high number of genes encoding regulatory proteins and those involved in the biosynthesis of natural products.

1.2 Features of *Myxococcus xanthus*: the favorite among the lab strains

The aforementioned *Myxococcus xanthus* (family: Myxococcaceae, suborder: Cystobacterineae), the well-known model organism used for most molecular genetic studies, is also the central subject of investigation for the studies of this thesis. Its individual cells are slender rods with tapered ends, somewhat flexible, up to 10 µm in length with a diameter of up to 1 µm (see Thaxter's drawing in **Figure 1.1 b** and SEM image **i**)[44]. They produce extensive extracellular matrix with fibrils consisting of polysaccharides and proteins in which the whole colony is embedded when grown on a solid surface. *M. xanthus* is motile and, like most myxobacteria, feeds on other

microorganisms including bacteria and unicellular fungi by collectively swarming about and killing and digesting them using secreted lytic enzymes. This "hunting" behavior resembles the "wolf-pack" strategy of some carnivorous living animals[45].

The fruiting bodies formed in response to unfavorable conditions (see **Figure 1.1 h** and **j**), especially nutrient deprivation, are rather simple, mound-like structures, coated with a gelatinous matter in contrast to the highly complex and impressive tree-like fruiting bodies formed by *Chondromyces* species (see **Figure 1.1 a** and **c**-**g**). This process has been partially deciphered by researchers up to date. **Chapter 1.3.1** outlines those findings in more detail. Fruiting body formation, however, cannot transpire without the cells motility.

1.2.1 Moving forward: motility of *M. xanthus*

As mentioned before, all myxobacteria are motile, which means that they can glide on solid surfaces along their length axis. For *M. xanthus*, the speed of progressing individual cells ranges from 1-20 µm/min and, as a distinctive feature, they reverse directions once every 2-8 minutes depending on the conditions by swapping the leading and lagging cell pole[46,47]. They move in groups in an organized, collective manner. The microscopic image **a** in **Figure 1.2** shows the resulting locomotion patterns. They form "streams" in which cells follow slime trails secreted by their forerunners, "ripples" indicating a high reversal frequency of the individual cells (not shown) and "aggregates" leading to "mounds", originating from a reduced reversal frequency of moving cells. Individual cells can also leave the edge of colonies and roam on their own. Macroscopically, this behavior results in a starburst-like growth pattern (see **Figure 1.2 b**)[48-50].

Myxobacteria cannot move freely through liquid media and do not use flagella, but possess two different motility systems that work synergistically: The so-called "S"- (for social) and "A"- (for adventurous motility) motility systems. Those terms were coined as a result of observations made with mutants that show defects in either system[51,52]. The S-motility is required for coordinated group movements and the A-motility system is required for individual cells to move independently off the colony. Both systems use their own, genetically mostly independent, "engines".

1.2.2 Type IV pili and S-motility: climbing forward horizontally

S-motility, also referred to as "twitching" motility, is based on the utilization of Type IV pili, a homopolymeric filamentous protein emerging from one pole of the cell towards the

direction of movement[53]. The atomic force microscopy image in **Figure 1.2 c** visualizes those pili emanating from swarming *M. xanthus* individuals[54]. Their cell-averted ends attach to either the fibril network surrounding the bacteria in a colony or directly to the extracellular matrix of another cell and pull the cells together by retraction whereat the pilus is being simultaneously disassembled at the inner membrane[55,56]. By this means, the cells assist each other to move by providing the necessary anchor points for the retraction force. This perspective is supported by observations that S-motility is strongly impaired or absent not only when genes encoding elements of the pilus assembly are mutated but also when fibril or extracellular matrix formation is hampered[57,58]. Apart from myxobacteria, genes encoding proteins for the Type IV pili machinery are conserved in several other gliding bacteria like *Pseudomonas aeruginosa, Neisseria gonorrhoeae, Neisseria meningitides, Synechocystis sp.* and the function of their protein products is partly known. By combining these findings, a working model for the molecular mode of action of the pilus apparatus has been constructed (see **Figure 1.2 d**)[59,60].

Figure 1.2 │ Motility motors in *Myxococcus xanthus*

a: Still picture of a phase contrast microscopic time-lapse video. Single cells are able to leave the colony leaving a slime trail on which following cells preferably travel. Collectively swarming cells form rafts in which they are closely aligned abreast. When swarms of cells collide, they form mounds. **b**: Macroscopic swarming pattern of a *M. xanthus* colony after a few days of growth on nutrient agar. The colony adopts a radial pattern with an irregular edge and is rather flat. **c**: Image taken by atomic force microscopy. Arrows point on the clearly visible polar Type IV pili that confer S-motility to *M. xanthus*. **d**: Contemporary working model on how Type IV pili work on a molecular level. For details see text. **e**: Transmission electron microscopic images of the polar cell area unveiled ring-shaped nozzles with an inner diameter of about 6.5 nm and a total diameter of about 14 nm, resembling a very similar structure previously described for Cyanobacteria. **f**: Ribbons of mucilage emanate from the posterior cell pole with the same speed as the cell moves ahead, an observation leading to the slime secretion model (see text). **g**: Shock frozen and dried motile *M. xanthus* cells exhibit a helical band (arrows indicate nodes where the band intersects) that spans the entire length of the cell. **h**: Discovery of protein clusters that remain stationary during cell movement (note: red dots are fluorescently labeled proteins associated with the helix; protein clusters remaining stationary at the basal side are connected with a straight line) (**i**) led to the focal adhesion model (see text). **j**: The helical rotor model proposes rearwards moving surface waves provoked by motor proteins that move along the helical cytoskeletal filament. Photo credits (each with permission): **a**: Wu *et al.*[48]; **b**: Jelsbak and Kaiser[61]; **c**: Li *et al.*[54]; **d**: reproduced from Kaiser; **e** and **f**: Wolgemuth *et al.*[62]; **g**: Lünsdorf and Schairer[63]; **h-j**: Nan and Zusman[64].

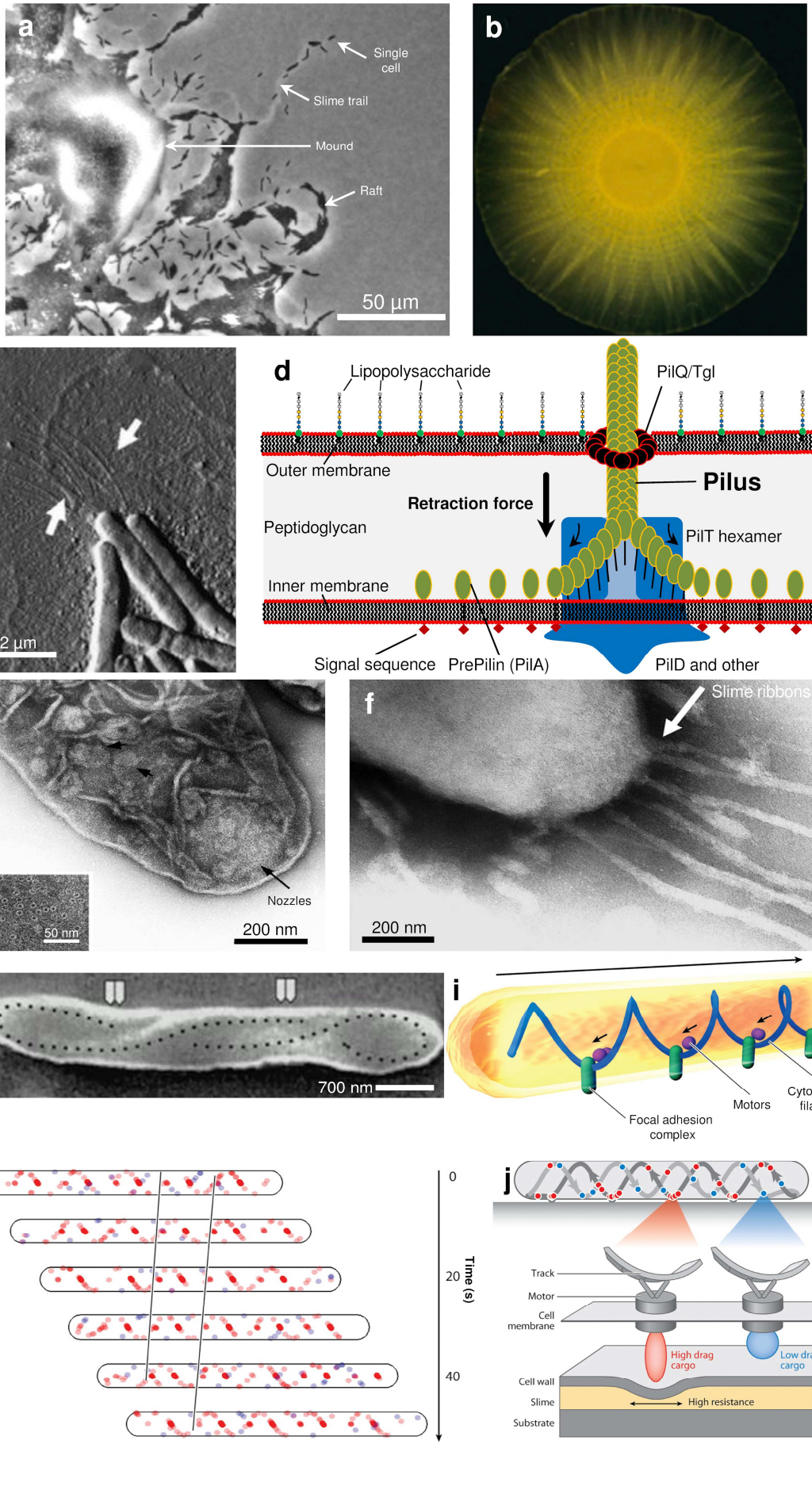
a
Single cell
Slime trail
Mound
Raft
50 µm
b
c
2 µm
d
Lipopolysaccharide
PilQ/TgI
Outer membrane
Pilus
Retraction force
Peptidoglycan
PilT hexamer
Inner membrane
Signal sequence
PrePilin (PilA)
PilD and other
e
Nozzles
50 nm
200 nm
f
Slime ribbons
200 nm
g
700 nm
i
Motors
Cytoskeletal filament
Focal adhesion complex
h
0
20
40
Time (s)
j
Track
Motor
Cell membrane
High drag cargo
Low drag cargo
Cell wall
Slime
High resistance
Substrate

According to this model, the pilus is made up of polymerized PilA monomers after their procession by PilD in the inner membrane. On the whole, the pilus spans the cytoplasm and penetrates the outer membrane through a pore made up of PilQ secret in monomers. After attaching to extracellular material or the surface of other cells, the pilus is retracted by the actions of PilT, an ATP-dependent motor protein, exerting the necessary force to drag the cell forward while the pilus is disassembled in the inner membrane simultaneously. Another motor protein, PilB, is responsible for the extension of the pilus. With a diameter of about 10 nm, it is very thin. As a result, the load force of the extending pilus is too weak to push the cell backwards[53].

In summary, the S-motility engine provides a basis for the coordinated propagation of a myxobacterial cell swarm. However, its' single cells cannot move as individuals because of missing extracellular matrix outside the colony so that a different kind of engine is required.

1.2.3 The secret of gliding motility: of microbial rocket engines and snakes

A-motility, referred to as "gliding" motility, a phenomenon also observed from cyanobacteria, flavobacteria and mycoplasmas, excels in movement of cells without the help of pili, flagella or any other visible motor structures outside the cells' envelope or the change of their morphology[65]. This made the investigations of the underlying mechanisms difficult. To date there are three, partially competing, models about how gliding motility exactly works for myxobacteria. Even so, some important elements involved in myxobacterial gliding motility engine were recently unveiled.

The production of slime is a prerequisite for gliding in myxobacteria[62]. The distal poles of the bacteria exhibit nozzles assumedly involved in slime secretion (**Figure 1.2 e-f**). The force produced by the secretion and hydration of the polyelectrolyte chains are considered to produce the sufficient thrust that pushes the cell forward in a rocket-engine-like manner. Backed up by a mathematical model this hypothesis led to the "slime secretion model"[62,64].

Later, scanning electron microscopical observations of freeze-dried *M. xanthus* cells revealed dynamic, helical bands spanning the interior site of the cells' envelopes along their entire length, described as a "closed band-shaped continuum which is twisted along the longitudinal axis of the cell"[63]. Those structures were also discovered in other bacterial species that translocate by gliding like *Flavobacterium johnsoniae* and *Flexibacter*

filiformis (**Figure 1.2 g**). Moreover, these filaments are absent in cells, immobilized by poisoning or genetic defects. Further time-laps fluorescence microscopy video analysis of cells featuring fluorescently labeled proteins associated with this structure disclosed its clockwise rotation when the cells glide with a pitch and speed consistent with the progress of the cell[66,67]. When the cell reverses, the helix turns to the opposite direction[68]. Several proteins were identified that form "traffic-jam" like clusters at the basis of the cell along this helical ribbon (**Figure 1.2 h**). While the cell moves forward, those protein clusters are being assembled at the anterior cell pole and remain virtually immobile while staying attached to the rotating helix until they reach the posterior cell pole to get dissembled again[64]**.** But how can these proteins cause a propulsive force? About 40 genes are involved in gliding motility, and several proteins being associated with the protein motor clusters or the intracellular helix structure were identified[69]. The helix as a whole is associated with the actin-like structural homolog MreB, an actin-like homolog, which itself forms helical filaments, represents an element of the myxobacterial cytoskeleton and is furthermore vital for the integrity of the gliding machinery. MreB is associated with the myosin domain containing protein AglZ[67]. Together with AgmU, a central interaction partner of proteins involved in gliding motility, it is the first observed constituent of the motor protein cluster that moves along the helical structures. Homologues of MotA/B, *E. coli* stator flagella proteins[70,71] and as such important elements for the production of thrusting force, designated AglX/AglV and AglR/AglS/AglQ respectively, were also identified as part of the gliding engine[68,72]. They may be responsible for the production of the required force. Those motor proteins also interact with AgmU[66] and likewise MotAB homologues, their source of energy is dependent on the proton gradient across the cytoplasmic membrane, also referred to the "proton motive force"[68].

Although this information may not be sufficient to fully assign functions to the potentially involved proteins, two working models for the mechanism of gliding were suggested. The "focal adhesion model"[73] (**Figure 1.2 i**) suggests that adhesion complexes connecting the substratum with the cell are being transported from the front to the back of the cell by the movement of the helical structure in order to mediate the cell movement similar to the tracks of a tank or tractor crawler. However, as there seem to be no such cell surface associated adhesion proteins present in *M. xanthus*, the competing "helical rotor model"[64,74] proposes that proteins riding as cargo on the helical track accumulate when reaching the ventral side of the cell causing transverse protrusion along the basal surface.

When propagated from the front to the back by the action of the turning helix, they cause driving force mediated by the secreted slime sticking to the substrate just like the waves of muscle contractions cause propulsion in a snail's body (**Figure 1.2 j**). The mechanisms underlying the myxobacterias' ability to glide again reveal the genetic and mechanistic versatility of the organisms. But the ability to move is only an easily conceivable prerequisite to what makes these bacteria master builders among the prokaryotes: fruiting body formation.

1.3 Intercellular communication during fruiting body formation: from complementation groups over genetic loci and proteins to small molecules

1.3.1 The process of fruiting body formation in *M. xanthus*

As already mentioned, most studies on the environmental prerequisites, the process and the molecular basis such as regulation, intra- and intercellular communication, were carried out on *M. xanthus*[44]. The reason for this is probably its relatively easy and reliable handling in a laboratory environment compared to other myxobacteria. If the conditions, especially temperature, media composition and cell density, are well-defined, the process in the order of the single events is temporally highly reproducible[9,75]. **Figure 1.3 a-c** depicts this process on a macroscopic (**a)** microscopic (**b)** and schematic (**c)** level respectively. Within 72 h, disordered, vegetative cells on a solid surface form the typical mound-shaped, spore filled fruiting bodies. Those fruiting bodies are made of up to 10^5 cells being transformed to round, thick-coated, refractive, metabolically quiescent spores, which are able to form a whole colony again when environmental conditions become favorable. Most interestingly, during the process of fruiting body formation, three types of cells emerge. About 10 % of all cells become the actual spores, another 10% stay rod like unable to fruit and are called "vegetative rods"[10], and 80% of the remaining cells undergo a programmed cell death (PCD)[76], thus sacrificing themselves to provide sufficient resources for the developmental process. The exact ratio between these cell populations is however strain specific[10].

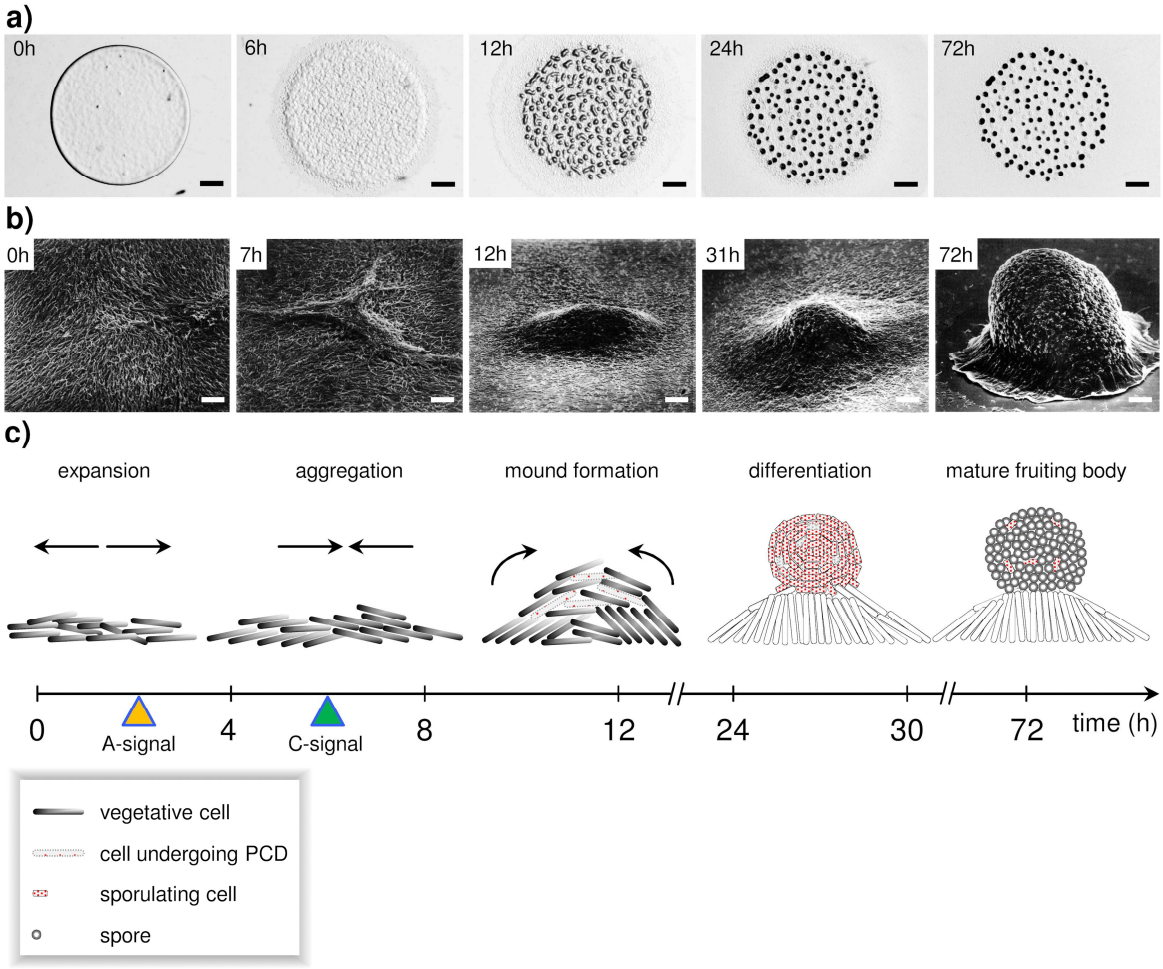

Figure 1.3 | Fruiting body formation in *M. xanthus*

a: Series of binocular loupe view of ~2.5x10^7 *M. xanthus* cells on a starvation agar during the process of starvation induced fruiting body formation. Black bar is 500 µm. **b**: Scanning electron microscopy images of the origination of a single fruiting body in a submersed culture. White bar is 10 µm. **c**: Schematic view of cell differentiation during development. Motile cells start to swarm away from the colony but limited food supply causes the initiation of the developmental program leading to the formation of aggregation centers first (6 h) that successively transform into mounds (12 h) which are the basis of the fruiting bodies (24 h) that gain increasing optical density while vegetative cells transform into spores (72 h and ongoing). Triangles indicate points when A- and S- signal come into effect. For details see text. Pictures **a** are taken from preliminary studies for publication shown in **Chapter 6.2** Pictures **b** are taken from Kuner and Kaiser[9]. Scheme **c** was created from references quoted in **Chapter 1.3**.

1.3.2 The exigency of intercellular communication as the prerequisite for the developmental program gradually unraveled: how do *M. xanthus* cells "talk" to each other?

As there is an obvious need for cell-cell communication between the individual cells, one major interest of researchers in the field of myxobacteria has been to find, define and identify distinct signals that mediate the spatial and temporal coordinative behavior of the cells during the course of the well-defined process of fruiting body formation. The

outcomes and the degree of precision of the research done on this topic were strongly determined by the availability of methods in the past. Most research was performed utilizing molecular genetic methods which focus on the requirement and temporal expression of genes with respect to an observable phenotype[77]. The exact functions of the gene products and the involvement of small molecules as "signals" are a rather new subject. Investigations anent the A-, C-, and particularly E- group of conditionally non-sporulating mutants[78,79](see next chapter) led to the non-exhaustive identification of individual proteins and, to some extent, their functions that are central elements at certain stages of fruiting body formation. However, no small molecules with a distinctive chemical structure and a defined mode of action acting as signals were identified to date. At least, for the myxobacterium *Stigmatella aurantiaca*, a close relative of *M. xanthus*, a substance named stigmolone was isolated, its structure verified, and a clear dose-response curve exhibited its function as a pheromone[80,81]. Still, a molecular target responsible for this biological activity is unknown. The following paragraphs summarize the present knowledge about genes, proteins and small molecules that are somehow involved or at least associated with the intercellular communication during fruiting body formation.

1.3.3 The long-lasting struggle: from complementation groups over genetic loci and proteins to small molecules

In a first step after the application of random mutagenesis on *M. xanthus* cells and the investigation of their resulting phenotypes with respect to the developmental process, it was possible to determine several groups of "conditionally non-sporulating mutants" subdivided into groups A-D (later named *asg*, *bsg*, *csg* and *dsg* mutants respectively)[78]. In addition to the four initially described complementation groups, a fifth (designated as *esg*) group of conditionally non-sporulating mutants with one relevant genetic locus was identified[79]. These mutants feature defects at various points of fruiting body formation and sporulation, but can regain their ability to sporulate at least to some extent when mixed with either wild type cells or mutant cells that belong to another complementation group, without transfer of genetic material[78]. Those properties indicate the transfer of somewhat signaling molecule(s), which are missing or have become ineffective within the respective complementation group.

Transposon mutagenesis using Tn5::kan constructs[82] and eventually the use of transposable promoter probes[83] helped to identify the location as well as the moment of the expression

of genetic elements in the developmental process[84]. As a result, it has been possible to assign distinctive genetic loci which are no longer active after starvation induced morphogenesis in the respective complementation groups. Finally, molecular cloning and sequencing disclose for what kind of protein they encode [85]. These experiments indicated that each complementation group bears not only one but several distinctive mutations in different genetic loci[86]. For example, for the *asg* mutants three loci (*asgA*-*asgC*) were initially described[87]and two other loci (*asgD* and *asgE*)[88] later.

1.3.4 The A-Signal: amino acids that make the difference

Mutants belonging to the *asg* group show an arrest within the first hours of the process of aggregation and fruiting body formation resulting in loose aggregates without myxospores[89]. Those mutants cannot only be rescued by mixing with wild type cells but interestingly also by the addition of cell culture supernatant of developing wild type cells. Two *M. xanthus* proteins with 27 and 10 kD in size respectively were found to be a heat-labile part of this signal[90]. These proteins in turn seem to generate a set of six different amino acids (Tyr, Phe, Trp, Leu, Ile) and small peptides consisting thereof by proteolytic activity. These amino acids are all also active by themselves and represent a heat-stable component of the A-signal[90]. The mutations behind the *asg* group were however not associated with those proteases. Instead, they were all within genes associated with signal transduction. Genes *asgA* and *asgD* encode for hybrid histidine kinases[90,91], *asgB* for a DNA binding protein[90], *asgC* for a sigma factor and *asgE* for a membrane bound amidohydrolase[88] together being proposed as a phosphorelay system that responses to the A-signal molecules in a concentration depended manner[92] so that the A-signal is regarded as a true quorum sensing system in myxobacteria[93].

1.3.5 The B-Signal: the arcane protease

For this group of conditionally non-sporulating mutants, only one gene defect was identified located in *bsgA* that encodes for an ATP-dependent LonD-like protease[94]. Mutations within this gene cause an early block in the developmental program resulting in mutants that produce less than 0.01% spores compared to the wild type[78,89]. However, it was not possible to assign specific signaling molecules to this group to date so that the nature of this signal remains elusive.

1.3.6 The C-signal: enzyme or not enzyme?

The developmental program of C-signal mutants is disturbed from 6 h after induction so that mutants fail to ripple and only form loose mounds until 24 h without sporulating and those aggregates start to disseminate again afterwards[95]. This phenotype is caused by a mutation in the *csgA* gene[96]. Two forms of this protein exist, named p17 and p25, with the apparent molecular mass of 17.7 and 25.5 kD respectively[97]. The former is a C-terminal fragment derived from the latter by proteolytic cleavage, which represents the full-length translation product of *csgA*. This cleavage is performed by the secretable protease PopC that is in turn usually kept inactive by PopD under vegetative conditions[98]. Protein p17 is found on the cell surface and able to rescue *csgA* mutants even when added to a starving culture as a recombinant protein[97]. The p25 CsgA protein belongs to the short-chain dehydrogenase (SCAD) like proteins. Mutagenesis experiments proved that the C-Signal activity of recombinant CsgA is abolished when either the NAD^+ binding motive or a motive known to be essential for SCAD activity is altered[99], which argues for the catalytic processing of another molecule by CsgA. However, the p17 form of CsgA lacks the N-terminal NAD^+ binding motive[97] and still possesses the full C-signal activity. This p17 form can be isolated from membrane fractions of developing *M. xanthus* cell[100]. As neither the specific receptor of p17 nor the substrate of p25 has been determined until now, the exact molecular mechanisms of C-signaling remain unclear. Interestingly, another SCAD-like enzyme encoding gene, designated as *socA*, was found to substitute for *csgA* defects when strongly overexpressed[101]. Recombinantly produced SocA is able to oxidize lysophosphatidylethanolamine *in-vitro*. It is most effective on PE(16:1ω5c/0:0), a lysophosphatidylethanolamine with the most abundant straight chain fatty acid in myxobacteria[102], but the structure of the product remains elusive[103].

1.3.7 D-Signal: mutants being too “slow” to aggregate

Mutants of the *dsg* group bear a mutation in *infC*, a gene encoding for an InfC-like protein, the essential ribosomally associated translation initiation factor[104] causing a growth defect on agar plates as well as an arrest in fruiting body formation and sporulation after 4 hours of induction. Mixing with wild type cells only restores sporulation to 10%[105] of the wild type level. By these observations, a perturbation of protein biosynthesis is held responsible for the perturbation of a normal development, and involvement of small molecule metabolites seems to be unlikely.

1.3.8 The branched-chain keto acid decarboxylase. lipids, secondary metabolites and the E-signal: one enzyme to rule them all

The E-group belongs to the latest discovered conditionally defective developmental mutants[79] and will be described in more detail as the E-signal is the superordinate topic of this thesis. An *esg* mutant aggregates but fails to form fruiting bodies and spores during the developmental program, shows less yellow pigmentation and a reduced adherence to hard surfaces. It was discovered that the *esg* phenotype is caused by a mutation in the E1 subunit of the branched-chain-2-oxo-acid dehydrogenase (BCKAD) complex[106] whereat they were consequently redefined as *bkd* mutants. The complex as a whole is central for the utilization of (for *M. xanthus* essential) branched-chain amino acids valine, leucine (**Figure 1.4**, **1**) and isoleucine after their deamination and decarboxylation yielding the branched-chain acids isobutyrate-CoA, isovaleryl-CoA (**Figure 1.4**, **2**) and 2-methylbuteryl-CoA respectively. The E1 subunit (encoded by genes *MXAN_4564* and *MXAN_4565)* is responsible for the decarboxylation of the branched-chain keto acids (**Figure 1.4**, 2-oxo-isocaproate **3**) to the corresponding branched-chain acid. Those organic acids are not only the starter units of the branched-chain fatty acids (e.g. isopentadecanoic acid (i15:0)), which constitute up to 60% of all fatty acids in *M. xanthus*[102], but are also incorporated into myxobacterial secondary metabolites like myxalamids[107], myxothiazols[108] and even terpenoids like aurachin and geosmin[109] as well as the steroid cycloartenol found in *Stigmatella aurantiaca*[110]. Accordingly, fatty acid composition with respect to the ratio between branched-chain and even-chain fatty acids is strongly growth medium dependent and *bkd* mutants show a reduced capability to produce branched-chain fatty acids[111]. These findings emphasize the centrality of the BCKAD in the metabolism of *M. xanthus* and other myxobacteria, but strongly impede the exact assignment of individual metabolites to specific functions in the process of fruiting body formation.

Still, *bkd* mutants produce a considerable amount of iso-fatty acids[111]. The observation that acetate is being incorporated into iso-branched hydrocarbon moieties of fatty acids and secondary metabolites[112] in these mutants led to the discovery of the mevalonate dependent branched-chain acid biosynthetic pathway.

1.3.9 The mevalonate dependent pathway: connection between iso-branched compounds and isoprenoids in *M. xanthus*

The observation of BCKAD-independent formation of iso-branched compounds led to the identification of a biosynthetic pathway branching off from the mevalonate-dependent isoprenoid biosynthetic pathway (see **Figure 1.4**). The mevalonate synthase (encoded by the *mvaS* (*MXAN_4267*) gene) is upregulated in *bkd* mutants, and a *bkd, mvaS* double mutant exhibits a more severe phenotype concerning fruiting body formation, sporulation and the synthesis of iso-branched fatty acids[55] than a *bkd* single mutant. Like the *bkd* single mutant, the phenotypes double mutant can be simply rescued by the addition of isovaleric acid[55,113]. This alternative pathway is strongly induced during fruiting body formation and in *bkd* mutants, but plays an inferior role under vegetative conditions and if rich food supply is provided[55] (see also **Figure 2** in **Chapter 6.1**). The full pathway is depicted in **Figure 1.4**. In more detail, 3-hydroxymethylglutaryl-Coenzyme A (3-HMG-CoA, **Figure 1.4**, **4**), which is provided by the action of the mevalonate synthase (MvaS), is dehydrated by the methylglutaconyl-CoA hydratase (LiuC, MXAN_3757) to 3-methylglutaconyl-CoA (3-MG-CoA, **Figure 1.4**, **5**), whereas LiuC can operate in both directions. A 3-Methylglutaconyl-CoA decarboxylase, which consists of two subunits AibA (MXAN_4264) and AibB (MXAN_4265), decarboxylates 3-MG-CoA to 3,3-dimethylacrylyl-CoA (DMAA-CoA, **Figure 1.4**, **6**), which is further reduced to isovaleryl-CoA (IV-CoA, **Figure 1.4**, **2**) by the action of the IV-CoA dehydrogenase AibC (MXAN_4266). Conversely, the short-chain-CoA dehydrogenase LiuA (MXAN_3760) can reverse these reactions together with the propionyl-CoA carboxyltransferase LiuB (MXAN_3759) and the methylglutaconyl-CoA hydratase LiuC. The resulting 3-HMG-CoA enters isoprenoid metabolism after its reduction to mevalonic acid (**Figure 1.4**, **7**)**.**

The protein functions were first deduced from the activities of homologues and confirmed by gene inactivation, gene complementation as well as metabolic labeling experiments[38,55]. Additionally, the complete reaction cascade from 3-HMG-CoA to IV-CoA was completely reconstructed *in-vitro* using heterologously expressed LiuC, AibA, AibB and AibC[114]. Thus, the *bkd* mutant is affected in the synthesis of various kinds of branched-chain compounds, including isoprenoids, secondary metabolites and any lipid that contains an iso-branched fatty acid or a moiety derived thereof. The deficiencies are partly, but not sufficiently, compensated by the shunt pathway. The complex interactions in this pathway

further complicate a prediction about which particular metabolite(s) or group of metabolites may be responsible for the *esg* phenotype.

1.3.10 Ether lipids in myxobacteria: just a biomarker?

Glycerophospholipids with a vinyl or alkyl ether linked fatty acid derived alkyl chain (plasmalogens) were found in *Myxococcus fulvus*[117] and *Stigmatella aurantiaca*[118] and their exact structures and occurrence in *M. xanthus* DK1622 were recently studied in detail [119,120]. Ether lipids PE(P-i15:0/i15:0), PE(*O*-i15:0/i15:0), and TG(*O*-i15:0/i15:0/i15:0) (named TG-1) were identified (see **Figure 1.4** for the structures and the "LIPID MAPS Lipid Classification System" (http://www.lipidmaps.org/data/classification/LM_classification_exp.php) for nomenclature of lipids in general[121,122]). Along with other triacylglycerols, they are specific biomarkers for cells that become spores in the process of starvation-induced fruiting body formation. Analogously, alkylglycerols were less abundant in *asg* and *csg* mutants that hardly sporulate. PE(P-i15:0/i15:0) and PE(*O*-i15:0/i15:0) also accumulate relative to PE(i15:0/i15:0), the most abundant glycerophospholipid in *M. xanthus*, when cells are starved, whereas PE(*O*-i15:0/i15:0) levels attain a maximum at 24 h after starvation-induced fruiting body formation. Additionally, and most notably, concerning the search for signal molecules, TG-1 is able to rescue a *bkd*, *mvaS* double mutant to a similar extent as i15:0 fatty acid for both, fruiting body formation and sporulation[119].

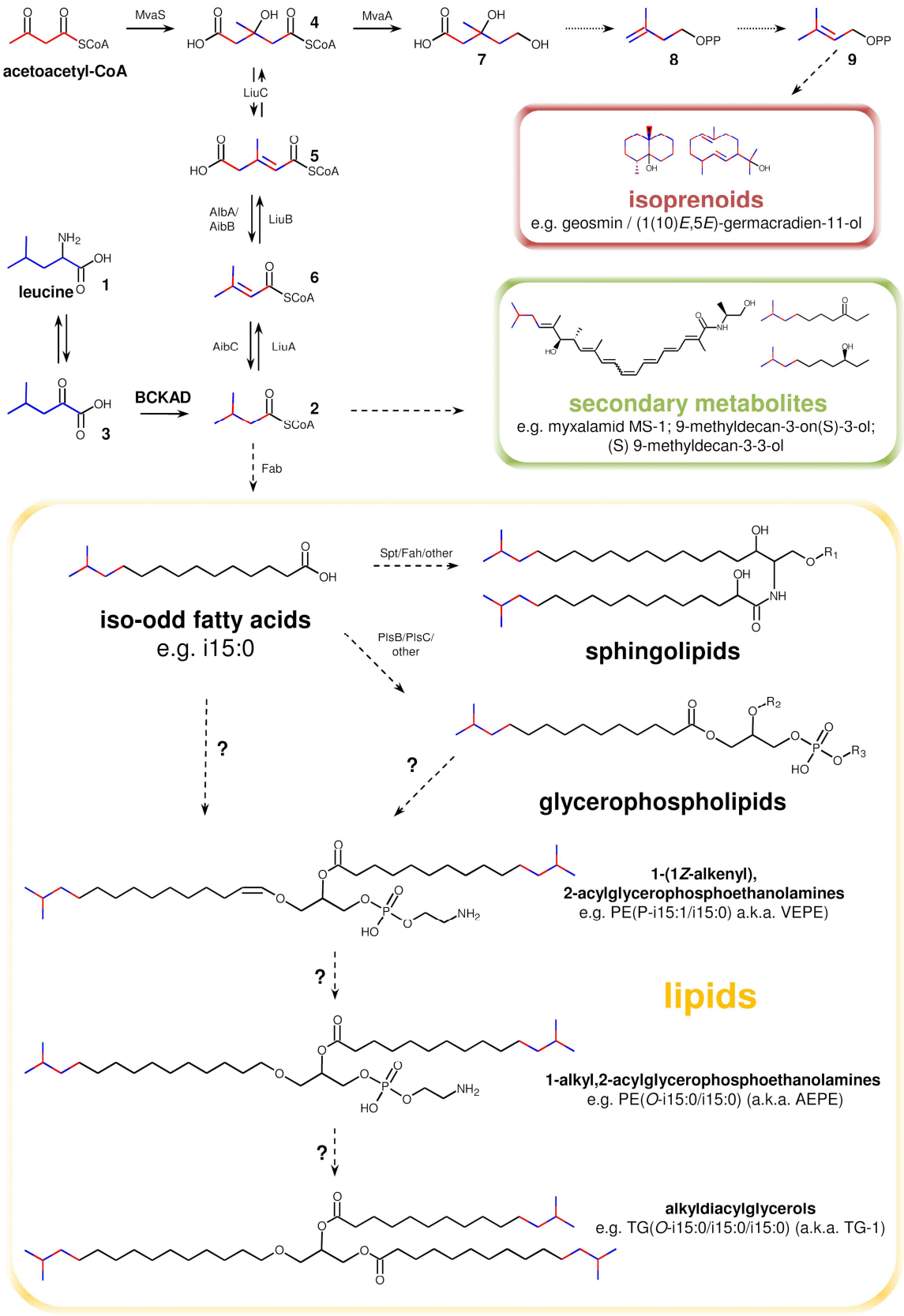

mevalonate pathway derived carbon

BkD pathway derived carbon

carbon derived from either pathway

Figure 1.4 | The molecular meaning of the E-signal: an all-encompassing unity

The complete metabolic link between isoprenoids (red), some secondary metabolites (green) and lipids (yellow) established by the mevalonate-dependent alternative pathway to isovaleryl-CoA, which can partly substitute for BCKAD activity on the one hand, but also provides a source for isoprenoid precursors on the other hand in *M. xanthus*. Proteins involved in reactions are indicated above arrows. Dashed arrows denote multiple enzymatic reaction steps. Dotted arrows indicate enzymatic conversions for those no gene product has been assigned to yet. See text for further details. Scheme was created by the information given in references quoted in **Chapters 1.3.8-10** and references [115,116]. MvaS: 3-HMG-CoA Synthase; MvaA: 3-HMG-CoA reductase; BCKAD: branched-chain-2-oxo-acid dehydrogenase; LiuA-C: leucine utilization enzymes; AibA-C: alternative IV-CoA biosynthetic enzymes; Fab: fatty acid biosynthesis; Spt: serine palmitoyl-CoA transferase; Fah: fatty acid hydroxylase; PlsC: 1-acylglycerol-3-phosphate O-acyltransferase; PlsB: glycerol-3-phosphate O-acyltransferase.

1.4 Aims of this work

Plenty of effort was invested in the description and investigation of the basis of cell-cell communication necessary for the process of fruiting body formation in *M. xanthus* (see **Chapter 1.3**). Most findings are related to genes, fewer on proteins and hardly any to small molecules involved in this process, with the pheromone stigmolone[80,81] produced by *Stigmatella aurantiaca* being the only molecule with a proven signaling function. The DKxanthenes produced by *M. xanthus* are essential for sporulation, but for which reasons remains elusive[123]. The work done on the shunt pathway between isovalerate and mevalonate (**Chapter 1.3.9**) as well as the discovery of the iso-branched ether lipids that are somehow involved in the process of fruiting body formation and sporulation of *M. xanthus* (**Chapter 1.3.10**) provided excellent starting points for the discovery of further elements in the fascinating spectacle of fruiting body formation and disclosed continuative research questions. Mutants with an isoprenoid biosynthesis being separated from amino acid utilization have become available[38]. Those mutants could be used to elucidate the extent of the participation of isoprenoids and branched-chain compounds in fruiting body formation. Furthermore, the urgent question arose how *M. xanthus* synthesizes the ether lipids as only the well-studied mammalian pathway was known. Once biosynthetic genes are found, one can also call on respective mutants to study the ether lipids relevance for the developmental process.

Additionally, the discovery of the ether lipids and the already known highly complex fatty acid pattern[115] of the myxobacteria necessitated the development of new methods to further explore and display the pattern of the complex lipids as a whole. With a method in hands to track individual lipid molecular species, a researcher can further explore how myxobacteria adapt their lipid composition during the different stages of cell differentiation and may lead

to the identification of lipid signaling molecules and/or biomarkers for fruiting body formation.

In the end, one central question is floating around over investigations associated with *bkd* derived compounds: What exactly is the “E-signal”? A particular small molecule, like a hormone or pheromone? A more or less structural coherent group of small molecules? Or is the “E-signal phenotype” after all the result of a less specific multifactorial disorder, caused by the drastic changes in the metabolism of a *bkd* mutant? The herein presented research results are intended to contribute to this basic question as part of the general effort to understand how myxobacteria manage their developmental cell differentiation, a process unparalleled in the kingdom of prokaryotes.

2 Manuscripts and publications

2.1 Publication: "Isoprenoids Are Essential for Fruiting Body Formation in *Myxococcus xanthus*"

Authors: Wolfram Lorenzen[1,2], Michael W. Ring[2], Gertrud Schwär[2] and Helge B. Bode[1,2]

[1]Molekulare Biotechnologie, Institut für Molekulare Biowissenschaften, Goethe Universität Frankfurt, 64038 Frankfurt am Main, Germany

[2]Pharmazeutische Biotechnologie, Universität des Saarlandes, 66123 Saarbrücken, Germany

Published in: Journal of Bacteriology, 15 September 2009, Volume 191, Number 18, page 5849-5853

Digital Object Identifier: 10.1128/JB.00539-09

For full article and declaration on the contribution of the authors see **Chapter 6.1**

2.2 Publication: “A multifunctional enzyme is involved in a novel bacterial ether lipid biosynthesis pathway”

Authors: Wolfram Lorenzen, Tilman Ahrendt, Kenan A J Bozhüyük & Helge B Bode

Merck-Stiftungsprofessur für Molekulare Biotechnologie, Fachbereich Biowissenschaften, Johann Wolfgang Goethe-Universität Frankfurt, Frankfurt, Germany

Published in: nature chemical biology, 11 Mai 2014, Volume 10, page 425-427

Digital Object Identifier: 10.1038/nchembio.1526

For full article and declaration on the contribution of the authors see **Chapter 6.2**.

2.3 Manuscript: "A comprehensive insight into the lipid composition of *Myxococcus xanthus* by UPLC ESI-MS"

Authors: Wolfram Lorenzen*, Kenan A. J. Bozhüyük*, Niña S. Cortina†, Helge B. Bode*

*Merck Stiftungsprofessur für Molekulare Biotechnologie, Fachbereich Biowissenschaften, Johann Wolfgang Goethe-Universität Frankfurt, Max-von-Laue Str. 9, D-60438 Frankfurt am Main, Germany

†Cluster of Excellence Macromolecular Complexes, Johann Wolfgang Goethe-Universität Frankfurt, Campus Riedberg, Buchmann Insitute for Molecular Life Sciences, Max-von-Laue-Str. 15, D-60438 Frankfurt am Main, Germany

Submitted in: The Journal of Lipid Research, 7 March 2014

Status: in revision

For full article and declaration on the contribution of the authors see **Chapter 6.3**.

3 Discussion

3.1 Isoprenoids in fruiting body formation and sporulation: how much isoprenoid is in the E-signal?

As described in **Chapter 1.3.9**, the mevalonate-dependent IV-CoA biosynthetic pathway provides a link between isoprenoid formation and that of iso-branched fatty acid derived compounds so that the majority of *bkd* associated developmental defects may be associated with either compound class. For example, the biosynthesis of isopentenyl pyrophosphate (IPP, **Figure 1.4**, **8**) and dimethylallyldiphosphate (DMAPP, **Figure 1.4**, **9**) from acetate units starting with acetoacetyl-CoA via 3-HMG-CoA (**Figure 1.4**, **4**) may be insufficient under starvation conditions. This can result in a depletion of IPP derived primary metabolites, like quinones from the respiratory chain or bactoprenols for cell wall biosynthesis. This unspecific effect would disagree with the signaling-deficiency hypothesis (**Chapter 1.3.8**).

Reinvestigation of several readily available mutants[38,55] provided an answer to the question how much "isoprenoid is in the E-signal". Especially the results from mutants HB002 (*Δbkd, liuC*) and HB015 (*Δbkd, MXAN_4265 (aibB)*) that successfully uncouple IPP from iso-branched fatty acid biosynthesis are of great importance. As evident by **Figure 3** from **Chapter 6.1**, the addition of excess the IPP biosynthesis complementing mevalonolactone to these mutants is able to partially complement the developmental phenotype with respect to timing and appearance of fruiting bodies without increasing the relative amount of i15:0 fatty acids. This was used as a proxy for IV-CoA supply. Interestingly, genetic complementation by addition of an extra copy of the mevalonate synthase *mvaS* (HB019 and HB020) proved to be more efficient in all tested cases. Under these circumstances, a *bkd* mutant is now able to produce almost wild type levels of i15:0 (HB019) so that one can conclude that the upregulation of the *mvaS* expression in a *bkd* mutant (see **Figure 2 B** from **Chapter 6.1**) seems to be insufficient to compensate for the loss of leucine utilization, whereas the conversion of 3-HMG-CoA to IV-CoA is not a limiting factor. In summary, an adequate level of isoprenoids is essential and sufficient to achieve fruiting body formation with or without wild type levels of iso-branched compounds.

After all, this perspective neglects one decisive parameter: the number of viable spores. A mutant may form fruiting bodies much alike the wild type, but still be incompetent in the formation of heat and sonication resistant spores that germinate when subjected to a

permissive temperature and nutrient levels. This has been shown for a mutant impaired in the biosynthesis of DKxanthenes for example[40]. However, Ring *et al.*, though with other intentions, already addressed this question by determining the relative number of viable spores of the *Δbkd, mvaS* (DK5624) double mutant in the presence of mevalonolactone and, amongst others, the neutral lipid tripalmitin (TG(16:0/16:0/16:0))[119]. Decomposition of this lipid only provides acetyl-CoA in the end, so that it is no use for the isoprenoid formation in *M. xanthus* via the IV-CoA dependent IPP formation (**Figure 1.4**). As expected, DK5624 produced only few (0.04%) spores and had a stronger phenotype than in **Figure 3** (**Chapter 6.1**) as less mevalonolactone was used for complementation. Astonishingly, addition of tripalmitin restored the phenotype of DK5624[119] and increased the level of spores to 1% wild type level similar to the *mvaS* complementation in strain HB019/020. Those observations taken together may suggest that there is another *mvaS* independent, still undiscovered, pathway to IPP in *M. xanthus*. Nevertheless, a sufficient isoprenoid level does not allow wild-type level of viable spores. Consequently, it is likely that a compound with an iso-branched moiety is required for spore formation at some point of the process.

3.2 Isobranched ether lipids and E-signaling: are they the missing signal?

Isovalerate and the fatty acid i15:0 derived thereof reconstitutes sporulation in DK5624 more effectively than any other tested compound. Their addition in excess to starvation media results in 40% and 30% spore formation relative to the wild type respectively. Synthetic TG-1 (TG(*O*-i5:0/i15:0/i15:0), see **Figure 1.4**) restores 25% of the spore formation in the same mutant[119]. Additionally, the cells seem to be attracted by this lipid as fruiting body formation preferentially took place around droplets of TG-1, phenomena that were absent when tripalmitin was used. These findings were recently confirmed in more detailed experiments, for which the dose-dependent ability of i15:0, TG-1, 16:0 and TG(i15:0/i15:0/i15:0) (the latter two served as controls) to restore the sporulation efficiency of a *Δbkd, MXAN_4265 (aibB)* mutant (LS1191) was established[124]. Both i15:0 and TG-1 rescued LS1191 in physiological concentrations, meaning that 1/3 of the molar amount of i15:0 and twice the amount of TG-1 compared to wild-type levels had 50% of maximum rescue capacity, whereas the other two lipids failed to do so. Again, i15:0 was more effective than TG-1, yet TG-1 stimulated the expression of the heretofore unknown developmental marker *MXAN_2146*. Is then i15:0 the true precursor of the E-signal and not

the alkylglycerol TG-1? This conclusion seems natural, but the occurrence of TG-1 has to be discussed together with the appearance of lipid bodies in *M. xanthus* over the course of the developmental program.

When subjected to stress, to be more precise, antibiotics, anoxic conditions or nutrient deprivation, the cells start to form lipid bodies beginning from the cell poles[120]. Their size ranges from 50-500 nm in diameter and consist of glycerolipids including monoalkydiacyl- and alkylmonoacylglycerols and are surrounded by a monolayer of glycerophospholipids, mainly VEPE (PE(P-i15:0/i15:0) and AEPE (PE(*O*-i15:0/i15:0). The severer the stress, the more pronounced is lipid body formation. More importantly, these lipid bodies are only formed by cells that either undergo programmed cell death or sporulation and not by cells that become peripheral rods during the course of starvation induced fruiting body formation. In wild type cells, maximum lipid body production is observable at 24 h after initiation of the developmental program[120]. The most abundant lipids are alkylglycerolipids with TG-1 as the principal component. With ongoing transformation to resistant spores, lipid bodies disappear and quantities of glycerolipids resume wild type levels. In spite of this, methanolyzed spores retain high levels of *O*-i15:0-glycerol[119].

Certain mutants (e.g. DK5608 (*csgA (MXAN_1294)*) or DK5624 (*Δbkd, mvaS*), which neither fruit nor sporulate, do not form lipid bodies and they produce only small amounts of glycerolipids[120]. The same is true for peripheral rods which seem to have lost the ability to perform fruiting body formation and sporulation. Additionally, mutants *asgA (MXAN_2670), csgA (MXAN_1294), fruA (MXAN_3117)* accumulate vinyl ether lipids, but there are only small amounts of alkylglycerol lipids suggesting a link between alkyldiacylglycerols and triacylglycerol formation[119]. But are these observations only symptoms or the actual cause of a defect in E-signaling, as *asg* and *csg* mutants reveal the same symptoms?

At this point, the findings presented in **Chapter 6.2** come into play. **SI Table 4** in **Chapter 6.2.5** shows triradylglycerol levels of starved *elbD (MXAN_1528)* mutant cells. As expected, they are on a low level in both cases in vegetative cells and strongly accumulate after 24 h of nutrient downshift in the wild type. In contrast to this, the *elbD* mutant shows a rather selective loss in alkylglycerol formation with a similar increase in all other glycerolipid species, which suggests the formation of lipid bodies without the formation of alkylglycerols and no impact on the overall relative amount of iso-branched fatty acids (**SI**

Table 3, **Chapter 6.2.5**). Contrary to the LS1191/HB015 mutants, all molecular species from any biosynthetic pathways, including the IV-CoA dependent isoprenoid formation but except those derived from alkylglycerols, are available at wild type levels. Considering the phenotype of *elbD* (**SI Figure 1**, **Chapter 6.2.5**), the early developmental events like aggregation and mound formation are delayed and viable spores are not detectable, whereas the overall fruiting body formation is similar to the wild type. In a situation where *elbD* is genetically complemented with *elbD* under the control of a constitutive promoter, alkylglycerol levels as well as the developmental phenotype are restored with an improved, but still strongly disturbed, differentiation into viable spores. A mutant with the same constitutive expression of *elbD* in a wild type background (*elbD*$^{+}$) yielded a similar phenotype with the expected higher levels of alkylglycerols (**SI Figure 1**, **Chapter 6.2.5**).

This line of evidence strongly suggests that the iso-branched ether lipids are an important component of the E-signal. They need to be formed chronologically in sufficient amounts in order to ensure timed aggregation as well as formation of viable spores. But why is i15:0 such a good remedy for mutants LS1191 and DK5624, even better than TG-1? In the light of the data from **Chapter 6.1**, it seems that one investigates two parameters at a time when i15:0 is used to complement a *bkd*, *bkd/mvaS* or *bkd/MXAN_4265 (aibB)* mutant. In all cases, formation of iso-branched compounds is more (*bkd/mvaS*, *bkd/MXAN_4265 (aibB)*) or less (*bkd)* severely hampered. At the same time IPP biosynthesis from IV-CoA is only reduced in a way that IV-CoA cannot be acquired from leucine (all mutants) or leucine and 3-HMG-CoA (*bkd/mvaS* , *bkd/MXAN_4265 (aibB)* mutants). However, IVA and DMAA, intermediates in the mevalonate-dependent IVA biosynthesis, can both be effectively utilized for isoprenoid biosynthesis as shown for geosmin[109]. The same is easily imaginable for i15:0 as its final β-oxidation product is IVA, which would mean that i15:0 does not only substitute for iso-branched lipids but also for insufficient isoprenoid biosynthesis. The developmental phenotype of HB020 (**Figure 3**, **Chapter 6.1**) suggests that a restoration of the *bkd* phenotype is possible on a macroscopic level, solely by providing more 3-HMG-CoA for isoprenoid biosynthesis. Unfortunately, no microscopic images from 6-24 h of starvation induced fruiting body formation are available, so that a comparison of strain HB020 with the *elbD* mutant is not possible for this time frame and it has never been shown directly that iso-odd fatty acids are precursors for terpenoids in *M. xanthus* so that the final evidence for this hypothesis is missing. At least, extensive β-

oxidation of externally fed [$^2H_7$]i15:0 is proven for *bkd* mutants of *Stigmatella aurantiaca* under vegetative conditions[125] so that this hypothesis is not far-fetched at all.

In conclusion, the presented data shows that a sufficient IPP supply for isoprenoid biosynthesis is important for fruiting body formation and the timely defined biosynthesis of iso-branched alkylglycerols in some, yet to be determined form, yields important signaling molecules that orchestrate the proper differentiation into viable, heat and sonication resistant spores. In order to unveil the true nature of the morphogenic iso-branched ether lipid molecule(s) the author suggests to check first if externally fed MG(*O*-15:0/0:0/0:0) is able to complement the phenotype of *elbD* and, a *bkd, liuC* double mutant, in a dose dependent manner. Utilization of this molecule ensures that no additional i15:0 fatty acid is present and the bioavailability should be improved compared to TG-1 due to the amphiphilic nature of this molecule. If this molecule proves to be active, feeding a chemically labeled analog of this molecule (may it be deuterated, radiolabeled or azido/alkyne labeled to allow click chemistry) during the course of development and cell differentiation along with appropriate analytics will auspiciously lead to the molecules which are so crucial for sporulation.

No matter how the actual E-signal molecule looks like: lipids are no molecules that can easily diffuse between cells through an aqueous environment and penetrate membranes of due to their poor water solubility and unfavorable partition coefficient[126]. Apart from the exact nature of the E-signal molecule(s), the way they are transferred from on cell to the other should be a subject for further research. An investigation of the proteome of outer membrane vesicles shed from vegetatively growing and starved *M. xanthus* cells led to the astonishing result that E1 subunit BCKAD proteins are transported within these vesicles[127] so that cells are probably able to deliver the enzyme activity necessary for E-signal formation or a lipophilic small molecule representing the E-signal. The same study also found a FadL homologue MXAN_7040 (putatively responsible for fatty acid uptake) and at least one putative lipase (MXAN_0220) so that it seems not unlikely that the complementation activity of TG-1 towards *bkd* mutants might be mediated by the i15:0 fatty acids after their hydrolytic release from the glycerol backbone. As a peculiar feature of motile *M. xanthus* cells, it was discovered that they are able to transfer lipids and proteins of their outer membrane upon direct contact on a solid surface as it was demonstrated for the motility proteins Tgl, CglB[128] as well as for fluorescent proteins directed to the outer membrane[129] and lipophilic dyes[130]. This kind of contact dependent

intercellular signaling is an easily conceivable way to transfer a lipophilic signaling molecule. Testing the concentration dependent ability of purified subcellular fractions of wild type cells for complementation activity on *bkd* mutants should demonstrate if there is a distinct spatial distribution of the E-signal.

3.3 The biosynthesis of vinyl ether lipids by the action of ElbD: a proposal for a new biosynthetic pathway.

Extensive characterization of *elb* gene mutants with regard to fruiting body formation, sporulation, fatty acid and lipid profile demonstrated the pivotal role of the multidomain enzyme ElbD in ether lipid formation (**Chapter 6.2**). In addition to this, *in-vitro* and *in-silico* experiments on ElbD suggested the activities of the respective domains. By summarizing all the presented data, the author proposes a biochemical route as a working model of how this enzyme achieves the stepwise formation of an ether bond (**Figure 3.1 a**). It has to be emphasized that this working model is very likely incomplete in terms of missing *in-vitro* data of the acyltransferase and reductase domains activities. Nevertheless, the stepwise ether bond formation may occur like this:

The fatty acyl-CoA ligase activates a free isopentadecanoic acid via adenylation and transfer onto a phosphopantethein moiety attached to the T domain as it was shown *in-vitro* (see **SI Figure 6**, **Chapter 6.2.5 a** and **b**). Then the activated fatty acid is reduced to yield an aldehyde intermediate and then transferred to the 2-isopentadecanoyl-*sn*-glycero-3-phosphoethanolamine (PE(0:0/i15:0)) to yield a hemiacetal intermediate to be dehydrated to a vinyl ether probably by the action of ElbE (**Figure 3.1 a**, pathway **A**) afterwards. However, observed aldehyde formation could also exclusively derive from hemiacetal decomposition, so that it is also conceivable that the activated fatty acid is first transferred on PE(0:0/i15:0) and the resulting ester bond is subsequently reduced in an unusual reaction to a hemiacetal intermediate, which is later dehydrated (**Figure 3.1 a,** pathway **B**). The proposed involvement of PE(0:0/i15:0) is consistent with our *in-silico* data of the acylglycerol acyltransferase domain and the observed accumulation of PE(0:0/i15:0) in the *elbD* mutant (see **SI Table 6**, **Chapter 6.2.5**). The final product of this proposed pathway, VEPE (PE(*O*-i15:0/i15:0), see **Figure 1.4**), accumulates during starvation induced fruiting body formation[119]. Further reactions by yet-to-be determined enzymes comprise hydrogenation of the Δ^1 double bond, hydrolysis of the 1-alkyl,2-acylglycerophosphoethanolamine head group (by a phospholipase C) and acylation of the free *sn*-3 hydroxyl group of the alkylacylglycerol (via a diacylglycerol *O*-acyltransferase)

with an activated isopentadecanoic acid to yield TG-1 or isoheptanoic acid to form its derivative TG(*O*-i15:0/i15:0/i17:0), which both accumulate in the aforementioned lipid bodies[120].

To date, there are no experimentally confirmed examples for neither the reduction and dehydration of an ester bond nor the transfer of a fatty aldehyde. Acetal formation is well known from starch biosynthesis elicited by the starch synthase (EC 2.4.1.21), but this reaction requires activation of the glucose with ATP so that there is no need to stabilize a hemiacetal intermediate[131].

Nevertheless, there is one important, well-described example of 1-(1*Z*-alkenyl),2-acylglycerophosphoethanolamines formation with inextricability of acetal formation in literature: metabolic pulse and pulse-chase labeling studies with [^{32}P] orthophosphate on *Clostridium butyricum*, whose membranes are also made of substantial amounts of 1-(1*Z*-alkenyl),2-acylglycerophosphoethanolamines, showed that these bacteria form first diacylglycerophosphoethanolamines, then unusual glycerol acetals of glycerophosphoethanolamines, then 1-(1*Z*-alkenyl),2-acylglycerophosphoethanolamines, which can be finally converted into the complex glycerophosphoethanolamine acetals of 1-(1*Z*-alkenyl),2-acylglycerophosphoethanolamines (**Figure 3.1 b**[132,135,136]).

Figure 3.1 | Formation of 1-(1*Z*-alkenyl),2-acylglycerophosphoethanolamines

a: Proposed ElbD mediated ether lipid biosynthesis in *M. xanthus* and other myxobacteria as deduced from experimental data presented in **Chapter 6.2**. For details see text. **b**: Order of [^{32}P] orthophosphate incorporation in glycerophosphoethanolamine species of *Clostridium butyricum*[132] (**A**) and proposed biosynthesis of 1-(1*Z*-alkenyl),2-acylglycerophosphoethanolamines species for *C. novyi*[133] (**B**). Note the formation of diacylglycerol species before 1-(1*Z*-alkenyl),2-acylglycerophosphoethanolamines are formed. 1-alkyl,2-acylglycerophosphoethanolamines are absent in *Clostridia.* **c**: Ether bond formation as determined for humans and other mammals[134]. The ether bond is formed before the polar headgroup is introduced. Vinyl ether bond formation is the last step. Enzymes in pathway **c**): **A**: glycerone-phosphate O-acyltransferase (EC 2.3.1.42); **B**: alkylglycerone-phosphate synthase (EC 2.5.1.26); **C**: acylglycerone-phosphate reductase (EC 1.1.1.101); **D**:alkylglycerolphosphate 2-O-acyltransferase ((EC 2.3.1.-); **E**: phosphatidate phosphatase (EC 3.1.3.4); **F**: ethanolamine-phosphotransferase (EC 2.7.8.1); F: ethanolamine-phosphotransferase (EC 2.7.8.1); **G**: plasmanylethanolamine desaturase (EC 1.14.99.19); Abbreviations: P: phosphate; CoA: coenzyme A; CDP-Etn: cytidin diphosphate ethanolamine; CMP: cytidin monophosphate; X: uncharacterized hydrogen donor; PE: phosphatidylethanolamine; Re: acyl-CoA(ACP)-like reductase; A: fatty acyl-CoA (ACP) synthetase; T: acyl carrier protein /thiolation domain; AT: acylglyceronephosphate acyltransferase. Dashed arrows indicate multiple reaction steps.

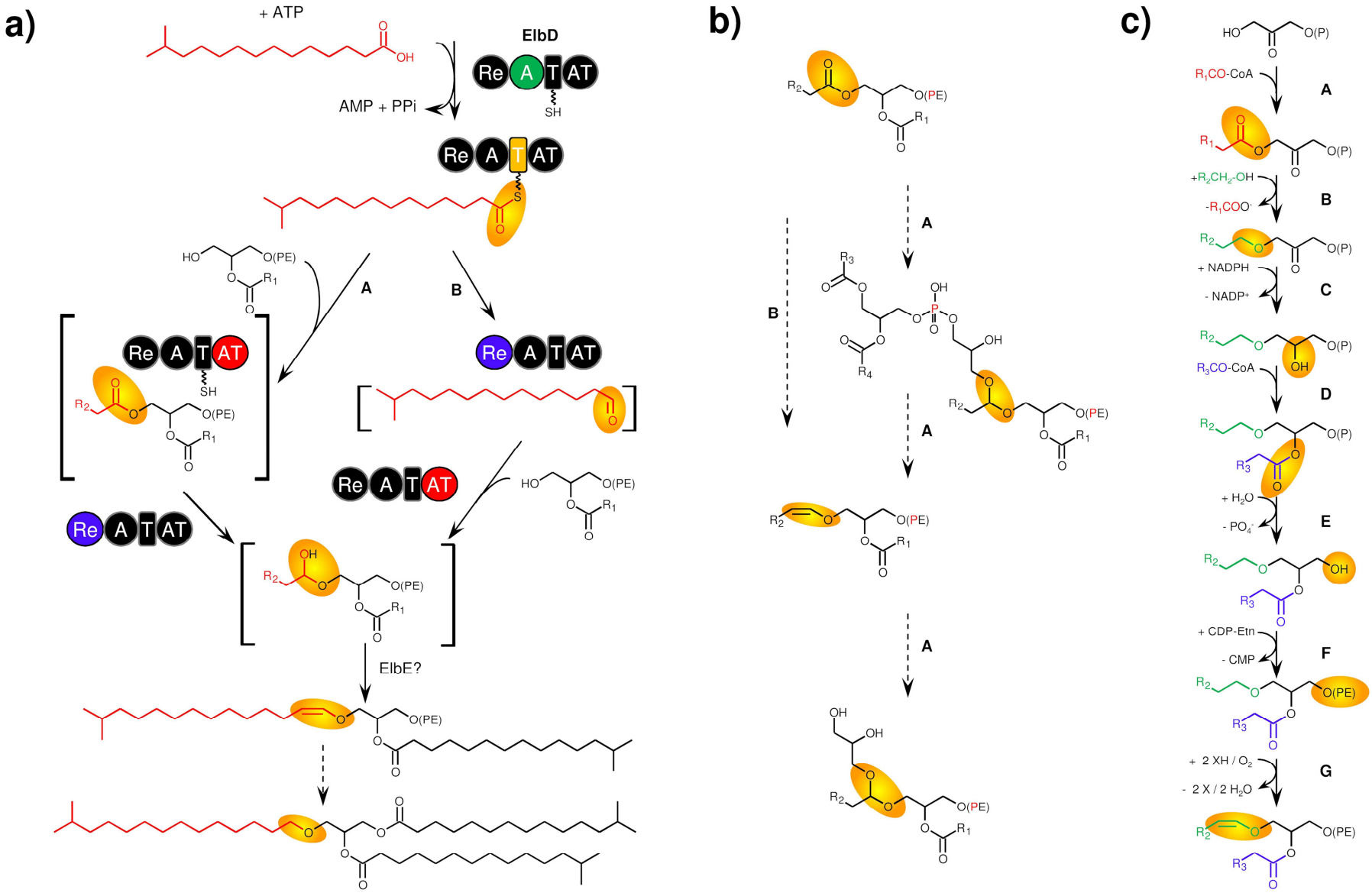
a)
+ ATP
AMP + PPi
ElbD
Re A T AT
SH
HO
O(PE)
R1
A
B
R2
ElbE?
b)
R3
R4
OH
P
c)
HO
O(P)
R1CO-CoA
+R2CH2-OH
-R1COO-
+ NADPH
- NADP+
R3CO-CoA
+ H2O
- PO4-
+ CDP-Etn
- CMP
+ 2 XH / O2
- 2 X / 2 H2O
C
D
E
F
G

These results were later confirmed for *Clostridium novyi* NT[137] and *Clostridium tetani*[133] strains, whereas they do not form glycerol acetals, but also exhibit a high proportion of 1-(1*Z*-alkenyl),2-acylglycerophosphoethanolamines. Additionally, 1-enyl chains were barely detectable in precursor lipids like glycerophosphates, CDP-diacylglycerols and glycerophosphoserines, thus further strengthening the hypothesis of a glycerophosphoethanolamine being formed before the introduction of the vinyl ether bond. Glycerol acetals were not found in *M. xanthus* during the study presented in **Chapter 6.3**, but they might be present in vanishingly small traces. There are no clear homologues of *elbD* or its single domains present in sequenced *Clostridium* genomes, but both a fatty-acyl CoA reductase activity yielding aldehydes as well as the formation of plasmalogens by incorporating exogenously added fatty aldehydes were demonstrated for *C. butyricum*[138-140]. These observations contrast with the well-studied mammalian ether lipid biosynthetic pathway[134] (**Figure 3.1 c**). Here, alkyl ether bond formation occurs via a substitution of an esterified fatty acid with a fatty alcohol (**Figure 3.1 c**, step **B**). The dehydrogenation reaction to yield a vinyl ether bond takes place in the last step of 1-(1*Z*-alkenyl),2-acylglycerophosphoethanolamines formation (**Figure 3.1 c**, step **G**).

The intensive and unsuccessful efforts spent on obtaining fully active, heterologously expressed ElbD (see online methods, **Chapter 6.1**) *in-vitro* and *in-vivo* promise a complex and exciting biochemistry behind ether bond formation. Even $ElbD_{DW}$, which is the ElbD homologue from *Stigmatella aurantiaca*, failed to be active when expressed in *M. xanthus* (**SI Figure 1 a** and **b**, **Chapter 6.2.5**) despite its high level of sequence identity (**SI Data Set 2, Chapter 6.2.5**). The direct overexpression of tagged ElbD in *M. xanthus* cells will be a potentially more promising method to achieve fully active ElbD than the use of other bacteria as heterologous host. Additionally, this will also conceivably offer means for the discovery of additional enzymes required for the underlying biochemistry. Only during starvation induced fruiting body formation, there is a strong increase in ether lipid formation in $elbD^{-}/elbD^{+}$ mutants, although the complementing gene is under control of a constitutive promoter (**SI Figure 1 b**, **Chapter 6.2.5**), which argues for other developmentally controlled genes being involved in ether lipid formation. The purification of homologously expressed ElbD under carefully controlled conditions potentially results in the co-purification of additional biosynthetic enzymes, which should be identifiable by means of peptide mass fingerprinting[141]. Such an approach was already successfully

utilized during the investigation of A-motility. It enabled researchers to unveil the interplay of several A-motility proteins[64,66](see **Chapter 1.2.3**).

3.4 Known biological functions of alkyl ether lipids and their putative roles in *M. xanthus*.

The data presented in **Chapter 6.2** and those from previous investigations on myxobacterial ether lipids[119,124] strongly suggest signaling functions elicited by an alkylglycerol containing lipid or some other molecule derived thereof. The observation that i15:0 is an even better agent to complement the E-Signal deficient *bkd, bkd/mvaS* or *bkd/MXAN_4265 (aibB)* mutant is explainable as it acts as both a precursor of the isoprenoids and iso-branched ether lipids (see **Chapter 3.2**). But what do these molecules possibly look like and what could be their molecular target? Two signaling functions of ether lipids are known from higher organisms: The pro-inflammatory activity of the platelet-activating factor (PAF, 1-*O*-hexadecyl-2-acetyl-sn-glycero-3-phophocholine) and the protein kinase C (PKC) activity modulating alkylacylglycerols.

PAF is produced by numerous cells of the human body that are associated with immune defense and hemostasis such as macrophages, monocytes, neutrophils, platelets, and endothelial cells. Its release mediates a number of pro-inflammatory effects like increase in vascular permeability, degranulation, release of cytokines and platelet activation[142]. Numerous other physiological and developmental processes including neuronal activity, spermatogenesis and embryo development also involve PAF. Its activity is transduced into target cells by its own G-protein coupled receptor[143] and the signal is further propagated by release of the second messengers inositol-1,4,5,-trisphosphate (IP_3) that usually derive from the phospholipase C mediated hydrolysis of glycerophosphoinositol-4,5-trisphosphate (PIP_2)[144]. The activation of several protein kinases typically involved in signal transduction (e.g. protein kinase C (PKC) and A (PKA) as well as mitogen activated protein kinase (MAPK)) were also found to be part of PAF signaling pathways[142]. Astonishingly, this provides a link to the activity of 1-alkyl,2-acylglycerols. As mentioned before, they affect the activity of protein kinases *in-vitro.* PKCs that are overactivated due to a mutation or the activity of the strongly agonistically acting phorbol esters are involved in tumorigenesis[145]. Contrary to this, alkylacylglycerols can inhibit the activity of PKCs as well as growth of certain tumorous cell lines *in-vitro*[146,147], and when supplemented in human dietary, they were shown to increase the survival of cancer patients or reduce the extent of side effects by radiation treatment[148,149]. It should not go unmentioned that the activity of

alkylmonoacylglycerols depends on the isoforms of PKCs. For example PKC β is stimulated by ether linked diglycerides but PKC isoforms δ and ε show significant inhibition *in-vitro*[150]. PKCs belong to the serine-threonine kinase family proteins (EC 2.7.11.-). As mentioned in **Chapter 1.1.2**, there is a striking number of serine-threonine kinases encoded in the genome of *M. xanthus,* but they are essentially uncharacterized so that one can only speculate about their involvement in alkylglycerol mediated signaling in myxobacteria[27].

Yet, a signaling role cannot solely explain the strikingly high amounts of alkyldiacylglycerol lipids found in lipid bodies during sporulation. They may simply be a special kind of temporary carbon storage similar to the triacylglycerols in adipocytes. At the same time, alkylglycerols are possibly covalently incorporated into the spore coat: Firstly, alkylglycerols in the form of i15:0-*O*-alkylglycerol bisTMS make up a high proportion of methanolyzed spore material as determined by GC-MS[119]. Secondly, during spore differentiation the spore coat thickens while the lipid bodies diminish[120]. However, further evidence for this hypothesis is missing as the exact composition of the myxobacteria spore coat is hardly established[151,152].

3.5 Plasmalogens: putative functions in an unusual host

Fatty acid derived vinyl ether lipids show a highly remarkable distribution among the tree of life. They are highly abundant in strictly anaerobically living organisms (e.g. bacteria comprising genera *Clostridia*, *Megasphaera*, *Vellonella,* and protozoa comprising *Isotricha* and *Dasytricha*; they are virtually absent in aerobically and facultatively anaerobic bacteria, plants and fungi and again common among all vertebrates including mammals and invertebrates[153,154]. Thus, the usually strictly aerobically (with the exception of *Anaeromyxobacter*[20] species) living myxobacteria are a remarkable exception. Membranes inhering plasmalogens show a number of physicochemical differences compared with those exclusively made up of diacylglycerophospholipids. With respect to their thermal phase behavior, lipids exclusively containing alk-(1Z)-enyl residues attached to the *sn*-1 position of the glycerol backbone show a slightly smaller (4-6 °C) transition temperature from the ordered gel phase to the liquid crystalline phase and a strongly (~38 °C) reduced transition temperature from the liquid crystalline to the non-lamellar reversed hexagonal phase[150,155,156]. These changes cause an increased permeability for ions (as shown for K^+ ions[157]) and promote their ability to fuse with other membranes[158]. These

properties may explain their high abundance in conductive tissue (e.g. myelin sheath) or synaptosomal membranes in which vesicular fusion events occur with high frequency[159]. In addition to this, the high susceptibility of the vinyl-ether bond to oxidation by reactive oxygen species (ROS) seems to serve as part of a general protection mechanism of cells against those harmful oxidants. Cells defective in the peroxisomal ether lipid biosynthesis are more susceptible to ROS and regain wild type susceptibility when plasmalogen levels are replenished by addition of alkylglycerols that serve as precursors for plasmalogens biosynthesis[160].

Both the change in membrane behavior and the antioxidative properties are beneficial for myxobacteria during sporulation and may explain their increased formation. Rod-shaped vegetative cells have to be reshaped to spherical spores thus increasing the overall curvature of the membranes. The outer membrane sloughs off in favor of the mounting spore coat by outer membrane transfer[127,128] whereat the lipid bodies bud at the inner membrane[120,124] at the same time so that there is a need of greater membrane flexibility. It is unknown if oxidative stress increases during sporulation, but an alleged role of myxobacterial plasmalogens in protection against ROS similar to those evident from mammalian cells does not seem devious. Here again, an in-depth analysis of the lipidome, lipid body formation and cell differentiation of mutant cells compared to that of wild type cells during the course of fruiting body formation and sporulation, particularly with respect to metabolic intermediates, can help identify additional roles of these peculiar lipids.

3.6 A new UPLC-MS based lipidomics analysis: a perspective for the investigation of lipid biosynthesis in myxobacteria as well as molecules that orchestrate development and differentiation

There are only few reports in the literature on lipid composition in myxobacteria[116,117,161,118], only one on biosynthesis of polar lipids[116] and none that displays the individual molecular composition of a myxobacterial lipidome with respect to all expected lipid classes. The method described in **Chapter 6.3** has a number of attractive, favorable features: a standard column chemistry, the use of a fairly simple solvent system and a common buffer system without any further additives plus a sample workup based on the well-known lipid extraction procedure first described by Bligh and Dyer[162]. The resulting data set is suitable for both statistical analysis and sophisticated data display as shown by MathLab plots in **Figures 11-12** (**Chapter 6.3**). The sensitivity and specificity of this method can be further extended by increasing the bed length of the column or the

use of a high resolution mass spectrometer. An increase in accuracy concerning the relative abundance of lipid molecular species is achieved by the additional use of appropriate internal standards, and absolute quantification of individual molecules is imaginable as long as the respective genuine standards are available. Though we could not establish an example, this method can be used to read out *in-vitro* assays for enzymes involved in lipid biosynthesis without the, still very common[137,163-165], use of radioactively labeled substrates as many conceivable lipid substrates, intermediates or final products are detectable with respect to abundance and molecular composition. Nonetheless, a comparative lipidomics approach will become crucial for the exact assignment of genes potentially involved in complex lipid biosynthesis as a common pitfall in assigning genes to their specific functions in myxobacteria is the presence of paralogous genes and convergent biosynthetic routes. For example, two biosynthetic routes lead to the formation of precursors for branched-chain fatty acids as shown in **Figure 1.4** and there are five different genes encoding 1-acylglycerol-3-phosphate *O*-acyltransferase homologues (EC 2.3.1.51, PlsC1, MXAN_3330; PlsC2, MXAN_3969; PlsC3, MXAN_5578; PlsC4, MXAN_0955; PlsC5, MXAN_0147) present in the genome[116] of *M. xanthus* so that gene inactivation experiments do not necessarily result in an unambiguous loss of a certain metabolite just as shown for ether lipids in **Chapter 6.2**. Statistical analysis of mutant vs. wild type lipidome may unveil the subtle changes that are caused by the inactivation of genes whose functions can be partially complemented by paralogous genes. A comparable, but exclusively qualitative, approach was successfully applied in the attempt to identify novel secondary metabolites from *M. xanthus*, as described in **Chapter 1.1.2**,[39,166] and statistical analysis was applied in **Chapter 6.2** to unambiguously show the involvement of ElbD in ether lipid formation. Based upon their homology[29], candidate proteins that may be involved in lipid biosynthesis are, apart from the aforementioned 1-acylglycerol-3-phosphate *O*-acyltransferase homologues, the putative phosphatidate cytidyltransferase MXAN_2556 (EC 2.7.7.41, CdsA) and phosphatidylserine decarboxylase MXAN_3724 (EC 4.1.1.65, Psd), both probably involved in glycerophosphoethanolamine biosynthesis. Phosphatidylglycerolphosphate synthase MXAN_4626 (EC 2.7.8.5, PgsA) and cardiolipin synthase homolog MXAN_0537 (EC 2.7.8.-, Cls) are candidates for glycerophosphoglycerol and cardiolipin synthesis, respectively and CDP-diacylglycerol-inositol 3-phosphatidyltransferase MXAN_0450 (EC 2.7.8.11), inositol phosphorylceramide synthase MXAN_0451 (EC 2.7.1.-) and *myo*-inositol-1-phosphate

synthase MXAN_0452 (EC 5.5.1.4) may all be responsible for the biosynthesis of the newly discovered ceramide phosphoinositols described in **Chapter 6.3**.

Analogously, it is now possible to determine changes in the lipid composition qualitatively and quantitatively during different stages of growth and development, e.g. at certain time points of starvation induced fruiting body formation so that the remodelling of the membranes can be precisely tracked.

4 Concluding remarks

4.1 The biochemistry of proteins as a future challenge

The introduction of this thesis and the references in particular demonstrate how the ever advancing molecular genetic methods in combination with phenotypic analysis allowed researchers to learn an impressive quantum about the way *M. xanthus* organizes its fascinating lifestyle by utilizing its genomic potential. Nevertheless, in most cases data on the true activity of the identified proteins are lacking. Consequently, many questions remain unanswered: What are the receptors for the A-signal amino acids or for the CsgA proteins, respectively (**Chapter 1.3.4** and **1.3.6**)? What are the substrates of the LonD-like protease that is inactivated in the *bsg* mutants (**Chapter 1.3.5**)? What is the oxidation product from monoacylglycerophosphoethanolamine after oxidation by SocA (**Chapter 1.3.6**)? Finally, an issue that concerns this thesis: what is the mode of action of ElbD (**Chapter 6.2**)? Those questions could be continued ad infinitum. The fundamental issue at hand is that it is by far more laborious, time and resource demanding to find specific substrates and/or interaction partners of particular proteins than to perform certain molecular genetic experiments. Nowadays, whole genomes can be sequenced and annotated with reasonable efforts[167] and a few researchers can easily produce and screen hundreds of mutants yielded by transposon mutagenesis[84] but will hardly be able to screen the same number of protein products for their activity. All the *in-silico* methods known to infer protein functions by sequence comparisons may be sufficient to guide experiments but fail if the moot protein belongs to a previously unknown class or unfolds a different function than expected[168]. Heterologous expression of genes with the intention to acquire soluble, active proteins to test their functions with the appropriate assay is still a subject of trial and error and rather resembles throwing the dice than rational science[169]. The only feasible and rational approach to perform such a task in a large scale is an increased use of automation systems in combination with thorough and rational test designs. Though hardly used in academic laboratory environments, all sorts of laboratory automation systems are already in use for high-throughput applications such as automated cloning[170], protein expression and purification[171,172] as well as protein crystallization[173,174]. Additionally, countless methods to screen for enzyme activity are known[175-178] and there are examples for automated protein production strategies from DNA preparation to protein purification and analysis[179,180] indicating that they are no dreams of the future. It is rather a general

question of resource allocation, division of labor and organizational structures if these technical achievements speed up progress in the quest to decipher protein functions or remain barely used. Such data sets can be used to answer particular questions as well as to provide valid bases for activity predictions. Recently, it was shown that as long as sufficient data on the substrate specificity and the structural constitution of a certain enzyme class is available, mathematical models can be constructed which allow the prediction of the substrate specificity of an unknown protein sequence from the same enzyme class[181]. This approach still has to prove itself, however could mean a real breakthrough in enzymology. A switch from individual, manually performed biochemical efforts to elucidate protein functions to thoroughly planned, automated large-scale endeavors will provide more facile and comprehensive answers on the mechanisms that protein evolve to shape the processes in myxobacterial cells.

4.2 Publications derived from additional projects: gas chromatography coupled to mass spectrometry as a versatile tool to fathom and monitor biological processes

Throughout the whole work, GC-MS was one of the most important tools to monitor changes in the composition of the fatty acid pattern of *M. xanthus* with the vinyl ether derived dimethylacetales and the alkylglycerol derived of i15:0-*O*-alkylglycerol bisTMS being the most important target components to monitor changes in the ether lipid production in the *elb* mutants (see **Chapter 6.2**). However, it should not go unmentioned that my expertise in GC-MS operation and method development was also required for numerous additional projects for which I supported colleagues and cooperation partner in their effort to elucidate different biological and biochemical questions. For a variety of reasons, some of these projects did not result in publications but others did with my humble self being co-author. Here are short summaries of the central subjects of those publications including short descriptions of my contributions. Details on these investigations are available in the original publications.

In "Myxotyrosides A and B, Unusual Rhamnosides from *Myxococcus* sp."[182], Ohlendorf *et al.* describe a novel group of natural products from *Myxococcus* sp. strain 131 named the myxotyrosides A and B. These molecules contain a tyrosine-related core structure, glycosylated with rhamnose at the phenolic hydroxy group and additionally acylated with fatty acids that are unsaturated at the Δ^2 position. My analysis of the fatty acid methyl ester pattern of *Myxococcus* sp. strain 131 provided the information that this strain does not have

these kinds of fatty acids as constitutive components of its cell membranes. This finding indicates that the Δ^2 unsaturated fatty acid moieties in the myxotyrosides are not acquired from primary metabolism but probably formed by the myxotyroside biosynthetic enzymes as discussed in the paper.

In an extensive metabolic engineering project, Brat *et al.* strived after the improvement of isobutanol production in *Saccharomyces cerevisiae* strains by relocalizing the valine biosynthetic genes from the mitochondrial matrix to the cytosol and overexpressing several other genes which protein products are involved in the catabolism of valine[183]. My effort was to establish and routinely carry out a GC-MS based method to analyze isobutanol formation from the headspace of cell culture supernatants including absolute quantification. Hence, the extent of isobutanol formation by fermenting *Saccharomyces* strains was traceable.

In the publication "Determination of the Absolute Configuration of Peptide Natural Products by Using Stable Isotope Labeling and Mass Spectrometry" we demonstrated that structures of peptides synthesized by NRPS can be fully elucidated by combining metabolic feeding experiments with HPLC-MS^n analysis, thus circumventing compound isolation and NMR analysis[184]. In order to determine the absolute configuration of the α-carbons within the peptide backbones, mutants defective in their amino acid transaminase activity were constructed, fed with fully deuterated amino acids and the relevant natural products were analyzed for the loss of label at the α-carbons. A loss of deuterium label indicates D-, a preservation of the label L-configuration. As GC-MS is an excellent tool to analyze amino acids[185], I established a method to determine the extent of the loss of deuterium label from the α-carbons of fully labeled deuterated amino acids in cell free media supernatant at various time points. As a result, we were able to assess the decline of transaminase activity in transaminase mutants.

For the publication "Reciprocal Cross Talk between Fatty Acid and Antibiotic Biosynthesis in a Nematode Symbiont" GC-MS based determination of the fatty acid methyl ester pattern derived from methanolyzed cells was needed again[186]. In this work, we provided evidence that the BCKAD complex from *Xenorhabdus nematophila* HGB081 is involved in both the provision of starter units for branched-chain fatty acids as well as isobutyryl-ACP starting units for the biosynthesis of the natural product pristinamycin II_a. GC-MS analysis confirmed that *E. coli* cells produce branched-chain fatty acids when

expressing genes encoding for the BCKAD complex from *Photorhabdus luminescens TT01*. In *Xenorhabdus nematophila* HGB081 the homologue of the gene encoding the E2 subunit of the BCKAD complex is part of the pristinamycin II_a PKS/NRPS biosynthetic gene cluster. When disrupted, mutants lack pristinamycin II_a production as well as formation of iso-branched fatty acids as determined by GC-MS.

5 References

1. Shapiro S. Antony van Leeuwenhoek; a review of his life and work. *J. Biol. Photogr. Assoc.* 1955;23(2-3):49-57.

2. Singer C. Notes on the Early History of Microscopy. *Proc. R. Soc. Med.* 1914;7 (Sect Hist Med):247-79.

3. Tan SY, Berman E. Robert Koch (1843-1910): father of microbiology and Nobel laureate. *Singapore Med. J.* 2008;49(11):854-5.

4. Münch R. Robert Koch. *Microbes Infect.* 2003;5(1):69-74.

5. Thaxter R. On the Myxobacteriaceæ, a New Order of Schizomycetes. *Bot. Gaz.* 1892;17(12):389-406.

6. Dworkin M. Biology of the myxobacteria. *Annu. Rev. Microbiol.* 1966;20:75-106.

7. Berkeley MJ, Curtis MA. Notices of the North American Fungi. *Grevillea*. 1874;3:49-64.

8. Grilione PL, Pangborn J. Scanning Electron Microscopy of Fruiting Body Formation by Myxobacteria. *J. Bacteriol.* 1975;124(3):1558-65.

9. Kuner JM, Kaiser D. Fruiting Body Morphogenesis in Submerged Cultures of *Myxococcus xanthus*. *J. Bacteriol.* 1982;151(1):458-61.

10. O'Connor KA, Zusman DR. Development in *Myxococcus xanthus* Involves Differentiation into Two Cell Types, Peripheral Rods and Spores. *J. Bacteriol.* 1991;173(11):3318-33.

11. Kearns DB, Shimkets LJ. Lipid chemotaxis and signal transduction in *Myxococcus xanthus*. *Trends Microbiol.* 2001;9(3):126-9.

12. Licking E, Gorski L, Kaiser D. A Common Step for Changing Cell Shape in Fruiting Body and Starvation-Independent Sporulation of *Myxococcus xanthus*. *J. Bacteriol.* 2000;182(12):3553-8.

13. Garcia R, Gerth K, Stadler M, Dogma IJ Jr, Müller R. Expanded phylogeny of myxobacteria and evidence for cultivation of the 'unculturables'. *Mol. Phylogenet. Evol.* 2010;57(2):878-87.

14. Dawid W. Biology and global distribution of myxobacteria in soils. *FEMS Microbiol. Rev.* 2000;24(4):403-27.

15. Zhou X, Li S, Li W, *et al*. Myxobacterial community is a predominant and highly diverse bacterial group in soil niches. *Environ. Microbiol. Rep.* 2014;6(1):45-56.

16. Dawid W, Gallikowski C, Hirsch P. 3.8 Psychrophilic Myxobacteria from Antarctic Soils. *Polarforschung*. 1988;58(213):271-278.

17. Fudou R, Jojima Y, Iizuka T, Yamanaka S. *Haliangium ochraceum* gen. nov., sp. nov. and *Haliangium tepidum* sp. nov.: novel moderately halophilic myxobacteria isolated from coastal saline environments. *J. Gen. Appl. Microbiol.* 2002;48(2):109-16.

18. Iizuka T, Jojima Y, Fudou R, Tokura M, Hiraishi A, Yamanaka S. *Enhygromyxa salina* gen. nov., sp. nov., a Slightly Halophilic Myxobacterium from the Coastal Areas of Japan. *Syst. Appl. Microbiol.* 2003;26(2):189-96.

19. Iizuka T. *Plesiocystis pacifica* gen. nov., sp. nov., a marine myxobacterium that contains dihydrogenated menaquinone, isolated from the Pacific coasts of Japan. *Int. J. Syst. Evol. Microbiol.* 2003;53(1):189-195.

20. Sanford RA, Cole JR, Tiedje JM. Characterization and Description of *Anaeromyxobacter dehalogenans* gen. nov., sp. nov., an Aryl-Halorespiring Facultative Anaerobic Myxobacterium. *Appl. Environ. Microbiol.* 2002;68(2):893-900.

21. Han K, Li Z, Peng R, *et al*. Extraordinary expansion of a *Sorangium cellulosum* genome from an alkaline milieu. *Sci. Rep.* 2013;3:2101.

22. Engel SR, Dietrich FS, Fisk DG, *et al*. The reference genome sequence of *Saccharomyces cerevisiae*: then and now. *G3: Genes, Genomes, Genet.* 2014;4(3):389-98.

23. Goldman BS, Nierman WC, Kaiser D, *et al*. Evolution of sensory complexity recorded in a myxobacterial genome. *Proc. Natl. Acad. Sci. U. S. A.* 2006;103(41):15200-5.

24. Thomas S, Wagner R, Arakaki A, *et al*. The mosaic genome of *Anaeromyxobacter dehalogenans* strain 2CP-C Suggests an Aerobic Common Ancestor to the Delta-Proteobacteria. *PLoS One*. 2008;3(5):e2103.

25. Iguchi A, Thomson NR, Ogura Y, *et al*. Complete Genome Sequence and Comparative Genome Analysis of Enteropathogenic *Escherichia coli* O127:H6 Strain E2348/69. *J. Bacteriol.* 2009;191(1):347-54.

26. Wenzel SC, Müller R. Myxobacteria—"microbial factories" for the production of bioactive secondary metabolites. *Mol. BioSyst.* 2009;5(6):567-74.

27. Pérez J, Castañeda-García A, Jenke-Kodama H, Müller R, Muñoz-Dorado J. Eukaryotic-like protein kinases in the prokaryotes and the myxobacterial kinome. *Proc. Natl. Acad. Sci. U. S. A.* 2008;105(41):15950-5.

28. Jakobsen JS, Jelsbak L, Jelsbak L, *et al*. σ^{54} Enhancer Binding Proteins and *Myxococcus xanthus* Fruiting Body Development. *J. Bacteriol.* 2004;186(13):4361-8.

29. Yang Z, Duan X, Kaplan, *et al*. Structure and Metabolism. In: Whitworth DE, ed. *Myxobacteria - Multicellularity and Differentiation*. Washington, DC: ASM Press; 2008 ; p.227-282.

30. Reichenbach H, Höfle G. Biologically active secondary metabolites from myxobacteria. *Biotechnol. Adv.* 1993;11(2):219-77.

31. Gerth K, Pradella S, Perlova O, Beyer S, Müller R. Myxobacteria: proficient producers of novel natural products with various biological activities—past and future biotechnological aspects with the focus on the genus *Sorangium*. *J. Biotechnol.* 2003;106(2-3):233-53.

32. Reichenbach H, Höfle G. Discovery and development of the epothilones : a novel class of antineoplastic drugs. *Drugs R&D*. 2008;9(1):1-10.

33. Bentley SD, Chater KF, Cerdeño-Tárraga A, *et al*. Complete genome sequence of the model actinomycete *Streptomyces coelicolor* A3(2). *Nature*. 2002;417(6885):141-7.

34. Omura S, Ikeda H, Ishikawa J, *et al*. Genome sequence of an industrial microorganism *Streptomyces avermitilis*: deducing the ability of producing secondary metabolites. *Proc. Natl. Acad. Sci. U. S. A.* 2001;98(21):12215-20.

35. Ikeda H, Ishikawa J, Hanamoto A, *et al*. Complete genome sequence and comparative analysis of the industrial microorganism *Streptomyces avermitilis*. *Nat. Biotechnol.* 2003;21(5):526-31.

36. Krug D, Zurek G, Revermann O, Vos M, Velicer GJ, Müller R. Discovering the Hidden Secondary Metabolome of *Myxococcus xanthus*: a Study of Intraspecific Diversity. *Appl. Environ. Microbiol.* 2008;74(10):3058-68.

37. Schley C, Altmeyer MO, Swart R, Müller R, Huber CG. Proteome analysis of *Myxococcus xanthus* by Off-line Two-Dimensional Chromatographic Separation Using Monolithic Poly-(styrene-divinylbenzene) Columns Combined with Ion-Trap Tandem Mass Spectrometry. *J. Proteome Res.* 2006;5(10):2760-8.

38. Bode HB, Ring MW, Schwär G, *et al*. Identification of Additional Players in the Alternative Biosynthesis Pathway to Isovaleryl-CoA in the Myxobacterium *Myxococcus xanthus*. *ChemBioChem*. 2009;10(1):128-40.

39. Cortina NS, Krug D, Plaza A, Revermann O, Müller R. Myxoprincomide: A natural Product from *Myxococcus xanthus* Discovered by Comprehensive Analysis of the Secondary Metabolome. *Angewandte Chemie (International ed. in English)*. 2012;51(3):811-6.

40. Meiser P, Bode HB, Müller R. The unique DKxanthene secondary metabolite family from the myxobacterium *Myxococcus xanthus* is required for developmental sporulation. *Proc. Natl. Acad. Sci. U. S. A.* 2006;103(50):19128-33.

41. Goldman BS, Nierman WC, Kaiser D, *et al*. Evolution of sensory complexity recorded in a myxobacterial genome. *Proc. Natl. Acad. Sci. U. S. A.* 2006;103(41):15200-5.

42. Deutscher J, Saier MH Jr. Ser/Thr/Tyr protein phosphorylation in bacteria - for long time neglected, now well established. *Journal of molecular microbiology and biotechnology*. 2005;9(3-4):125-31.

43. Maurice P, Guillaume J, Benleulmi-Chaachoua A, Daulat AM, Kamal M, Jockers R. GPCR-interacting proteins, major players of GPCR function. *Advances in pharmacology (San Diego, Calif.)*. 2011;62:349-80. doi:10.1016/B978-0-12-385952-5.00001-4.

44. Whitworth DE. *Myxobacteria - Multicellularity and Differentiation*. (Whitworth DE, ed.). Washington, DC: ASM Press; 2008.

45. Dworkin M. Recent advances in the social and developmental biology of the myxobacteria. *Microbiol. Rev.* 1996;60(1):70-102.

46. Spormann AM, Kaiser AD. Gliding Movements in *Myxococcus xanthus*. *J. Bacteriol.* 1995;177(20):5846-52.

47. Spormann AM, Kaiser D. Gliding Mutants of *Myxococcus xanthus* with High Reversal Frequencies and Small Displacements. *J. Bacteriol.* 1999;181(8):2593-601.

48. Wu Y, Jiang Y, Kaiser AD, Alber M. Self-organization in bacterial swarming: lessons from myxobacteria. *Phys. Biol.* 2011;8(5):055003.

49. Kaiser D, Crosby C. Cell Movement and Its Coordination in Swarms of *Myxococcus xanthus*. *Cell Motil.* 1983;3(3):227-245.

50. Wu Y, Jiang Y, Kaiser D, Alber M. Social interactions in myxobacterial swarming. *PLoS Comput. Biol.* 2007;3(12):e253.

51. Hodgkin J, Kaiser D. Genetics of gliding motility in *Myxococcus xanthus* (Myxobacterales): Genes Controlling Movement of Single Cells. *Mol. Gen. Genet.* 1979;171(2):167-176.

52. Hodgkin J, Kaiser D. Genetics of gliding motility in *Myxococcus xanthus* (Myxobacterales): Two Gene Systems Control Movement. *Mol. Gen. Genet.* 1979;171(2):177-191.

53. Kaiser D. Social gliding is correlated with the presence of pili in *Myxococcus xanthus*. *Proc. Natl. Acad. Sci. U. S. A.* 1979;76(11):5952-6.

54. Li Y, Lux R, Pelling AE, Gimzewski JK, Shi W. Analysis of type IV pilus and its associated motility in *Myxococcus xanthus* using an antibody reactive with native pilin and pili. *Microbiology (Reading, U. K.)*. 2005;151(Pt 2):353-60.

55. Bode HB, Ring MW, Schwär G, Kroppenstedt RM, Kaiser D, Müller R. 3-Hydroxy-3-Methylglutaryl-Coenzyme A (CoA) Synthase Is Involved in Biosynthesis of Isovaleryl-

CoA in the Myxobacterium *Myxococcus xanthus* during Fruiting Body Formation. *J. Bacteriol.* 2006;188(18):6524-8.

56. Jakovljevic V, Leonardy S, Hoppert M, Søgaard-Andersen L. PilB and PilT Are ATPases Acting Antagonistically in Type IV Pilus Function in *Myxococcus xanthus*. *J. Bacteriol.* 2008;190(7):2411-21. doi:10.1128/JB.01793-07.

57. Lu A, Cho K, Black WP, *et al*. Exopolysaccharide biosynthesis genes required for social motility in *Myxococcus xanthus*. *Mol. Microbiol.* 2005;55(1):206-20.

58. Li Y, Sun H, Ma X, *et al*. Extracellular polysaccharides mediate pilus retraction during social motility of *Myxococcus xanthus*. *Proc. Natl. Acad. Sci. U. S. A.* 2003;100(9):5443-8.

59. Kaiser D. Bacterial motility: How do pili pull? *Curr. Biol.* 2000;10(21):R777-80.

60. Kaiser D. *Myxococcus*—from Single-Cell Polarity to Complex Multicellular Patterns. *Annu. Rev. Genet.* 2008;42(1):109-130.

61. Jelsbak L, Kaiser D. Regulating Pilin Expression Reveals a Threshold for S Motility in *Myxococcus xanthus*. *J. Bacteriol.* 2005;187(6):2105-12.

62. Wolgemuth C, Hoiczyk E, Kaiser D, Oster G. How Myxobacteria Glide. *Curr. Biol.* 2002;12(5):369-77.

63. Lünsdorf H, Schairer HU. Frozen motion of gliding bacteria outlines inherent features of the motility apparatus. *Microbiology (Reading, U. K.).* 2001;147(Pt 4):939-47.

64. Nan B, Zusman DR. Uncovering the mystery of gliding motility in the myxobacteria. *Annu. Rev. Genet.* 2011;45:21-39.

65. Kearns DB. A field guide to bacterial swarming motility. *Nat. Rev. Microbiol.* 2010;8(9):634-44.

66. Nan B, Mauriello EMF, Sun I, Wong A, Zusman DR. A multi-protein complex from *Myxococcus xanthus* required for bacterial gliding motility. *Mol. Microbiol.* 2010;76(6):1539-54.

67. Mauriello EMF, Mouhamar F, Nan B, *et al*. Bacterial motility complexes require the actin-like protein, MreB and the Ras homologue, MglA. *EMBO J.* 2010;29(2):315-26.

68. Nan B, Chen J, Neu JC, Berry RM, Oster G, Zusman DR. Myxobacteria gliding motility requires cytoskeleton rotation powered by proton motive force. *Proc. Natl. Acad. Sci. U. S. A.* 2011;108(6):2498-503.

69. Diodati ME, Gill RE, Plamann L, *et al*. Development and Motility. In: Whitworth DE, ed. *Myxobacteria - Multicellularity and Differentiation*. Washington, DC: ASM Press; 2008; p.41-132.

70. Cascales E, Lloubès R, Sturgis JN. The TolQ-TolR proteins energize TolA and share homologies with the flagellar motor proteins MotA-MotB. *Mol. Microbiol.* 2001;42(3):795-807.

71. Minamino T, Imada K, Namba K. Molecular motors of the bacterial flagella. *Curr. Opin. Struct. Biol.* 2008;18(6):693-701.

72. Youderian P, Burke N, White DJ, Hartzell PL. Identification of genes required for adventurous gliding motility in *Myxococcus xanthus* with the transposable element *mariner*. *Mol. Microbiol.* 2003;49(2):555-70.

73. Mignot T, Shaevitz JW, Hartzell PL, Zusman DR. Evidence That Focal Adhesion Complexes Power Bacterial Gliding Motility. *Science*. 2007;315(5813):853-6.

74. Nan B, McBride MJ, Chen J, Zusman DR, Oster G. Bacteria that Glide with Helical Tracks. *Curr. Biol.* 2014;24(4):R169-R173.

75. Dworkin M, Voelz H. The formation and germination of microcysts in *Myxococcus xanthus*. *J. Gen. Microbiol.* 1962;28:81-5.

76. Nariya H, Inouye M. MazF, an mRNA Interferase, Mediates Programmed Cell Death during multicellular *Myxococcus* Development. *Cell*. 2008;132(1):55-66.

77. Higgs PI, Merlie JP Jr., Müller F, *et al*. Myxobacterial Methods. In: Whitworth DE, ed. *Myxobacteria: Multicellularity and Differentiation*. Washington DC: ASM Press; 2007; p.463-513.

78. Hagen DC, Bretscher AP, Kaiser D. Synergism Between Morphogenetic Mutants of *Myxococcus xanthus*. *Dev. Biol.* 1978;64(2):284-96.

79. Downard J, Ramaswamy SV, Kil KS. Identification of esg, a Genetic Locus Involved in Cell-Cell Signaling during *Myxococcus xanthus* Development. *J. Bacteriol.* 1993;175(24):7762-70.

80. Plaga W, Stamm I, Schairer HU. Intercellular signaling in *Stigmatella aurantiaca*: Purification and characterization of stigmolone, a myxobacterial pheromone. *Proc. Natl. Acad. Sci. U. S. A.* 1998;95(19):11263-7.

81. Hull WE, Berkessel A, Plaga W. Structure elucidation and chemical synthesis of stigmolone, a novel type of prokaryotic pheromone. *Proc. Natl. Acad. Sci. U. S. A.* 1998;95(19):11268-73.

82. Kuner JM, Kaiser D. Introduction of transposon Tn*5* into *Myxococcus* for analysis of developmental and other nonselectable mutants. *Proc. Natl. Acad. Sci. U. S. A.* 1981;78(1):425-9.

83. Kroos L, Kaiser D. Construction of Tn*5lac*, a transposon that fuses *lacZ* expression to exogenous promoters, and its introduction into *Myxococcus xanthus*. *Proc. Natl. Acad. Sci. U. S. A.* 1984;81(18):5816-20.

84. Kroos L, Kuspa A, Kaiser D. A Global Analysis of Developmentally Regulated Genes in *Myxococcus xanthus*. *Dev. Biol.* 1986;117(1):252-66.

85. Kroos L, Kaiser D. Expression of many developmentally regulated genes in *Myxococcus* depends on a sequence of cell interactions. *Genes Dev.* 1987;1(8):840-54.

86. Kuspa A, Kroos L, Kaiser D. Intercellular Signaling is Required for Developmental Gene Expression in *Myxococcus xanthus*. *Dev. Biol.* 1986;117(1):267-76.

87. Kuspa A, Kaiser D. Genes Required for Developmental Signalling in *Myxococcus xanthus*: Three *asg* Loci. *J. Bacteriol.* 1989;171(5):2762-72.

88. Garza AG, Harris BZ, Pollack JS, Singer M. The *asgE* locus is required for cell-cell signalling during *Myxococcus xanthus* development. *Mol. Microbiol.* 2000;35(4):812-24.

89. LaRossa R, Kuner J, Hagen D, Manoil C, Kaiser D. Developmental Cell Interactions of *Myxococcus xanthus*: Analysis of Mutants. *J. Bacteriol.* 1983;153(3):1394-404.

90. Plamann L, Kuspa A, Kaiser D. Proteins That Rescue A-Signal-Defective Mutants of *Myxococcus xanthus*. *J. Bacteriol.* 1992;174(10):3311-8.

91. Cho K, Zusman DR. AsgD, a new two-component regulator required for A-signalling and nutrient sensing during early development of *Myxococcus xanthus*. *Mol. Microbiol.* 1999;34(2):268-81.

92. Kaplan HB, Plamann L. A *Myxococcus xanthus* cell density-sensing system required for multicellular development. *FEMS Microbiol. Lett.* 1996;139(2-3):89-95.

93. Kaiser D. Signaling in myxobacteria. *Annu. Rev. Microbiol.* 2004;58:75-98.

94. Gill RE, Bornemann MC. Identification and Characterization of the *Myxococcus xanthus bsgA G*ene Product. *J. Bacteriol.* 1988;170(11):5289-97.

95. Kaiser D. Coupling cell movement to multicellular development in myxobacteria. *Nat. Rev. Microbiol.* 2003;1(1):45-54.

96. Shimkets LJ, Rafiee H. CsgA, an Extracellular Protein Essential for *Myxococcus xanthus* Development. *J. Bacteriol.* 1990;172(9):5299-306.

97. Lobedanz S, Søgaard-Andersen L. Identification of the C-signal, a contact-dependent morphogen coordinating multiple developmental responses in *Myxococcus xanthus*. *Genes Dev.* 2003;17(17):2151-61.

98. Rolbetzki A, Ammon M, Jakovljevic V, Konovalova A, Søgaard-Andersen L. Regulated Secretion of a Protease Activates Intercellular Signaling during Fruiting Body Formation in *M. xanthus*. *Developmental cell*. 2008;15(4):627-34.

99. Lee BU, Lee K, Mendez J, Shimkets LJ. A tactile sensory system of Myxococcus xanthus involves an extracellular NAD(P)(+)-containing protein. *Genes Dev.* 1995;9(23):2964-73.

100. Kim SK, Kaiser D. Purification and properties of *Myxococcus xanthus* C-factor, an intercellular signaling protein. *Proc. Natl. Acad. Sci. U. S. A.* 1990;87(10):3635-9.

101. Lee K, Shimkets LJ. Suppression of a signaling defect during *Myxococcus xanthus* development. *J. Bacteriol.* 1996;178(4):977-84.

102. Ware JC, Dworkin M. Fatty Acids of *Myxococcus xanthus*. *J. Bacteriol.* 1973;115(1):253-61.

103. Avadhani M, Geyer R, White DC, Shimkets LJ. Lysophosphatidylethanolamine Is a Substrate for the Short-Chain Alcohol Dehydrogenase SocA from *Myxococcus xanthus*. *J. Bacteriol.* 2006;188(24):8543-8550.

104. Cheng YL, Kalman LV, Kaiser D. The *dsg G*ene of *Myxococcus xanthus* Encodes a Protein Similar to Translation Initiation Factor IF3. *J. Bacteriol.* 1994;176(5):1427-33.

105. Cheng Y, Kaiser D. *dsg*, a Gene Required for *Myxococcus* Development, is Necessary for Cell Viability. *J. Bacteriol.* 1989;171(7):3727-31.

106. Toal DR, Clifton SW, Roe BA, Downard J. The *esg* locus of *Myxococcus xanthus* encodes the E1α and E1β subunits of a branched-chain keto acid dehydrogenase. *Mol. Microbiol.* 1995;16(2):177-89.

107. Bode HB, Meiser P, Klefisch T, *et al*. Mutasynthesis-Derived Myxalamids and Origin of the Isobutyryl-CoA Starter Unit of Myxalamid B. *ChemBioChem*. 2007;8(17):2139-44.

108. Mahmud T, Wenzel SC, Wan E, *et al*. A Biosynthetic Pathway to Isovaleryl-CoA in Myxobacteria: the Involvement of the Mevalonate Pathway. *ChemBioChem*. 2005;6(2):322-30.

109. Dickschat JS, Bode HB, Mahmud T, Müller R, Schulz S. A Novel type of Geosmin Biosynthesis in Myxobacteria. *J. Org. Chem.* 2005;70(13):5174-82.

110. Bode HB, Zeggel B, Silakowski B, Wenzel SC, Reichenbach H, Müller R. Steroid biosynthesis in prokaryotes: identification of myxobacterial steroids and cloning of the first bacterial 2,3(S)-oxidosqualene cyclase from the myxobacterium *Stigmatella aurantiaca*. *Mol. Microbiol.* 2003;47(2):471-81.

111. Bartholomeusz G, Zhu Y, Downard J. Growth Medium-Dependent Regulation of *Myxococcus xanthus* Fatty Acid Content Is Controlled by the *esg* Locus. *J. Bacteriol.* 1998;180(19):5269-72.

112. Mahmud T, Bode HB, Silakowski B, *et al*. A Novel Biosynthetic Pathway Providing Precursors for Fatty Acid Biosynthesis and Secondary Metabolite Formation in Myxobacteria. *J. Biol. Chem.* 2002;277(36):32768-74.

113. Dickschat JS, Bode HB, Kroppenstedt RM, Müller R, Schulz S. Biosynthesis of iso-fatty acids in myxobacteria. *Org. Biomol. Chem.* 2005;3(15):2824.

114. Li Y, Luxenburger E, Müller R. An alternative isovaleryl CoA biosynthetic pathway involving a previously unknown 3-methylglutaconyl CoA decarboxylase. *Angew. Chem., Int. Ed. Engl.* 2013;52(4):1304-8.

115. Ring MW, Schwär G, Bode HB. Biosynthesis of 2-Hydroxy and *iso*-even Fatty Acids is Connected to Sphingolipid Formation in Myxobacteria. *ChemBioChem*. 2009;10(12):2003-10.

116. Curtis PD, Geyer R, White DC, Shimkets LJ. Novel lipids in *Myxococcus xanthus* and their role in chemotaxis. *Environ. Microbiol.* 2006;8(11):1935-49.

117. Kleinig H. Membranes from *Myxococcus fulvus* (Myxobacterales) containing carotenoid glucosides. I. Isolation and composition. *Biochim. Biophys. Acta*. 1972;274(2):489-98.

118. Caillon E, Lubochinsky B, Rigomier D. Occurrence of Dialkyl Ether Phospholipids in *Stigmatella aurantiaca* DW4. *J. Bacteriol.* 1983;153(3):1348-51.

119. Ring MW, Schwär G, Thiel V, *et al*. Novel Iso-branched Ether Lipids as Specific Markers of Developmental Sporulation in the Myxobacterium *Myxococcus xanthus*. *J. Biol. Chem.* 2006;281(48):36691-700.

120. Hoiczyk E, Ring MW, McHugh CA, *et al*. Lipid body formation plays a central role in cell fate determination during developmental differentiation of *Myxococcus xanthus*. *Mol. Microbiol.* 2009;74(2):497-517.

121. Fahy E, Subramaniam S, Brown HA, *et al*. A comprehensive classification system for lipids. *J. Lipid Res.* 2005;46(5):839-61.

122. Fahy E, Subramaniam S, Murphy RC, *et al*. Update of the LIPID MAPS comprehensive classification system for lipids. *J. Lipid Res.* 2009;50 Suppl:S9-14.

123. Meiser P, Bode HB, Muller R. The unique DKxanthene secondary metabolite family from the myxobacterium *Myxococcus xanthus* is required for developmental sporulation. *Proc. Natl. Acad. Sci. U. S. A.* 2006;103(50):19128-19133.

124. Bhat S, Ahrendt T, Dauth C, Bode HB, Shimkets LJ. Two lipid signals guide fruiting body development of *Myxococcus xanthus*. *mBio*. 2014;5(1):e00939-13.

125. Bode HB, Dickschat JS, Kroppenstedt RM, Schulz S, Müller R. Biosynthesis of Iso-Fatty Acids in Myxobacteria: Iso-Even Fatty Acids Are Derived by α-Oxidation from Iso-Odd Fatty Acids. *J. Am. Chem. Soc.* 2005;127(2):532-533.

126. Dahan A, Miller JM. The Solubility-Permeability Interplay and Its Implications in Formulation Design and Development for Poorly Soluble Drugs. *AAPS J.* 2012;14(2):244-51.

127. Kahnt J, Aguiluz K, Koch J, *et al*. Profiling the Outer Membrane Proteome during Growth and Development of the Social Bacterium *Myxococcus xanthus* by Selective Biotinylation and Analyses of Outer Membrane Vesicles. *J. Proteome Res.* 2010;9(10):5197-208.

128. Nudleman E, Wall D, Kaiser D. Cell-to-Cell Transfer of Bacterial Outer Membrane Lipoproteins. *Science*. 2005;309(5731):125-7.

129. Wei X, Pathak DT, Wall D. Heterologous protein transfer within structured myxobacteria biofilms. *Mol. Microbiol.* 2011;81(2):315-26.

130. Pathak DT, Wei X, Bucuvalas A, Haft DH, Gerloff DL, Wall D. Cell Contact-Dependent Outer Membrane Exchange in Myxobacteria: Genetic Determinants and Mechanism. *PLoS Genet.* 2012;8(4):e1002626.

131. Streb S, Zeeman SC. Starch metabolism in *Arabidopsis*. *The Arabidopsis book / American Society of Plant Biologists*. 2012;10:e0160.

132. MacDonald DL, Goldfine H. Phosphatidylglycerol acetal of plasmenylethanolamine as an intermediate in ether lipid formation in *Clostridium butyricum*. *Biochem. Cell Biol.* 1990;68(1):225-30.

133. Johnston NC, Aygun-Sunar S, Guan Z, *et al*. A phosphoethanolamine-modified glycosyl diradylglycerol in the polar lipids of *Clostridium tetani*. *J. Lipid Res.* 2010;51(7):1953-61.

134. Watschinger K, Werner ER. Orphan enzymes in ether lipid metabolism. *Biochim.* 2013;95(1):59-65.

135. Koga Y, Goldfine H. Biosynthesis of Phospholipids in *Clostridium butyricum*: Kinetics of Synthesis of Plasmalogens and the Glycerol Acetal of Ethanolamine Plasmalogen. *J. Bacteriol.* 1984;159(2):597-604.

136. Johnston NC, Goldfine H. Isolation and characterization of new phosphatidylglycerol acetals of plasmalogens. A family of ether lipids in C*lostridia*. *European journal of biochemistry / FEBS*. 1994;223(3):957-63.

137. Guan Z, Johnston N, Aygun-Sunar S, Daldal F, Raetz C, Goldfine H. Structural characterization of the polar lipids of *Clostridium novyi* NT. Further evidence for a novel anaerobic biosynthetic pathway to plasmalogens. *Biochim. Biophys. Acta*. 2011;1811(3):186-93.

138. Baumann NA, Hagen P, Goldfine H. Phospholipids of *Clostridium butyricum*. Studies on Plasmalogen Composition and Biosynthesis. *J. Biol. Chem.* 1965;240:1559-67.

139. Day JL, Goldfine H, Hagan P. Enzymic reduction of long-chain acyl-CoA to fatty aldehyde and alcohol by extracts of *Clostridium butyricum*. *Biochim. Biophys. Acta*. 1970;218(1):179-82.

140. Day JI, Goldfine H. Partial Purification and Properties of Acyl-CoA Reductase from *Clostridium butyricum*. *Arch. Biochem. Biophys.* 1978;190(1):322-31.

141. Shevchenko A, Tomas H, Havlis J, Olsen JV, Mann M. In-gel digestion for mass spectrometric characterization of proteins and proteomes. *Nat. Protoc.* 2006;1(6):2856-60.

142. Liu L, Xia S. Role of platelet-activating factor in the pathogenesis of acute pancreatitis. *World J. Gastroenterol.* 2006;12(4):539-45.

143. Seyfried CE, Schweickart VL, Godiska R, Gray PW. The human platelet-activating factor receptor gene (PTAFR) contains no introns and maps to chromosome 1. *Genomics*. 1992;13(3):832-4.

144. Stafforini DM, McIntyre TM, Zimmerman GA, Prescott SM. Platelet-Activating Factor, a Pleiotrophic Mediator of Physiological and Pathological Processes. *Crit. Rev. Clin. Lab. Sci.* 2003;40(6):643-72.

145. Nishizuka Y. The role of protein kinase C in cell surface signal transduction and tumour promotion. *Nature*. 1984;308(5961):693-8.

146. Warne TR, Buchanan FG, Robinson M. Growth-dependent accumulation of monoalkylglycerol in Madin-Darby canine kidney cells. Evidence for a role in the regulation of protein kinase C. *J. Biol. Chem.* 1995;270(19):11147-54.

147. Pedrono F, Martin B, Leduc C, *et al*. Natural alkylglycerols restrain growth and metastasis of grafted tumors in mice. *Nutr. Cancer*. 2004;48(1):64-9.

148. Hallgren B. Therapeutic effects of ether lipids. In: Mangold HK, Paltauf F, eds. *Ether Lipids: Biochemical And Biomedical Aspects*. New York: Academic Press, New York; :261-275.

149. Berdel WE, Okamoto S. Ether lipids in cancer chemotherapy. *Keio J. Med.* 1990;39(2):75-8.

150. Nagan N, Zoeller RA. Plasmalogens: biosynthesis and functions. *Prog. Lipid Res.* 2001;40(3):199-229.

151. Bacon K, Clutter D, Kottel RH, Orlowski M, White D. Carbohydrate Accumulation During Myxospore Formation in *Myxococcus xanthus*. *J. Bacteriol.* 1975;124(3):1635-6.

152. Kottel RH, Bacon K, Clutter D, White D. Coats from *Myxococcus xanthus*: Characterization and Synthesis During Myxospore Differentiation. *J. Bacteriol.* 1975;124(1):550-7.

153. Řezanka T, Křesinová Z, Kolouchová I, Sigler K. Lipidomic analysis of bacterial plasmalogens. *Folia Microbiol. (Dordrecht, Neth.)*. 2012;57(5):463-72.

154. Magnusson CD, Haraldsson GG. Ether lipids. *Chem. Phys. Lipids*. 2011;164(5):315-40.

155. Lohner K, Balgavy P, Hermetter A, Paltauf F, Laggner P. Stabilization of non-bilayer structures by the etherlipid ethanolamine plasmalogen. *Biochim. Biophys. Acta*. 1991;1061(2):132-40.

156. Goldfine H. The appearance, disappearance and reappearance of plasmalogens in evolution. *Prog. Lipid Res.* 2010;49(4):493-8.

157. Zeng Y, Han X, Gross RW. Phospholipid subclass specific alterations in the passive ion permeability of membrane bilayers: separation of enthalpic and entropic contributions to transbilayer ion flux. *Biochem.* 1998;37(8):2346-55.

158. Glaser PE, Gross RW. Plasmenylethanolamine facilitates rapid membrane fusion: a stopped-flow kinetic investigation correlating the propensity of a major plasma membrane constituent to adopt an HII phase with its ability to promote membrane fusion. *Biochem.* 1994;33(19):5805-12.

159. Braverman NE, Moser AB. Functions of plasmalogen lipids in health and disease. *Biochim. Biophys. Acta*. 2012;1822(9):1442-52.

160. Zoeller RA, Morand OH, Raetz CR. A possible role for plasmalogens in protecting animal cells against photosensitized killing. *J. Biol. Chem.* 1988;263(23):11590-6.

161. Orndorff PE, Dworkin M. Separation and Properties of the Cytoplasmic and Outer Membranes of Vegetative cells of *Myxococcus xanthus*. *J. Bacteriol.* 1980;141(2):914-27.

162. Bligh E, Dyer W. A rapid method of total lipid extraction and purification. *Can. J. Biochem. Physiol.* 1959;37(8):911-7.

163. Guan Z, Johnston NC, Raetz CR, Johnson EA, Goldfine H. Lipid diversity among botulinum neurotoxin-producing clostridia. *Microbiology (Reading, U. K.).* 2012;158(Pt 10):2577-84.

164. Prasad SS, Garg A, Agarwal AK. Enzymatic activities of the human AGPAT isoform 3 and isoform 5: localization of AGPAT5 to mitochondria. *J. Lipid Res.* 2011;52(3):451-462.

165. Agarwal AK, Sukumaran S, Cortes AV, *et al*. Human 1-Acylglycerol-3-phosphate O-Acyltransferase Isoforms 1 and 2: Biochemical Characterization and Inability to Rescue Hepatic Steatosis in Agpat2-/- Gene Lipidystrophic Mice. *J. Biol. Chem.* 2011;286(43):37676-37691.

166. Krug D, Zurek G, Schneider B, Garcia R, Müller R. Efficient mining of myxobacterial metabolite profiles enabled by liquid chromatography-electrospray ionisation-time-of-flight mass spectrometry and compound-based principal component analysis. *Anal. Chim. Acta*. 2008;624(1):97-106.

167. Dark MJ. Whole-genome sequencing in bacteriology: state of the art. *Infect. Drug Resist.* 2013;6:115-123.

168. Bernardes JS, Pedreira CE. A Review of Protein Function Prediction Under Machine Learning Perspective. *Recent Pat. Biotechnol.* 2013;7(2):122-41.

169. Leibly DJ, Nguyen TN, Kao LT, Hewitt SN, Barrett LK, van Voorhis WC. Stabilizing Additives Added during Cell Lysis Aid in the Solubilization of Recombinant Proteins. Riggs PD, ed. *PLoS One*. 2012;7(12):e52482.

170. Klock HE, White A, Koesema E, Lesley SA. Methods and results for semi-automated cloning using integrated robotics. *J. Struct. Funct. Genomics*. 2005;6(2-3):89-94.

171. Jeon WB, Aceti DJ, Bingman CA, *et al*. High-throughput purification and quality assurance of *Arabidopsis thaliana* proteins for eukaryotic structural genomics. *J. Struct. Funct. Genomics*. 2005;6(2-3):143-7.

172. Kim Y, Dementieva I, Zhou M, *et al*. Automation of protein purification for structural genomics. *J. Struct. Funct. Genomics*. 2004;5(1-2):111-8.

173. Santarsiero, Santarsiero BD, Yegian, *et al*. An approach to rapid protein crystallization using nanodroplets. *J. Appl. Crystallogr.* 2002;35(2):278-281.

174. Snell G, Cork C, Nordmeyer R, *et al*. Automated Sample Mounting and Alignment System for Biological Crystallography at a Synchrotron Source. *Structure*. 2004;12(4):537-45.

175. Jackson CR, Tyler HL, Millar JJ. Determination of microbial extracellular enzyme activity in waters, soils, and sediments using high throughput microplate assays. *J. Visualized Exp.* 2013;(80).

176. Pohn B, Gerlach J, Scheideler M, *et al*. Micro-colony array based high throughput platform for enzyme library screening. *J. Biotechnol.* 2007;129(1):162-70.

177. Bell CW, Fricks BE, Rocca JD, Steinweg JM, McMahon SK, Wallenstein MD. High-throughput fluorometric measurement of potential soil extracellular enzyme activities. *J. Visualized Exp.* 2013;(81):e50961.

178. Rachinskiy K, Kunze M, Graf C, Schultze H, Boy M, Büchs J. Extension and application of the “enzyme test bench” for oxygen consuming enzyme reactions. *Biotechnol. Bioeng.* 2013.

179. Kohl T, Schmidt C, Wiemann S, Poustka A, Korf U. Automated production of recombinant human proteins as resource for proteome research. *Proteome Sci.* 2008;6:4.

180. Tegel H, Steen J, Konrad A, *et al*. High-throughput protein production - lessons from scaling up from 10 to 288 recombinant proteins per week. *Biotechnol. J.* 2009;4(1):51-7.

181. Khurana P, Gokhale RS, Mohanty D. Genome scale prediction of substrate specificity for acyl adenylate superfamily of enzymes based on active site residue profiles. *BMC Bioinf.* 2010;11:57.

182. Ohlendorf B, Lorenzen W, Kehraus S, Krick A, Bode HB, König GM. Myxotyrosides A and B, Unusual rhamnosides from *Myxococcus* sp. *J. Nat. Prod.* 2009;72(1):82-6.

183. Brat D, Weber C, Lorenzen W, Bode HB, Boles E. Cytosolic re-localization and optimization of valine synthesis and catabolism enables inseased isobutanol production with the yeast *Saccharomyces cerevisiae*. *Biotechnol. Biofuels*. 2012;5(1):65.

184. Bode HB, Reimer D, Fuchs SW, *et al*. Determination of the Absolute Configuration of Peptide Natural Products by Using Stable Isotope Labeling and Mass Spectrometry. *Chemistry (Weinheim, Ger.)*. 2012;18(8):2342-8.

185. Kawana S, Nakagawa K, Hasegawa Y, Yamaguchi S. Simple and rapid analytical method for detection of amino acids in blood using blood spot on filter paper, fast-GC/MS and isotope dilution technique. *J. Chromatogr. B: Anal. Technol. Biomed. Life Sci.* 2010;878(30):3113-8.

186. Brachmann AO, Reimer D, Lorenzen W, *et al*. Reciprocal Cross Talk between Fatty Acid and Antibiotic Biosynthesis in a Nematode Symbiont. *Angew. Chem., Int. Ed. Engl.* 2012;51(48):12086-9.

6 Attachments

6.1 Publication: "Isoprenoids Are Essential for Fruiting Body Formation in *Myxococcus xanthus*"

Authors: Wolfram Lorenzen[1,2], Michael W. Ring[2], Gertrud Schwär[2] and Helge B. Bode[1,2]

[1]Molekulare Biotechnologie, Institut für Molekulare Biowissenschaften, Goethe Universität Frankfurt, 64038 Frankfurt am Main, Germany

[2]Pharmazeutische Biotechnologie, Universität des Saarlandes, 66123 Saarbrücken, Germany

Published in: Journal of Bacteriology, 15 September 2009, Volume 191, Number 18, page 5849-5853

Digital Object Identifier: 10.1128/JB.00539-09

Erklärung über Anteile der Autoren/Autorinnen an den einzelnen Kapiteln der Promotionsarbeit

Titel der Publikation: "Isoprenoids Are Essential for Fruiting Body Formation in *Myxococcus xanthus*"

	Beiträge des Promovierenden und der Co-Autoren/innen
(1) Entwicklung und Planung	HBB: 100%
(2) Durchführung der einzelnen Untersuchungen/Experimente	MWR+WLO: Durchführung der Fettsäuremethylesteranalysen; GS: Kultivierung und Entwicklungsexperimente *M. xanthus*
(3) Erstellung der Datensammlung und Abbildungen	HBB: Darstellung der Stoffwechselwege; GS: Entwicklungsbilder; WLO+MWR: Auswertung Fettsäuremethylesteranalysen
(4) Analyse/Interpretation der Daten	MWR+WLO: Interpretation der Fettsäuremethylesteranalysen; HBB: Ergebniszusammenfassung und Interpretation
(5) übergeordnete Einleitung/Ergebnisse/Diskussion	HBB: 50%; MWR: 25%; WLO: 25%

Isoprenoids Are Essential for Fruiting Body Formation in *Myxococcus xanthus*[▽]

Wolfram Lorenzen,[1,2] Michael W. Ring,[2] Gertrud Schwär,[2] and Helge B. Bode[1,2]*

Molekulare Biotechnologie, Institut für Molekulare Biowissenschaften, Goethe Universität Frankfurt, 60438 Frankfurt am Main,Germany,[1] and Pharmazeutische Biotechnologie, Universität des Saarlandes, 66123 Saarbrücken, Germany[2]

Received 22 April 2009/Accepted 13 July 2009

* Corresponding author. Mailing address: Molekulare Biotechnologie, Institut für Molekulare Biowissenschaften, Biozentrum/Campus Riedberg, Goethe Universität Frankfurt, Max-von-Laue-Str. 9, 60438 Frankfurt am Main, Germany. Phone: 49 69 798 29522. Fax: 49 69 79829527. E-mail: h.bode@bio.uni-frankfurt.de.

[▽]Published ahead of print on 17 July 2009.

6.1.1 Abstract

It was recently shown that *Myxococcus xanthus* harbors an alternative and reversible biosynthetic pathway to isovaleryl coenzyme A (CoA) branching from 3-hydroxy-3-methylglutaryl-CoA. Analyses of various mutants in these pathways for fatty acid profiles and fruiting body formation revealed for the first time the importance of isoprenoids for myxobacterial development.

6.1.2 Main text

Myxobacteria are unique among the prokaryotes as (i) they can form highly complex fruiting bodies under starvation conditions, even up to microscopic tree-like structures (28); (ii) they can move on solid surfaces using different motility mechanisms (16); (iii) they produce some of the most cytotoxic secondary metabolites, with epothilone already in clinical use against cancer (2, 3); and (iv) they harbor the largest prokaryotic genomes found so far (15, 27). The large genome might be directly related to their complex life-style and the diverse secondary (3) and primary (9) metabolisms. Already in 2002 we found that myxobacteria are able to produce isovaleryl coenzyme A (IV-CoA) and compounds derived thereof via a new pathway that branches from 3-hydroxy-3-methylglutaryl-CoA (HMG-CoA), which is the central intermediate of the well-known

mevalonate-dependent isoprenoid biosynthesis (**Fig. 1**) (22, 23). Usually IV-CoA is derived from leucine degradation via the branched-chain keto acid dehydrogenase (BKD) complex (24), which is also the preferred pathway to IV-CoA in the myxobacteria *Myxococcus xanthus* and *Stigmatella aurantiaca* (**Fig. 2A**). However, in *bkd* mutants, where no or only residual leucine degradation is possible (30), the alternative pathway is induced (**Fig. 2B**), presumably to ensure the production of iso-fatty acids (iso-FAs) (5). A possible reason for this alternative pathway is the importance of IV-CoA-derived compounds in the complex myxobacterial life cycle, which is the starvation-induced formation of fruiting bodies in which the cells differentiate into myxospores. We showed that this pathway is induced during fruiting body formation in *M. xanthus* when leucine is limited. Under these conditions, this pathway might be more important for protein synthesis than for lipid remodeling, as lipids are present in excess during development due to the surface reduction from vegetative rods to round myxospores as described previously (29). Examples of IV-CoA-derived compounds are the unusual iso-branched ether lipids, which are almost exclusively produced in the developing myxospores. They might serve as structural lipids and signalling compounds during fruiting body formation (26).

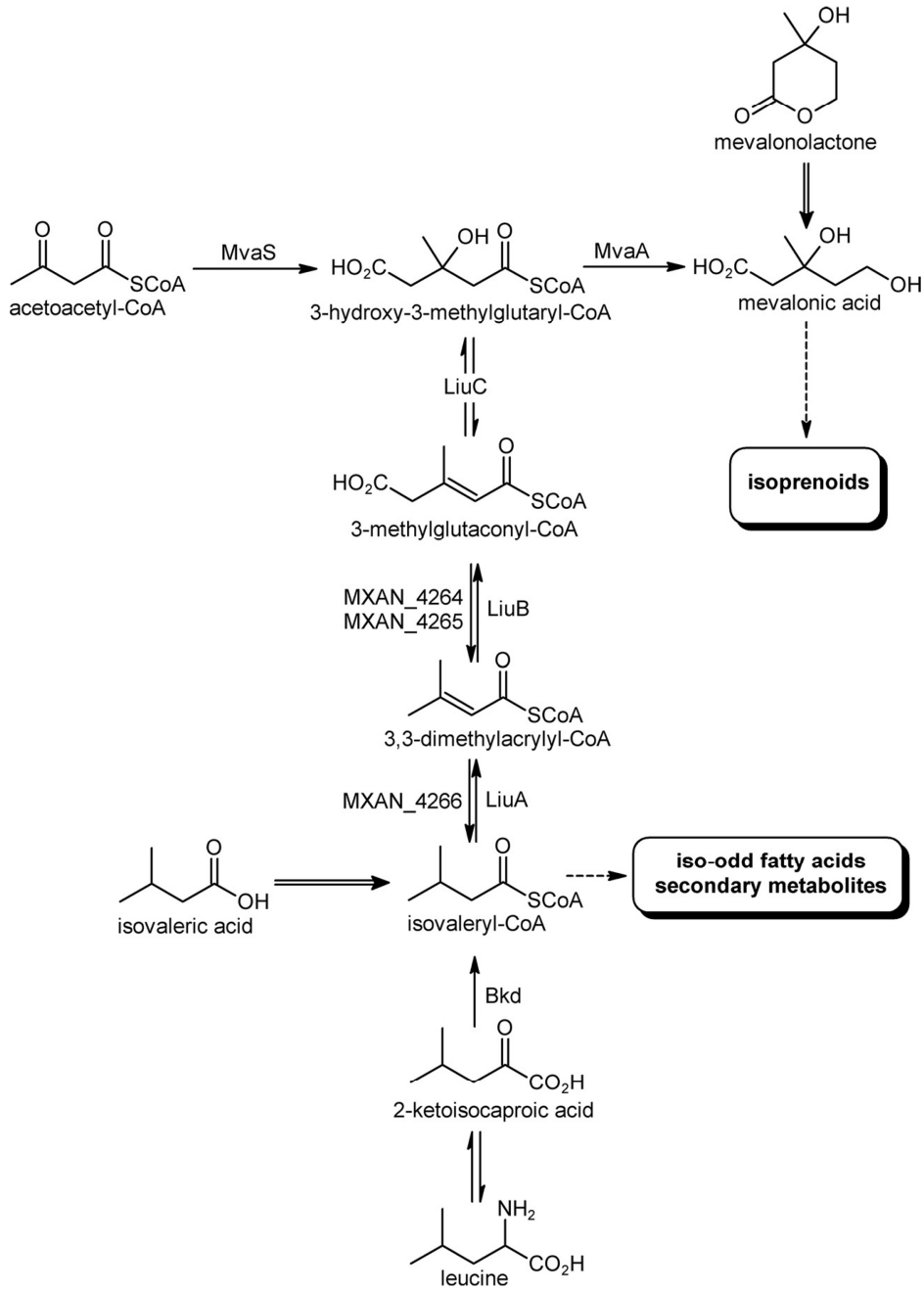

FIG. 1. Biosynthesis of IV-CoA and compounds derived thereof and biosynthesis of isoprenoids in *M. xanthus*. Broken arrows indicate multistep reactions; supplementation (double-lined arrows) with MVL and IVA can be used to complement selected mutants.

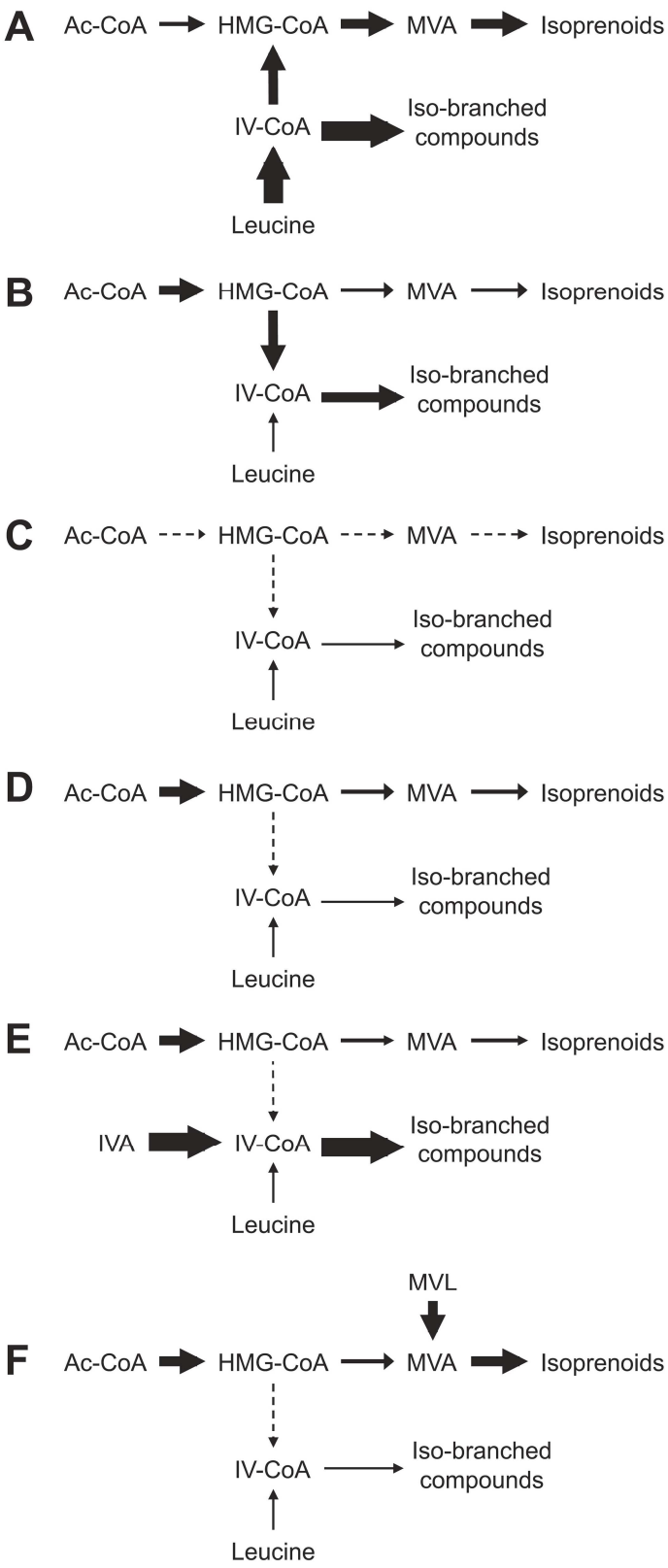

FIG. 2. Short representations of proposed metabolic fluxes through the IV-CoA/isoprenoid network. Broken arrows indicate no metabolic flux. (A) DK1622 (wild type); (B) DK5643 (Δ*bkd*); (C) DK5624 (Δ*bkd mvaS*::*kan*); (D) HB002 (Δ*bkd liuC*::*kan*); (E) HB002 with 1 mM IVA; (F) HB002 with 1 mM MVL. Ac-CoA, acetyl-CoA; MVA, mevalonic acid.

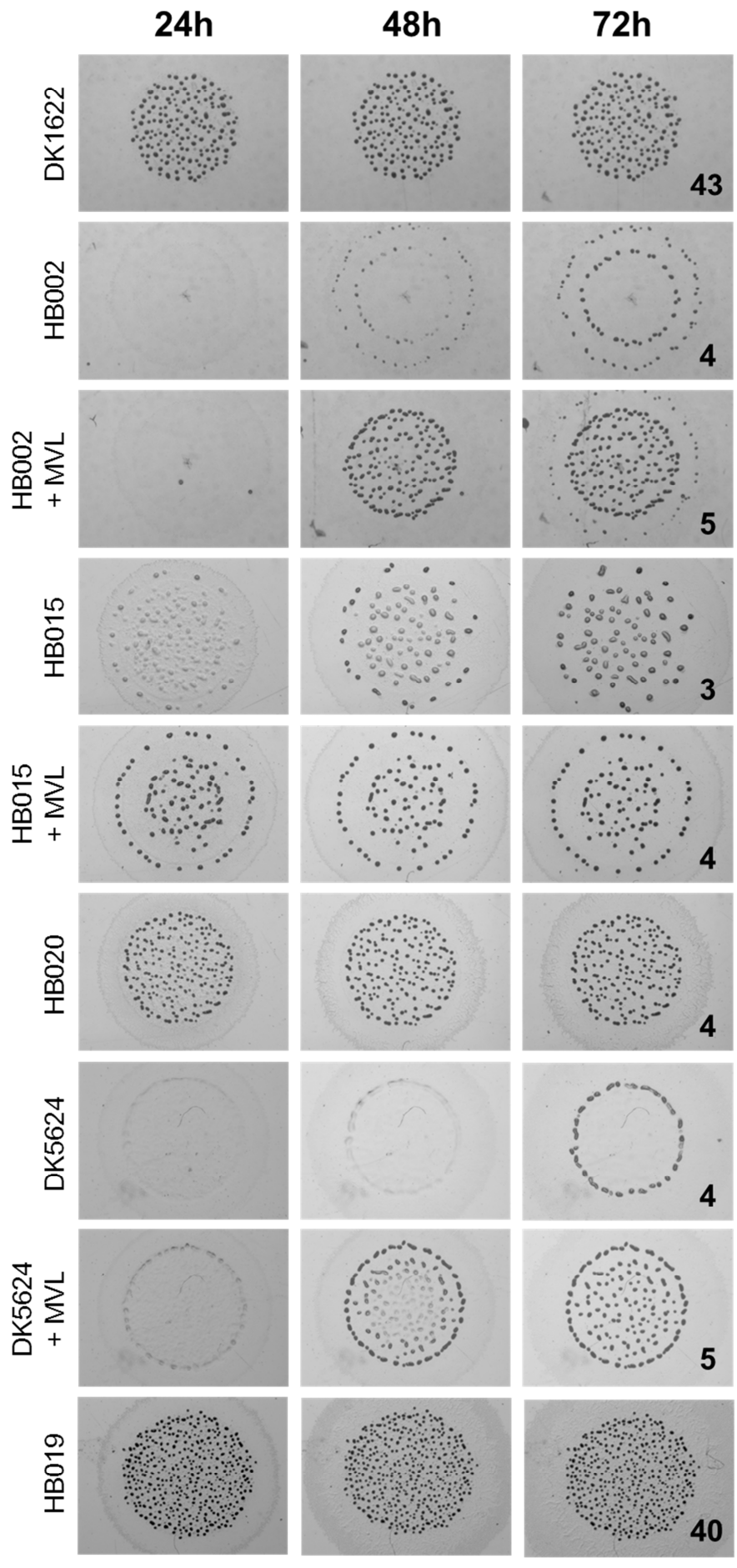
24h
48h
72h
DK1622
43
HB002
4
HB002 + MVL
5
HB015
3
HB015 + MVL
4
HB020
4
DK5624
4
DK5624 + MVL
5
HB019
40

FIG. 3 (previous page). Fruiting body formation on TPM agar in selected mutants at 24, 48, and 72 h after starvation. Numbers refer to the relative amounts (in percentages) of the most abundant iso-FA, iso-15:0, which is indicative of iso-FAs in general. Strains were DK1622 (wild type), HB002 (Δ*bkd liuC*::*kan*), HB015 (Δ*bkd* MXAN_4265::*kan*), DK5624 (Δ*bkd mvaS*::*kan*), HB019 (Δ*bkd mvaS*::*kan mvaS*$^+$), and HB020 (Δ*bkd* MXAN_4265::*kan mvaS*$^+$). DK5624 was grown with 0.3 mM MVL prior to starvation, and the cells were washed and plated on TPM with or without 1 mM of MVL.

In *M. xanthus*, we could recently identify candidate genes involved in the alternative pathway from HMG-CoA to IV-CoA. We also described the genes required for the degradation pathway of leucine and subsequently also those involved in the transformation of IV-CoA to HMG-CoA (4). In myxobacteria leucine is an important precursor for isoprenoid biosynthesis, as was already shown elsewhere for the biosynthesis of steroids (7) and prenylated secondary metabolites like aurachin (22) or leupyrrins (6), as well as volatiles like geosmin or germacradienol in *M. xanthus* and *S. aurantiaca* (11, 13). The interconnection of iso-FAs and isoprenoid biosynthesis made it difficult to assign functions to these compound classes during fruiting body formation in *M. xanthus* because it cannot be excluded that reduced leucine degradation also impairs isoprenoid biosynthesis. A mutant strain of *M. xanthus* that was blocked in the degradation of leucine and the alternative pathway had a deletion in the *bkd* locus as well as a plasmid insertion in the *mvaS* gene encoding the HMG-CoA synthase (strain DK5624). This double mutation severely affected isoprenoid biosynthesis (5), and cultures of DK5624 must be supplemented with mevalonolactone (MVL; the cyclized form of mevalonic acid) in order to enable growth (**Fig. 2C**). Since we have identified the genes involved in IV-CoA biosynthesis and the mevalonate pathway (4), we can now start to identify differences between strains that show deficiencies in iso-Fas and strains that show deficiencies in isoprenoids via simple analysis of the FA profile and analysis of the myxobacterial development of selected mutants.

All mutants used in this study (HB002 [Δ*bkd liuC*::*kan*], HB015 [Δ*bkd* MXAN_4265::*kan*], DK5624 [Δ*bkd mvaS*::*kan*], HB019 [Δ*bkd mvaS*::*kan mvaS*$^+$], and HB020 [Δ*bkd* MXAN_4265::*kan mvaS*$^+$]) have been published previously (4), and FA analysis as well as myxobacterial fruiting body formation has also been described previously (26).

M. xanthus HB002 (Δ*bkd liuC*) shows only residual amounts of iso-FAs, as both leucine degradation and the alternative pathway to IV-CoA are blocked (**Fig. 2D**) and its capability to form fruiting bodies is strongly reduced (**Fig. 3**). The residual amount of iso-FAs results

from a second BKD activity in *M. xanthus* that has been identified by residual leucine incorporation as well as by residual enzymatic activity in *bkd* mutants (23, 30). This second BKD activity might be a side activity of the pyruvate dehydrogenase or a related chemical oxidative decarboxylation, as no second *bkd* locus could be identified in the genome (unpublished results). Moreover, growth of HB002 is not MVL dependent because the block in the alternative pathway does not affect isoprenoid biosynthesis, as *liuC* encodes a dehydratase/hydratase that is involved in the conversion of HMG-CoA to 3-methylglutaconyl-CoA and vice versa (4). As expected, the FA profile (4) as well as the developmental phenotype (data not shown) can be complemented (**Fig. 2E**) by the addition of isovaleric acid (IVA), the free acid of IV-CoA, indicating the importance of iso-branched compounds for development in *M. xanthus*. Unexpectedly, addition of MVL (**Fig. 2F**) also partially restored fruiting body formation without restoring the FA profile (**Fig. 3**). Similarly, *M. xanthus* HB015 (Δ*bkd* MXAN_4265::*kan*) can produce only traces of iso-FAs, as both pathways to IV-CoA are blocked. MXAN_4265 encodes a protein with similarity to a glutaconyl-CoA transferase subunit, but from our previous results, we postulated it to be involved in the alternative pathway to IV-CoA (**Fig. 1**) (4). The respective mutant shows a severely impaired developmental phenotype, which can be complemented not only by the addition of IVA (not shown) but also by the addition of MVL (**Fig. 3**). Again, no change in the FA profile was observed after the addition of MVL. However, a plasmid insertion into MXAN_4265 has a polar effect on *mvaS*, which is the last gene in this five-gene operon and which is crucial for HMG-CoA formation from acetoacetyl-CoA and acetyl-CoA. Therefore, we assume that both pathways to HMG-CoA are blocked in HB015: no HMG-CoA can be made from acetyl-CoA and hardly any can be made via leucine degradation. In order to prove this hypothesis, we complemented HB015 with an additional copy of mvaS under the constitutive T7A1 promoter as described previously, using the plasmid pCK4267exp (4). The resulting strain, HB020 (Δ*bkd*, MXAN_4265*::kan mvaS*$^{+}$), showed a restored developmental phenotype but still produced only trace amounts of iso-FAs.

The data from HB002, HB015, and HB020 indicate an important function of the mevalonate-dependent isoprenoid pathway for fruiting body formation in *M. xanthus*. Therefore, MVL addition can at least partially complement the developmental phenotype of DK5624, which cannot form fruiting bodies without MVL (**Fig. 3**). However, genetic

complementation with *mvaS* in HB019 resulted in the expected complementation of the fruiting body formation and the FA profile (**Fig. 3**, bottom row).

Leucine is one of the most abundant proteinogenic amino acids. It is also an essential amino acid for *M. xanthus* (8), which has a predatory life-style (1), as it lives on other bacteria and fungi that contain a lot of leucine. Moreover, leucine is very efficiently incorporated into isoprenoids like geosmin and aurachin (10, 22). Thus, one can conclude that in fact leucine degradation is the major pathway for HMG-CoA biosynthesis instead of the usual formation via acetoacetyl-CoA and acetyl-CoA by the HMG-CoA synthase MvaS as indicated in **Fig. 2A**. No difference in growth was observed between culture with and culture without MVL for HB002 (Δ*bkd liuC*::*kan*) and HB015 (Δ*bkd* MXAN_4265::*kan*) in rich medium (data not shown), probably due to the complete MvaS activity (in HB002) or residual BKD activity (in HB002 and HB015), resulting in all precursors for the mevalonate-dependent isoprenoid biosynthesis still being present in excess under these conditions. However, under starvation conditions a small reduction in HMG-CoA biosynthesis caused by completely blocked leucine degradation (as in HB002 due to the mutation in *liuC* [**Fig. 2D**]) or reduced leucine degradation and a mutation in *mvaS* (as in HB015) might each result in a reduced isoprenoid level, which can be complemented at least partially by the addition of MVL. This would also explain the difference in the developmental phenotypes of HB002 and HB015, with the phenotype being more severe in HB002 (**Fig. 3**). The fact that complementation with IVA is in all cases more efficient than that with MVL can be explained by the role of the already-mentioned isolipids. They can be produced only after IVA addition, which also complements the (developmental) phenotype of some of these mutants (26).

As isoprenoids represent probably the most diverse class of natural products (14), it is very hard to predict which particular isoprenoids might be responsible for the observed effects. Several isoprenoids (7, 11–13), prenylated secondary metabolites (6, 22), and carotenoids (18–21) are known from myxobacteria in general, and a major volatile compound from *M. xanthus* is the terpenoid geosmin (13). In order to test whether geosmin might be required for fruiting body formation, we constructed a plasmid insertion mutant in MXAN_6247, which is involved in the cyclization of farnesyl diphosphate to geosmin, following published procedures (4, 5). The resulting strain, HB022, showed the expected loss in geosmin production but no developmental phenotype (data not shown).

Additionally, it cannot be excluded that prenylated proteins, sugars, or quinones from the respiratory chain are important for fruiting body formation. Moreover, stigmolone has been described as a pheromone involved in fruiting body formation in *S. aurantiaca* (25). Although its biosynthesis has not been elucidated yet, stigmolone could be an isoprenoid as well, which is deducible from the two iso-branched residues within its chemical structure (17). Nevertheless, the importance of isoprenoids for *M. xanthus* is evident from the data presented, and clearly more work is needed to identify the compound(s) involved.

Acknowledgements

We are grateful to Rolf Müller for his continuous support and for critical reading of the manuscript. We are also grateful to the Deutsche Forschungsgemeinschaft for financial support within the Emmy Noether program.

6.1.3 References

1. **Berleman, J. E., and J. R. Kirby.** 2007. Multicellular development in *Myxococcus xanthus* is stimulated by predator-prey interactions. J. Bacteriol. **189:**5675–5682.

2. **Bode, H. B., and R. Müller.** 2006. Analysis of myxobacterial secondary metabolism goes molecular. J. Ind. Microbiol. Biotechnol. **33:**577–588.

3. **Bode, H. B., and R. Müller.** 2007. Secondary metabolism in myxobacteria, p.259–282. *In* D. Whitworth (ed.), Myxobacteria: multicellularity and differentiation.ASM Press, Washington, DC.

4. **Bode, H. B., M. W. Ring, G. Schwär, M. O. Altmeyer, C. Kegler, I. R. Jose, M. Singer, and R. Müller.** 2009. Identification of additional players in the alternative biosynthesis pathway to isovaleryl-CoA in the myxobacterium *Myxococcus xanthus*. Chembiochem **10:**128–140.

5. **Bode, H. B., M. W. Ring, G. Schwär, R. M. Kroppenstedt, D. Kaiser, and R. Müller.** 2006. 3-Hydroxy-3-methylglutaryl-coenzyme A (CoA) synthase is involved in the biosynthesis of isovaleryl-CoA in the myxobacterium *Myxococcus xanthus* during fruiting body formation. J. Bacteriol. **188:**6524–6528.

6. **Bode, H. B., S. C. Wenzel, H. Irschik, G. Höfle, and R. Müller.** 2004. Unusual biosynthesis of leupyrrins in the myxobacterium *Sorangium cellulosum*. Angew. Chem. Int. Ed. **43:**4163–4167.

7. **Bode, H. B., B. Zeggel, B. Silakowski, S. C. Wenzel, H. Reichenbach, and R. Müller.** 2003. Steroid biosynthesis in prokaryotes: identification of myxobacterial steroids and cloning of the first bacterial 2,3(S)-oxidosqualene cyclase from the myxobacterium *Stigmatella aurantiaca*. Mol. Microbiol. **47:**471–481.

8. **Bretscher, A. P., and D. Kaiser.** 1978. Nutrition of *Myxococcus xanthus*, a fruiting myxobacterium. J. Bacteriol. **133:**763–768.

9. **Curtis, P. D., and L. J. Shimkets.** 2007. Metabolic pathways relevant to predation, signaling, and development, p. 241–258. *In* D. Whitworth (ed.), Myxobacteria: multicellularity and differentiation. ASM Press, Washington, DC.

10. **Dickschat, J. S., H. B. Bode, T. Mahmud, R. Müller, and S. Schulz.** 2005. A novel type of geosmin biosynthesis in myxobacteria. J. Org. Chem. **70:**5174–5182.

11. **Dickschat, J. S., H. B. Bode, S. C. Wenzel, R. Müller, and S. Schulz.** 2005. Biosynthesis and identification of volatiles released by the myxobacterium *Stigmatella aurantiaca*. Chembiochem **6:**2023–2033.

12. **Dickschat, J. S., T. Nawrath, V. Thiel, B. Kunze, R. Müller, and S. Schulz.** 2007. Biosynthesis of the off-flavor 2-methylisoborneol by the myxobacterium *Nannocystis exedens*. Angew. Chem. Int. Ed. **46:**8287–8290.

13. **Dickschat, J. S., S. C. Wenzel, H. B. Bode, R. Müller, and S. Schulz.** 2004. Biosynthesis of volatiles by the myxobacterium *Myxococcus xanthus*. Chembiochem **5:**778–787.

14. **Gershenzon, J., and N. Dudareva.** 2007. The function of terpene natural products in the natural world. Nat. Chem. Biol. **3:**408–414.

15. **Goldman, B. S., W. C. Nierman, D. Kaiser, S. C. Slater, A. S. Durkin, J. Eisen, C. M. Ronning, W. B. Barbazuk, M. Blanchard, C. Field, C. Halling, G. Hinkle, O. Iartchuk, H. S. Kim, C. Mackenzie, R. Madupu, N. Miller, A. Shvartsbeyn, S. A. Sullivan, M. Vaudin, R. Wiegand, and H. B. Kaplan.** 2006. Evolution of sensory

complexity recorded in a myxobacterial genome. Proc. Natl. Acad. Sci. USA **103:**15200–15205.

16. **Hartzell, P., W. Shi, and P. Youderian.** 2007. Gliding motility in *Myxococcus xanthus*, p. 103–122. *In* D. Whitworth (ed.), Myxobacteria: multicellularity and differentiation. ASM Press, Washington, DC.

17. **Hull, W. E., A. Berkessel, and W. Plaga.** 1998. Structure elucidation and chemical synthesis of stigmolone, a novel type of prokaryotic pheromone. Proc. Natl. Acad. Sci. USA **95:**11268–11273.

18. **Jansen, R., A. Nowak, B. Kunze, H. Reichenbach, and G. Höfle.** 1995. Four new carotenoids from *Polyangium fumosum* (Myxobacteria): 3,3',4,4'-tetradehydro-1,1',2,2'-tetrahydro-1,1'-dihydroxy-y,y-carotene (di-O-demethylspirilloxanthin), its beta-glucoside fatty acid esters. Liebigs Ann. Recl. **1995:**873–876.

19. **Kleinig, H., and H. Reichenbach.** 1969. Carotenoid pigments of *Stigmatella aurantiaca* (Myxobacterales). I. The minor carotenoids. Arch. Mikrobiol. **68:**210–217.

20. **Kleinig, H., and H. Reichenbach.** 1970. A new type of carotenoid pigment isolated from myxobacteria. Naturwissenschaften **57:**92–93.

21. **Kleinig, H., H. Reichenbach, and H. Achenbach.** 1970. Carotenoid pigments of Stigmatella aurantiaca (Myxobacterales). II. Acylated carotenoid glucosides. Arch. Mikrobiol. **74:**223–234.

22. **Mahmud, T., S. C. Wenzel, E. Wan, K. W. Wen, H. B. Bode, N. Gaitatzis, and R. Müller.** 2005. A novel biosynthetic pathway to isovaleryl-CoA in myxobacteria: the involvement of the mevalonate pathway. Chembiochem **6:**322–330.

23. **Mahmud, T., H. B. Bode, B. Silakowski, R. M. Kroppenstedt, M. Xu, S. Nordhoff, G. Höfle, and R. Müller.** 2002. A novel biosynthetic pathway providing precursors for fatty acid biosynthesis and secondary metabolite formation in myxobacteria. J. Biol. Chem. **277:**32768–32774.

24. **Michal, G.** 1999. Biochemical pathways. Spektrum Akademischer Verlag, Heidelberg, Germany.

25. **Plaga, W., I. Stamm, and H. U. Schairer.** 1998. Intercellular signaling in *Stigmatella aurantiaca*: purification and characterization of stigmolone, a myxobacterial pheromone. Proc. Natl. Acad. Sci. USA **95:**11263–11267.

26. **Ring, M. W., G. Schwär, V. Thiel, J. S. Dickschat, R. M. Kroppenstedt, S. Schulz, and H. B. Bode.** 2006. Novel iso-branched ether lipids as specific markers of developmental sporulation in the myxobacterium *Myxococcus xanthus*. J. Biol. Chem. **281:**36691–36700.

27. **Schneiker, S., O. Perlova, O. Kaiser, K. Gerth, A. Alici, M. O. Altmeyer, D. Bartels, T. Bekel, S. Beyer, E. Bode, H. B. Bode, C. J. Bolten, J. V. Choudhuri, S. Doss, Y. A. Elnakady, B. Frank, L. Gaigalat, A. Goesmann, C. Groeger, F. Gross, L. Jelsbak, L. Jelsbak, J. Kalinowski, C. Kegler, T. Knauber, S. Konietzny, M. Kopp, L. Krause, D. Krug, B. Linke, T. Mahmud, R. Martinez-Arias, A. C. McHardy, M. Merai, F. Meyer, S. Mormann, J. Munoz-Dorado, J. Perez, S. Pradella, S. Rachid, G. Raddatz, F. Rosenau, C. Ruckert, F. Sasse, M. Scharfe, S. C. Schuster, G. Suen, A. Treuner-Lange, G. J. Velicer, F. J. Vorholter, K. J. Weissman, R. D. Welch, S. C. Wenzel, D. E. Whitworth, S. Wilhelm, C. Wittmann, H. Blöcker, A. Pühler, and R. Müller. 2007.** Complete genome sequence of the myxobacterium *Sorangium cellulosum*. Nat. Biotechnol**. 25:**1281–1289.

28. **Shimkets, L., M. Dworkin, and H. Reichenbach.** 2006. The myxobacteria, p.31–115. *In* M. Dworkin (ed.), The prokaryotes, vol. 7. Springer, Berlin, Germany.

29. **Shimkets, L., and T. W. Seale.** 1975. Fruiting-body formation and myxospores differentiation and germination in *Myxococcus xanthus* viewed by scanning electron microscopy. J. Bacteriol. **121:**711–720.

30. **Toal, D. R., S. W. Clifton, B. A. Roe, and J. Downward.** 1995. The *esg* locus of *Myxococcus xanthus* encodes the E1 alpha and E1 beta subunits of a branched-chain keto acid dehydrogenase. Mol. Microbiol. **16:**177–189.

6.2 Publication: “A multifunctional enzyme is involved in a novel bacterial ether lipid biosynthesis pathway”

Authors: Wolfram Lorenzen, Tilman Ahrendt, Kenan A J Bozhüyük & Helge B Bode

Merck-Stiftungsprofessur für Molekulare Biotechnologie, Fachbereich Biowissenschaften, Johann Wolfgang Goethe-Universität Frankfurt, Frankfurt, Germany

Published in: nature chemical biology, 11 Mai 2014, Volume 10, page 425-427

Digital Object Identifier: 10.1038/nchembio.1526

Erklärung über Anteile der Autoren/Autorinnen an den einzelnen Kapiteln der Promotionsarbeit

Titel der Publikation: "A multifunctional enzyme is involved in bacterial ether lipid biosynthesis"

	Beiträge des Promovierenden und der Co-Autoren/innen
(1) Entwicklung und Planung	WLO: 75%; HBB: 25%
(2) Durchführung der einzelnen Untersuchungen/Experimente	WLO: Alle Experimente außer: TA: Auskeimungsexperimente *M. xanthus*; KAJB: Molecular Modeling
(3) Erstellung der Datensammlung und Abbildungen	WLO: Alle Tabellen und Abbildungen außer: TA: Ergebnissammlung Auskeimungsexperimente *M. xanthus*; KAJB: Dockings ElbD Acyltransferase u. Adenylierungsdomäne
(4) Analyse/Interpretation der Daten	WLO: Sämtlich Daten außer: KAJB: Dockings ElbD Acyltransferase u. Adenylierungsdomäne
(5) übergeordnete Einleitung/Ergebnisse/Diskussion	WLO: 75%; HBB: 25%

A multifunctional enzyme is involved in bacterial ether lipid biosynthesis

Wolfram Lorenzen, Tilman Ahrendt, Kenan AJ Bozhüyük & Helge B Bode*

Merck-Stiftungsprofessur für Molekulare Biotechnologie, Fachbereich Biowissenschaften, Johann Wolfgang Goethe-Universität Frankfurt, Frankfurt, Germany. *e-mail: h.bode@bio.uni-frankfurt.de

published online: 11 may 2014

6.2.1 Abstract

Fatty acid–derived ether lipids are present not only in most vertebrates but also in some bacteria. Here we describe what is to our knowledge the first gene cluster involved in the biosynthesis of such lipids in myxobacteria that encodes the multifunctional enzyme ElbD, which shows similarity to polyketide synthases. Initial characterization of *elbD* mutants in *Myxococcus xanthus* and *Stigmatella aurantiaca* showed the importance of these ether lipids for fruiting body formation and sporulation.

6.2.2 Main text

Vinyl ether lipids are frequently found in extremophile prokaryotes[1], but to date, no genes related to their biosynthetic have been described. However, for *Megasphera elsdenii*, *Veillonella parvula* and *Clostridium butyricum*, several studies showed that plasmalogen biosynthesis is not performed via dihydroxyacetone but with glycerol, and in *C. butyricum*, diacylglycerols were identified as precursors of plasmalogens[2,3]. We investigated ether lipid formation in the myxobacteria *M. xanthus* and *S. aurantiaca*[4]. These bacteria belong to the order myxococcales, which comprises Gram-negative, soil-dwelling, almost ubiquitous deltaproteobacteria that show social twitching motility and cooperative, wolf pack–like predatory feeding. Upon adverse environmental conditions, a temporally defined developmental program takes place, including aggregation, cell differentiation, fruiting body formation and sporulation[5]. We identified a number of unusual iso-branched vinyl- and alkyl ether lipids in *M. xanthus*, including plasmenylphosphatidylethanolamine (**Fig. 1a**; VEPE (PE(P-i15:0/i15:0), **1**; notation is as described by LIPID MAPS,

http://www.lipidmaps.org/data/classification/LM_classification_exp.php) and plasmanylphosphatidylethanolamine (AEPE (PE(*O*-i15:0/i15:0), **2**), 1-*O*-alkyl-*sn*-glycerol, 1-*O*-alkyl-2-acyl-*sn*-glycerol and 1-*O*-alkyl-2,3-diacyl-*sn*-glycerol, whereas the latter mentioned neutral ether lipids strongly accumulate in lipid bodies during the process of starvation-induced fruiting body formation[4,6]. In addition to that, a diacylmonoalkyl ether lipid named TG-1 (TG(*O*-i15:0/i15:0/i15:0) (**3**)) was recently found to act as a signaling molecule involved in the developmental program of *M. xanthus*[7]. Thus, we sought to further investigate the biosynthesis of these important molecules in myxobacteria.

As a starting point, we searched the genome of *M. xanthus* for possible gene candidates. The gene product of *MXAN_1676* has 92% sequence coverage and about 42% identity to the human alkylglycerone-phosphate synthase (E.C. 2.5.1.26), which catalyzes the second step in peroxisomal ether lipid formation. However, gene disruption caused only a small reduction in ether lipid formation, indicating the existence of an alternative pathway (**Supplementary Results**, **Supplementary Fig. 1**). Therefore, we searched the genome for acyltransferases related to glycerolipid biosynthesis that have been previously disregarded8, resulting in the discovery of *MXAN_1528*, which encodes a multifunctional protein with a domain annotated as acylglycerolphosphate acyltransferase of glycerophospholipid biosynthesis (AT). The gene is embedded in a five-gene operon (*MXAN_1531–1527*), and its protein product additionally features a fatty acyl CoA–like reductase (Re), an acyl–carrier protein/thiolation domain (T) and an acyl-CoA synthetase domain (A) (**Fig. 1a**).

Insertion mutagenesis of *MXAN_1528* yielded a phenotype with delayed aggregation between 6 h and 24 h after starvation-induced fruiting body formation, a strongly reduced content of vinyl and alkyl ethers under both vegetative and starvation conditions and no detectable viable spores and fewer fruiting bodies compared to the wild type (**Fig. 1b** and **Supplementary Fig. 1**, **Supplementary Data Set 1** and **Supplementary Table 2**). Accordingly, the *MXAN_1531–1527* operon was renamed as *elbA–elbE* (where *elb* stands for ether lipid biosynthesis). Complementation of the *elbD* mutant restored both ether lipid formation and the developmental phenotypes, whereas overexpression in the wild-type background resulted in an acceleration of aggregation as well as a significant ($P = 0.0011$) increase in monoalkylgylcerol formation; in both cases, the strain's ability to form viable spores is strongly reduced (**Supplementary Fig. 1** and **Supplementary Table 2**). The changes in phenotype suggest a putative signaling function of a yet-to-be-determined ether

lipid molecule. Signaling functions of ether lipids have been shown in humans for the platelet-activating factor or monoacylmonoalkylglycerols inhibiting phosphokinase C (ref. 9), and, indeed, the development-specific alkyldiacylglycerol TG-1 can rescue the developmental phenotype of an *esg* mutant, which is impaired in the formation of a yet-to-be-determined intercellular signal[7].

Gene disruption experiments in *elbA*, *elbB* and *elbE* (**Supplementary Fig. 1** and **Supplementary Table 2**) suggested that *elbA* is probably not involved in ether lipid formation as its disruption did not result in a specific phenotype. Disruption of *elbB* led to a similar but less pronounced phenotype than *elbD* in terms of ether lipid formation, which was partially restored by expression of *elbD*, suggesting that *elbD* is probably translationally coupled with *elbB* so that the observed effect was most likely due to a polar effect of *elbB* disruption. Finally, *elbE* seems to have a role in ether lipid formation as its inactivation caused a decrease in ether lipid formation that cannot be complemented by an extra copy of *elbD*. Concerning the developmental phenotype of the complementation mutants, it seemed that the constitutive expression of *elbD* disturbed the formation of viable spores. We did not deem this observation surprising as the amount of ether lipids is normally dependent on the stage of fruiting body formation[4]. Similarly, it has been shown that PE(16:1ω5c/16:1ω5c), a chemotaxis signal in *M. xanthus*, is only active at a specific concentration[10] and that the ability to complement an *esg* mutant by ether lipids follows a concentration-dependent saturation kinetics so that a high concentration is not necessarily beneficial for sporulation[7].

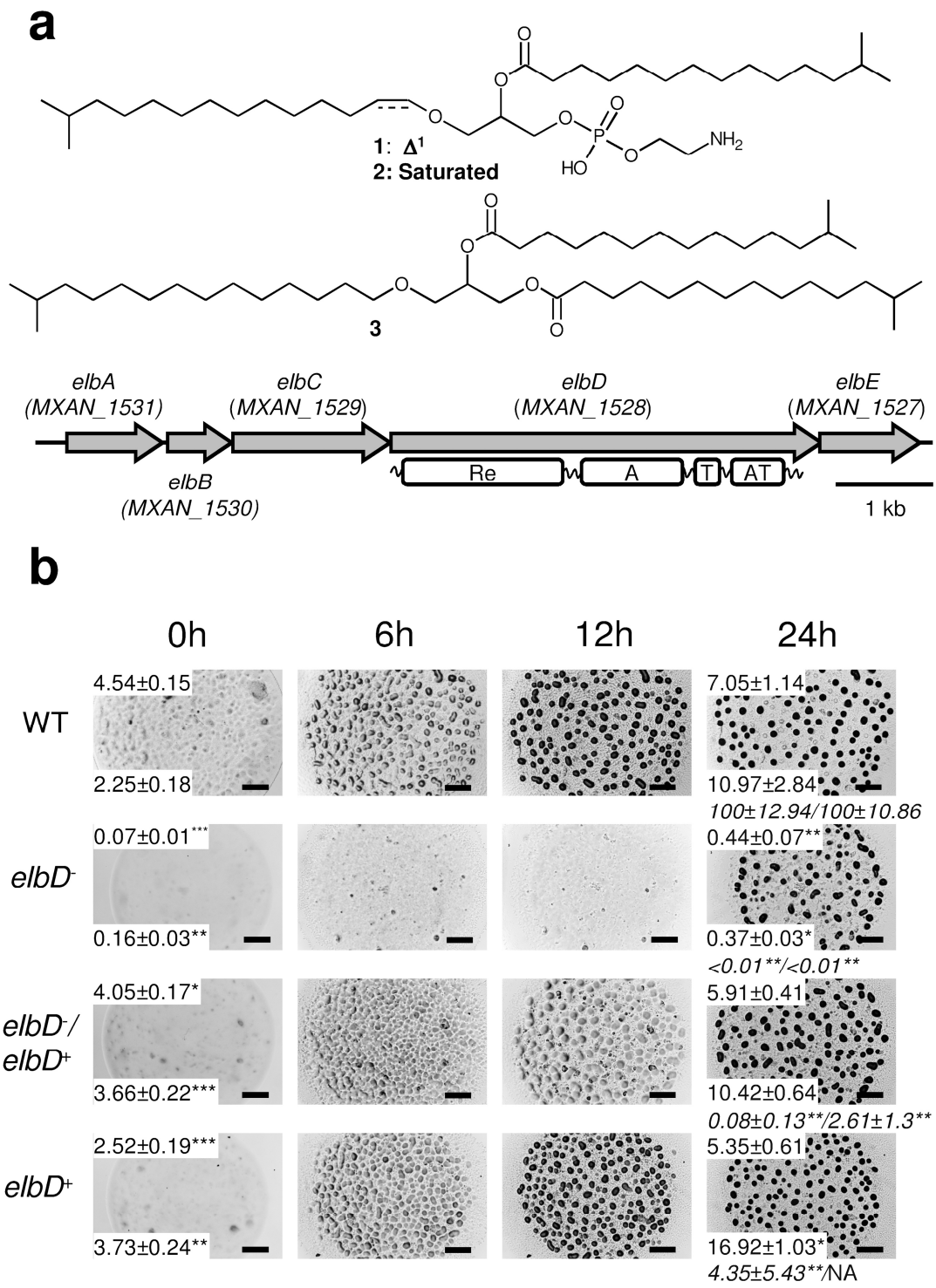

Figure 1 | Phenotypic investigation of the *elbD* mutant. (**a**) Structures of the myxobacterial ether lipids VEPE(**1**), AEPE(**2**), the major diacylmonoalkyl ether lipid TG-1 (**3**); the constitution of the proposed ether lipid biosynthesis gene cluster in *M. xanthus*; and the predicted domain structure within ElbD (**Supplementary Data Set 2**). (**b**) Microscopic plan view on developing *M. xanthus* cells (scale bars, 500 μm) with mean (n = 3) ± s.d. of relative amounts of i15:0-DMA (top of each image) and of i15:0-OAG (bottom of each image), measured as the percentage of total fatty acid methyl esters. The results of the sporulation assay (italicized numbers in the '24 h' column) are shown as mean (n = 3) ± s.d. number of colony-forming units of percent wild type at 72 h and 120 h (values separated by slash), after starvation-induced fruiting body formation. *P < 0.05; **P < 0.01; ***P < 0.001 relative to wild type. NA: data not available. Details are in **Supplementary Figure 1**, **Supplementary Table 2** and **Supplementary Data Set 1**.

As the notorious background level of vinyl- and alkyl ether lipids was a challenge for data evaluation and interpretation, we investigated *elbA*, *elbB* and *elbD* insertion mutants in *S. aurantiaca* DW4/3-1. The genes are arranged in the same way as in *M. xanthus*, and their protein products exhibit a very high homology (up to 90%). Additionally, *S. aurantiaca* does not have a *MXAN_1676* homolog (**Supplementary Fig. 2** and **Supplementary Data Set 2**). As with *M. xanthus*, inactivation of *elbA* in *S. aurantiaca* did not result in a phenotype, but inactivation of *elbB* strongly decreased ether lipid content, and *elbD* brought ether lipid formation below the detection limit, strengthening the hypothesis that ElbD is involved in ether lipid synthesis. Starvation-induced aggregation behavior proved to be different in the *elbA*, *elbB* and *elbD* mutants compared to the wild type (**Supplementary Fig. 1** and **Supplementary Table 2**). Notably, *elbD* from *S. aurantiaca* was not able to complement the *M. xanthus elbD* mutant despite their high homology. All of the sequenced myxobacterial strains feature close homologs of at least *elbB–E* (**Supplementary Fig. 2**) and some homologs of *MXAN_1676* (**Supplementary Data Set 2**), and all of the strains analyzed by gas chromatography (GC)/MS[11] contained ether lipids (**Supplementary Fig. 3**).

TLC analysis of total lipid extracts showed no obvious changes in phospholipid composition in an *elbD* mutant under vegetative conditions and 24 h after starvation induction, which is the time point with the highest abundance of ether lipids in the wild type[4], but it did show a loss of one lipid species in the neutral lipid fraction (**Supplementary Fig. 4**). Additionally, GC/MS analysis of the methanolized fractions revealed that residual amounts of alkyl ether lipids were only detectable in the lysophospholipid fraction of the *elbD* mutant (**Fig. 2a** and **Supplementary Table 3**). This finding matches well with the eukaryotic peroxisomal ether lipid biosynthetic pathway, where 1-*O*-alkyl-*sn*-glycero-3-phosphates, not 1-*O*-alkenyl-*sn*-glycero-3-phosphates, are the first intermediates[12]. The lost neutral lipid species mentioned before turned out to be the 1-alkyl-2,3-diacyl-*sn*-glycerol that usually accumulates in lipid bodies under starvation conditions, whereas overall triglyceride biosynthesis was less affected (**Fig. 2b** and **Supplementary Tables 4**, **5** and **11**)[6]. At the same time, lysophosphatidylethanolamines strongly accumulated in the lipid extract of starved *elbD* mutant cells (**Supplementary Tables 6** and **11**). High-performance LC (HPLC)/MS runs of freshly prepared lysophosphatidylethanolamine extracts from *elbD* mutants suggested that the fatty acyl

residue is bound to the *sn*-2 hydroxyl group of the glycerol backbone (**Supplementary Fig. 5**).

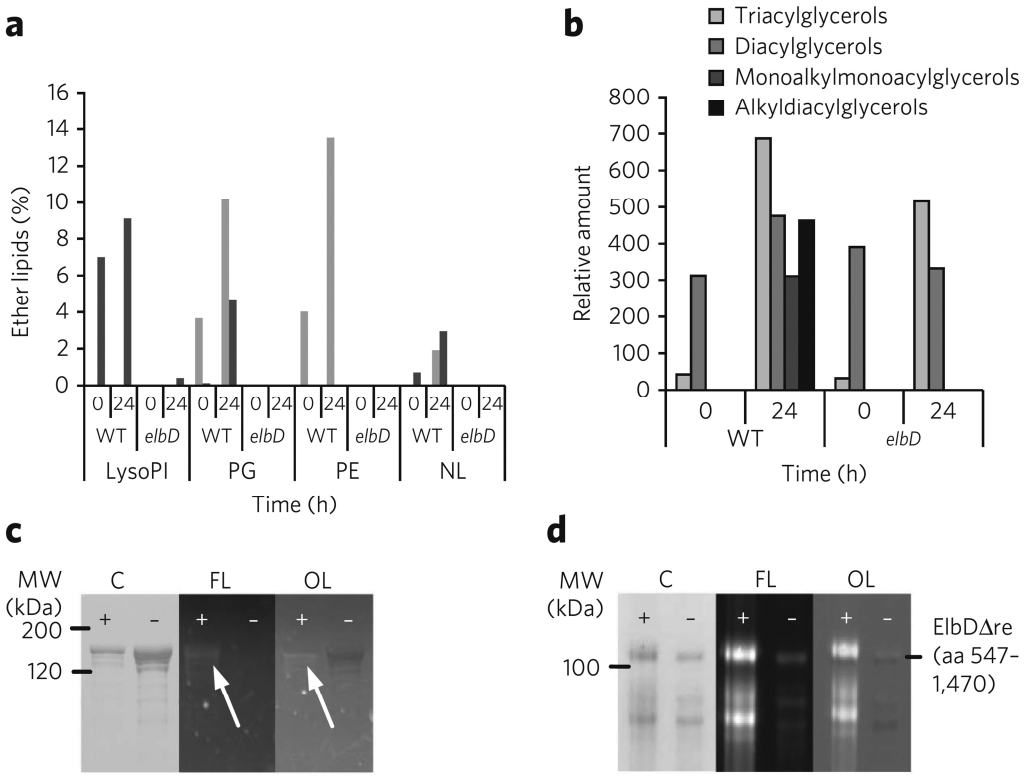

Figure 2 | Differential analysis of lipid fractions and biochemical characterization of ElbD. (**a**) Relative amounts of i15:0-OAG (dark gray) and i15:0-DMA (light gray), measured in percentage (n = 1) of lipid fractions, as determined by fatty acid methyl ester (FAME) GC/MS analysis. NL, neutral lipids; PE, glycerophosphoethanolamine; PG, glycerophosphoglycerol; LysoPl, lysophospholipid. (**b**) High-temperature GC/MS analysis of neutral lipid fractions (n = 1). Bars indicate amounts of lipids relative to the internal standard palmitylpalmitate (1,000 arbitrary units). (**c**) Enzymatic labeling of ElbD with fluorescent BODIPY-FL-CoA with (+) and without (−) Sfp. Average normalized fluorescence intensity is 5.3 × above control (n = 2; R = 2.2–8.4). (**d**) F488-DBCOlabeling of az15:0 loaded onto phosphopantetheinylated ACP domain of ElbDΔre with (+) and without (−) az15:0 in the assay. Average normalized fluorescence intensity is 4.7× above control (n = 2; R = 2.8–6.6). C, Coomassie blue stain; FL, fluorescence; OL, overlay. Numbers indicate apparent molecular weight in kDa. Additional protein bands proved to be C-terminally truncated translation products (full gel pictures are in **Supplementary Figs. 6** and **7**, and MS analysis of the protein bands is in **Supplementary Tables 12–16**).

For initial biochemical characterization, ElbD was labeled *in vitro* with the fluorescent CoA analog BODIPY-FL-CoA by the phosphopantetheinyltransferase Sfp[13], confirming a functional ACP domain (**Fig. 2c**). Similarly, auto-acylation of phosphopantetheinylated ElbDΔre (ElbD without the reduction domain) was observed after treatment with ATP and a free azido fatty acid following the addition of a clickable fluorescent dye (**Fig. 2d**), demonstrating the protein's ability to activate long chain fatty acids, as further supported by *in silico* docking (**Supplementary Figs. 8** and **9**) and bioinformatic analysis[14] (**Supplementary Tables 7** and **8**). Unfortunately, attempts to functionally express *MXAN_1531–1527* in *E. coli* did not result in ether lipid formation, as assessed by GC/MS.

For isolated ElbD, no acyltransferase domain protein activity was observable, preventing the exact evaluation of the activity elicited by the acyl transferase and reductase domain (Online Methods and **Supplementary Notes 1** and **2**). A phylogeny-based approach suggested that the acyl acceptor (**Supplementary Note 3**, **Supplementary Data Set 3** and **Supplementary Fig. 10**) could be 2-lysophosphatidylethanolamine. This was further supported by its accumulation in *elbD* mutants (**Supplementary Tables 6** and **11**) as well as by *in silico* docking experiments with the predicted acyl acceptor substrates into the ElbD AT domain modeled upon the crystal structure of the glycerolphosphate acyltransferase from *Curcubita moscata* (**Supplementary Figs. 8b** and **11**).

The reductase domain of ElbD is annotated as an acyl-CoA reductase (**Supplementary Data Set 2**). Such enzymes usually reduce CoA-bound fatty acids to fatty aldehydes or alcohols as part of wax ester biosynthesis[15]. However, we found neither fatty alcohols nor wax esters in the lipid extracts of *M. xanthus*. Therefore, we analyzed *M. xanthus* and *S. aurantiaca* cells for aldehyde formation as described[16]. Only i15:0 aldehyde could be identified in wild-type strains, and it was abolished in *elbD* mutants (**Supplementary Fig. 12**). We conclude from these findings that i15:0 aldehyde is the most likely product of the acyl-CoA reductase domain and is probably also involved in the formation of the vinyl ether bond.

Taking all of the results together, we have provided evidence that ElbD is involved in ether lipid biosynthesis, but more work will be needed to determine its biochemical mechanism. Although the exact functions of ElbABC remain unclear, it seems that they are dispensable for ether lipid formation or that their function can be complemented by other homologs encoded in the genome. Clues for a possible mechanism also come from Clostridia, which contain exclusively vinyl and no alkyl ether lipids. Here, metabolic labeling studies showed that, contrary to mammalian ether lipid biosynthesis[12], diacylglycerophosphoethanolamines are formed before the vinyl moiety is introduced[3], so our finding that only alkenyl- and not alkylacylglycerophosphoethanolamines are detectable in *M. xanthus* under both vegetative and developmental conditions (**Fig. 2a**) points to a possible 'reductive' ether lipid formation pathway. Additionally, the phosphatidylglycerol acetal of plasmenylethanolamine species, which require a hemiacetal intermediate in their biosynthesis, were described for *C. botulinum*[17]. *elbD* homologs can be found in many other bacterial genera, though the reductase domain is absent in most cases (**Supplementary Fig. 13**). Recently the multidomain enzyme DWA1, which is

involved in drought resistance and cuticular wax formation in *Oryza sativa* japonica rice, was described[18]; it has a domain structure similar to that of ElbD and has many homologs in other green vascular plants and bacteria but with an additional allene oxide synthase–like domain at the N terminus. The authors were able to prove A-domain activity but did not further investigate the activities of the other domains.

In summary, we have identified genes in myxobacteria that are involved in the formation of fatty acid derived ether lipids and provide a starting point for the evaluation of the sought-after ether lipid biosynthetic pathway in bacteria and their functions as well as the biotechnological production of ether lipids in bacteria. The latter aspect is of major ecological and technical importance because ether lipids for industrial, cosmetic and medicinal purposes are mainly obtained from shark liver oils[19], which are highly complex mixtures that strongly hamper the extraction of pure, defined lipids[20] and, further, threaten an increasing number of endangered species whose overall population is assumed to be decreasing steadily[21]. As ether lipids are part of the regulation cascade for myxobacterial fruiting body formation, we expect that future work concerning the regulation of their biosynthesis as well as the identification of their molecular target (or targets) will unveil the molecular basis of this fascinating process.

Received 14 September 2013; accepted 14 April 2014; published online 11 May 2014

6.2.3 Online methods

Bacterial strains, culture condition, imaging and chemicals. *M. xanthus* DK1622 and *S. aurantiaca* DW4/3-1 were grown in liquid CTT[22] and TS medium[23], respectively, at 30 °C and 200 r.p.m. on a rotary shaker until the desired optical density was obtained. All strains of *E. coli* were grown in liquid or on solid Luria Bertani (LB)[24] medium. For growth on agar plates, 1.5% agarose was added to the medium before autoclaving for solidification. Cultures of antibiotic-resistant mutant strains were supplemented with kanamycin (40 μg/ml) and/or chloramphenicol (34 μg/ml) to maintain plasmid stability or inserted gene disruption constructs. A complete list of all strains used in this study is in **Supplementary Table 10**.

All chemicals and analytical standards used for the experiments were, if not stated otherwise, obtained from Sigma-Aldrich Corporation or Carl-Roth GmbH and were at least

of analytical grade. Water was obtained from an Elga LabWater Model PL 5241 (VWS Deutschland GmbH) water purification system.

Pictures of protein gels were taken with transillumination by a light box using a model D90 reflex camera (Nikon GmbH, Germany) with a 60-mm prime lens, an aperture of f/16, an ISO value of 200 and an exposure time of 1/60 s at a resolution of 12 megapixels and saved in the NEF format. Pictures of western blots were taken under daylight the same way but with an aperture of f/3.5.

All pictures of fluorescent protein gels and primuline-stained thin layer chromatography (TLC) plates were acquired in a model UVIprochemi 2026 WL/UV26M (Biometra GmbH) gel documentation system. Gels were transilluminated with UV light at a wavelength of 366 nm and with an ethidium bromide filter (cutoff: λ = 580 nm) mounted in front of the camera lens. Fluorescent TLC pictures were taken with the UV light coming from the top (λ = 366 nm) and without a cutoff filter in front of the camera lens. The resolution of the pictures was 1.3 megapixels, and they were initially saved in the TIF format.

Cropping and adjustment of contrast and brightness to enhance the visibility of all details in the pictures and conversion into JPEG images were carried out using Lightroom 3 (Adobe Systems GmbH).

Pictures of developing *S. aurantiaca* cells on an agar surface were taken using a 1.4-megapixel Zeiss Axiocam Mrc digital camera (Carl Zeiss AG) attached to a SZH binocular (Olympus Europa Holding GmbH). Image data were acquired by the AxioVision Software (Carl Zeiss AG). The aperture was set to f/4.5, exposure time was 20 ms and JPEG was chosen as the image data format. The pictures of developing *M. xanthus* cells were recorded with a D90 reflex camera (Nikon GmbH) mounted on a Leica DM750 microscope (Leica microsystems GmbH) equipped with a 2.5× object lens. The aperture of the transmitted light was maximally closed, the exposure time was set to 1/125 s, the ISO value was 200 and NEF was chosen as the file format. Small deviations in brightness due to fluctuating thickness of the agar were adjusted afterwards.

For quantification of fluorescent bands as well as the corresponding Coomassie blue-stained bands obtained by the ACP loading assay and the adenylation domain assay (described below), ImageJ (version 1.47) was used. To calculate a normalized fluorescence, the quotient of control to sample in the Coomassie blue-stained picture of the

SDS-PAGE gels was multiplied with the quotient of the control to the sample band of their fluorescent images.

Starvation induced development in *M. xanthus.* Cells were grown vegetatively to an optical density (OD600) of ~1.2 (~3.8 × 10^8 cells/ml), pelleted, washed twice in MC7 buffer[25] and resuspended again in MC7 medium to a cell density to 5 × 10^9 cells/ml, of which 5 μl were spotted onto TPM agar[25] and incubated at 30 °C for up to 120 h. Sufficient cells for a FAME analysis or a lipid extract were obtained by plating 7.5 × 109 cells in 25 ml MC7 medium in petri dishes or 6 × 10^{10} cells in 150 ml MC7 medium in rectangular cell culture plates (25 cm × 25 cm), respectively, and incubated as mentioned above. For the sporulation assay, 1.27 × 10^9 vegetative cells in 3.5 ml MC7 buffer were developed in triplicate for 72 h and 120 h in petri dishes with a diameter of 3.5 cm.

Sporulation assay. The developed cells were incubated at 56 °C for 2 h to inactivate vegetative cells, harvested and resuspended in 10 ml water before treating with ultrasonic sound. 50 μl of this suspension in the case of the *elbD* mutant and 50 μl of a tenfold dilution for all of the other strains investigated were plated on CTTYE agar[26] plates for germination. The plates were incubated at 30 °C for 5 d, and colonies were counted. Mean and s.d. as well as *P* values were calculated analogously to those for the FAME data (**Supplementary Note 2**). Colony numbers were normalized to the wild type, which was defined as 100%. Detection limits were defined as less than one colony in one of the triplicates relative to wild-type colonies at the given time point.

Heterologous expression of *elbD* constructs in *E. coli* for protein purification. Two versions of *MXAN_1528* were heterologously expressed: A full-length version (*elbD)* was amplified using primers elbDmx_redom_BamHI-1 and elbDmx_-re_XhoI-2 and a shortened version without the reduction domain (*elbD*Δre) with elbDmx_-re_BamHI-1 and elbDmx_-re_XhoI-2; both fragments were subsequently cloned into the BamHI and XhoI restriction sites of pSUMO3_ck4 vector, giving rise to pSUMO3_ck4_elbD and pSUMO3_ck4_elbD_Δ_re. When induced, *elbD* and *elbD*Δre are expressed as fusion proteins with an N-terminal His_6SUMO3 tag to enhance correct folding of the protein product. The sequence of the constructs was verified by DNA sequencing of both strands. *E. coli* strain BL21(DE3) was used as an expression host. To further enhance correct folding and solubility, *elbD* and *elbD*Δre were coexpressed with the trigger factor gene *tig* from plasmid pTf16 (ref. 27). Expression procedures were carried out according to

standard procedures (pET System Manual, Merck-Millipore KGaA). Briefly, the expression strains were inoculated 1:100 (v/v) from an overnight culture in 1 l LB medium supplemented with chloramphenicol, kanamycin and 0.25 mg/ml arabinose, grown at 30 °C and 160 r.p.m. to an optical density of ~1.2. Protein expression was induced by adding isopropyl β-D-1-thiogalactopyranoside (IPTG) to a final concentration of 0.1 mM. Expression was performed at 16 °C and 160 r.p.m. for 16 h.

Heterologous expression of *elbA–E* in *E. coli* for testing *in vivo* activity. Genes *elbA–elbE* were heterologously expressed in *E. coli* BL21(DE3) while fed with i15:0 fatty acid and were subsequently analyzed for the presence of alkyl or vinyl ethers by FAME GC/MS. Genes *MXAN_1531*, *MXAN_1530*, *MXAN_1529* and *MXAN_1527* were synthesized with codon optimization for *E. coli* at Life Technologies and provided as cloning vectors pMK-RQ_MXAN_1527-1531exp_synth and pMK-RQ_MXAN_1530-1529exp_synthm, whereas *MXAN_1527* and *MXAN_1531* on the one hand and *MXAN_1530* and *MXAN_1529* on the other hand were made as artificial operons in a single reading frame.

Cloning procedures were executed as follows: in the first step, *elbD* was amplified from pSUMO3_ck4_elbD using primers elbDmx_exp_NdeI-3 and elbDmx_-re_XhoI-2, subcloned into pJet1.2/blunt (Thermo Scientific), sequenced and afterwards cloned into pCOLA_tacI/I via restriction sites NdeI and XhoI, giving rise to pCOLA_tacI/I_MCSII_*MXAN_1528*exp. Genes *MXAN_1530* and *MXAN_1529* were directly cloned into pCOLA_tacI/I_MCSII_MXAN_1528exp via restriction sites EcoRI and SdaI, giving rise to pCOLA_tacI/I_MCSI_MXAN_1530-1529exp_MCSII_MXAN_1528exp.

MXAN_1527 and *MXAN_1531* were cloned into pACYC_tacI/I using NdeI and XhoI, resulting in plasmid pACYC_tacI_MCSII_*MXAN*_1527_1531. To enable *E. coli* to form branched-chain fatty acids, genes *bkdA–C* from *Photorhabdus luminescens* TT01 (ref. 28) were cloned from plasmid pCOLA_bkd_C into pACYC_tacI_MCSII_ MXAN_1527_1531 using SacI and PstI, giving rise to pACYC_tacI_MCSI_bkdA-C_MCSII_ MXAN_1527_1531.

As both plasmids have compatible origins of replication and confer different antibiotic resistances, all of the genes were expressible together in *E. coli*. Additionally, the tacI

promoter in front of the genes enabled IPTG-dependent transcription with comparable transcript numbers.

For the expression experiment plasmids, *E. coli* BL21(DE3) cells were transformed with pCOLA_tacI/I_MCSI_MXAN_1530-1529exp_MCSII_MXAN_1528exp, pACYC_tacI_MCSI_bkdA-C_MCSII_ MXAN_1527_1531 and pET32a_mtaA_NdeI/XhoI in the samples and pCOLA_tacI/I, pACYC_tacI/I and pET32a in the controls.

Cells were grown at 37 °C overnight in Tanaka medium without IPTG. Expression experiments were performed in 1.5-ml volumes and adjusted to an OD600 of 1.0 with the following variables: medium: Tanaka or LB; IPTG concentrations: 0.05 mM, 0.1 mM or 0.4 mM; expression time and temperature: 16 h at 16 °C or 6 h at 23 °C; iso15:0 fatty acid concentration: 0.25 mM or 1 mM.

Cells were pelleted after the aforementioned expression times of 6 h or 16 h, subjected to FAME derivatization and analyzed by GC/MS as described above, and the resulting spectra were surveyed for the presence of dimethylacetals (indicative ion: m/z = 75) and *O*-alkylglycerols (indicative ion; m/z = 205) in general and i15:0 DMA and i15:0-OAG in particular as surrogates for the formation of alkylglycerols and 1*Z*-alkenylglycerols.

Heterologous expression of *sfp* and *mtaA* constructs in *E. coli.* The phosphopantetheinyltransferases Sfp from *Bacillus subtilis* and MtaA *from S. aurantiaca* DW4/3-1 were expressed in a similar way to *MXAN_1528*, but for Sfp, the sequence for the SUMO3 tag was removed during the cloning procedure using the *Pst*I and *Mun*I restriction sites of pSUMO3_ck5. Genomic DNA *B. subtilis* and *S. aurantiaca* DW4/3-1 were used as templates to amplify *sfp* and *mtaA*, respectively. For the *mtaA* PCR product, BglII/EcoRI restriction sites were used. The sequences of the constructs were verified by DNA sequencing. Expression conditions were identical to those mentioned above.

Purification of His6SUMO3ElbD and His6SUMO3ElbDΔre. Heterologously expressed proteins were purified from soluble fractions of cell lysates by nickel-NTA column chromatography and gel filtration chromatography. An ÄKTApurifier 10 FPLC system upgraded with a column screening kit, a sample application kit, air sensor kit and a fraction Collector Frac-950 (all from GE Corp.) was used for this purpose. All of the purification steps were monitored using SDS-PAGE[29] with normalized gel loading (pET System

Manual, Merck-Millipore KGaA). The pelleted cells form the protein expression were resuspended in 7 ml binding buffer (20 mM Tris-HCl 20 mM imidazole, 20% (w/v) glycerol, 0.1% (w/v) Triton X-100, pH 7.5) supplemented with 100 µl Protease Inhibitor Cocktail Set II (Calbiochem, Merck KGaA) and 25 U/ml benzonase (Merck KgaA) and lysed by adding 10,000 U/ml lysozyme and incubating for 30 min at room temperature. After centrifugation at 15,000*g* for 45 min, the supernatant was filtered through a 0.45-µM filter membrane and loaded to a 1-ml HisTrap HP column (GE corp.) and washed with 15 ml binding buffer (without Triton X-100). Recombinant proteins were eluted stepwise with 5 ml of 50 mM, 100 mM, 200 mM and 500 mM imidazole, respectively. Fractions containing the expressed proteins were pooled and concentrated to ~2 ml using Amicon ultra centrifugal filter units (Merck Millipore KGaA). Buffer exchange to gel filtration buffer (50 mM Tris-HCl, 10 mM MgCl2, 500 mM NaCl, 20% (w/v), pH 7.5, concentrated again to ~1 ml and treated with 60 U SUMO protease 2 (LifeSensors Inc.) in each case. For gel filtration, 500 µl of the SUMO protease digestion was separated on a Superdex 200 10/300 GL column (GE Corp.) and separated into 1-ml fractions at a constant flow rate of 0.3 ml/min. Again, fractions containing either ElbD or ElbDΔre were pooled, and buffer was exchanged to protein storage buffer (50 mM Tris-HCl, 10 mM MgCl2, 50% (w/v) glycerol, pH 7.5) and concentrated again using a Vivaspin500 Ultra Centrifugal filter units (Sartorius AG) to ~100 µl (ElbD) and ~200 µl (ElbDΔre). Protein concentrations were 0.6 µg/µl for ElbDΔre and 4.0 µg/µl for ElbD.

Protein fractionation for *in vitro* acyltransferases assay. Solubilized membrane fractions of *E. coli* cells expressing ElbD were used for this assay. The preparation of this fraction was performed very similarly to a method described in ref. 30. As a control, proteins from equally treated *E. coli* cells bearing only the empty expression vector were used.

Protein expression and cell lysis was carried out as described above. Unlysed cells were pelleted by centrifugation at 8,000*g* for 15 min at 4 °C. The supernatant was then again subjected to ultracentrifugation at 105,000*g* for 90 min at 4 °C to pellet the membranes and inclusion bodies of the lysed cells. The pellet was then resuspended in a buffer containing 100 mM Tris-HCl, pH 8.0, 300 mM NaCl, mixed with an equal amount of 1% sodium lauroyl sarcosinate, incubated for 20 min at room temperature under agitation and centrifuged again at 105,000*g* for 90 min at 4 °C to remove indissoluble protein. Protein

concentrations were 1.1 mg/ml in the control preparation and 0.8 mg/ml in the sample preparation.

Purification of His_6Sfp and His_6SUMO3MtaA. For His_6Sfp, purification was performed as mentioned above, but fractions from the nickel-NTA affinity chromatography were directly buffer exchanged to a storage buffer containing 50 mM 2-(4-(2-hydroxyethyl)-1-piperazinyl)-ethanesulfonic acid (HEPES), pH 7.6, 100 mM NaCl, 10% glycerol after combination of protein containing fractions and concentration. 4.1 mg of protein were obtained from 500 ml expression culture.

His_6SUMO3MtaA was purified using the Protino-Kit (Macherey-Nagel GmbH) according to the manufacturer's instructions and concentrated, and the buffer was exchanged as described for His_6Sfp, yielding 2.3 mg of protein from a 500-ml expression culture.

Fluorescent labeling of ACP domain using a CoA analog. BODIPY-CoA analogs were synthesized from BODIPY FL maleimide (Life Technologies) and coenzyme A as described previously[31] and *in vitro* labeling of ACP was performed similarly to a published procedure[31]. In short, 1 µl of ElbD or ElbDΔre was incubated overnight at 30 °C in a mixture of 5 µl 10× reaction buffer (750 mM 2-(*N*-morpholino)ethanesulfonic acid (MES), 100 mM $MgCl_2$, 1,500 mM NaCl, pH 6.0), 1 µl of ~200 µM BODIPY-Fl-CoA solution and 1 µl of Sfp solution filled up to 50 µl with water. After incubation, proteins were precipitated with 12.5 µl of 3 M trichloroacetic acid (TCA), pelleted, washed with water and pelleted again. After removal of the supernatant, the pellets were dried and redissolved in 10 µl 1 M Tris-HCl, pH 6.0, and 5 µl of 3× SDS-PAGE loading buffer at 95 °C for 5 min. Proteins were resolved on an 8% sodium dodecyl sulfate polyacrylamide gel (SDS-PAGE), and fluorescence was recorded as stated above with an aperture of f/1.4, a focal length of 95 mm and an exposure time of 15 s.

Acyl-ACP loading assay. The activity of the adenylation domain of ElbD has been determined by testing the ability of its shortened version, ElbDΔre, to load an azido-labeled fatty acid on its own ACP-domain, in a procedure similar to that published for the visualization of lipoproteins[32]. In the first step, ElbDΔre was phosphopantetheinylated by mixing 8.3 µl protein solution with 5 µl 50 mM Tris-HCl buffer, 10 mM $MgCl_2$, pH 7.5, buffer, 0.5 µl 10 mM Coenzyme A solution and 0.5 µl of a 10 µM MtaA solution; filled up to 50 µl with water; and incubated at 30 °C for 4 h. Afterward, 0.5 µl of a 100 mM solution of ATP (ATP) and 0.5 µl of a 10 µM of 15-azidopentadecanoic acid (az15:0) in DMSO

was added, followed by a further incubation at 30 °C for 5 h. To remove unreacted az15:0, the reaction mixture buffer was exchanged to 50 mM triethylamine (TEA), 150 mM NaCl, 0.1% (w/v) sodium dodecyl sulfate using PD SpinTrap G25 columns (GE Corp.). Acylated protein was fluorescently labeled by adding 3 µl of a 10-mM dibenzcyclooctyne-Fluor 488 (Fluor 488-DBCO) (Jena Bioscience GmbH) in dimethyl sulfoxide solution and incubating overnight at 37 °C. Proteins in the reaction mixture were precipitated as described in ref. 33, washed twice with 500 µl methanol and redissolved in 50 µl 1× SDS-PAGE loading buffer. 20 µl was resolved on a 10% SDS-PAGE. Pictures of the fluorescence were acquired as mentioned above with a focal length of 96 mm, an aperture of f/5.6 and an exposure time of 1 s.

In vitro **acyltransferase assay.** The AT assay was carried out under the following conditions: 100 mM Tris-HCl, pH 7.5, 10 mM $MgCl_2$, 1 mM ATP, 600 µM acyl donor (**Supplementary Note 2**), 150 µM of acyl acceptor (**Supplementary Note 2**) and 1 mg/ml BSA in a total volume of 100 µl. Incubation was performed at 30 °C for 45 min. Each sample contained 10 µg of tested protein. A sample without acyl donor served as a control. Lipids were extracted from the assay by the method described in ref. 34. In the samples in which monoacylglycerophosphates were used as test substrates, 10 µl of 10 M hydrochloric acid was added before the extraction procedure to protonate those lipids for a higher hydrophobicity. The lipids were dissolved in a mixture of dichloromethane:methanol:water 65:35:8 (v/v/v) when monoacylglycerophosphoethanolamines were used and dichloromethane:methanol:acetic acid 40:10:1 (v/v/v) when the samples contained monoacylglycerophosphates. Those samples were subjected to HPLC/MS analysis with a similar setup as described in **Supplementary Note 2** except that the gradient started at 30% B, was increased to 99% in a linear manner over 30 min and held for 7 min before reequilibration. HPLC/MS chromatograms were checked for *m*/*z* 671.5 in the positive ion mode and 626.5 in the negative ion mode, which would indicate incorporation of d7-i15:0 into PE(0:0/i15:0) or PA(0:0/i15:0), respectively.

Accession codes

GenBank: Sequences of expression plasmids pSUMO3_ck4, pSUMO4_ck5, pMK-RQ_MXAN_1527-1531exp_synth and pMK-RQ_MXAN_1530-1529exp_synth are

available under accession numbers KJ633124, KJ633125, KJ633122 and KJ633123, respectively.

6.2.4 References

1. Řezanka, T., Křesinová, Z., Kolouchová, I. & Sigler, K. *Folia Microbiol.* (*Praha*) **57**, 463–472 (2012).

2. Prins, R.A. & van Golde, L.M. *FEBS Lett.* **63**, 107–111 (1976).

3. Guan, Z. *et al. Biochim. Biophys. Acta* **1811**, 186–193 (2011).

4. Ring, M.W. *et al. J. Biol. Chem.* **281**, 36691–36700 (2006).

5. Whitworth, D.E. *Myxobacteria* (ASM Press, 2007).

6. Hoiczyk, E. *et al. Mol. Microbiol.* **74**, 497–517 (2009).

7. Bhat, S., Ahrendt, T., Dauth, C., Bode, H.B. & Shimkets, L.J. *mBio* **5**, e000939–13 (2014).

8. Curtis, P.D., Geyer, R., White, D.C. & Shimkets, L.J. *Environ. Microbiol.* **8**, 1935–1949 (2006).

9. Magnusson, C.D. & Haraldsson, G.G. *Chem. Phys. Lipids* **164**, 315–340 (2011).

10. Kearns, D.B. *et al. Proc. Natl. Acad. Sci. USA* **98**, 13990–13994 (2001).

11. Garcia, R.O., Reichenbach, H., Ring, M.W. & Müller, R. *Int. J. Syst. Evol. Microbiol.* **59**, 1524–1530 (2009).

12. Watschinger, K. & Werner, E.R. *Biochimie* **95**, 59–65 (2013).

13. Lambalot, R.H. *et al. Chem. Biol.* **3**, 923–936 (1996).

14. Khurana, P., Gokhale, R. & Mohanty, D. *BMC Bioinformatics* **11**, 57 (2010).

15. Lee, S.B. & Suh, M.C. *Mol. Plant* **6**, 246–249 (2013).

16. Wichard, T., Poulet, S.A. & Pohnert, G. *J. Chromatogr. B Analyt. Technol. Biomed. Life Sci.* **814**, 155–161 (2005).

17. MacDonald, D.L. & Goldfine, H. *Biochem. Cell Biol.* **68**, 225–230 (1990).

18. Zhu, X. & Xiong, L. *Proc. Natl. Acad. Sci. USA* **110**, 17790–17795 (2013).

19. Vannuccini, S. *Shark Utilization, Marketing and Trade* (Food and Agriculture Organization of the United Nations, 1999).

20. Fernández, Ó., Vázquez, L., Reglero, G. & Torres, C.F. *Food Chem.* **136**, 464–471 (2013).

21. Clarke, S.C., Harley, S.J., Hoyle, S.D. & Rice, J.S. *Conserv. Biol.* **27**, 197–209 (2013).

22. Bretscher, A.P. & Kaiser, D. *J. Bacteriol.* **133**, 763–768 (1978).

23. Mahmud, T. *et al. J. Biol. Chem.* **277**, 32768–32774 (2002).

24. Bertani, G. *J. Bacteriol.* **62**, 293–300 (1951).

25. Jakobsen, J.S. *et al. J. Bacteriol.* **186**, 4361–4368 (2004).

26. Rosario, C.J. & Singer, M. *J. Bacteriol.* **189**, 8793–8800 (2007).

27. Nishihara, K., Kanemori, M., Yanagi, H. & Yura, T. *Appl. Environ. Microbiol.* **66**, 884–889 (2000).

28. Brachmann, A.O. *et al. Angew. Chem. Int. Ed. Engl.* **51**, 12086–12089 (2012).

29. Laemmli, U.K. *Nature* **227**, 680–685 (1970).

30. Heath, R.J. & Rock, C.O. *J. Bacteriol.* **180**, 1425–1430 (1998).

31. La Clair, J.J., Foley, T.L., Schegg, T.R., Regan, C.M. & Burkart, M.D. *Chem. Biol.* **11**, 195–201 (2004).

32. Rangan, K.J., Yang, Y.Y., Charron, G. & Hang, H.C. *J. Am. Chem. Soc.* **132**, 10628–10629 (2010).

33. Wessel, D. & Flügge, U.I. *Anal. Biochem.* **138**, 141–143 (1984).

34. Bligh, E.G. & Dyer, W.J. *Can. J. Biochem. Physiol.* **37**, 911–917 (1959).

Acknowledgments

The authors are grateful to M. Ring for the identification of the *elb* operon; O. Schimming for providing the phosphopantetheinyl transferases; C. Kegler for providing expression plasmids pSUMO3_CK4, pSUMO3_CK5, pCOLA_tacI/I and pACYC_tacI/I; S. Fuchs for the MALDI-MS measurements; and A. Perèz for providing acyl donors. H.B.B. is grateful to the German Research Foundation (DFG) for an Emmy Noether fellowship that initiated this work.

Author contributions

H.B.B. conceived the work, W.L. and T.A. designed and performed the myxobacterial sporulation assay, and W.L. designed and performed all of the other experiments. Molecular modeling and ligand docking experiments were performed by K.A.J.B. H.B.B. and W.L. wrote the paper.

Competing financial interests

The authors declare no competing financial interests.

Additional information

Supplementary information is available in the online version of the paper. Reprints and permissions information is available online at http://www.nature.com/reprints/index.html. Correspondence and requests for materials should be addressed to H.B.B.

6.2.5 Supplementary Information

A multifunctional enzyme is involved in bacterial ether lipid biosynthesis

Wolfram Lorenzen, Tilman Ahrendt, Kenan A.J. Bozhüyük, Helge B. Bode

Supplementary Results

Supplementary Figure 1 | (next page) Phenotypes of *elbA, B, D, E* disruption mutants.

a) Microscopic plan view of developing M. xanthus cells with results of sporulation assay (italics numbers within 72 h images: mean % and standard deviation of colony forming units relative to wild type; n=3) at 72 / 120 h after starvation induced fruiting body formation (scale bars= 500 μm). Values greater than 10 % were rounded for the sake of readability. b) Changes of i15:0-OAG (dark grey) and i15:0-DMA (light grey) in mutant vegetative and developed cells compared to wild type (mean % and standard deviation; n=3). Asterisks indicate level of significance for the respective analyte (* $p<0.05$, ** $p<0.01$, *** $p<0.001$). c) Microscopic plan view of aggregating *S. aurantiaca* cells. Sporulation experiments of *S. aurantiaca* were not feasible as strain DW4/3-1 does not form fruiting bodies under our laboratory conditions. However, note the „spot“ like aggregate of the elbD mutant in comparison to the „ring“ like aggregates of the wild type (scale bars= 1000 μm). d) Changes of i15:0-OAG (dark grey), i15:0-DMA (light grey), 15:0-OAG (dotted) and 16:1-OAG (shaded) in mutant vegetative cells compared to wild type (mean % and standard deviation; n=3). Asterisks indicate level of significance for the respective value referred to wild type result (* $p<0.05$, ** $p<0.01$, *** $p<0.001$). See Supplementary Data Set 1, Supplementary Table 2 and 3 for full FAME patterns, results of sporulation assay and statistics. n.a.: data not available.

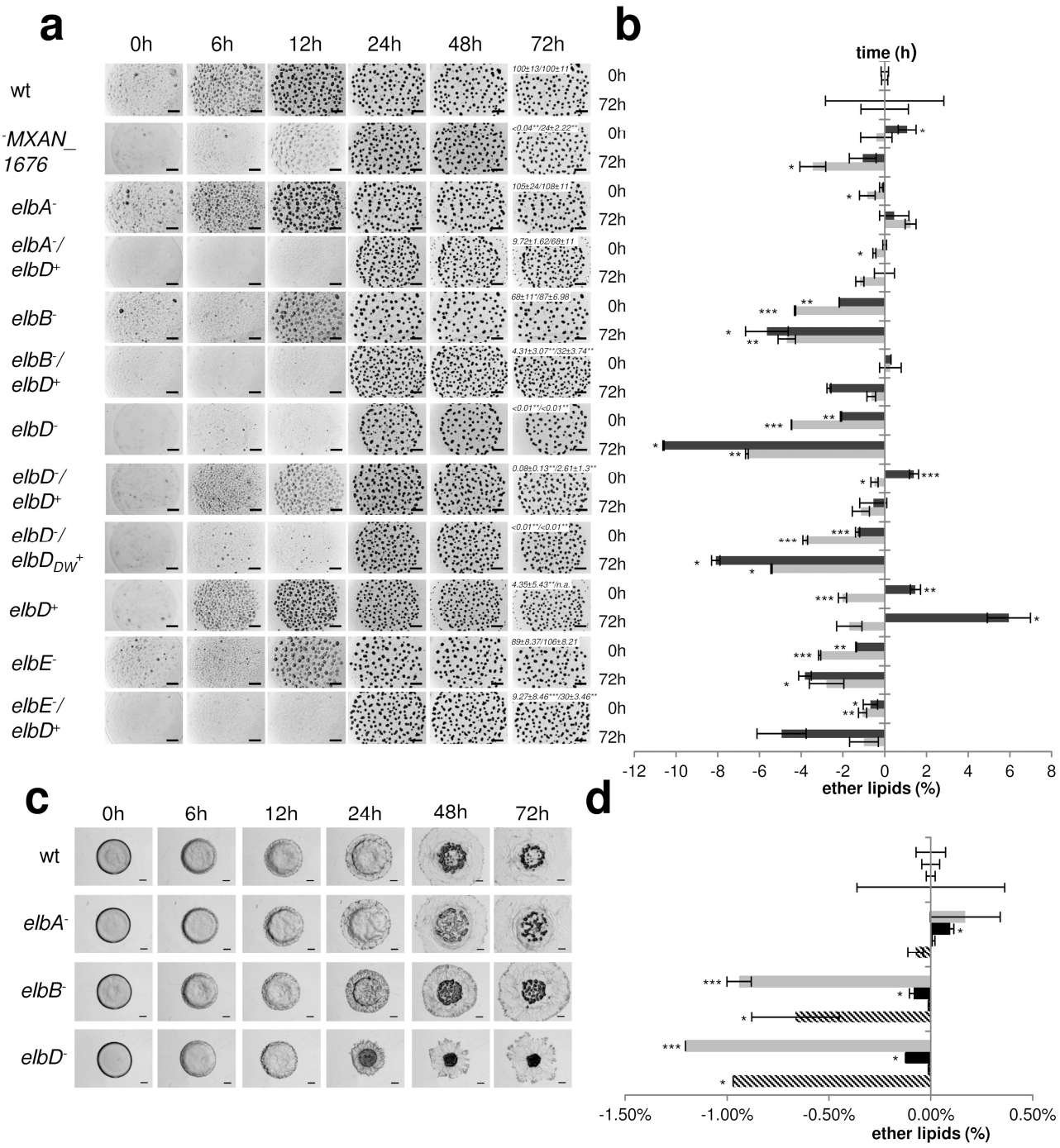
a
0h
6h
12h
24h
48h
72h
wt
-MXAN_1676
elbA-
elbA-/elbD+
elbB-
elbB-/elbD+
elbD-
elbD-/elbD+
elbD-/elbDDW+
elbD+
elbE-
elbE-/elbD+
100±13/100±11
<0.04**/24±2.22**
105±24/108±11
9.72±1.62/68±11
68±11*/87±6.98
4.31±3.07**/32±3.74**
<0.01**/<0.01**
0.08±0.13**/2.61±1.3**
<0.01**/<0.01**
4.35±5.43**/n.a.
89±8.37/106±8.21
9.27±8.46**/30±3.46**
b
time (h)
0h
72h
-12
-10
-8
-6
-4
-2
0
2
4
6
8
ether lipids (%)
c
0h
6h
12h
24h
48h
72h
wt
elbA-
elbB-
elbD-
d
-1.50%
-1.00%
-0.50%
0.00%
0.50%
ether lipids (%)

Supplementary Figure 2 | (next page) *elbA-E* homologues in all sequenced myxobacteria

The operon structure of *elbA-E* orthologous in myxobacteria is shown. *elbD* and *elbE* are in all but one case overlapping, *elbB* and *elbC* are located either close to *elbD* and *elbE* upstream or can be found somewhere else in the genome. *elbA* is more separated from *elbB-E* or absent in some of the genomes. This provides further evidence for the hypothesis that the decreased ether lipid formation in *elbB* insertion mutants is rather due to diminished *elbD* expression by polar effects than due to an involvement of *elbB* and *elbC* in ether lipid formation (Supplementary Figure 1). For further details see Supplementary Data Set 2. Italic numbers indicate gene length and length between genes in base pairs respectively.

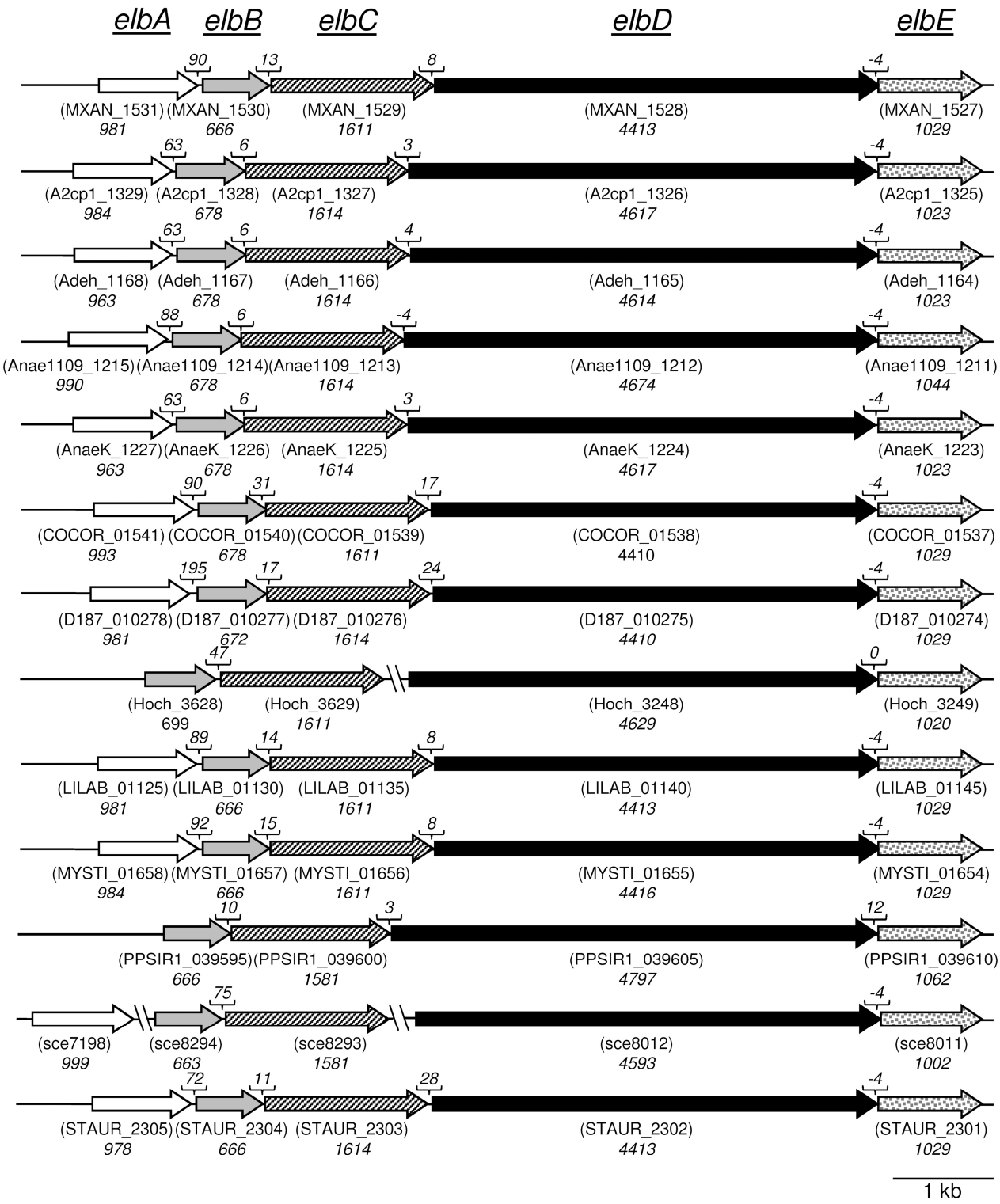
elbA
elbB
elbC
elbD
elbE
90
13
8
-4
(MXAN_1531) (MXAN_1530) (MXAN_1529) (MXAN_1528) (MXAN_1527)
981 666 1611 4413 1029
63
6
3
-4
(A2cp1_1329) (A2cp1_1328) (A2cp1_1327) (A2cp1_1326) (A2cp1_1325)
984 678 1614 4617 1023
63
6
4
-4
(Adeh_1168) (Adeh_1167) (Adeh_1166) (Adeh_1165) (Adeh_1164)
963 678 1614 4614 1023
88
6
-4
-4
(Anae1109_1215) (Anae1109_1214) (Anae1109_1213) (Anae1109_1212) (Anae1109_1211)
990 678 1614 4674 1044
63
6
3
-4
(AnaeK_1227) (AnaeK_1226) (AnaeK_1225) (AnaeK_1224) (AnaeK_1223)
963 678 1614 4617 1023
90
31
17
-4
(COCOR_01541) (COCOR_01540) (COCOR_01539) (COCOR_01538) (COCOR_01537)
993 678 1611 4410 1029
195
17
24
-4
(D187_010278) (D187_010277) (D187_010276) (D187_010275) (D187_010274)
981 672 1614 4410 1029
47
0
(Hoch_3628) (Hoch_3629) (Hoch_3248) (Hoch_3249)
699 1611 4629 1020
89
14
8
-4
(LILAB_01125) (LILAB_01130) (LILAB_01135) (LILAB_01140) (LILAB_01145)
981 666 1611 4413 1029
92
15
8
-4
(MYSTI_01658) (MYSTI_01657) (MYSTI_01656) (MYSTI_01655) (MYSTI_01654)
984 666 1611 4416 1029
10
3
12
(PPSIR1_039595) (PPSIR1_039600) (PPSIR1_039605) (PPSIR1_039610)
666 1581 4797 1062
75
-4
(sce7198) (sce8294) (sce8293) (sce8012) (sce8011)
999 663 1581 4593 1002
72
11
28
-4
(STAUR_2305) (STAUR_2304) (STAUR_2303) (STAUR_2302) (STAUR_2301)
978 666 1614 4413 1029
1 kb

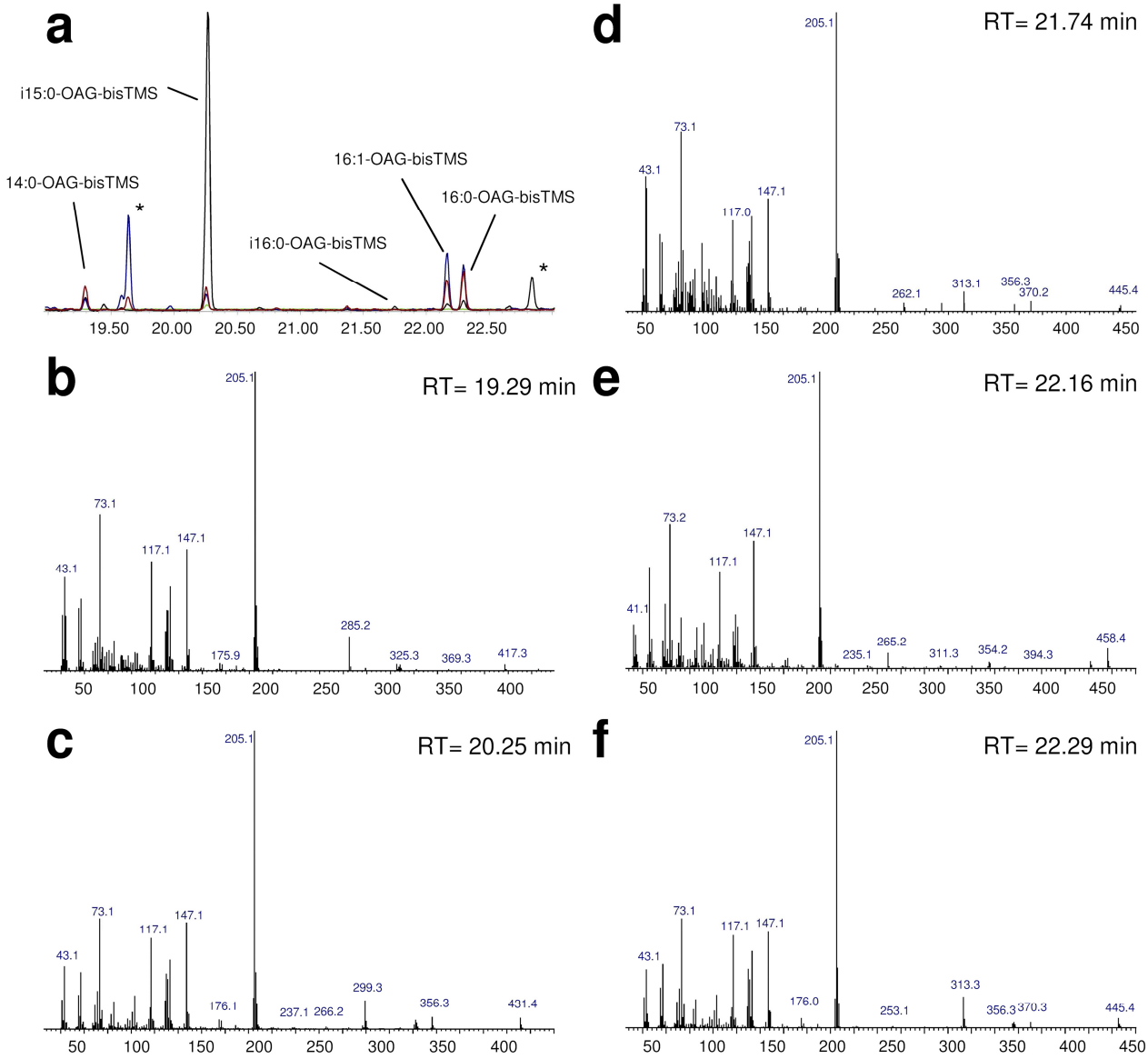

Supplementary Figure 3 | EI-MS chromatograms of *O*-alkylglycerols from various myxobacteria.

a) Excerpt of GC-MS total ion chromatograms of different myxobacterial wild type strains from whole cell fatty acid methyl esters. Asterisks indicate signals of non-ether lipid molecules. blue: *Sorangium cellulosum* So ce377; black: *Cystobacter sp.* SBCb004; green: *Myxococcus xanthus* DK897; red: *Sorangium cellulosum* So ce56 **b-f)** Electron impact mass spectra of 14:0-, i15:0-, i16:0-, 16:1- and 16:0-OAG-bisTMS respectively. Spectra were interpreted as described previously[4].

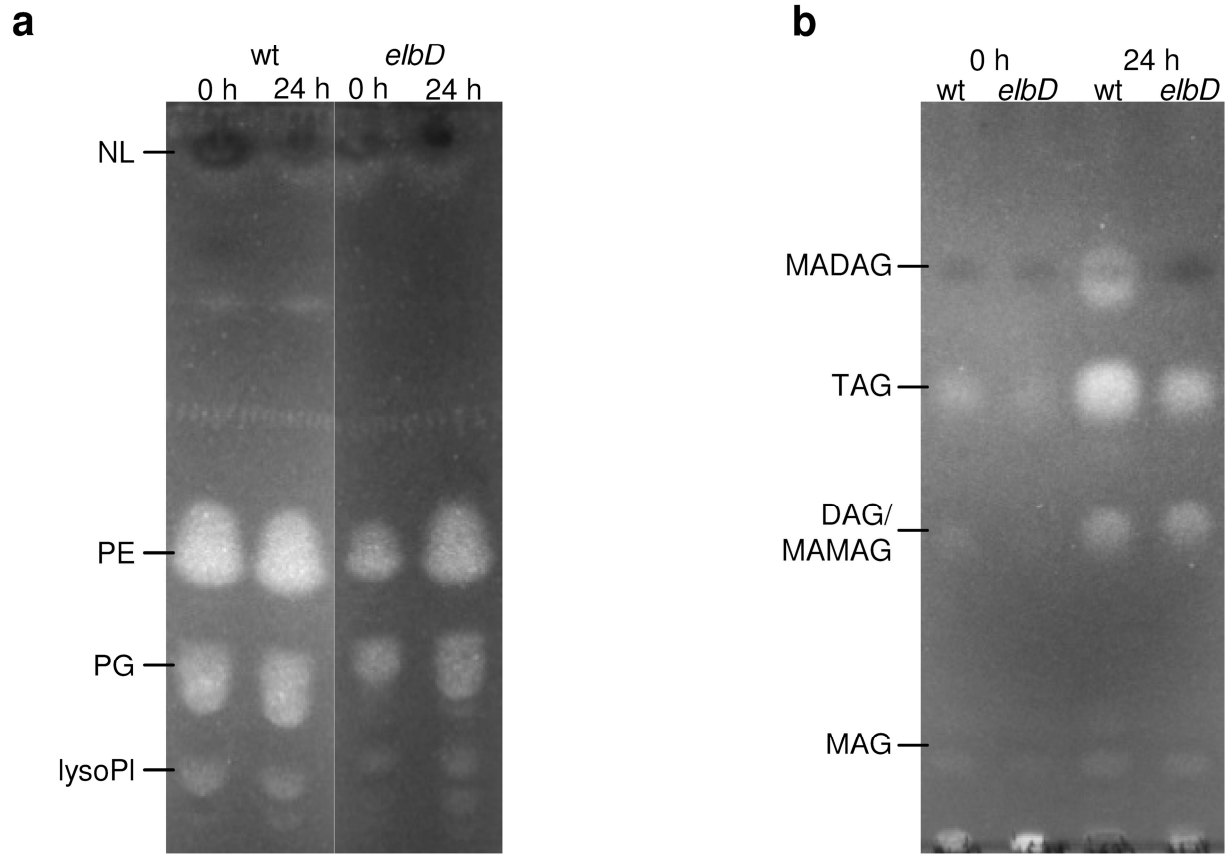

Supplementary Figure 4 | Lipid composition of *M. xanthus* and its *elbD* mutant.

Primuline-stained TLC plates of lipid extracts from vegetative *M. xanthus* cells (0 h) and those developed for 24 h, with resolved phospholipids (**a**) and neutral lipids (**b**). NL, neutral lipids; PE, glycerophosphoethanolamine; PG, glycerophosphoglycerol; LysoPl, lysophospholipid; MADAG, alkyldiacylglycerol; TAG, triacylglycerol; DAG, diacylglycerol; MAMAG, monoalkylmonoacylglycerol; MAG, monoacylglycerol. Note the loss of the MADAG spot in the lipid extract of *elbD* after 24 h of development.

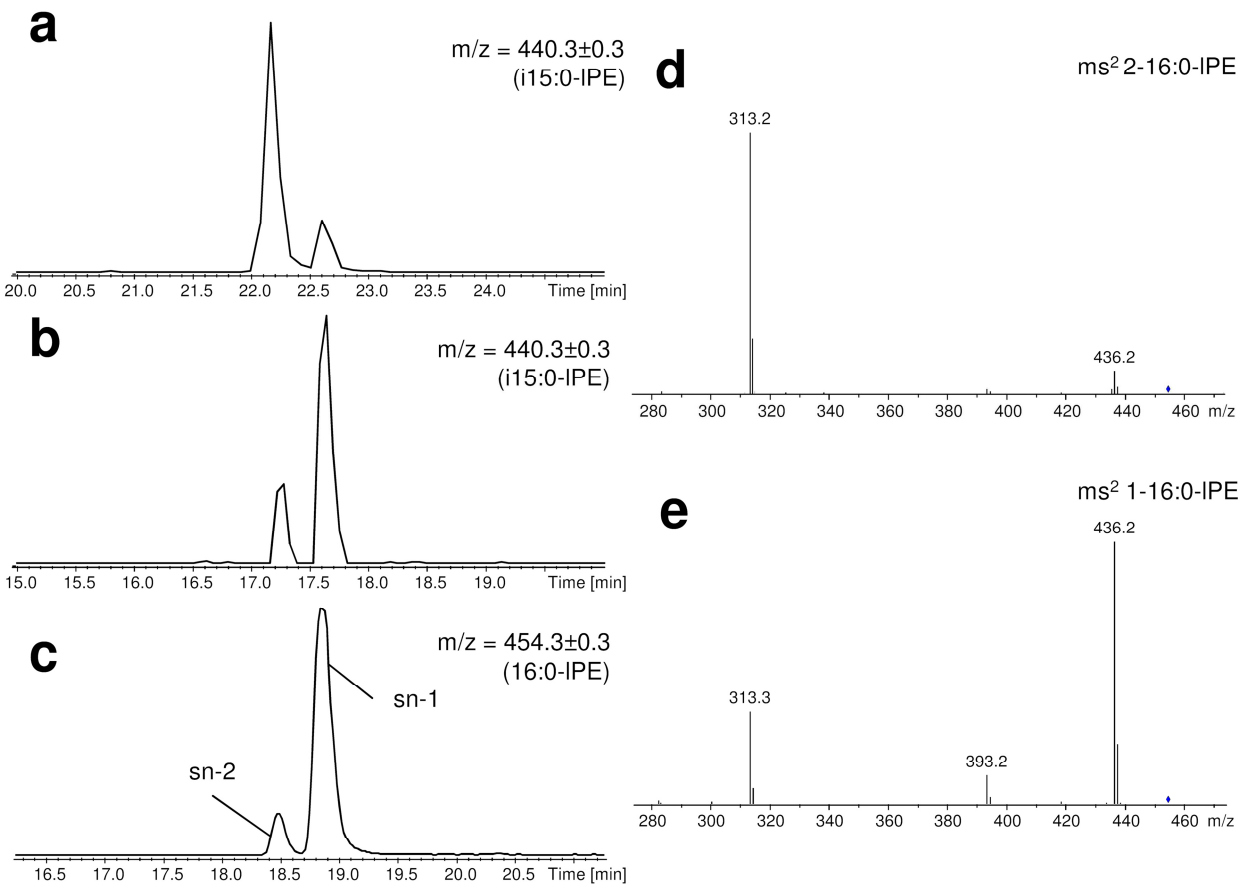

Supplementary Figure 5 | 2-acyl-lyso-PEs are formed by *M. xanthus*

Extracted ion chromatograms of lysophosphosphatidylethanolamines from a freshly prepared DK1622 lipid extract **a)**, an extract stored for a prolonged time **b)** and a 1-acyllyso-PE standard from Sigma **c)** with the typical ~9:1 molar ratio of *sn*-1 to *sn*-2 isomer[35]. Mass spectra **d)** and **e)** show that in loss of the polar headgroup is favored over the loss of water in the case of the *sn*-2 isomer whereas it is vice versa in the case of the sn-1 isomer. The differing retention times derive from the instance that different HPLC-MS systems and gradients were used.

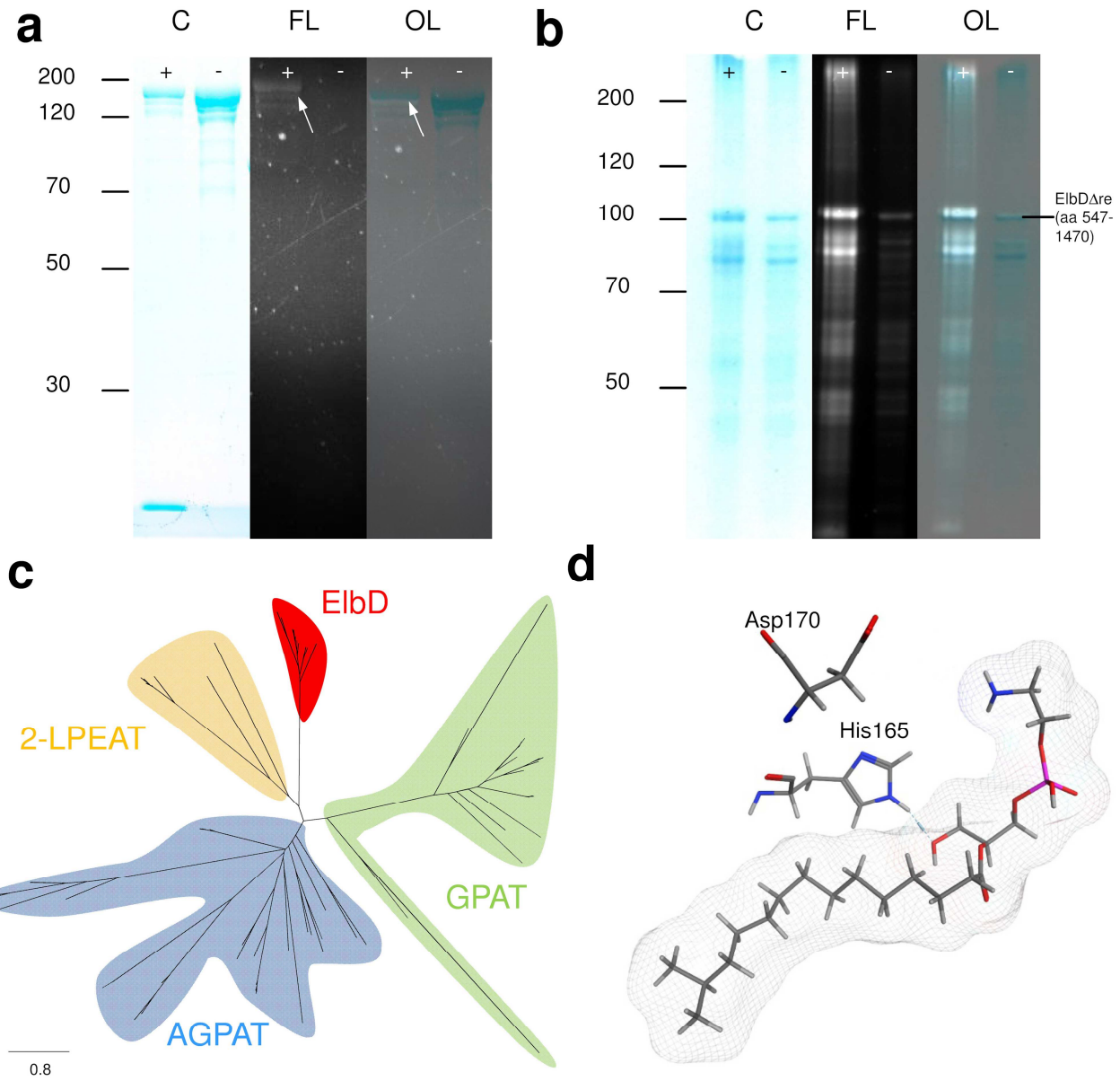
a
C
FL
OL
200
120
70
50
30
+
-
b
C
FL
OL
200
120
100
70
50
ElbDΔre
(aa 547-
1470)
c
ElbD
2-LPEAT
GPAT
AGPAT
0.8
d
Asp170
His165

Supplementary Figure 6 | (previous page) Biochemical characterization of ElbD.

a) Full gel image of Figure 2c. Enzymatic labeling of ElbD with fluorescent BODIPY-FL Coenzyme A with (+) and without (-) Sfp. Average normalized fluorescence intensity is 5.3× above control (n = 2; R = 2.2-8.4). **b)** Full gel image of Figure 2d. F488-DBCO labeling of az15:0 loaded onto phosphopantetheinylated ACP domain of ElbDΔre with (+) and without (-) az15:0 in the assay. Average normalized fluorescence intensity is 4.7× above control (n = 2; R = 2.8-6.6). C: coomassie stain; FL: fluorescence; OL: overlay. Numbers indicate apparent molecular weight in kD. **c)** Phylogenetic tree (PHYML) of trimmed sequences from long chain acyltransferases from various organisms that cluster well according to their specificity. 2-LPEAT: 2-lysophosphatidylethanolamine acyltransferase; AGPAT: 1-acylglycerolphosphate acyltransferase; GPAT: glycerolphosphate acyltransferase; for details see Supplementary Figure 9 and Supplementary Data Set 3 **d)** *In-silico* docking of 2-i15:0-lysophosphatidylethanolamine into the acyltransferase domain of ElbD. Grid shows electron cloud of the substrate. Note the interaction between the hydroxyl group in the *sn*-2 position of the glycerol moiety with the putative charge relay system of Asp170 and His165.

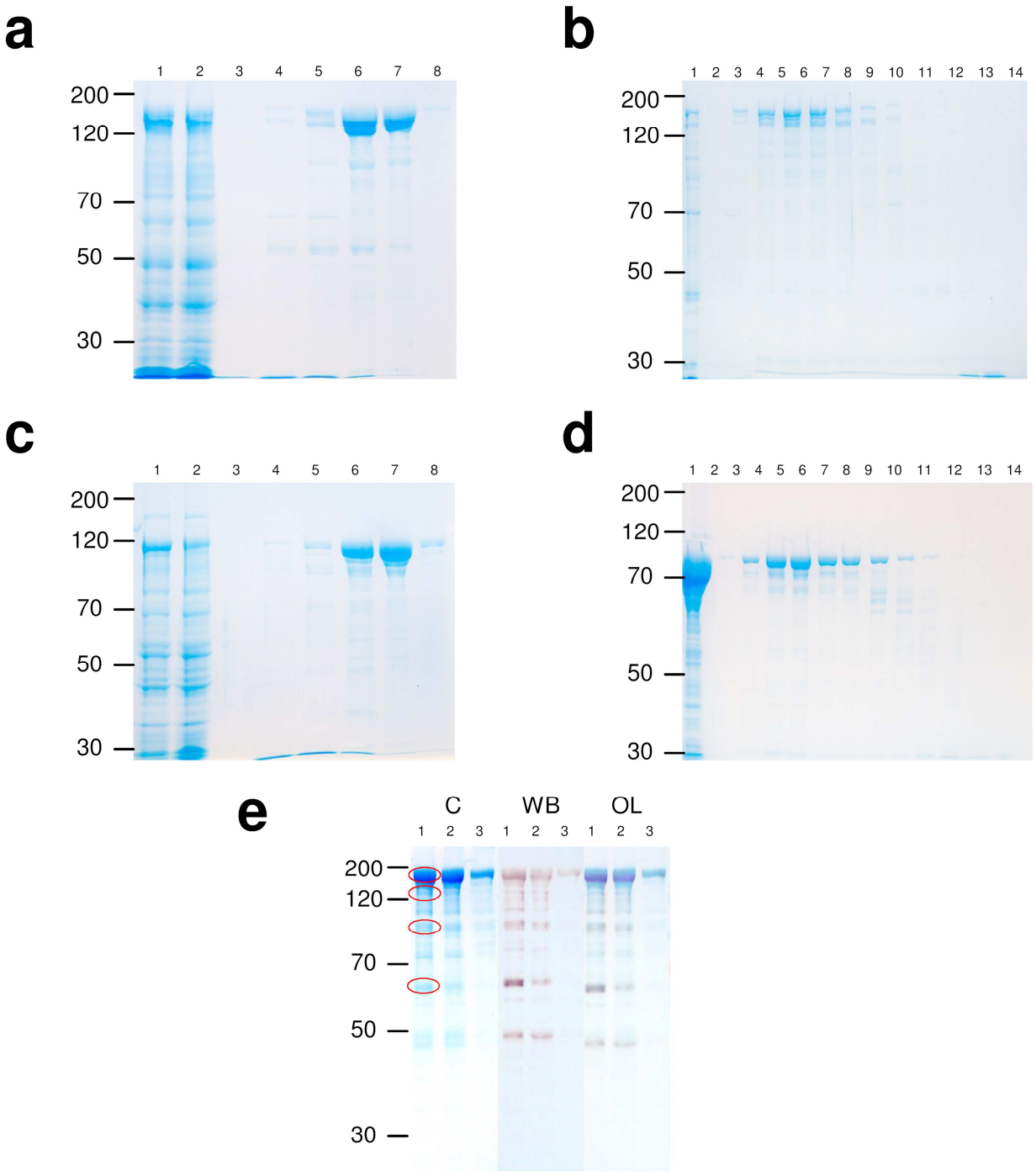
a
1 2 3 4 5 6 7 8
200
120
70
50
30
b
1 2 3 4 5 6 7 8 9 10 11 12 13 14
200
120
70
50
30
c
1 2 3 4 5 6 7 8
200
120
70
50
30
d
1 2 3 4 5 6 7 8 9 10 11 12 13 14
200
120
70
50
30
e
C
WB
OL
1 2 3 1 2 3 1 2 3
200
120
70
50
30

Supplementary Figure 7 | (previous page) Truncated translation products of ElbD when expressed in *E. coli.*

SDS-PAGE of Ni-NTA affinity chromatography fractions (3-8) of His6SUMO3ElbD (**a**) and His6SUMO3ElbDΔre (**c**) (1: pellet fraction; 2: soluble fraction). SDS-PAGE of SEC fractions (2-14) of the respective Sumo2 protease treated Ni-NTA chromatography fractions of ElbD (**b**) and ElbDΔre (**d**) (1: pellet fraction). **e**) Coomassie stained SDS-PAGE (left), western blot (center) and merge (right) of various Nickel-NTA affinity chromatography fractions. Co-eluting bands are products of flawed His_6SUMO3ElbD translation. Numbers indicate apparent molecular weight. Additional bands with smaller molecular weight than the target protein proved to be truncated translation products as shown by western blot and peptide mass finger print (see Supplementary Table 12-16). C: coomassie stain; WB: western blot; OL: overlay

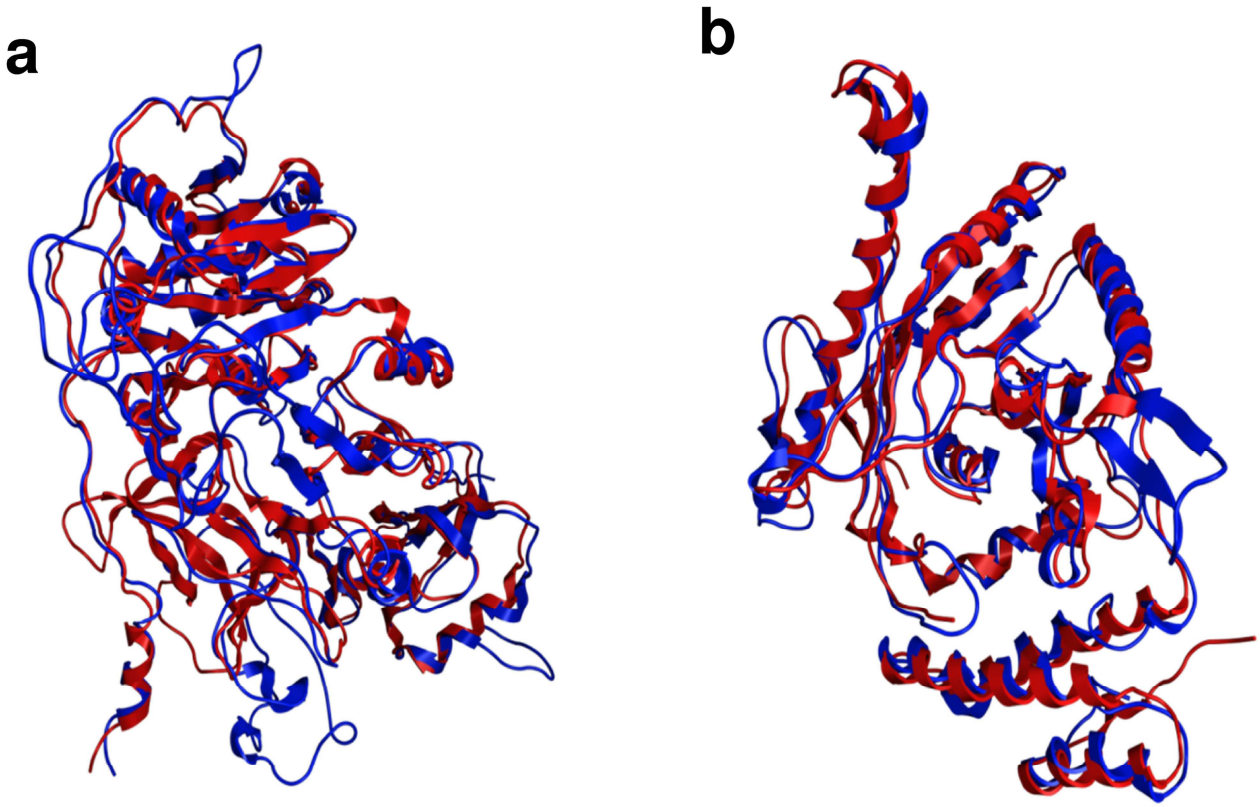

Supplementary Figure 8 | Modeling of A- and AT-domain of ElbD

a) Superposition of the ElbD A-Domain (blue) homology model (RMSD: 1.7 Å) modelled on the 1.9 Å chrystal structure of PheA from the gramicidin synthetase from *Bacillus brevis* (red) **b)** Superposition of a 364aa stretch comprising the ACP and AT domain of ElbD modelled on the chrystal structure of the stromal GPAT from *Curcubita moscata* (RMSD: 1.4 Å).

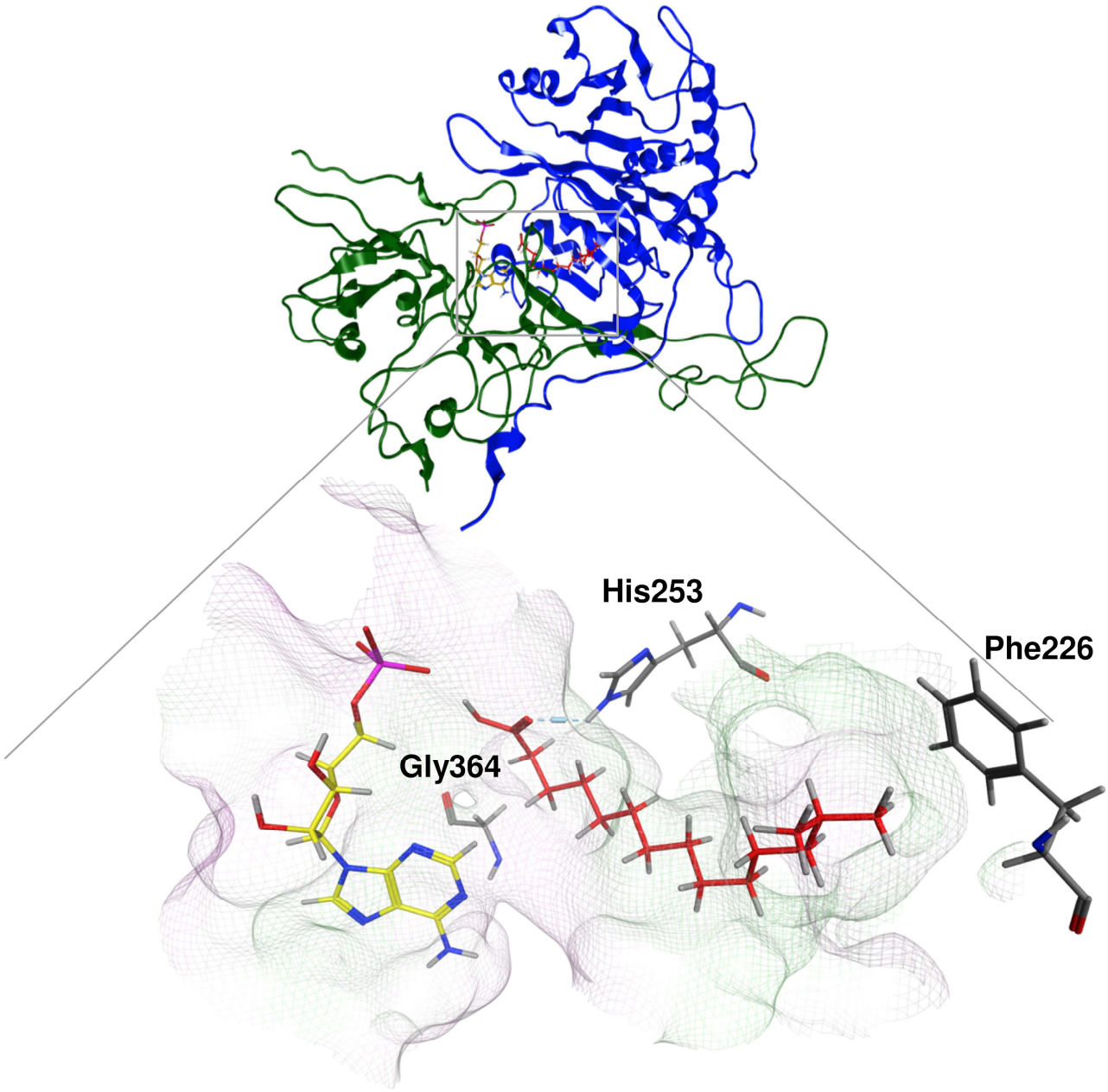

Supplementary Figure 9 | Docking of fatty acyl substrate in ElbD A-Domain.

Ribbon representation of ElbD A-domain (top view; blue: N-terminal subdomain; green: C-terminal subdomain) with docked AMP (CHEMPLP-score: 43.34) and iso15:0 (CHEMPLP-score: 65.24). The active site is located in the cleft between the two subdomains. Magnified view (bottom view) of the binding pocket shows hydrophobic (green) and hydrophilic (purple) surfaces. Gly364 provides the necessary space to access the hydrophobic tunnel for long chain fatty acids, Phe226 is limiting the maximal length and His253 is necessary for the binding of the fatty acid by interacting with its carboxy moiety.

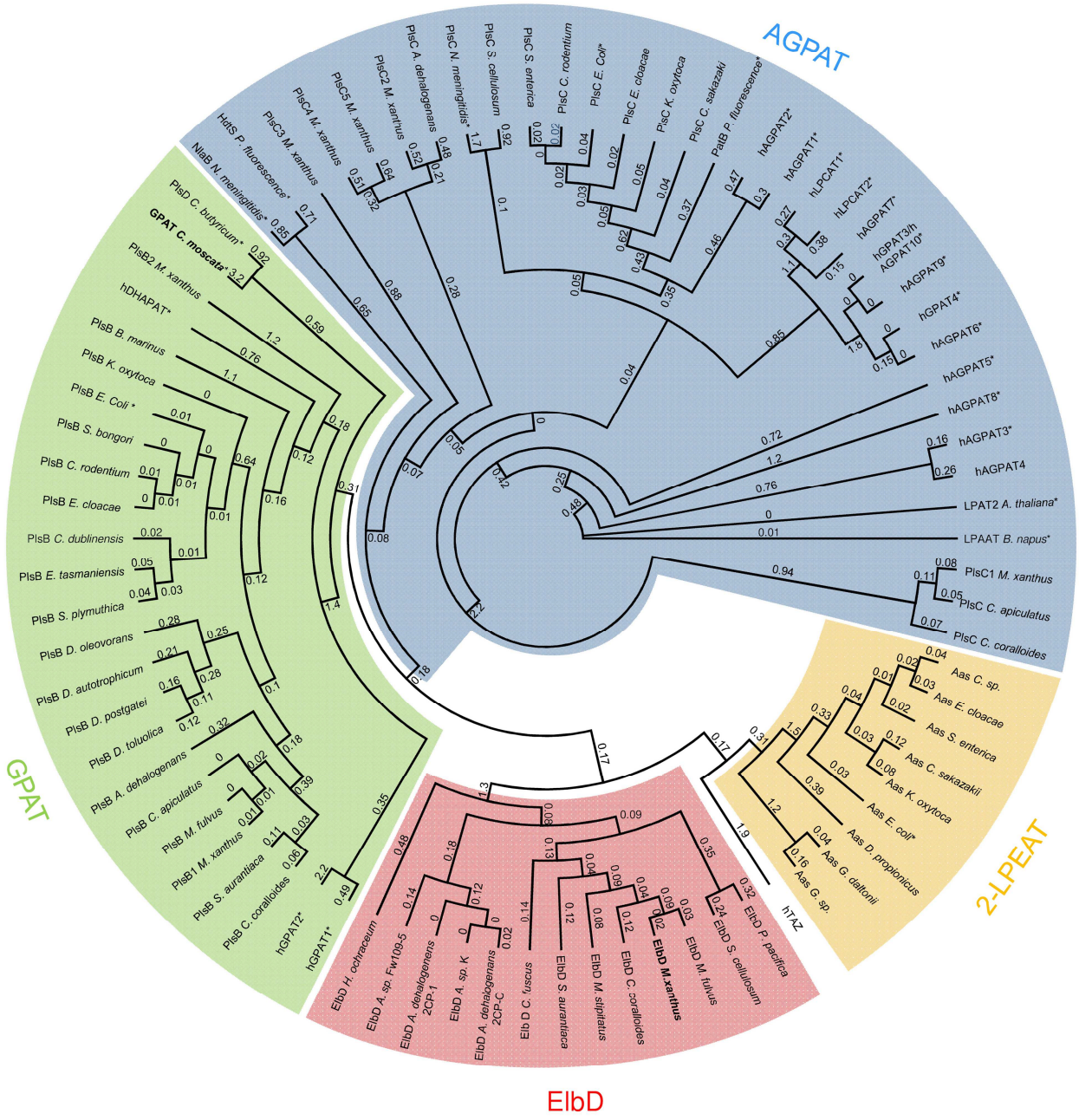
AGPAT
GPAT
2-LPEAT
ElbD
PlsC S. cellulosum
PlsC S. enterica
PlsC C. rodentium
PlsC E. Coli*
PlsC E. cloacae
PlsC K. oxytoca
PlsC C. sakazakii
PatB P. fluorescence*
hAGPAT2*
hAGPAT1*
hLPCAT1*
hLPCAT2*
hAGPAT7*
hGPAT3/h AGPAT10*
hAGPAT9*
hGPAT4*
hAGPAT6*
hAGPAT5*
hAGPAT8*
hAGPAT3*
hAGPAT4
LPAT2 A. thaliana*
LPAAT B. napus*
PlsC1 M. xanthus
PlsC C. apiculatus
PlsC C. coralloides
PlsC N. meningitidis*
PlsC A. dehalogenans
PlsC2 M. xanthus
PlsC5 M. xanthus
PlsC4 M. xanthus
PlsC3 M. xanthus
HdtS P. fluorescence*
NlaB N. meningitidis*
PlsD C. butyricum*
GPAT C. moscata*
PlsB2 M. xanthus
hDHAPAT*
PlsB B. marinus
PlsB K. oxytoca
PlsB E. Coli *
PlsB S. bongori
PlsB C. rodentium
PlsB E. cloacae
PlsB C. dublinensis
PlsB E. tasmaniensis
PlsB S. plymuthica
PlsB D. oleovorans
PlsB D. autotrophicum
PlsB D. postgatei
PlsB D. toluolica
PlsB A. dehalogenans
PlsB C. apiculatus
PlsB M. fulvus
PlsB1 M. xanthus
PlsB S. aurantiaca
PlsB C. coralloides
hGPAT2*
hGPAT1*
hTAZ
Aas C. sp.
Aas E. cloacae
Aas S. enterica
Aas C. sakazakii
Aas K. oxytoca
Aas E. coli*
Aas D. propionicus
Aas G. daltonii
Aas G. sp.
ElbD H. ochraceum
ElbD A. sp. Fw109-5
ElbD A. dehalogenens 2CP-1
ElbD A. sp. K
ElbD A. dehalogenans 2CP-C
Elb D C. tuscus
ElbD S. aurantiaca
ElbD M. stipitatus
ElbD C. coralloides
ElbD M.xanthus
ElbD M. fulvus
ElbD S. cellulosum
ElbD P. pacifica

Supplementary Figure 10 |(previous page) Phylogenetic analysis of acyltransferase domains with different substrate specificities.

Unrooted cladogram of phylogenetic analysis of acyltransferase domains from various sources (Supplementary Table 9) derived from a trimmed MAFFT alignment (Supplementary Data Set 3). Acyltransferases with various preferences concerning the hydroxyl functions of the glycerol phosphate acceptor (*sn-1* or *sn-2*, acylation or no acylation) cluster within distinct branches, whereupon the acyltransferase domains of the ElbD homologues forms its own branch with 2-lysophosphatidylethanolamine acyltransferase (2-LPEAT) domains that exhibit a specificity towards 2-acylglycerolphosphoethanolamine. Numbers indicate distance given in substitutions per site. Asterisks indicate acyltransferases with experimentally determined substrate specificities. GPAT from *C. moscata* and AT-domain of ElbD from *M. xanthus* are highlighted in bold. For details concerning the alignment see Supplementary Data Set 3 Supplementary Table 9. 2-LPEAT: 2-lysophosphatidylethanolamine acyltransferase; AGPAT: 1-acylglycerolphosphate acyltransferase; GPAT: glycerolphosphate acyltransferase.

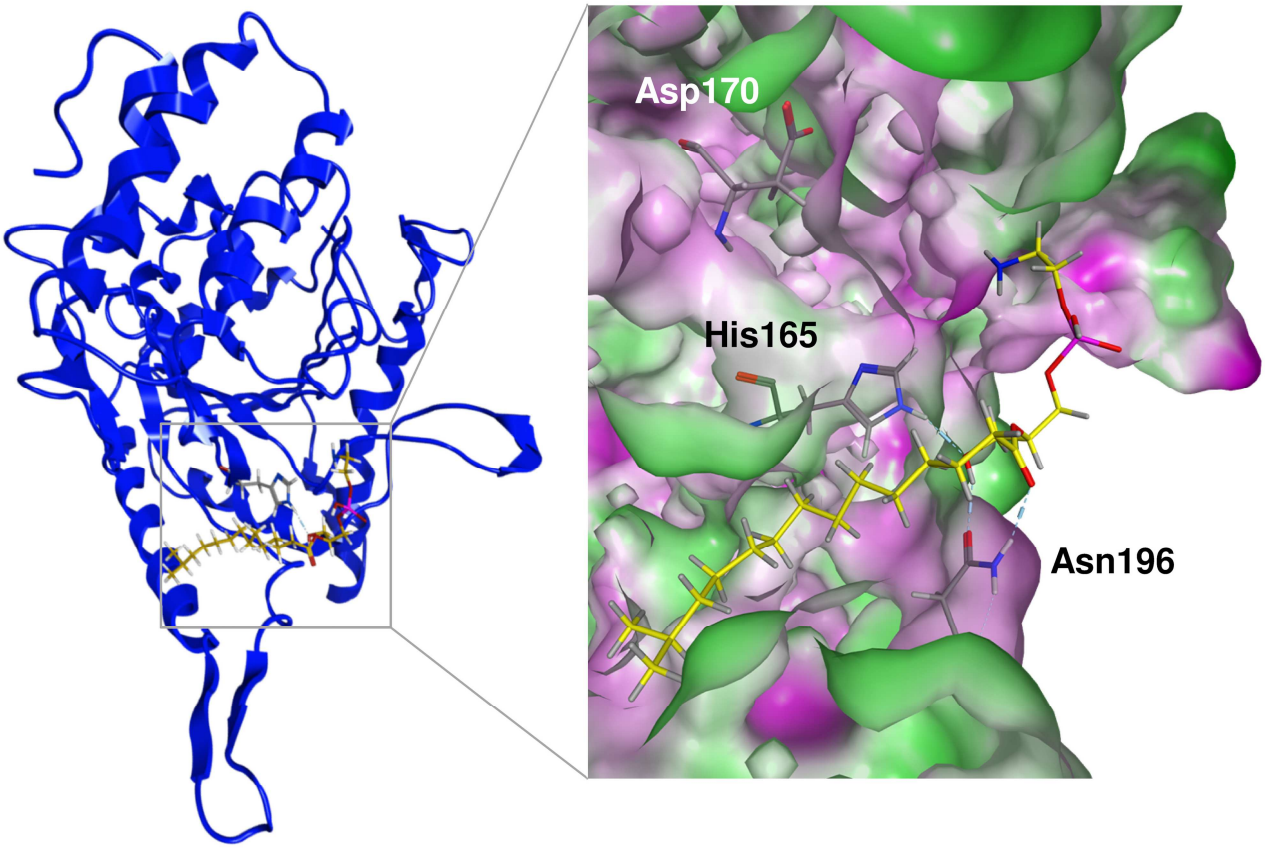

Supplementary Figure 11 | Docking of putative ElbD substrate in acyl transferase model.

Ribbon representation (left) of ElbD AT domain with docked 2-i15:0-lysophosphatidylethanolamine (CHEMPLP-score: 71.75). Magnified view (right) of 2-i15:0-lysophosphatidylethanolamine docked into the putative binding pocket of the AT -domain (green and purple hydrophobic and hydrophilic surfaces respectively). The docking experiments for the ElbD AT domain with 2-isopentadecanoylphosphatidylethanolamine proposed interactions with $H(X)_4D$ motif of the amino acids Asp170 and His165 which are invariant in homologues sequences[36] forming a putative charge relay system that can abstract the hydrogen from the free 1-hydroxy group, which in turn enables the attack of this hydroxyl oxygen at the carbonyl carbon of the acyl donor during the ester formation. This arrangement resembles the active site of serine proteases and epoxide hydrolases and was also postulated for acyltransferases[37].

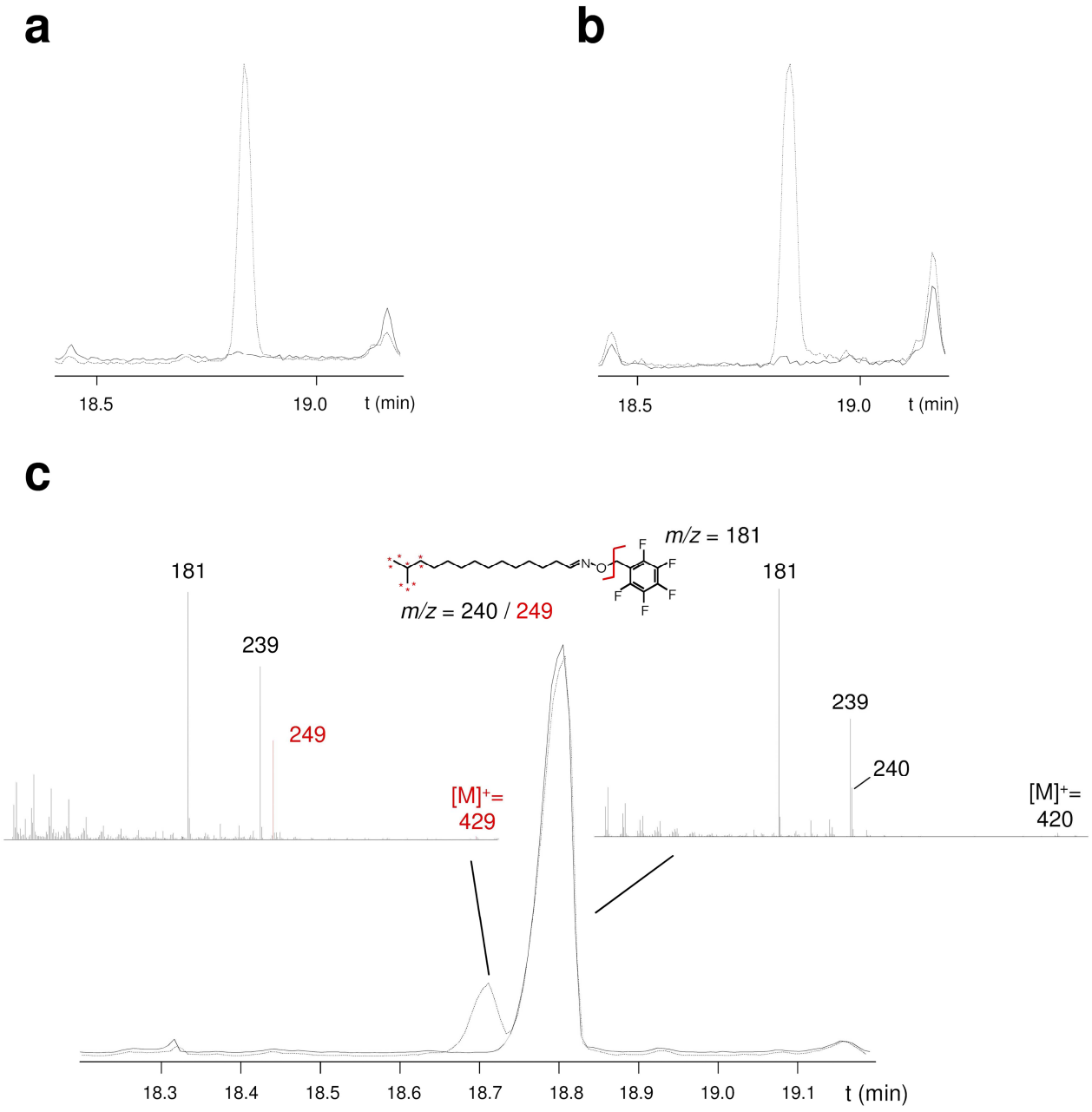

Supplementary Figure 12 | Formation of i15:0 aldehyde is abolished in *elbD* mutants.

Total ion chromatograms of wt (dashed) and *elbD* (solid line) cells of *M. xanthus* (**a**) and *S. aurantiaca* (**b**). c) i15:0 aldehyde was identified by comparing mass spectra and chromatograms of d_9-i15:0-PFB oxime (left spectrum) with i15:0-PFB oxime (right spectrum) obtained from analyzing metabolically labeled cells as described in methods section; solid line: unlabeled sample; dashed line: sample from d_{10}-Leucine fed cells.

Protein Domains	Organism	Accession No.
	***Myxococcus xanthus* DK1622**	**YP_629780 (Query)**
	*Candidatus Poribacteria sp.* WGA-4E	WP_020383835
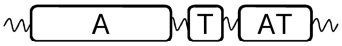	*Desulfobacca acetoxidans*	YP_004371800
	*Hydrogenobaculum sp.*	YP_007500146
	*Persephonella marina*	YP_002730949
	*Calothrix sp.* PCC 7103	WP_019496682
	*Geobacter metallireducens* RCH3	YP_006720580
	*Hydrogenivirga sp.* 128-5-R1-1	WP_008286326
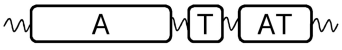	*Sulfurihydrogenibium sp.*	YP_001930344
	*Aquifex aeolicus*	NP_213682
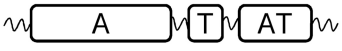	*Fusobacterium mortiferum*	WP_005886937
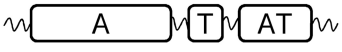	*Fusobacterium ulcerans*	WP_005981858

Supplementary Figure 13 | (previous page) ElbD–like homologues with similar domain architecture outside the order Myxococcales

Examples of ElbD homologues found by BLAST P search in decreasing order of homology. Note the broad range of clades, in which ElbD like homologues are detectable. Sequence identity is between 28-33%. Presence of plasmalogens was confirmed for *Fusobacterium mortiferum* (*Sphaerophorus rediculosis*)[38] while *Fusobacterium ulcerans* is an important pathogen found in tropical ulcers[39]. Etherlipids have also been identified from various sponges[40,41,42] in which Poribacteria are frequently encountered as endosymbionts. However, a clear fatty acyl-CoA reductase domain homologue could not be detected for the organisms other than *Candidatus Poribacteria*. Re: fatty-acyl-CoA like reductase domain; A: acyl-CoA synthetase domain; T: acylcarrier protein / thiolation domain; AT: acylglycerolphosphate acyltransferase domain.

Supplementary Table 1 | FAME-GC-MS data of vegetatively grown DW4/3-1 cells in per cent of total fatty acid methyl esters. Averages and standard deviations were calculated from three independent biological samples. Values following less-than sign indicate analytes below detection limit. Colors indicate level of significance (green: p<0.05; yellow: p<0.01; magenta: p<0.001). For details see method section. DMA: Vinyl ether derived dimethylacetales; OAG: alkyl ether derived *O*-alkylglycerols.

	wt		*elbA*⁻			*elbB*-			*elbD*⁻		
	0h		0h		p-Value	0h		p-Value	0h		p-Value
iso-13:0	0.67	±0.02	0.75	±0.08	0.164	0.62	±0.05	0.170	0.33	±0.02	0.000
14:1ω9c	0.03	±0.00	0.01	±0.00	0.008	0.01	±0.00	0.015	0.00	±0.00	0.003
14:1ω3c	0.72	±0.04	0.70	±0.10	0.496	0.67	±0.04	0.148	0.47	±0.03	0.001
14:0	1.18	±0.05	1.11	±0.13	0.321	0.81	±0.06	0.001	0.58	±0.02	0.000
iso-15:1w9c	<0.02	<0.02	0.37	±0.33	0.132	0.58	±0.05	0.002	0.44	±0.04	0.001
iso-15:0	12.13	±0.36	14.45	±1.36	0.063	10.56	±1.00	0.070	7.92	±0.23	0.000
15:0	1.67	±0.09	1.87	±0.22	0.168	1.18	±0.06	0.001	0.77	±0.06	0.000
15:1ω10c	0.06	±0.03	0.20	±0.02	0.005	0.25	±0.01	0.004	0.21	±0.01	0.010
15:1ω4c	0.49	±0.01	1.14	±0.14	0.010	0.97	±0.13	0.015	0.85	±0.05	0.004
iso-16:0	6.42	±0.25	6.19	±0.76	0.424	8.12	±0.68	0.026	9.65	±0.21	0.000
16:2w5c,11c	<0.02	<0.02	0.10	±0.17	0.286	0.09	±0.04	0.037	0.17	±0.03	0.006
16:1w11c	0.12	±0.02	0.09	±0.02	0.095	0.08	±0.00	0.025	0.07	±0.02	0.016
16:1w5c	17.72	±0.97	22.06	±2.52	0.057	25.25	±2.05	0.008	26.79	±0.36	0.001
16:0	11.89	±0.77	6.67	±0.84	0.001	4.95	±0.27	0.001	2.91	±0.03	0.002
iso-17:1w11c	<0.02	<0.02	0.30	±0.26	0.129	0.28	±0.49	0.286	<0.05	<0.05	1.000
iso-17:1w5c	0.50	±0.02	0.81	±0.06	0.004	1.39	±0.17	0.007	1.16	±0.08	0.002
iso-17:0	20.52	±0.66	14.00	±7.99	0.203	18.02	±7.23	0.396	21.17	±1.21	0.331
18:2	6.51	±0.17	5.12	±0.75	0.055	4.38	±0.10	0.000	3.91	±0.62	0.010
18:1	0.09	±0.02	1.16	±0.17	0.005	1.05	±0.02	0.000	0.67	±0.51	0.133
18:0	1.20	±0.08	0.66	±0.09	0.001	0.88	±0.06	0.005	0.86	±0.05	0.005
14:0 3-OH	0.18	±0.09	0.14	±0.01	0.340	0.23	±0.06	0.319	0.32	±0.05	0.069
iso-15:0 3-OH	1.74	±0.67	1.38	±0.16	0.308	2.19	±0.41	0.275	2.87	±0.32	0.059
16:0 2-OH	0.80	±0.19	1.02	±0.17	0.159	0.87	±0.09	0.395	1.04	±0.09	0.100
16:0 3-OH	0.10	±0.05	0.05	±0.01	0.140	0.09	±0.02	0.445	0.10	±0.02	0.508
iso-17:0 2-OH	12.95	±1.97	17.13	±0.97	0.034	15.86	±1.64	0.091	16.55	±0.42	0.057
iso-17:0 3-OH	0.00	±0.01	<0.01	<0.01	0.286	0.00	±0.01	0.570	0.18	±0.32	0.291
iso-15:0 DMA	1.20	±0.07	1.37	±0.17	0.157	0.26	±0.06	0.000	<0.05	<0.05	0.001
iso-15:0 OAG	0.12	±0.04	0.22	±0.02	0.034	0.04	±0.02	0.043	<0.05	<0.05	0.028
15:0 OAG	0.01	±0.02	0.02	±0.01	0.333	<0.01	<0.01	0.286	<0.05	<0.05	0.286
16:1 OAG	0.97	±0.36	0.90	±0.04	0.472	0.31	±0.21	0.048	<0.05	<0.05	0.031

Supplementary Table 2 | Results of the germination assay of all strains from developed cells harvested at 72 and 120 h after starvation induced fruiting body formation in % of germinated wild type spores. Colors indicate level of significance (green: $p<0.05$; yellow: $p<0.01$; magenta: $p<0.001$).

	wt				*elbD*$^-$				$^-$MXAN_1676				*elbD*$^-$ / *elbD*$^+$				*elbD*$^+$				*elbD*$^-$ / *elbD*$_{DW}$$^+$			
	mean		sdv	p-value	mean		sdv	p-value	mean		sdv	p-value	mean		sdv	p-value	mean		sdv	p-value	mean		sdv	p-value
72h	100.00	±	12.94	0.004	<0.01	±	-	0.004	<0.04	±	-	0.004	0.08	±	0.13	0.004	4.35	±	5.43	0.002	<0.01	±	-	0.004
120h	100.00	±	10.86	0.003	<0.01	±	-	0.004	24.47	±	2.22	0.003	2.61	±	1.30	0.003	-	±	-	-	<0.01	±	-	0.003

	elbA$^-$				*elbA*$^-$ / *elbD*$^+$				*elbB*$^-$				*elbB*$^-$ / *elbD*$^+$				*elbE*$^-$				*elbE*$^-$ / *elbD*$^+$			
	mean		sdv	p-value	mean		sdv	p-value	mean		sdv	p-value	mean		sdv	p-value	mean		sdv	p-value	mean		sdv	p-value
72h	104.73	±	24.04	0.509	9.72	±	1.62	0.004	67.78	±	11.25	0.024	4.31	±	3.07	0.003	89.18	±	8.37	0.217	9.27	±	8.46	0.001
120h	107.83	±	10.89	0.302	67.26	±	11.10	0.016	86.54	±	6.98	0.115	31.91	±	3.74	0.003	106.05	±	8.21	0.341	30.13	±	3.46	0.003

Supplementary Table 3 | Complete FAME-GC-MS data from Figure 2c in per cent of all fatty acid methyl esters. Values following less-than sign indicate analyte below detection limit. DMA: vinyl ether derived dimethylacetales; OAG: alkyl ether derived *O*-alkylglycerols.

	lyso-Phospholipid fraction				Phosphatidylglycerol fraction				Phosphatidylethanolamine fraction				Neutral Lipid fraction			
	wt		*elbD*		wt		*elbD*		wt		*elbD*		wt		*elbD*	
	0h	24h	0h	24h	0h	24h	0h	24h	0h	24h	0h	24h	0h	24h	0h	24h
12:0	<0.76	1.38	<0.57	<0.4	<0.13	0.21	<0.48	<0.08	<1.09	<0.81	0.02	0.10	0.52	0.17	0.48	0.15
iso-13:0	<0.76	<1.38	<0.57	<0.4	0.14	<0.09	<0.48	0.08	<1.09	<0.81	0.25	0.16	0.50	1.28	<0.48	0.31
iso-14:0	<0.76	<1.38	<0.57	<0.4	<0.13	<0.09	<0.48	<0.08	<1.09	<0.81	<0.02	<0.1	<0.5	0.25	<0.48	<0.15
14:1ω9c	<0.76	<1.38	<0.57	<0.4	0.61	0.09	<0.48	0.61	<1.09	<0.81	1.99	1.24	<0.5	0.28	<0.48	0.61
14:0	4.89	<1.38	6.66	2.60	4.86	2.85	5.04	4.22	<1.09	2.91	5.16	4.29	5.00	2.69	4.65	4.22
iso-15:1ω9c	<0.76	<1.38	<0.57	<0.4	<0.13	<0.09	<0.48	<0.08	<1.09	<0.81	0.70	0.68	<0.5	<0.07	<0.48	0.25
iso-15:0	48.34	22.88	45.28	21.35	56.24	44.96	36.87	42.44	47.50	52.53	46.93	44.28	30.92	41.91	27.69	40.16
15:0	3.73	<1.38	5.59	1.48	2.08	1.00	2.36	1.14	1.33	0.81	1.70	1.37	2.12	1.22	2.76	1.60
15:1ω10c	<0.76	<1.38	1.00	<0.4	1.99	0.93	4.19	3.20	2.88	1.47	5.15	5.03	1.52	1.60	3.44	3.06
15:1ω4c	<0.76	<1.38	2.94	3.65	2.12	0.90	5.64	3.04	3.03	1.28	3.91	3.53	2.50	1.87	3.50	3.36
iso-16:0	<0.76	<1.38	<0.57	<0.4	<0.13	0.78	<0.48	0.57	<1.09	<0.81	<0.02	0.33	<0.5	4.72	<0.48	1.37
16:2ω5c,11c	<0.76	<1.38	<0.57	5.44	2.07	1.05	4.27	3.79	6.76	3.03	6.81	6.44	7.33	3.41	8.94	5.38
16:1ω11c	<0.76	<1.38	<0.57	<0.4	<0.13	<0.09	1.16	0.84	1.09	<0.81	1.19	1.34	0.64	0.39	0.83	0.81
16:1w5c	3.09	8.69	8.96	25.77	11.52	7.32	16.42	16.14	13.30	8.61	12.57	15.18	10.98	13.56	11.59	17.29
16:0	10.81	43.39	10.74	5.50	2.55	9.51	3.74	2.91	5.75	7.98	1.79	2.52	23.68	7.45	22.78	8.69
iso-17:2ω5c,11c	<0.76	<1.38	0.57	2.84	1.53	0.61	2.30	2.25	4.57	1.80	4.37	4.39	4.38	2.09	4.84	3.11
iso-17:1ω11c	<0.76	<1.38	1.32	1.31	0.67	1.10	1.26	0.96	2.23	1.30	2.24	2.43	1.49	0.61	1.55	1.05
iso-17:1ω5c	<0.76	<1.38	<0.57	4.06	1.51	<0.09	3.29	2.61	3.24	1.63	2.82	2.89	2.11	2.58	2.25	3.10
iso-17:0	9.00	5.18	7.67	9.57	5.12	6.40	6.95	7.05	4.28	3.12	2.41	3.80	5.59	8.97	4.70	5.47
16:0 2-OH	0.76	<1.38	0.78	1.10	0.04	0.12	0.48	0.28	<1.09	<0.81	<0.02	<0.1	<0.5	<0.07	<0.48	<0.15
iso-17:0 2-OH	12.37	9.38	8.50	14.95	3.15	7.33	6.04	7.87	<1.09	<0.81	<0.02	<0.1	<0.5	0.07	<0.48	<0.15
iso-15:0 DMA	<0.76	<1.38	<0.57	<0.4	3.66	10.18	<0.48	<0.08	4.03	13.53	<0.02	<0.1	<0.5	1.93	<0.48	<0.15
iso-15:0 OAG	7.00	9.11	<0.57	0.40	0.13	4.66	<0.48	<0.08	<1.09	<0.81	<0.02	<0.1	0.71	2.96	<0.48	<0.15

Supplementary Table 4 | Complete htGC-MS data from Figure 2d. Intensities normalized to those of the internal standard palmitylpalmitate (=1000). Values following less-than sign indicate analytes below detection limit. Alkylether containing molecular species are highlighted in bold.

	wt		¯*elbD*	
	0h	24h	0h	24h
Palmitylpalmitate	1000	1000	1000	1000
TG(14:0/i15:0/i15:0)	<11	17	<14	<4
TG(i15:0/i15:0/i15:0)	31	247	19	231
TG(14:0/i15:0/16:1)	11	98	14	89
TG(i15:0/i15:0/16:1)	<11	205	<14	137
TG(i15:0/16:1/16:1)	<11	10	<14	16
TG(i15:0/16:1/i17:0)	<11	87	<14	37
TG(i15:0/i17:0/i17:0)	<11	19	<14	4
TG(16:1/i17:0/i17:0)	<11	4	<14	<4
TG(*O*-i15:0/i15:0/i15:0)	<11	**259**	<14	<4
TG(*O*-i15:0/i15:0/16:0)	<11	**44**	<14	<4
TG(*O*-i15:0/i15:0/i17:0)	<11	**66**	<14	<4
MG(*O*-i15:0/0:0/0:0)	<11	**94**	<14	<4
MG(i15:0/0:0/0:0)	271	1274	286	1980
MG(0:0/i15:0/0:0)	31	109	57	123
DG(*O*-i15:0/i15:0/0:0)	<11	**61**	<14	<4
DG(*O*-i15:0/i15:0/0:0)	<11	**249**	<14	<4
DG(i15:0/i15:0/0:0)	312	475	390	333

Supplementary Table 5 | htGC-MS data from the analysis of neutral lipid fraction of the wild type sample 24 h after starvation induction. Intensities normalized to those of the internal standard palmitylpalmitate (=1000). Values following less-than sign indicate analytes below detection limit. Alkylether containing molecular species are highlighted in bold. “Monoradylglycerols” and “diradylglycerols” are terms corresponding to class GL01 and GL02 of the LIPID MAPS classification system (www.lipidmaps.org/data/classification/LM_classification_exp.php).

	Monoradylglycerols	Diradylglycerols	Triacylglycerols	Alkyldiacylglycerols
Palmitylpalmitate	1000	1000	1000	1000
TG(14:0/i15:0/i15:0)	<4	<1	<11	43
TG(i15:0/i15:0/i15:0)	<4	19	332	558
TG(14:0/i15:0/16:1)	<4	3	77	<28
TG(i15:0/i15:0/16:1)	<4	4	144	<28
TG(i15:0/16:1/16:1)	<4	1	14	<28
TG(i15:0/i16:1/i17:0)	<4	<1	45	48
TG(*O*-i15:0/i15:0/i15:0)	<4	1	<11	**287**
TG(*O*-i15:0/i15:0/16:0)	<4	<1	<11	**184**
TG(*O*-i15:0/i15:0/i17:0)	<4	<1	**20**	**219**
MG(*O*-i15:0/0:0/0:0)	**5**	<1	<11	<28
MG(i15:0/0:0/0:0)	570	13	<11	**109**
MG(0:0/i15:0/0:0)	8	26	<11	<28
DG(*O*-i15:0/i15:0/0:0)	<4	**100**	<11	28
DG(*O*-i15:0/i15:0/0:0)	<4	**15**	<11	<28
DG(i15:0/i15:0/0:0)	4	146	11	181
DG(i15:0/0:0/i15:0)	<4	19	<11	<28

Supplementary Table 6 | Relative AUCs of lysophosphatidylethanolamine species detected in the lysophospholipid fraction by means of HPLC-ESI-MS. All peak areas were calculated relative to the i15:0-lysophosphatidylethanolamine AUC of the vegetative wild type culture.

name	m/z	RT (min)	wt		*elbD*	
			0h	24h	0h	24h
14:0-lPE	426.3	10.1	5	3	1	26
15:1-lPE	438.3	9.9	5	7	2	46
15:0-lPE	440.3	10.5	100	36	16	329
16:2-lPE	450.3	9.9	4	7	2	27
16:1-lPE	452.3	10.4	10	15	6	93
16:0-lPE	454.3	11.0	13	2	1	11
17:2-lPE	464.3	10.2	3	3	3	7
17:1-lPE	466.3	10.7	5	4	5	23
17:0-lPE	468.4	11.5	9	4	3	32
		Total	154	80	39	594

Supplementary Table 7 | Results retrieved from the acyl-adenylate superfamily substrate predictor by Khurana *et al.*[14] for the profile-based HMMER prediction. Best hit is highlighted in bold.

Best Match	Score	E-Value
Long Chain	**309.2**	**5.00E-93**
NRPS	35.0	2.20E-21
Medium Chain	-55.5	8.80E-18
Coumarate	-6.2	2.40E-13
Luciferase	-143.5	2.30E-12
Acetyl	-231.5	5.30E-12

Supplementary Table 8 | Results retrieved from the acyl-adenylate superfamily substrate predictor by Khurana *et al.*[14] for the position specific scoring matrix. Best hit is highlighted in bold.

Best Match	Template Active Site Residues	Query Active Site Residues	Raw Score	Percentile	Alignment
Long Chain	**HGFFLAGGGYGLSAK**	**HTFAVVGGGYGLPV-**	**26.097**	**73.63**	**Long-chain-CoA ligases**
Medium Chain	HGFFLAGGGYGLSAK	HTFAVVGGGYGLPV-	12.006	31.55	Medium-chain-CoA ligases
Luciferase	HGFFLAGGGYGLSAK	HTFAVVGGGYGLVL-	13.054	30.56	Luciferases
Coumarate	HGFFLAGGGYGLSAK	TFEAVVGGGYGLPV-	8.046	18.99	Coumarate-CoA ligases
NRPS	FDAWTIAGAYGPICK	TFEAVFSRRNNI--E	-35.166	-	NRPS
Acetyl	WVTSYGVGTWWQGFK	HTFAVFSRNRNNKLH	-47.704	-	Acetyl-CoA ligases

Supplementary Table 9 | Protein sequences used for the construction of the phylogenetic trees in Supplementary Figure 5 and 9. Functions were assigned from published data. 2-LPEAT: 2-lysophosphatidyletanolamineacyltransferase; 1-LPEAT: 1-lysophosphatidylethanolaminetransferase; LPAT: lysophosphatidicacidacyltransferase; LPCAT: lysophosphatidylcholinacytransferase; LPIAT: lysophosphatidylinositolacyltransferase; GPAT: glycerolphosphateacyltransferase

Name	Organism	Accession No.	Confirmed Substrates
Aas *K. oxytoca*	*Klebsiella oxytoca* 10-5245	ZP_17103746	
Aas *C. sakazakii*	*Cronobacter sakazakii* 696	ZP_18226439	
Aas *E. cloacae*	*Enterobacter cloacae subsp. dissolvens* SDM	YP_006479085	
Aas *S. enterica*	*Salmonella enterica subsp. enterica serovar Choleraesuis str.* SC-B67	YP_217936	
Aas *C. sp*.	*Citrobacter sp.* A1	ZP_10409702	
Aas E. coli (confirmed)	*Escherichia coli* str. K-12 substr. W3110	BAE76905	2-LPEAT[30]
Aas D. propionicus	*Desulfobulbus propionicus* DSM 2032	YP_004195979	
Aas *G. sp.*	*Geobacter sp.* M18	YP_004197112	
Aas *G. daltonii*	*Geobacter daltonii* FRC-32	YP_002535553	
ElbD *P. pacifica*	*Plesiocystis pacifica* SIR-1	ZP_01905621	
ElbD *S. cellulosum*	*Sorangium cellulosum* So ce56	YP_001618662	
ElbD *M. fulvus*	*Myxococcus fulvus* HW-1	YP_004663238	
ElbD *M.xanthus*	Myxococcus xanthus DK 1622	YP_629780	
ElbD *M. stipitatus*	*Myxococcus stipitatus* DSM 14675	YP_007358671	
ElbD *C. coralloides*	*Corallococcus coralloides* DSM 2259	YP_005367541	
ElbD *S. aurantiaca*	*Stigmatella aurantiaca* DW4/3-1	ZP_01459699	
Elb D *C. fuscus*	*Cystobacter fuscus*	WP_002629080	
ElbD *A. sp.* K	*Anaeromyxobacter* sp. K	YP_002133586	
ElbD *A. dehalogenans* 2CP-C	*Anaeromyxobacter dehalogenans* 2CP-C	YP_464376	
ElbD *A. dehalogenens* 2CP-1	*Anaeromyxobacter dehalogenans* 2CP-1	YP_002491736	
ElbD *A. sp.* Fw109-5	*Anaeromyxobacter* sp. Fw109-5	YP_001378404	
ElbD *H. ochraceum*	*Haliangium ochraceum* DSM 14365	YP_003267643	
PlsC2 *M. xanthus*	*Myxococcus xanthus* DK 1622	YP_632149	
PlsC5 *M. xanthus*	*Myxococcus xanthus* DK 1622	YP_628430	
PlsC4 *M. xanthus*	*Myxococcus xanthus* DK 1622	YP_629216	
PlsC *A. dehalogenans*	*Anaeromyxobacter dehalogenans* 2CP-C	YP_467128	
HdtS *P. fluorescence* (confirmed)	*Pseudomonas fluorescens* F113	YP_005205437	LPAT[43]
NlaB *N. meningitidis* (confirmed)	*Neisseria meningitidis* NMB	AAD38301	LPAT[44]
PlsC *S. cellulosum*	*Sorangium cellulosum* So ce56	YP_001614071	
PlsC3 *M. xanthus*	*Myxococcus xanthus* DK 1622	YP_633717	
PlsC *C. apiculatus*	*Chondromyces apiculatus* DSM 436	ZP_11022903	
PlsC1 *M. xanthus*	*Myxococcus xanthus* DK 1622	YP_631529	
PlsC *C. coralloides*	*Corallococcus coralloides* DSM 2259	YP_005369050	
hAGPAT5 (confirmed)	*Homo sapiens*	NP_060831	LPAT, LPCAT, 1-LPEAT[45]
hAGPAT8 (confirmed)	*Homo sapiens*	NP_001002257	LPAT (LPEAT) [46]
hAGPAT3 (confirmed)	*Homo sapiens*	AAQ89067	LPAT, LPCAT,

			LPIAT[45]
hAGPAT4	*Homo sapiens*	NP_064518	LPAT[47]
LPAT2 *A. thaliana* (confirmed)	*Arabidopsis thaliana*	Q8LG50	LPAT[48]
LPAAT *B. napus* (confirmed)	*Brassica napus*	ADC97478	LPAT[49]
PlsC *C. rodentium*	*Citrobacter rodentium* ICC168	YP_003367015	
PlsC *S. enterica*	*Salmonella enterica subsp. enterica serovar Schwarzengrund* str. SL480	ZP_02663187	
PlsC *E. Coli* (confirmed)	*Escherichia coli* str. K-12 substr. W3110	YP_491210	LPAT[30]
PlsC *K. oxytoca*	*Klebsiella oxytoca* 10-5245	ZP_17104077	
PlsC *E. cloacae*	*Enterobacter cloacae subsp. cloacae* ENHKU01	YP_006580226	
PlsC *C. sakazaki*	*Cronobacter sakazakii* E899	ZP_12437444	
PatB *P. fluorescence* (confirmed)	*Pseudomonas fluorescens* F113	AEV64097	[43]
hAGPAT1 (confirmed)	*Homo sapiens*	Q99943	LPAT[50]
hAGPAT2 (confirmed)	*Homo sapiens*	O15120	LPAT[50]
hAGPAT7 (confirmed)	*Homo sapiens*	NP_705841	1-LPEAT[51]
hLPCAT2 (confirmed)	*Homo sapiens*	Q7L5N7	LPAFAT[52]
hLPCAT1 (confirmed)	*Homo sapiens*	NP_079106	LPCAT[53]
hGPAT3/hAGPAT10 (confirmed)	*Homo sapiens*	NP_116106	GPAT, LPAT[54,55,56]
hAGPAT9 (confirmed)	*Homo sapiens*	AAH73136	LPAT
hAGPAT6 (confirmed)	*Homo sapiens*	AAH51377	GPAT[57]
hAGPAT4	*Homo sapiens*	NP_064518	GPAT, (LPAT)[47]
NlaA N. meningitidis (confirmed)	*Neisseria meningitidis* WUE 2594	YP_005892021	LPAT[44]
hGPAT2 (confirmed)	*Homo sapiens*	NP_997211	GPAT[58]
hGPAT1 (confirmed)	*Homo sapiens*	NP_065969	GPAT[59,60]
PlsB *M. fulvus*	*Myxococcus fulvus* HW-1	YP_004667818	
PlsB1 *M. xanthus*	*Myxococcus xanthus* DK 1622	YP_631487	
PlsB *C. apiculatus*	*Chondromyces apiculatus* DSM 436	ZP_11026508	
PlsB *S. aurantiaca*	*Stigmatella aurantiaca* DW4/3-1	YP_003953342	
PlsB *C. coralloides*	*Corallococcus coralloides* DSM 2259	YP_005369008	
PlsB *A. dehalogenans*	*Anaeromyxobacter dehalogenans* 2CP-1	YP_002493070	
PlsB *D. postgatei*	*Desulfobacter postgatei* 2ac9	ZP_10171403	
PlsB *D. toluolica*	*Desulfobacula toluolica* Tol2	YP_006762008	
PlsB *D. autotrophicum*	*Desulfobacterium autotrophicum* HRM2	YP_002603729	
PlsB *D. oleovorans*	*Desulfococcus oleovorans* Hxd3	YP_001529872	
PlsB *C. rodentium*	*Citrobacter rodentium* ICC168	YP_003367145	
PlsB *E. cloacae*	*Enterobacter cloacae subsp. cloacae* ENHKU01	YP_006576829	
PlsB *S. bongori*	*Salmonella bongori* NCTC 12419	YP_004732477	
PlsB *E. Coli* (confirmed)	*Escherichia* coli str. K-12 substr. W3110	YP_492184	GPAT[30]
PlsB *K. oxytoca*	*Klebsiella oxytoca* 10-5246	ZP_17105746	
PlsB *C. dublinensis*	*Cronobacter dublinensis* 582	ZP_19160269	
PlsB *E. tasmaniensis*	*Erwinia tasmaniensis* Et1/99	YP_001909017	
PlsB *S. plymuthica*	*Serratia plymuthica* PRI-2C	ZP_10110453	
PlsB *B. marinus*	*Bacteriovorax marinus* SJ	YP_005035807	
PlsB2 *M. xanthus*	*Myxococcus xanthus* DK 1622	YP_629927	
PlsD *C. butyricum*	*Clostridium butyricum*	AAC46006	GPAT[61]
GPAT *C. moscata* (confirmed, crystal)	*Cucurbita moschata*	1IUQ_A	GPAT[62]

Supplementary Table 10 | Strains, oligonucleotides and plasmids used in the study. Restriction sites used for cloning are marked bold within the sequences.

Strain Name	Characteristics	Reference
E. Coli		
DH10B	F- mcrA Δ(mrr-hsdRMS-mcrBC) Φ80dlacZΔM15 ΔlacX74 endA1 recA1 deoR Δ(ara,leu)7697 araD139 galU galK nupG rpsL λ-	63
S17-1 λpir	TpR SmR recA, thi, pro, hsdR-M+RP4: 2-Tc:Mu: Km Tn7 λpir	64
BL21(DE3)	dcm ompT hsdS(rB-mB-) gal	65
ElbDexp	BL21(DE3) / pSUMO3_CK4_elbD_delta_re	This study
ElbDΔre_exp	BL21(DE3) / pSUMO3_CK4_elbD	This study
Myxococcus xanthus		
DK1622	wild type	66
DK897	wild type	67
ˉMXAN_1531	DK1622::pCRII-TOPO MXAN1531, Km^r	This study
ˉMXAN_1530	DK1622::pCRII-TOPO MXAN1530, Km^r	This study
ˉMXAN_1527	DK1622::pCRII-TOPO MXAN1527, Km^r	This study
ˉMXAN_1528	DK1622::pMRMXAN_1528ko-2, Km^r	This study
Stigmatella aurantiaca		
DW4/3-1	wild type	68
ˉSTAUR_2305	DW4/3-1::pWL_STIAU2023ko, Km^r	This study
ˉSTAUR_2304	DW4/3-1::pWL_STIAU2025ko, Km^r	This study
ˉSTAUR_2302	DW4/3-1::pMRSTAUR_2302ko, Km^r	This study
Sorangium cellulosum		
So ce56	wild type	69
So ce377	wild type	70
Cystobacter sp.		
SBCb004	wild type	71

Oligo Name	(5'-3') Sequence	Characteristics
MXAN_1531-1	ATGAGAGCCCTCATCACCGG	419 BP internal fragment of MXAN_1531, forward
MXAN_1531-2	CTCTCCCCATACCATTCGTGG	419 BP internal fragment of MXAN_1531, reverse
MXAN_1530-1	ATGTCCTCGAAAGCTGCCTT	306 BP internal fragment of MXAN_1530, forward
MXAN_1530-2	GTCGATGAGGTCCTGCGTCT	306 BP internal fragment of MXAN_1530, reverse
MXAN_1527-1	TCGTGAAGCTGCTGGTGACG	545 BP internal fragment of MXAN_1527, forward
MXAN_1527-2	TGTGGAGGACAGCCGGTCAT	545 BP internal fragment of MXAN_1527, reverse
STAUR_2305_EcoRI-1	AGAC**GAATTC**TCGCTGAAGCAGGCTG	430 BP internal fragment of STAUR_2305, forward

STAUR_2305_HindIII-2	ATAC**AAGCTT**CGTCCACCAGGGTCAG	430 BP internal fragment of STAUR_2305, reverse
STAUR_2304_EcoRI_1	ATAG**GAATTC**ATGCCCGCCAAAGCT	327 BP internal fragment of STAUR_2304, forward
STAUR_2304_BAM HI_2	ATAT**GGATCC**GCAGCCGGAGC	327 BP internal fragment of STAUR_2304, reverse
STAUR_2302ko_EcoRI-1	ATAA**GAATTC**AGCGAGCCCTTCCAAC	664 BP internal fragment of STAUR_2302, forward
STAUR_2302ko_SalI-2	ATAT**GTCGAC**TTGGTGTACGTGTACG	664 BP internal fragment of STAUR_2302, reverse
elbDmx_-re_BamHI-1	ATAT**GGATCC**ATGGAGTCGGAGCGC	expression of *elbD* without reduction domain (BP1649-4423), forward
elbDmx_redom_BamHI-1	ATAT**GGATCC**ATGGCCGCCCTTCCC	expression of *elbD*, forward
elbDmx_-re_XhoI-2	ATAT**CTCGAG**TCACGAGTCCTTCCCTTCCGTGGACG	expression of *elbD* with and without reduction domain, reverse
elbDmx_exp_NdeI-3	ATAT**CATATG**GCCGCCCTTCCCGAGC	expression of *elbD*, forward
sfp_PstI_for	GATCTA**CTGCAG**ATGAAGATTTACGGAATTTATATGG	707 BP including primers of Sfp, forward
sfp_EcoRI_rev	TGAGCC**GAATTC**TTATAAAAGCTCTTCGTACGAG	707 BP including primers of Sfp, reverse
mtaA_*Bgl*II_for	TACATA**AGATCT**CCGACGTCCTCCCCT	853 BP including primers of MtaA, forward
mtaA_*Eco*RI_rev	TACCGC**GAATTC**ACCCTCCTCCC	853 BP including primers of MtaA, reverse
Control_1_MXAN1531-1	AACGTTATCTTCCCTCGGGA	integration control of pCRII-TOPO MXAN1531, upstram region, forward
Control_1_MXAN1531-2	GCGAGAAAGGAAGGGAAGAA	integration control of pCRII-TOPO MXAN1531, upstram region, reverse
Control_2_MXAN1531-1	AAGAACTCTGTAGCACCGCC	integration control of pCRII-TOPO MXAN1531, downstream region, forward
Control_2_MXAN1531-2	TCTCCATAGGAGAAGGCGAT	integration control of pCRII-TOPO MXAN1531, downstream region, reverse
Control_1_MXAN1530-1	AGGCCCTGGGACTGAC	integration control of pCRII-TOPO MXAN1530, upstram region, forward
Control_1_MXAN1530-2	TCCCAGTCACGACGTTG	integration control of pCRII-TOPO MXAN1530, upstram region, reverse
Control_2_MXAN1530-1	AAGGTAACTGGCTTCAGCAGA	integration control of pCRII-TOPO MXAN1530, downstream region, forward
Control_2_MXAN1530-2	GACAATCTTGCAGCCGCT	integration control of pCRII-TOPO MXAN1530, downstream region, reverse
Control_1_MXAN1527-1	CGCGCTCGGAGGGATA	integration control of pCRII-TOPO MXAN1527, upstram region, forward
Control_1_MXAN1527-2	CGCTATTACGCCAGCTGG	integration control of pCRII-TOPO MXAN1527, upstram region, reverse
Control_2_MXAN1527-1	GACTCAAGACGATAGTTACCG	integration control of pCRII-TOPO MXAN1527, downstream region, forward
Control_2_MXAN1527-2	AACTTCACCACCGTCCATGT	integration control of pCRII-TOPO MXAN1527, downstream region, reverse
SENSE_STIAU2023ko_Control	GTAGTAGCACGCCCGAGGC	integration control of pWL_STIAU2023ko, upstream region, forward
SENSE_STIAU2025ko_Control	GTGGAAGACGTGGTGGACCT	integration control of pWL_STIAU2025ko, upstream region, forward
SENSE_STIAU2027-3	CACAAGTACGAGCGCGAGTTCG	integration control of pMRSTAUR_2302ko, upstream region, forward
ANTISENSE_STIAU2023ko_Control	GCGTAATAGGCGTAGACGTGAAC	integration control of pWL_STIAU2023ko, downstream region, reverse
ANTISENSE_STIAU2025ko_Control	AACTCCAGGACGACCTCCAG	integration control of pWL_STIAU2025ko, downstream region, reverse

ANTISENSE_STIAU2027-4	TTCTCCGAGACCAGCAGCAC	integration control of pMRSTAUR_2302ko, downstream region, reverse
pUCin	GACGTTGTAAAACGACGGCCAG	integration control of pWL_STIAU2023/2025/2027/2028ko, upstream region, reverse
pUCout	ACACAGGAAACAGCTATGACCATG	integration control of pWL_STIAU2023/2025/2027/2028ko, downstream region, forward
T7	TAATACGACTCACTATAGGG	sequencing *elbD* expression forward
T7term_r	TAGTTATTGCTCAGCGGTGG	sequencing *elbD* expression reverse
seq_elbD-1	TTCATCCGCCAGAAGGTG	sequencing *elbD* expression forward
seq_elbD-2	GGCCGGACGATGGAGTAG	sequencing *elbD* expression reverse
seq_elbD-3	CTGGCCCAACACGTACAC	sequencing *elbD* expression forward
seq_elbD-4	CGGAAGACGTAGCGGTTC	sequencing *elbD* expression reverse
seq_elbD-5	GTCAGCAAGAAGGAGTTCGAG	sequencing *elbD* expression forward
seq_elbD-6	GCAGGATGCCGAAGTAGC	sequencing *elbD* expression reverse
seq_elbD-7	GCGGGCATCAAGCAC	sequencing *elbD* expression forward
seq_elbD-8	CCTGCGTAATCTTGCGATG	sequencing *elbD* expression reverse
seq_elbD-9	ATCGCAAGATTACGCAGGAG	sequencing *elbD* expression forward
seq_elbD-10	AGGCACGCCACCTTCTC	sequencing *elbD* expression reverse
seq_elbD-11	GGCCTGCCCGACGAC	sequencing *elbD* expression forward
seq_elbD-12	GCCGTAGAGCACCTTCTGC	sequencing *elbD* expression reverse
seq_elbD-13	GCGGAAGAGGTGGAGATTC	sequencing *elbD* expression forward
seq_elbD-14	GCCCGCATGGAGTCCT	sequencing *elbD* expression reverse
seq STAUR_2302exp-0	AGACGAGGCCGCTGCGGTT	sequencing STAUR_2302 expression reverse
seq STAUR_2302exp-1	TACTTTCCGAAGAAGGACGA	sequencing STAUR_2302 expression forward
seq STAUR_2302exp-2	ACGCGCCGCTCGTGCACCGT	sequencing STAUR_2302 expression reverse
seq STAUR_2302exp-3	ACCTGGCCTCCGGCGACGAGAA	sequencing STAUR_2302 expression forward
seq STAUR_2302exp-4-6	CTCGGCGGACTGGTCCGACA	sequencing STAUR_2302 expression reverse
seq STAUR_2302exp-4	AGCAGATCCCGGTACGCGGCA	sequencing STAUR_2302 expression reverse
seq STAUR_2302exp-5	CCGGGATCTGCTCGAACTCT	sequencing STAUR_2302 expression forward
seq STAUR_2302exp-6	GAACACGTCGCCCAGCCGGT	sequencing STAUR_2302 expression reverse
seq STAUR_2302exp-7	TGGCCGGCGCCTTCTCCATT	sequencing STAUR_2302 expression forward
seq STAUR_2302exp-8	GACGTCCTTCTTGCGGCCCA	sequencing STAUR_2302 expression reverse
seq STAUR_2302exp-9	ATCGAGTTCCGCATCGACCA	sequencing STAUR_2302 expression forward
seq STAUR_2302exp-10	AGGTCCTCCACCGTGTTCAC	sequencing STAUR_2302 expression reverse
seq STAUR_2302exp-11	GACGGGCGGCGTGAGCGATT	sequencing STAUR_2302 expression forward
seq STAUR_2302exp-12	AAGGTGCCCCGCAGGTAGAG	sequencing STAUR_2302 expression reverse
seq STAUR_2302exp-13	CGGACCTGATCCCCATGGAT	sequencing STAUR_2302 expression forward
STAUR_2302_NdeI-1	ATGC**CATATG**AGCCAGCTGCCCGAACTGA	primer for full length STAUR_2302 forward
STAUR_2302_EcoRI-2	ATGC**GAATTC**TTCACGCGTCCTGTCCTCCA	primer for full length STAUR_2302 reverse
MXAN1528_NdeI-1	ATAT**CATATG**GCCGCCCTTCCCGAGCT	primer for full lenth MXAN_1528 forward

MXAN1528_BamHI-2	ATAT**GGATCC**TCACGAGTCCTTCCCTTCCGT	primer for full lenth MXAN_1528 reverse
pUCorilac_PauI-1	AACCTC**GCGCGC**ACACATGCAG	pUC18_oriR forward
pUCorilac_BglII-2	TCGTTC**AGATCT**CTGAGCGTCAGAC	pUC18_oriR reverse
orilac_BcuI-1	CAGGAA**ACTAGT**ACATGTGAGCAAAAGGC	cloning primer, amplifying pMR06tet forward
orilac_XhoI-2	AAAGCG**CTCGAG**TGAGCGCAACG	cloning primer, amplifying pMR06tet reverse
oriT_SalI-1	GTAGG**CGTCGAC**ACAGGCTCATGCC	RP4/RK2 oriT from pCOM9 forward
oriT_XbaI-2	AGCCAT**TCTAGA**ATCCTCTCTCGCCTGTC	RP4/RK2 oriT from pCOM9 reverse
pCOLA-NheI_for	GTTTCTGCGTCTAGCATGCCT	cloning primer for pCOLA_tacI/I
pCOLA-NheI_rev	GTCCTAGAAGATGCCAGGAGG	cloning primer for pCOLA_tacI/I
tacI_NcoI_up	CATGAGCTGTTGACAATTAATCATCGGCTCGTATAATGTGTG GAATTGTGAGCGGATAACAATTTCACACAGGAGGGAATTCCA TGGC	cloning primer for pCOLA_tacI/I
tacI_NcoI_dw	AATTGCCATGGAATTCCCTCCTGTGTGAAATTGTTATCCGC TCACAATTCCACACATTATACGAGCCGATGATTAATTGTCAA CAGCT	cloning primer for pCOLA_tacI/I
tacI_up	GGAGCTGTTGACAATTAATCATCGGCTCGTATAATGTGTG GAATTGTGAGCGGATAACAATTTCACACAGGAGGCTAGCA	cloning primer for pCOLA_tacI/I
tacI_dw	TATGCTAGCCTCCTGT GTGAAATTGTTATCCGCTCACAATTCCACACATTATACGAGC CGATGATTAATTGTCAACAGCTCCTGCA	cloning primer for pCOLA_tacI/I
pACYC-NheI_for	GGAGTGTATAC TGGCTTACTATGTTGGC	cloning primer for pACYC_tacI/I
pACYC-NheI_rev	GGAGTGTATAC TGGCTTACTATGTTGGC	cloning primer for pACYC_tacI/I
pCKT7A1_attB_blunt-1	TCATGACCAAAATCCCTTAACGT	cloning primer for pWL02zeo_att
pCKT7A1_attB_blunt-2	TTTCGCGACATGGAGGACT	cloning primer for pWL02zeo_att

Plasmid Name	**Function**	**Reference**
pJet1.2/blunt	cloning vector	Thermo Scientific
pCR®II-TOPO®	cloning vector	life technologies inc.
pCRII-TOPO MXAN1527	suicide plasmid, pCRII-TOPO carrying internal fragment of MXAN_1527	This study
pCRII-TOPO MXAN1530	suicide plasmid, pCRII-TOPO carrying internal fragment of MXAN_1530	This study
pCRII-TOPO MXAN1531	suicide plasmid, pCRII-TOPO carrying internal fragment of MXAN_1531	This study
pMRMXAN_1528ko-2	suicide plasmid, pMR06kan carrying internal fragment of MXAN_1528	This study
pMR06kan	cloning vector, Km^r	72
pMR08kanT	cloning vector, harbouring RP4 *oriT*, Km^r	72
pMR10_kanT	cloning vector, harbouring RP4 *oriT*, Km^r	This study
pWL_STIAU2023ko	suicide plasmid, pMR10_kanT carrying internal fragment of STAUR_2305	This study
pWL_STIAU2025ko	suicide plasmid, pMR10_kanT carrying internal fragment of STAUR_2304	This study
pMRSTAUR_2302ko	suicide plasmid, pMR08_kanT carrying internal fragment of STAUR_2302	This study
pSUMO3_ck4	expression plasmid	This study
pSUMO3_ck4_elbD_delta_re	expression plasmid, for ElbD AA547-1470, N-terminal His_6 and SUMO-tag	This study
pSUMO3_ck4_elbD	expression plasmid, for ElbD, N-terminal His_6 and SUMO-tag	This study

pSUMO3_ck5	expression plasmid	This study
pSUMO_mtaA	expression plasmid, for MtaA, N-terminal His_6 and SUMO-tag	This study
pSUMO_sfp	expression plasmid, for Sfp, N-terminal His_6-tag	This study
pTf16	expression plasmid, for coexpression of the chaperone coding *tig* gene	TAKARA BIO INC.
pET32a	expression plasmid, T7 promotor, amp^r	Novagen
pCOLA_tacI/I_MCSI_MXAN_1530-1529exp_MCSII_MXAN_1528exp	expression plasmid for MXAN_1530, MXAN_1529, MXAN_1528	This study
pACYC_tacI_MCSI_bkdA-C_MCSII_ MXAN_1527_1531	expression plasmid for MXAN_1527, MXAN_1531	This study
pET32a_mtaA_NdeI/XhoI	expression plasmid for MtaA	73
pCOLA_tacI/I	expression plasmid for two inserts, colA oriR, two mcs with tacI promotors, Km^r	This study
pACYC_tacI/I	expression plasmid for two inserts, pACYC oriR, two mcs with tacI promotors, Cm^r	This study
pMK-RQ_MXAN_1527-1531exp_synth	cloning vector containing MXAN_1527 and MXAN_1531 codon optimized for *E. Coli*	This study/life technology
pMK-RQ_MXAN_1530-1529exp_synth	cloning vector containing MXAN_1530 and MXAN_1529 codon optimized for *E. Coli*	This study/life technology
pWL02zeo_att	expression vector for *M. xanthus*, Zeo^r	This study
pWL02zeo_MXAN_1528exp	expression vector for MXAN_1528	This study
pWL02zeo_MXAN_2027exp	expression vector for STAUR_2302	This study

Supplementary Table 11 | Total weight in mg of lipid extracts from *M. xanthus* DK1622 and TLC fractions derived thereof.

	Total Extract	Lysophospholipid Fraction	Phosphatidylglycerol Fraction	Phosphatdiylethanolamine Fraction	Neutral Lipid Fraction
wt veg I	2.2				
wt veg II	2.3	1.2	3.1	2.4	5.4
wt veg III	2.1				
elbD veg I	2.3				
elbD veg II	2.2	1.8	3.8	2.4	3.3
elbD veg III	2.2				
wt 24h I	3.1				
wt 24h II	4	1.3	0.5	1.8	6
wt 24h III	2.4				
elbD dev I	2.2				
elbD dev II	2.1	**2.9**	3.9	2	5.8
elbD dev III	2.6				

Supplementary Table 12 | Query sequence for peptide mass fingerprint of His_6SUMO3ElbD.

1-100
MGHHHHHHGGMSEEKPKEGVKTENDHINLKVAGQDGSVVQFKIKRHTPLSKLMKAYCERQGLSMRQIRFRFDGQPINETDTPAQLEMEDEDTIDVFQQQT
101-200
GGSTGSMAALPELNVTQTFTGKRLLFAGATGFVGKVTLSMLLTRYGQDLDKVYVLVRKGSAASAERRFFDKVATSEPFQPLRDSLGDEGALAFIRQKVEV
201-300
LDGDITDPWMGLEEPQVEALTGKVHAFINCAGLVSFNPSLEVGLNVNTHGLKFAAALAVRWSVPLIHMSTAFVAGNRSGLVFEDEEVRGYFPKREEMDGR
301-400
DFSLEQELQDAARIVARLREQAEDRALTSTFRKKALDRLEEEGRDPNDEKTLRLAVGRERKLWLSGELVRAGMERAAHWGWPNTYTYTKSLGEQVLAATP
401-500
GLRYSIVRPSIVESARHFPFPGWNEGFTTSAPLAFAGIKGPGGIPAGENTILDIIPVDQVAGATIGITAHAMDVEERRIYQLASGDMNPFYAGRSVELVG
501-600
LYRRRYYRNRESGNALMNKLRSRVEPQPVSKKEFELFSAPMLSRGARFLKKAIDEVRPAWGAPAVQAMLDKAKVSLDEVDDNAQGIIALTELFLPFLYEN
601-700
RYVFRCDNTRSVYARMAHADRLKVPWDPEHIDWREYFLGTHLPGLEKWVFPGMESEREKRTVIPAHRDLLELMEATVHAYRHRVAFRMVAGEKEERFTYG
701-800
EVHRYAARVGSFLLAAGIKHGDRVLLVSENRPEWGISYFGILRAGATVVPVDPGLSEAELVNIARRADARACLVSEDAARDFPGLFAALGDGVTVASLAE
801-900
AMTGDPAHPDRIGPVRRSAAADDLASIIFTSGTTGTPKGVMLTHRNFAALVAKLAGTFDIGVGDGVLSVLPLHHTFEFAAGFLTPFWRGAEITYIDELTS
901-1000
DRLGEVFETGRITAMVGVPALWQLLHRKITQEFASRPPFIEQALKALMATHGELRNRNNINLGKLLFWPVHRKFGGRIKVIVSGGSALPDDVHKAFHELG
1001-1100
FNITEGYGLTEAAPVLAVTKPGNKRQPGTVGRALPGIELRILNPDNDGLGEVLAKGPNVMPGYFGDREATEAVLKDGWLHTGDLGRLDAEGHLYLVGRAK
1101-1200
DVIIDHNGKNIYPDELEELYQDHTHIKELSIVGLPDDAGGEKVACLCVPDYADRPREEVRRELEEHFRKVSAGMPFYRRVKVLRLWDGELPRTAK
1201-1300
KQVVEELKRQERMAASASKAREKAANPTTGGIADWLFPLIADVSHRPVSDVRPDALLSGDLGFDSLMLTELSSALEAAGVPLPAVEDLTQVQTVEDLRKV
1301-1400
VASSGKRPTVETRAKEISKENERAEEVEIPVPDVVADVGRQLLSFGQKVLYGGVFDVKVTGKSFIPQNRNFLVIANHSSHLDAGLVRVALGDQGERLVSL

1401-1500

AARDYFFNTPLKRAWFENFTNLIPIERQGSLRESLRMAGEALRQGFNVLIFPEGTRSTTGELMEFKSTLGYLALTFNMDVLPLYIGGAFDALPKGSVLPK

1501-1576

TKTPLRVNIGPALGHADLRTRVQGMARSEGYRYVTRIAEDSMRALRDGRVLNLERVDLPPAGASPRASTSTEGKDS

Supplementary Table 13 | Result table of peptide mass fingerprint from ~175 kD band of Supplementary Figure 6e. Abbreviations: Meas.: Measured; Calc.: Calculated; Dev.: Deviation.

Sequence	Range	Partials	Meas. M/z	Calc. MH+	Meas. Mr	Calc. Mr	Dev.(Da)	Dev.(ppm)
TENDHINLKVAGQDGSVVQFK	22 - 42	1	2299.175	2299.168	2298.167	2298.16	0.007	3.042
VAGQDGSVVQFK	31 - 42	0	1234.643	1234.643	1233.636	1233.635	0	0.347
YGQDLDKVYVLVR	145 - 157	1	1567.848	1567.848	1566.84	1566.841	0	-0.14
FFDKVATSEPFQPLR	168 - 182	1	1781.926	1781.922	1780.918	1780.915	0.003	1.939
VATSEPFQPLR	172 - 182	0	1244.663	1244.663	1243.656	1243.656	0	-0.184
VATSEPFQPLRDSLGDEGALAFIR	172 - 195	1	2589.331	2589.331	2588.324	2588.323	0.001	0.232
DSLGDEGALAFIR	183 - 195	0	1363.686	1363.685	1362.678	1362.678	0	0.292
SGLVFEDEEVR	278 - 288	0	1279.617	1279.616	1278.61	1278.609	0.001	0.528
SGLVFEDEEVRGYFPK	278 - 293	1	1871.919	1871.917	1870.912	1870.91	0.002	0.845
REEMDGRDFSLEQELQDAAR	294 - 313	2	2395.096	2395.094	2394.089	2394.087	0.002	0.666
REEMDGRDFSLEQELQDAAR 4: Oxidation (M)	294 - 313	2	2411.092	2411.089	2410.084	2410.082	0.003	1.058
EEMDGRDFSLEQELQDAAR	295 - 313	1	2238.994	2238.993	2237.987	2237.986	0.001	0.333
DFSLEQELQDAAR	301 - 313	0	1521.718	1521.718	1520.711	1520.711	0	0.181
LREQAEDR	318 - 325	1	1016.512	1016.512	1015.505	1015.505	0	-0.114
ALDRLEEEGRDPNDEKTLR	335 - 353	3	2256.123	2256.121	2255.116	2255.114	0.001	0.599
AAHWGWPNTYTYTK	376 - 389	0	1695.798	1695.791	1694.791	1694.784	0.006	3.753
SLGEQVLAATPGLR	390 - 403	0	1411.792	1411.79	1410.784	1410.783	0.001	0.866
YSIVRPSIVESAR	404 - 416	0	1476.819	1476.817	1475.811	1475.81	0.002	1.105
RIYQLASGDMNPFYAGR	478 - 494	1	1958.955	1958.954	1957.948	1957.947	0.001	0.611
RIYQLASGDMNPFYAGR 10: Oxidation (M)	478 - 494	1	1974.951	1974.949	1973.944	1973.942	0.002	1.191
IYQLASGDMNPFYAGR	479 - 494	0	1802.854	1802.853	1801.847	1801.846	0.001	0.467
IYQLASGDMNPFYAGR 9: Oxidation (M)	479 - 494	0	1818.849	1818.848	1817.842	1817.841	0.002	0.855
SVELVGLYR	495 - 503	0	1035.583	1035.583	1034.576	1034.576	0	-0.438
SVELVGLYRR	495 - 504	1	1191.685	1191.684	1190.677	1190.677	0	0.068

KEFELFSAPMLSR	532 - 544	1	1554.8	1554.798	1553.793	1553.791	0.001	0.853
EFELFSAPMLSR 9: Oxidation (M)	533 - 544	0	1442.699	1442.698	1441.692	1441.691	0.001	0.728
EFELFSAPMLSR	533 - 544	0	1426.704	1426.704	1425.697	1425.696	0.001	0.574
AIDEVRPAWGAPAVQAMLDK	552 - 571	0	2138.11	2138.106	2137.102	2137.099	0.003	1.581
WVFPGMESER	648 - 657	0	1237.567	1237.567	1236.559	1236.56	0	-0.209
DLLELMEATVHAYR 6: Oxidation (M)	668 - 681	0	1676.832	1676.831	1675.825	1675.824	0.001	0.73
DLLELMEATVHAYR	668 - 681	0	1660.837	1660.836	1659.83	1659.829	0.001	0.495
VGSFLLAAGIK	709 - 719	0	1075.651	1075.651	1074.644	1074.644	0	-0.147
VLLVSENRPEWGISYFGILR	724 - 743	0	2348.278	2348.276	2347.27	2347.269	0.001	0.625
AGATVVPVDPGLSEAELVNIAR	744 - 765	0	2178.179	2178.176	2177.171	2177.169	0.002	0.975
ACLVSEDAAR 2: Carbamidomethyl (C)	771 - 780	0	1091.515	1091.515	1090.508	1090.508	0	0.262
SAAADDLASIIFTSGTTGTPK	818 - 838	0	2024.021	2024.018	2023.013	2023.011	0.003	1.25
GAEITYIDELTSDR	889 - 902	0	1582.76	1582.76	1581.753	1581.752	0	0.25
GAEITYIDELTSDRLGEVFETGR	889 - 911	1	2571.257	2571.257	2570.249	2570.25	-0.001	-0.226
LGEVFETGR	903 - 911	0	1007.515	1007.516	1006.508	1006.508	0	-0.147
KITQEFASRPPFIEQALK	928 - 945	1	2103.162	2103.16	2102.155	2102.152	0.002	1.032
ITQEFASRPPFIEQALK	929 - 945	0	1975.066	1975.065	1974.059	1974.057	0.002	0.815
ALMATHGELR	946 - 955	0	1098.573	1098.572	1097.565	1097.565	0	0.128
AFHELGFNITEGYGLTEAAPVLAVTKPGNK	995 - 1024	0	3144.638	3144.636	3143.631	3143.629	0.001	0.468
ALPGIELR	1033 - 1040	0	868.525	868.525	867.517	867.518	-0.001	-0.637
GPNVMPGYFGDR	1056 - 1067	0	1309.6	1309.599	1308.592	1308.592	0	0.133
GPNVMPGYFGDREATEAVLK 5: Oxidation (M)	1056 - 1075	1	2167.051	2167.049	2166.044	2166.042	0.002	0.978
GPNVMPGYFGDREATEAVLK	1056 - 1075	1	2151.057	2151.054	2150.05	2150.047	0.003	1.427
DGWLHTGDLGR	1076 - 1086	0	1226.591	1226.591	1225.584	1225.584	0	0.068
LDAEGHLYLVGR	1087 - 1098	0	1342.712	1342.711	1341.704	1341.704	0	0.275
VACLCVPDYADRPR 3: Carbamidomethyl (C) 5: Carbamidomethyl (C)	1143 - 1156	0	1691.801	1691.799	1690.793	1690.792	0.001	0.824
VACLCVPDYADRPREEVR 3: Carbamidomethyl (C) 5: Carbamidomethyl (C)	1143 - 1160	1	2205.055	2205.054	2204.048	2204.047	0.001	0.543
VACLCVPDYADRPREEVRR 3: Carbamidomethyl (C) 5: Carbamidomethyl (C)	1143 - 1161	2	2361.156	2361.155	2360.149	2360.148	0.001	0.579

KVSAGMPFYR	1169 - 1178	1	1155.598	1155.598	1154.59	1154.591	0	-0.159
VSAGMPFYR	1170 - 1178	0	1027.502	1027.503	1026.495	1026.496	-0.001	-0.564
LWDGELPR	1185 - 1192	0	985.51	985.51	984.503	984.503	0	-0.04
AKEISKENERAEEVEIPVPDVVADVGR	1314 - 1340	3	2978.542	2978.543	2977.534	2977.536	-0.001	-0.471
EISKENERAEEVEIPVPDVVADVGR	1316 - 1340	2	2779.412	2779.411	2778.405	2778.404	0.001	0.438
ENERAEEVEIPVPDVVADVGR	1320 - 1340	1	2322.161	2322.157	2321.154	2321.15	0.004	1.606
AEEVEIPVPDVVADVGR	1324 - 1340	0	1793.93	1793.928	1792.922	1792.921	0.002	0.945
NFLVIANHSSHLDAGLVR	1370 - 1387	0	1963.053	1963.051	1962.046	1962.044	0.002	1.061
DYFFNTPLKR	1404 - 1413	1	1300.669	1300.668	1299.661	1299.661	0	0.169
AWFENFTNLIPIER	1414 - 1427	0	1749.898	1749.896	1748.891	1748.889	0.002	1.399
VNIGPALGHADLR	1507 - 1519	0	1332.739	1332.738	1331.731	1331.731	0	0.33
VLNLERVDLPPAGASPR	1550 - 1566	1	1804.009	1804.008	1803.002	1803	0.002	1.057
VDLPPAGASPR	1556 - 1566	0	1079.584	1079.584	1078.577	1078.577	0	-0.109

Sequence coverage:	77.90%
Intensity coverage:	38.80%

Supplementary Table 14 | Result table of peptide mass fingerprint from ~140 kD band of Supplementary Figure 6e. Abbreviations: Meas.: Measured; Calc.: Calculated; Dev.: Deviation.

Sequence	Range	Partials	Meas. M/z	Calc. MH+	Meas. Mr	Calc. Mr	Dev.(Da)	Dev.(ppm)
TENDHINLKVAGQDGSVVQFK	22 - 42	1	2299.176	2299.168	2298.168	2298.16	0.008	3.45
LLFAGATGFVGKVTLSMLLTR 17: Oxidation (M)	124 - 144	1	2211.261	2211.257	2210.254	2210.25	0.004	1.788
YGQDLDKVYVLVR	145 - 157	1	1567.849	1567.848	1566.842	1566.841	0.001	0.701
FFDKVATSEPFQPLR	168 - 182	1	1781.926	1781.922	1780.919	1780.915	0.004	2.299
VATSEPFQPLRDSLGDEGALAFIR	172 - 195	1	2589.333	2589.331	2588.325	2588.323	0.002	0.744
DSLGDEGALAFIR	183 - 195	0	1363.686	1363.685	1362.678	1362.678	0	0.237
QKVEVLDGDITDPWMGLEEPQVEALTGK	196 - 223	1	3097.535	3097.54	3096.528	3096.533	-0.005	-1.523
SGLVFEDEEVRGYFPK	278 - 293	1	1871.92	1871.917	1870.913	1870.91	0.003	1.488
REEMDGRDFSLEQELQDAAR 4: Oxidation (M)	294 - 313	2	2411.09	2411.089	2410.082	2410.082	0	0.155
REEMDGRDFSLEQELQDAAR	294 - 313	2	2395.095	2395.094	2394.088	2394.087	0.001	0.459
DFSLEQELQDAAR	301 - 313	0	1521.717	1521.718	1520.71	1520.711	-0.001	-0.492
KLWLSGELVR	361 - 370	1	1200.71	1200.71	1199.702	1199.703	0	-0.21
AAHWGWPNTYTYTK	376 - 389	0	1695.794	1695.791	1694.786	1694.784	0.002	1.305
SLGEQVLAATPGLR	390 - 403	0	1411.791	1411.79	1410.783	1410.783	0	0.263
YSIVRPSIVESAR	404 - 416	0	1476.818	1476.817	1475.81	1475.81	0.001	0.581
HFPFPGWNEGFTTSAPLAFAGIK	417 - 439	0	2492.25	2492.24	2491.242	2491.232	0.01	3.995
RIYQLASGDMNPFYAGR	478 - 494	1	1958.956	1958.954	1957.948	1957.947	0.002	0.809
RIYQLASGDMNPFYAGR 10: Oxidation (M)	478 - 494	1	1974.951	1974.949	1973.944	1973.942	0.002	1.162
IYQLASGDMNPFYAGR	479 - 494	0	1802.854	1802.853	1801.846	1801.846	0.001	0.315
IYQLASGDMNPFYAGR 9: Oxidation (M)	479 - 494	0	1818.851	1818.848	1817.844	1817.841	0.003	1.885
SVELVGLYR	495 - 503	0	1035.583	1035.583	1034.575	1034.576	-0.001	-0.601
SVELVGLYRR	495 - 504	1	1191.685	1191.684	1190.678	1190.677	0	0.389
RYYRNRESGNALMNK	505 - 519	3	1871.92	1871.929	1870.913	1870.922	-0.009	-4.883
KEFELFSAPMLSR	532 - 544	1	1554.801	1554.798	1553.793	1553.791	0.002	1.445

EFELFSAPMLSR	533 - 544	0	1426.704	1426.704	1425.696	1425.696	0	0.168
AIDEVRPAWGAPAVQAMLDK	552 - 571	0	2138.112	2138.106	2137.105	2137.099	0.006	2.768
AIDEVRPAWGAPAVQAMLDKAK	552 - 573	1	2337.238	2337.238	2336.231	2336.231	0	-0.036
DLLELMEATVHAYR 6: Oxidation (M)	668 - 681	0	1676.831	1676.831	1675.824	1675.824	0	0.137
VLLVSENRPEWGISYFGILR	724 - 743	0	2348.279	2348.276	2347.271	2347.269	0.002	1.059
AGATVVPVDPGLSEAELVNIAR	744 - 765	0	2178.179	2178.176	2177.172	2177.169	0.003	1.35
SAAADDLASIIFTSGTTGTPK	818 - 838	0	2024.022	2024.018	2023.015	2023.011	0.004	1.905
GAEITYIDELTSDR	889 - 902	0	1582.76	1582.76	1581.753	1581.752	0	0.302
GAEITYIDELTSDRLGEVFETGR	889 - 911	1	2571.257	2571.257	2570.25	2570.25	0	0.058
LGEVFETGR	903 - 911	0	1007.515	1007.516	1006.508	1006.508	-0.001	-0.573
KITQEFASRPPFIEQALK	928 - 945	1	2103.163	2103.16	2102.155	2102.152	0.003	1.365
ITQEFASRPPFIEQALK	929 - 945	0	1975.067	1975.065	1974.059	1974.057	0.002	0.902
LLFWPVHR	965 - 972	0	1067.615	1067.615	1066.607	1066.608	0	-0.129
AFHELGFNITEGYGLTEAAPVLAVTKPGNK	995 - 1024	0	3144.635	3144.636	3143.628	3143.629	-0.002	-0.518
GPNVMPGYFGDREATEAVLK 5: Oxidation (M)	1056 - 1075	1	2167.049	2167.049	2166.042	2166.042	0.001	0.236
GPNVMPGYFGDREATEAVLK	1056 - 1075	1	2151.057	2151.054	2150.05	2150.047	0.003	1.415
DGWLHTGDLGR	1076 - 1086	0	1226.591	1226.591	1225.584	1225.584	0	-0.284
LDAEGHLYLVGR	1087 - 1098	0	1342.711	1342.711	1341.704	1341.704	0	-0.24
NIYPDELEELYQDHTHIK	1110 - 1127	0	2257.071	2257.077	2256.064	2256.07	-0.006	-2.671
VACLCVPDYADRPR 3: Carbamidomethyl (C) 5: Carbamidomethyl (C)	1143 - 1156	0	1691.801	1691.799	1690.793	1690.792	0.001	0.813
VACLCVPDYADRPREEVRR 3: Carbamidomethyl (C) 5: Carbamidomethyl (C)	1143 - 1161	2	2361.154	2361.155	2360.147	2360.148	-0.001	-0.241
LWDGELPR	1185 - 1192	0	985.51	985.51	984.502	984.503	0	-0.464
EISKENERAEEVEIPVPDVVADVGR	1316 - 1340	2	2779.406	2779.411	2778.398	2778.404	-0.005	-1.847
ENERAEEVEIPVPDVVADVGR	1320 - 1340	1	2322.156	2322.157	2321.149	2321.15	-0.001	-0.423
AEEVEIPVPDVVADVGR	1324 - 1340	0	1793.929	1793.928	1792.922	1792.921	0.001	0.79
NFLVIANHSSHLDAGLVR	1370 - 1387	0	1963.053	1963.051	1962.045	1962.044	0.002	0.934
DYFFNTPLKR	1404 - 1413	1	1300.668	1300.668	1299.661	1299.661	0	-0.167
AWFENFTNLIPIER	1414 - 1427	0	1749.898	1749.896	1748.89	1748.889	0.002	1.048
VNIGPALGHADLR	1507 - 1519	0	1332.737	1332.738	1331.73	1331.731	-0.001	-0.998

VLNLERVDLPPAGASPR	1550 - 1566	1	1804.013	1804.008	1803.005	1803	0.005	2.767

Intensity coverage:	52.50%
Sequence coverage:	40.50%

Supplementary Table 15 | Result table of peptide mass fingerprint from ~100 kD band of Supplementary Figure 6e. Abbreviations: Meas.: Measured; Calc.: Calculated; Dev.: Deviation.

Sequence	Range	Partials	Meas. M/z	Calc. MH+	Meas. Mr	Calc. Mr	Dev.(Da)	Dev.(ppm)
YGQDLDKVYVLVR	145 - 157	1	1567.849	1567.848	1566.842	1566.841	0.001	0.596
DSLGDEGALAFIR	183 - 195	0	1363.686	1363.685	1362.679	1362.678	0.001	0.867
SGLVFEDEEVRGYFPK	278 - 293	1	1871.914	1871.917	1870.906	1870.91	-0.004	-2.017
DFSLEQELQDAAR	301 - 313	0	1521.717	1521.718	1520.71	1520.711	-0.001	-0.631
AAHWGWPNTYTYTK	376 - 389	0	1695.793	1695.791	1694.786	1694.784	0.002	1.023
SLGEQVLAATPGLR	390 - 403	0	1411.791	1411.79	1410.783	1410.783	0	0.211
YSIVRPSIVESAR	404 - 416	0	1476.818	1476.817	1475.81	1475.81	0.001	0.428
RIYQLASGDMNPFYAGR 10: Oxidation (M)	478 - 494	1	1974.949	1974.949	1973.942	1973.942	0	0.15
RIYQLASGDMNPFYAGR	478 - 494	1	1958.956	1958.954	1957.948	1957.947	0.002	0.816
IYQLASGDMNPFYAGR	479 - 494	0	1802.854	1802.853	1801.847	1801.846	0.001	0.482
IYQLASGDMNPFYAGR 9: Oxidation (M)	479 - 494	0	1818.852	1818.848	1817.845	1817.841	0.004	2.469
SVELVGLYR	495 - 503	0	1035.583	1035.583	1034.575	1034.576	-0.001	-0.677
AIDEVRPAWGAPAVQAMLDK	552 - 571	0	2138.111	2138.106	2137.104	2137.099	0.005	2.136
DLLELMEATVHAYR 6: Oxidation (M)	668 - 681	0	1676.833	1676.831	1675.825	1675.824	0.001	0.837
VGSFLLAAGIK	709 - 719	0	1075.65	1075.651	1074.643	1074.644	-0.001	-0.515
AGATVVPVDPGLSEAELVNIAR	744 - 765	0	2178.179	2178.176	2177.171	2177.169	0.002	1.004

Intensity coverage:	33.80%
Sequence coverage:	12%

Supplementary Table 16 | Result table of peptide mass fingerprint from ~60 kD band of Supplementary Figure 6e. Abbreviations: Meas.: Measured; Calc.: Calculated; Dev.: Deviation.

Sequence	Range	Partials	Meas. M/z	Calc. MH+	Meas. Mr	Calc. Mr	Dev.(Da)	Dev.(ppm)
STGSMAALPELNVTQTFTGKR 5: Oxidation (M)	1-21	1	2225.121	2225.123	2224.114	2224.116	-0.002	-0.909
LLFAGATGFVGK	22 - 33	0	1180.672	1180.672	1179.664	1179.665	-0.001	-0.595
WSVPLIHMSTAFVAGNR 8: Oxidation (M)	159 - 175	0	1901.971	1901.969	1900.964	1900.962	0.002	1.222
WSVPLIHMSTAFVAGNR	159 - 175	0	1885.976	1885.974	1884.969	1884.967	0.002	1.223
SGLVFEDEEVR	176 - 186	0	1279.616	1279.616	1278.608	1278.609	-0.001	-0.568
REEMDGRDFSLEQELQDAAR 4: Oxidation (M)	192 - 211	2	2411.091	2411.089	2410.083	2410.082	0.001	0.597
EEMDGRDFSLEQELQDAAR 3: Oxidation (M)	193 - 211	1	2254.992	2254.988	2253.985	2253.981	0.004	1.789
DFSLEQELQDAAR	199 - 211	0	1521.718	1521.718	1520.711	1520.711	0	0.243
LREQAEDR	216 - 223	1	1016.511	1016.512	1015.504	1015.505	-0.001	-0.772
YGQDLDKVYVLVR	43 - 55	1	1567.847	1567.848	1566.84	1566.841	-0.001	-0.457
VATSEPFQPLR	70 - 80	0	1244.663	1244.663	1243.655	1243.656	-0.001	-0.519
DSLGDEGALAFIR	81 - 93	0	1363.685	1363.685	1362.678	1362.678	0	0.041
VEVLDGDITDPWMGLEEPQVEALTGK 13: Oxidation (M)	96 - 121	0	2857.382	2857.381	2856.375	2856.374	0.001	0.457
KLWLSGELVR	259 - 268	1	1200.709	1200.71	1199.702	1199.703	-0.001	-0.599
LWLSGELVR	260 - 268	0	1072.614	1072.615	1071.607	1071.608	-0.001	-0.635
AAHWGWPNTYTYTK	274 - 287	0	1695.793	1695.791	1694.786	1694.784	0.001	0.873
SLGEQVLAATPGLR	288 - 301	0	1411.791	1411.79	1410.783	1410.783	0	0.174
YSIVRPSIVESAR	302 - 314	0	1476.818	1476.817	1475.81	1475.81	0.001	0.529
HFPFPGWNEGFTTSAPLAFAGIK	315 - 337	0	2492.241	2492.24	2491.234	2491.232	0.001	0.521
IYQLASGDMNPFYAGR	377 - 392	0	1802.853	1802.853	1801.846	1801.846	0	0.068
SVELVGLYR	393 - 401	0	1035.583	1035.583	1034.575	1034.576	-0.001	-0.714

Intensity coverage:	48.50%
Sequence coverage:	17.00%

Supplementary Note 1: Molecular Biology Methods

General biomolecular procedures

Polymerase chain reaction, agarose gel electrophoresis, restriction enzyme digestion, DNA transfer into *E. coli*, plasmid isolation, protein gel electrophoresis and western blotting were carried out by established procedures[74], whereas anti-His_6 PentaHisTM monoclonal antibodies (Qiagen NV) and anti-mouse IgG alkaline phosphatase antibody conjugates (Sigma-Aldrich Corp.) were used as the respective primary and secondary antibody.

Tryptic protein digestion for peptide mass fingerprint (PMF) was done using a published protocol[75]. Sample preparation, instrumentation, acquisition of mass spectra and MS data analysis is described elsewhere[76] except that the obtained MGF-files were compared with an *in-silico* digest of His_6SUMO3ElbD using biotools 3.0 (Bruker Daltonics). The query sequence is accessible in Supplementary Table 12. Supplementary Tables 13-16 contain the matched peptide sequences of the PMF analysis of bands encircled in Supplementary Figure 5e. Those reveal additional bands in Supplementary Figure 5a-d as C-terminally truncated translation products.

All primers used for this study were designed in house utilizing either Vector NTI® (life technologies inc.) or GeneiousTM (Biomatters Ltd)[77] and were finally obtained from Sigma- Aldrich.

The construction of gene disruption vectors for *M. xanthus* were achieved by cloning internal PCR fragments of target genes into pCR®II-TOPO® plasmids using TOPO TA Cloning® Kit Dual Promotor (life technologies inc.) according to manufactures instructions. Plasmid DNA isolation, genomic DNA isolation and DNA extraction from agarose gels was performed using the GeneJET^{TM} Plasmid MiniPrep Kit (Thermo Scientific corp.), GeneJETTM Gel Extraction Kit (Thermo Scientific corp.) and Gentra Puregene Yeast/Bact. Kit B (Qiagen NV) respectively. Protein quantification was performed with Roti®-Quant (Carl Roth GmbH).

DNA Sequencing was carried out by Seq-IT GmbH & Co. KG (Kaiserslautern, Germany). For a complete list of primers and plasmids used in this study see Supplementary Table 10.

Plasmid pMR10kanT was obtained by the following procedure: Plasmid pMR06kan[72] was amplified using primers kan-BglII-BclI-1 and kan-PauI-PaeI-NcoI-2. The resulting

fragment was then used in a second round of PCR with pMR06kan as a template. After incubating the PCR mixture with *Dpn*I to degrade the template, the mixture was introduced into *E. coli* JM109 by electroporation, yielding an intermediate plasmid called pMR09kan which now contained an excisable kanamycin cassette. From this plasmid, a PCR product containing the kanamycin resistance gene was generated using primers kan_BglII-1 and kan_PauI-2. This PCR product was ligated into pMR06tetT after excision of its tetracycline resistance gene using restriction enzymes *Bgl*II and *Pau*I giving rise to pMR10kanT so that a plasmid for biparental conjugation was available.

pMR06tetT was obtained by the following steps: A tetracycline resistance gene (*tetA*) was amplified from pCOM9[78] with primers tetCOM_PauI-1 and tetCOM_BglII-2. Another 1.5 kb fragment containing the origin of replication and the *lacZα* gene with the multiple cloning site was amplified from pUC18 with primers pUCorilac_PauI-1 and pUCorilac_BglII-2. Both fragments were digested with *Pau*I and *Bgl*II and ligated to give rise to cloning vector pMR06tet. To obtain a mobilizable vector similar to pMR08kanT[72], new restriction sites were introduced by amplifying most of pMR06tet with primers orilac_BcuI-1 and orilac_XhoI-2 The RP4/RK2 oriT was obtained from pCOM9 with primers oriT_SalI-1 and oriT_XbaI-2. Both PCR products were digested and ligated, resulting in plasmid pMR06tetT.

Cloning of dual promoter vectors pCOLA_tacI/I and pACYC_tacI/I for heterologous expression in *E. Coli* was done in the following way: In a first step the NheI site of pCOLADuet-1 (Merck/Novagen) was deleted by a PCR using the primers pCOLA-NheI_for and pCOLA-NheI_rev. The PCR product was ligated leading to a single base deletion in the former NheI site and resulting in the new vector pCOLA-NheI. The annealed oligos tacI_NcoI_up and tacI_NcoI_dw were cloned into the *Nco*I/*Eco*RI sites of pCOLA-NheI resulting in the vector pCOLA_tacI-NheI. In a second promoter introduction step the annealed oligos tacI_up and tacI_dw were cloned into the PstI/NdeI sites of pCOLA_tacI-Nhe resulting in the final vector pCOLA_tacI/I harboring two tacI promoters driving the expression of potentially two cloned genes. In order to use the vector pACYCDuet-1 in a similar manner to pCOLA tacI/I independently of the T7 RNA polymerase the NheI site of the vector was deleted by amplifying the vector using pACYC-NheI_for and pACYCNheI_rev thereby deleting one nucleotide of the NheI site and the NheI site at that location. The PCR product was ligated leading to pACYC-NheI. The 896

bp fragment of a MluI/AvrII digest of pCOLA_tacI/I was cloned into the MluI/AvrII site of pACYC-NheI resulting in the final vector pACYC_tacI/I.

Vector pWL02zeo_att is a derivative of pCK_T7A1_attB, that was described previously[79]. It consists of a ligated PCR product obtained by using primers pCKT7A1_attB_blunt-1 and pCKT7A1_attB_blunt-2 and plasmid pCK_T7A1_attB. It enables the expression of genes in *M. xanthus* under the control of the constitutive T7A1 promoter via integration into the genome using the MX8 phage attachment site. Plasmids pWL02zeo_MXAN_1528exp and pWL02zeo_MXAN_2027exp were constructed by direct cloning of the PCR products obtained with primers STAUR_2302_NdeI-1, STAUR_2302_EcoRI-2 and MXAN1528_NdeI-1, MXAN1528_BamHI-2 respectively. Inserts were verified by sequencing.

Construction of gene disruption and complementation mutants in *M. xanthus* and *S. aurantiaca*

For construction of myxobacterial gene disruption and complementation mutants the respective constructs were transferred into *M. xanthus* by electroporation[80] or *S. aurantiaca* by biparental conjugation using established protocols[81,72]. The verification of the mutants was done by amplifying the integration sites from isolated genomic DNA using construct and genome specific primers[25].

Supplementary Note 2: Chemical analysis methods

Preparation of lipid extracts from bacteria

Lipid extracts of vegetative and developed *M. xanthus* cells were obtained by the method of Bligh and Dyer[34]. Pellets from three independent samples from vegetative cultures and after 24 h of starvation induced development were resuspended in 2 ml of water and mixed with 5 ml of methanol and 2.5 ml of DCM. After incubation for 20 minutes at 30 °C under agitation, phase separation was induced by addition of 2.5 ml water and 2.5 ml DCM. The lower phase was removed and cells were extracted again with 3.5 ml DCM. Combined DCM phases were filtered through solvent resistant filters with a pore size of 0.22 µm and

evaporated for determination of the total lipid mass. Amounts of lipid extracts and lipid fractions obtained by preparative TLC (see below) are depicted in (Supplementary Table 11).

Fractionation of lipid extracts using preparative thin layer chromatography (TLC)

and analytical thin layer chromatography

For the in-depth analysis of the bacterial extracts, the three replicate biological samples were pooled and 100 µl of a solution of 10 mg/ml bacterial extract was applied per cm of the starting line of a predeveloped 200 x 200 x 2 mm silica gel 60 plates with glass backing (Merck Millipore KgaA). Separation of lipid extracts was performed using a phospholipid (PL) eluant consisting of chloroform:methanol:water 95:35:5 (v/v/v). Assignment of lipid fractions was done with genuine lipid standards which were 3-*n*-lysophosphatidylethanolaminefrom egg yolk for the lysophospholipid fraction, 1,2-dipalmitoyl-s*n*-glycero-3-phosphoethanolamine, for the phosphatidylethanolamine fraction, rac-1,2-distearoylglycerol, for the phosphatidylglycerol fraction and glyceryl tristearate for the neutral lipid fraction. After chromatographic separation and evaporation of the eluant, lipids were visualized by spraying with 50 mg/L primuline solution in acetone:water 80:20 (v/v) and subsequent examination under UV-light[82]. Fluorescent bands were scratched off, extracted three times with chloroform/methanol 1:2 (v/v), each time with sonication for 15 minutes. Combined extracts were filtered through solvent resistant 0.45 and 0.22 µm membrane filter units and the solvent was evaporated for determination of dry weight (Supplementary Table 11). Neutral lipids were fractionated in an analogous way, except that the neutral lipid fraction from the previous step was used as the starting material and a mixture of hexane:diethylether:acetic acid 80:20:1 (v/v/v) was used as the eluent to resolve the lipids. 1-Stearoyl-rac-glycerol, rac-1,2-distearoylglycerol, and glyceryl tristearate were used as standards. Analytical TLC was performed the same way but aluminium backed 200 x 200 x 0.2 mm silica 60 plates (Merck Millipore KgaA) were used and lipid extract or lipid fraction equivalent to 100 µg was spotted on the starting lane as a 0.5 cm band each time. Pictures were taken after primuline staining as described above with a focal length of 11mm, an aperture of f/16 and an exposure time of 5 s.

Determination of fatty acid methyl acid (FAME) patterns and neutral lipid composition in bacteria, lipid extracts and fractions thereof

All GC-MS analysis were conducted on a 7890A model gas chromatograph (Agilent Technologies inc.) equipped with a CTC PAL Combi XT autosampler (CTC analytics AG) and coupled to a Series 5975C mass selective detector (Agilent Technologies inc.). A DB5ht column (Agilent Technologies inc.) with a length of 30 m, an inner diameter of 0.25 mm and a stationary phase of 0.1 μm in strength was used for the separation of the analytes.

The derivatization procedure as well as the temperature program and the data analysis workflow for both, the fatty acid methyl acid analysis[83] and neutral lipid analysis[6] were performed as described. Briefly to obtain fatty acid methyl esters, 1 mg of total lipid extract, TLC fraction of lipid extracts or a dried pellet of $7.5x10^9$ cells were used as the starting material, incubated over night at 56 °C in a mixture of toluol:methanol:sulphuric acid 50:50:2 (v/v/v) for complete methanolysis. Afterwards, a solution of 400 μl of 0.5 M ammoniumhydrogencarbonate and 3 M potassiumchloride was added. After phase separation, 75 μl of the fatty acid methyl ester containing upper phase was transferred into a glass vial and 25 μl of N-methyl-N-(trimethylsilyl) trifluoroacetamide (MSTFA) was added after which another 30 min incubation at 37 °C followed.

Individual detection limits for analytes not detected in a sample were calculated by dividing the peak area of the least abundant analyte by the sum of the peak areas of all analytes. Levels of significance between the individual analytes from the mutant samples compared to the wild type samples were calculated in the following way: A Welch's t-test was applied on the triplicate results of the respective mutant and wild type sample in order to obtain the t value using Excel's "T.TEST" function (two-tailed, heteroscedastic). The degrees of freedom were calculated by the Welch–Satterthwaite equation. The p-value was obtained by subtraction of the result from the T.DIST.2T function from[1].

Detection of i15:0 aldehyde in *M. xanthus* and *S. aurantiaca* cells

Aldehydes were detected after their derivatization to the corresponding *O*-(2,3,4,5,6-pentafluorobenzyl)-oximes as described by Wichard *et al.*[16]. About $7.5\ x10^9$ cells of vegetatively grown cells were harvested washed ones with purified water and resuspended in 1 ml of a solution containing 50 mM of *O*-(2,3,4,5,6-pentafluorobenzyl)-

hydroxylaminhydrochloride (PFBHA) in 10 mM Tris-HCl (pH 7.5) plus 10 µl benzaldehyde in hexane (1:1000 (v/v)) as the first internal standard. Cells were disrupted by treatment with ultrasound for 3 min after the addition of glass beads followed by an incubation for 2 h at 30 °C under agitation. Afterwards, 30 µl of PFB-undecanal (0.1 mg/ml) were added as a second internal standard. 3 ml of hexane and 0.5 ml of methanol were added, mixed and phase separation was achieved by centrifugation. 3 ml of the upper phase was withdrawn, dried under reduced pressure and dissolved in 80 µl hexane and 20 µl of MSTFA. After an additional incubation for 1 h at 57 °C samples were analyzed by GC-MS using the following parameters: sample volume: 1 µl; inlet temperature: 250 °C; gas flow: 1ml/min; temperature program: 60 to 85 °C in 1 min followed by a ramp to 310 °C with 9 °C/min. All other parameters were identical to those used for FAME analysis.

i15:0-PFB oxime was identified by feeding 1 mM d_{10}-Leucine thrice every 12 h to a culture until an optical density of 1.0-1.3 was reached. The resulting d_9-i15:0-PFB oxime was detected due to its increase of 9 mass units and slightly lower retention time as discussed by Dickschat *et al.*[84].

Analysis of lysophosphatidylethanolamine

Fractions containing lysophospholipds were analyzed by means of HPLC ESI-MS. They were dissolved to 10 mg/ml in methanol and 5 µl were subjected to a UltiMate 3000 system (Dionex/Thermo Scientific Corp.) coupled to an amaZon X mass spectrometer (Bruker Corp.). Analytes were separated on an Acquity UPLC BEH C18 1.7 µm RP column (Waters Corp.) with a length of 50 mm and an inner diameter of 2.1 mm in combination with a MeCN/0.1 % formic acid in water gradient ranging from 5 to 95 % in 22 min at a flow rate of 0.6 mL min^{-1}. Lysophosphatidylethanolamines were identified in the positive ion MS^2 mode by a neutral loss of 141 *m/z* corresponding to the loss of the polar head group. Areas under the curves (AUCs) of the extracted ion chromatograms of each lysophosphatidylethanolamine species were integrated and compared among the respective samples whereas AUCs of the main LPE i15:0-lPE in the vegetative wild type samples was set to 100%.

Synthesis of putative acyl acceptors for *in-vitro* acyltransferase assay

The putative substrates were synthesized similar to a published procedure[85]: About 2 mg of a lipid extracts from the DK1622 *elbD* was dissolved in 1 ml of peroxide free diethylether

by sonication, mixed with 600 µl 50 mM tris-malate pH 5.7, 100 µl of 100 mM $CaCl_2$, 800 µl methanol and 10 µl of phospholipase A1 preparation from *Thermomyces lanuginosus* (10 kU/ml; Sigma-Aldrich), vigorously mixed and incubated at 37 °C under agitation for 15 min. Reaction was stopped by the addition of 1.2 ml methanol and 1 ml of dichloromethane (DCM) and lipids were extracted by the method of Bligh and Dyer[34] as described below. Lysophospholipids were dissolved in an aqueous solution of 10 mM dodecylmaltoside (DDM) to a final concentration of about 10 mM. The in this way formed 2-monoacylglycerophosphoethanolamines (2-lPE) as well as 1-monoacylglycerophosphoethanolamines (1-lPE), 2- monoacylglycerophosphates (2-lPA) and 1 - monoacylglycerophosphates (1-lPA) were used as test substrates. 1-lPE was obtained by incubating 2-lPE in 100 mM Tris-HCl for 6 h at 37 °C by acyl migration[86]. 2-monoacylglycerophosphates were generated from 2-lPE by incubation with 2 units phospholipase D from *Streptomyces sp.* Type VII (Sigma-Aldrich) per µmol monoacylgylcerolphosphoethanolamine lipid in 50 mM Tris-malate 5 mM $CaCl_2$, 1 mM boric acid and 0.5 % (v/v) n-Butanol for 30 min at 30 °C. 1-lPA was generated from 2-lPA by acyl migration analogously to the formation of 1-lPE. d_7-i15:0 was used as the acyl donor.

Synthesis of putative acyl donors for *in-vitro* acyltransferase assay

As iso15:0 fatty acid is the predicted and most likely acyl donor for ElbD, we sought to use it in the acyl transferase assay. In order to enhance its detectability using mass spectroscopy, we synthesized the isotope-labeled derivative d_7-i15:0[87]. D_7-ispropylmagnesiumbromide (0.227 g, 1.74 mmole, 3 eq.), a small amount of iodine and magnesia shavings (0.085 g, 3.48 mmole, 6 eq.) were mixed under nitrogen and 10 ml of absolute tetrahydofurane (THF) was added. Grignard-reaction was initiated by short heating. Sodium(12-bromo)dodecanoate (0.175 g, 0.58 mmole, 1eq.) was resuspended in 5 ml THF with dilithiumcopper(I)tetrachloride (0.2 ml, 0.02 mmole, 0.03 eq.) added under agitation to the Grignard preparation. The preparation was stirred overnight and heated the following day for another six hours. After addition of 5 ml 6 M HCl solution and 10 ml water, the preparation was extracted thrice with 15 ml ethylacetate each. Combined organic phases were dried over sodiumsulfate and solvent was removed under removed pressure. The raw product was purified by silica gel column chromatography with a chloroform/methanol gradient (100 %→90 %). 60 mg purified product (41 % yield) was obtained.

This fatty acid was used as free acid and as an *N*-Acetylcysteamine thioester mimicking the activated, ACP-bound fatty acid88 synthesized as described in the following: 50 µmole of d_7-i15:0 was dissolved in 2 ml of DCM, subjected to N_2 atmosphere in order to ensure water free conditions, cooled to 0 °C, 1 equivalent of 1-hydroxybenzotriazole (HOBt) and 1.1 equivalent of *N*-(3-Dimethylaminopropyl)-*N′*-ethylcarbodiimide hydrochloride (EDC) were added under agitation. Finally, 1.4 equivalents of N-acetylcysteamine were added and reaction mixture was incubated for 18 h. Preparation was worked up by addition of 5 ml of DCM and 5 ml of aqueous 1 M HCl, separation of organic phase and aqueous phase was reextracted twice with 10 ml DCM. Combined organic phase was dried over Na_2SO_4, filtered and evaporated using a rotary evaporator. Formation of, d_7-i15:0-SNAC was confirmed with NMR. For the acyl transferase assay, d_7-i15:0-SNAC was dissolved in DMSO to final concentration of 10 mmole/L.

Supplementary Note 3: Bioinformatics methods

General Bioinformatics

Identification of homologues of proteins or domains mentioned in this study was performed using BLAST-P14[89,90] search within the nr database of NCBI. Prior to design of internal fragments or expression constructs, a frame plot 2.3.2 [91] analysis ensured the correct assignment of open reading frames. Sequence alignments were obtained using MUSCLE Alignment[92]. Search for primers suitable for PCR and sequences were constructed using Primer3[93,94].

The phylogenetic investigations of the ElbD acyltransferase domain were done as follows: Literature was reviewed for reports of acyl acceptor specificity of acyltransferases with known amino acid sequences involved in phospholipid biosynthesis with respect to the constitution of the polar headgroup and the hydroxyl group of the glycerol backbone that is being acylated. The following groups of ATs were included: glycerol-3-phosphate acyltransferases (PlsB/GPAT; EC 2.3.1.15), 1-acylglycerolphosphate acyltransferases (PlsC/AGPAT; EC 2.3.1.51), 2-acylglycerolphosphoethanolamine acyltransferases (Aas/2-LPEAT; EC 2.3.1.40), 1-acylglycerophosphocholine O-acyltransferase (LPCAT; EC 2.3.1.23) as well as all ElbD homologues found in myxobacterial genomes (Supplementary Table 9). For several of these enzymes, multiple substrate recognitions were reported.

Names given to the proteins in a publication were kept. Additional sequences from putative glyceride acylating acyl transferases were obtained by repeated BLAST searches against the nr library of NCBI[95]. Sequence alignments were done using MUSCLE with BLOSUM80 scoring matrix, gap open penalty of 1.53 and an offset value of 0.123. In order to maximize the clustering of the acyltransferase sequences according to their substrate specificity, the alignment was trimmed so that only sequences that align within the AT motifs I-V were taken into consideration resulting in a 325 aa consensus sequence. Sequence alignment was repeated with MUSCLE alignment, this time using BLSOUM30 cost matrix in order to refine the alignment of the now more similar sequences (Supplementary Data Set 3). Based on this trimmed multiple alignment a phylogenetic tree was built using PhyML[96]. Settings were as follows: Substitution model: Dayhoff; branch support: Bootstrap, 500 replicates; proportion of invariable sites fixed to 0; number of substitution rate categories: 4; Optimize: topology/length /rate; topology search: NNI; default, fast (Supplementary Figure 9). Substitution per site were calculated according Dayhoff *et al.*[97]

In-silico analysis of acyltransferase domains in ElbD

Homology-modelling of A and AT-domain of ElbD

The Molecular Operating Environment 2012.10 (MOE) was used to construct homology models of the A- and AT-domain of ElbD[98]. After loading the FASTA sequences into MOE, a BLAST search was performed to find appropriate template crystal structures[89]. Thereafter the primary structures, respectively, of the template and the corresponding target were aligned. To avoid deletions or insertions in conserved regions the alignments were inspected and corrected manually if necessary. Two series each consisting of ten models were constructed with MOE using a Boltzmann-weighted randomized procedure combined with specialized logic for the handling of sequence insertions and deletions[99,100]. The models with the best packing quality functions were selected for full energy minimization using Amber12 and Supporting Hueckel Theory (Amber12EHT). The stereo-chemical qualities of the models were assessed using Ramachandran plots.

A-Domain:

For homology modeling the 1.9 Å crystal structure of PheA from *Brevibacillus brevis* (PDBID: 1AMU_A) was used[101]. The sequence identity of ElbD A-Domain and 1AMU is

~17%. The model used for full energy minimization has a packing score of 2.3. The final model has a root-mean-square deviation (RMSD) of 1.7 Å in relation to the template structure.

AT-Domain:

For homology modelling the only available 1.5 Å crystal structure of a long chain fatty acid acyl transferase, the Chain A of the glycerol-3-phosphate 1-O-acyltransferase from chloroplasts of *Curcubita moscata* (PDB-ID: 1IUQ_A) was used as a template[102]. The target and template sequence identity is ~11%. The packing score of the model used for full energy minimization is 2.5. The RMSD between the final model and the template structure is 1.4 Å.

Ligand-Docking

To predict the binding mode, dockings were carried out by using GOLD version 5.1[103]. The empirical scoring function CEMPLP was used for advanced Protein-Ligand docking[104]. The Binding site of ElbD A-Domain was centered at His253 and for ElbD AT-Domain at His165. The default docking parameters were used.

Supplementary Data Set 1 | Complete FAME-GC-MS data from Figure 1b in per cent of all fatty acid methyl esters. Values following less-than signs indicate analytes below detection limit. Averages and standard deviations were calculated from three independent biological samples. Colors indicate level of significance (green: $p<0.05$; yellow: $p<0.01$; magenta: $p<0.001$). For details see Supplementary Note 2. DMA: Vinyl ether derived dimethylacetales; OAG: alkyl ether derived *O*-alkylglycerols**.**

	wt						*elbD*⁻							⁻*MXAN_1676*						
	0h			72h			0h			p-value	72h			p-value	0h			p-value	72h			p-value
12:0	0.09	±	0.02	<0.13	±	0.00	0.09	±	0.04	0.6020	<0.06	±	0.00	1.0000	0.11	±	0.04	0.3010	<0.12	±	0.00	1.0000
iso-13:0	1.00	±	0.06	0.80	±	0.15	0.58	±	0.05	0.0006	0.23	±	0.02	0.0133	0.76	±	0.08	0.0118	0.59	±	0.07	0.0775
iso-14:0	<0.07	±	0.00	0.14	±	0.13	<0.06	±	0.00	1.0000	0.08	±	0.01	0.3286	<0.11	±	0.00	1.0000	0.36	±	0.01	0.0660
14:1ω9c	1.49	±	0.06	0.26	±	0.03	0.42	±	0.37	0.0244	0.26	±	0.02	0.5279	0.48	±	0.51	0.0513	0.26	±	0.23	0.5670
14:1ω3c	<0.07	±	0.00	<0.13	±	0.00	<0.06	±	0.00	1.0000	<0.06	±	0.00	1.0000	<0.11	±	0.00	1.0000	<0.12	±	0.00	1.0000
14:0	3.97	±	0.32	0.86	±	0.06	3.11	±	0.05	0.0289	2.03	±	0.05	0.0000	4.05	±	0.53	0.5317	1.07	±	0.06	0.0081
iso-15:1ω9c	0.68	±	0.04	<0.13	±	0.00	0.28	±	0.03	0.0001	0.10	±	0.03	0.0138	0.47	±	0.09	0.0324	0.16	±	0.08	0.0579
iso-15:1ω3c	<0.07	±	0.00	<0.13	±	0.00	<0.06	±	0.00	1.0000	<0.06	±	0.00	1.0000	<0.11	±	0.00	1.0000	<0.12	±	0.00	1.0000
iso-15:0	42.92	±	0.55	39.18	±	7.45	33.88	±	1.51	0.0033	23.03	±	6.12	0.0339	28.38	±	9.87	0.0881	38.25	±	2.29	0.5167
15:0	0.73	±	0.02	0.08	±	0.13	2.05	±	0.11	0.0013	1.13	±	0.05	0.0014	2.20	±	0.38	0.0148	0.80	±	0.07	0.0028
15:1ω10c	1.04	±	0.02	<0.13	±	0.00	2.27	±	0.08	0.0006	1.61	±	0.12	0.0012	2.38	±	0.33	0.0132	0.76	±	0.07	0.0022
15:1ω4c	0.93	±	0.16	<0.13	±	0.00	2.06	±	0.18	0.0009	1.42	±	0.07	0.0006	2.58	±	0.34	0.0043	0.97	±	0.10	0.0027
iso-16:0	<0.07	±	0.00	2.56	±	0.34	<0.06	±	0.00	1.0000	2.15	±	0.29	0.1400	<0.11	±	0.00	1.0000	3.10	±	0.48	0.1376
16:2ω5c,11c	5.51	±	0.24	3.47	±	0.44	5.24	±	0.39	0.2663	4.55	±	0.63	0.0596	5.65	±	1.20	0.5176	3.11	±	0.30	0.2245
16:1ω11c	0.90	±	0.04	<0.13	±	0.00	1.19	±	0.02	0.0011	1.03	±	0.02	0.0001	1.08	±	0.26	0.2345	0.42	±	0.03	0.0012
16:1w5c	11.18	±	0.94	12.40	±	1.29	17.75	±	0.32	0.0024	20.28	±	1.62	0.0024	16.74	±	2.51	0.0339	14.53	±	0.24	0.0703
16:0	1.52	±	0.05	1.28	±	0.12	1.92	±	0.21	0.0535	2.34	±	0.05	0.0010	1.85	±	0.13	0.0241	1.86	±	0.14	0.0041
iso-17:2ω5c,11c	3.64	±	0.16	1.81	±	0.18	2.93	±	0.15	0.0037	2.40	±	0.17	0.0112	2.86	±	0.41	0.0452	1.32	±	0.00	0.0298
iso-17:1ω11c	1.73	±	0.08	0.36	±	0.31	1.37	±	0.03	0.0076	1.17	±	0.02	0.0327	1.35	±	0.19	0.0376	0.46	±	0.00	0.4055
iso-17:1ω5c	3.21	±	0.02	3.52	±	0.49	2.38	±	0.03	0.0000	3.37	±	0.13	0.4245	2.53	±	0.33	0.0476	2.69	±	0.17	0.0592
iso-17:0	5.79	±	1.35	6.42	±	0.98	4.93	±	0.44	0.2619	7.46	±	1.16	0.2168	4.38	±	1.16	0.1760	6.86	±	0.53	0.3717
14:0 3-OH	0.12	±	0.03	0.07	±	0.06	0.58	±	0.06	0.0017	0.52	±	0.02	0.0016	0.57	±	0.11	0.0119	0.20	±	0.06	0.0438
iso-15:0 3-OH	1.15	±	0.21	1.05	±	0.12	3.44	±	0.46	0.0040	3.50	±	0.34	0.0021	4.26	±	0.29	0.0002	1.84	±	0.72	0.1352
16:0 2-OH	0.23	±	0.12	0.50	±	0.19	0.88	±	0.05	0.0035	1.48	±	0.05	0.0065	0.72	±	0.13	0.0066	0.35	±	0.04	0.2079
16:0 3-OH	0.07	±	0.01	<0.13	±	0.00	0.24	±	0.02	0.0007	0.21	±	0.17	0.1167	0.29	±	0.06	0.0129	0.09	±	0.08	0.1290
iso-17:0 2-OH	5.11	±	1.44	6.97	±	0.21	10.48	±	1.21	0.0062	18.55	±	2.08	0.0071	8.38	±	2.09	0.0718	6.24	±	0.84	0.1853
iso-17:0 3-OH	0.20	±	0.13	0.26	±	0.05	1.72	±	2.76	0.2980	0.26	±	0.25	0.5740	0.45	±	0.21	0.1269	0.18	±	0.18	0.3692
iso-15:0 DMA	4.54	±	0.15	7.05	±	1.14	0.07	±	0.01	0.0002	0.44	±	0.07	0.0067	4.15	±	0.75	0.3075	3.60	±	0.62	0.0131
iso-15:0 OAG	2.25	±	0.18	10.97	±	2.84	0.16	±	0.03	0.0013	0.37	±	0.03	0.0163	3.33	±	0.42	0.0237	9.92	±	0.64	0.3852

	elbD⁻/ *elbD*⁺								*elbD*⁺							
	0h			p-value	72h			p-value	0h			p-value	72h			p-value
12:0	0.08	±	0.01	0.5172	<0.10	±	0.00	1.0000	0.11	±	0.03	0.2059	<0.16	±	0.00	1.0000
iso-13:0	0.69	±	0.02	0.0042	0.56	±	0.03	0.0682	0.79	±	0.06	0.0104	0.73	±	0.05	0.3301
iso-14:0	<0.06	±	0.00	1.0000	0.31	±	0.02	0.0976	<0.12	±	0.00	1.0000	0.23	±	0.04	0.2595
14:1ω9c	0.35	±	0.34	0.0173	0.36	±	0.25	0.3686	0.96	±	0.02	0.0015	0.54	±	0.04	0.0009
14:1ω3c	<0.06	±	0.00	1.0000	<0.10	±	0.00	1.0000	<0.12	±	0.00	1.0000	<0.16	±	0.00	1.0000
14:0	2.80	±	0.04	0.0161	0.75	±	0.35	0.4122	2.96	±	0.28	0.0115	0.91	±	0.08	0.2825
iso-15:1ω9c	0.14	±	0.12	0.0075	0.26	±	0.03	0.0038	0.19	±	0.17	0.0234	0.18	±	0.16	0.1294
iso-15:1ω3c	<0.06	±	0.00	1.0000	<0.10	±	0.00	1.0000	<0.12	±	0.00	1.0000	<0.16	±	0.00	1.0000
iso-15:0	36.53	±	1.30	0.0045	35.85	±	1.64	0.3470	39.47	±	2.72	0.1083	32.39	±	3.47	0.1761
15:0	1.57	±	0.04	0.0000	0.67	±	0.09	0.0037	0.92	±	0.04	0.0054	0.39	±	0.05	0.0301
15:1ω10c	1.58	±	0.05	0.0010	0.58	±	0.04	0.0013	0.95	±	0.03	0.0132	0.29	±	0.07	0.0116
15:1ω4c	1.53	±	0.09	0.0069	0.74	±	0.07	0.0022	0.78	±	0.06	0.1614	0.33	±	0.05	0.0052
iso-16:0	<0.06	±	0.00	1.0000	2.84	±	0.14	0.1956	<0.12	±	0.00	1.0000	2.19	±	0.22	0.1493
16:2ω5c,11c	4.97	±	0.45	0.1170	3.02	±	0.19	0.1497	4.34	±	0.41	0.0144	2.86	±	0.28	0.0932
16:1ω11c	1.04	±	0.05	0.0139	0.52	±	0.03	0.0008	0.97	±	0.09	0.2178	0.32	±	0.28	0.1297
16:1w5c	15.91	±	1.42	0.0090	15.01	±	0.65	0.0380	14.48	±	1.48	0.0295	12.24	±	2.06	0.5723
16:0	2.13	±	0.18	0.0151	2.02	±	0.11	0.0010	2.05	±	0.10	0.0030	1.46	±	0.22	0.2094
iso-17:2ω5c,11c	2.44	±	0.08	0.0012	1.25	±	0.07	0.0158	2.62	±	0.10	0.0013	1.33	±	0.17	0.0206
iso-17:1ω11c	1.29	±	0.06	0.0016	0.52	±	0.02	0.3164	1.47	±	0.10	0.0210	0.33	±	0.30	0.5679
iso-17:1ω5c	2.36	±	0.23	0.0167	2.62	±	0.14	0.0528	2.36	±	0.17	0.0092	2.75	±	0.24	0.0656
iso-17:0	5.75	±	0.95	0.5949	6.78	±	0.01	0.3826	5.53	±	1.84	0.5421	6.17	±	0.33	0.4516
14:0 3-OH	0.54	±	0.04	0.0002	0.25	±	0.07	0.0205	0.50	±	0.02	0.0000	0.32	±	0.03	0.0054
iso-15:0 3-OH	3.86	±	0.19	0.0001	2.10	±	0.65	0.0724	3.66	±	0.31	0.0005	3.03	±	0.50	0.0118
16:0 2-OH	0.52	±	0.05	0.0280	0.29	±	0.02	0.1426	0.42	±	0.05	0.0727	0.23	±	0.08	0.0870
16:0 3-OH	0.23	±	0.02	0.0003	0.12	±	0.03	0.0153	0.21	±	0.03	0.0036	0.18	±	0.03	0.0078
iso-17:0 2-OH	5.73	±	1.31	0.4143	6.13	±	0.98	0.1876	7.63	±	0.03	0.0663	7.53	±	0.94	0.2776
iso-17:0 3-OH	0.25	±	0.19	0.4933	0.11	±	0.05	0.0175	0.38	±	0.35	0.3188	0.79	±	0.68	0.2134
iso-15:0 DMA	4.05	±	0.17	0.0153	5.91	±	0.41	0.1524	2.52	±	0.19	0.0001	5.35	±	0.61	0.0772
iso-15:0 OAG	3.66	±	0.22	0.0010	10.42	±	0.64	0.4798	3.73	±	0.24	0.0011	16.92	±	1.03	0.0386

	elbD⁻ / *elbDDW+*								*elbA*⁻							
	0h			p-value	72h			p-value	0h			p-value	72h			p-value
12:0	0.10	±	0.08	0.5247	<0.11	±	0.00	1.0000	0.08	±	0.02	0.3918	<0.08	±	0.00	1.0000
iso-13:0	0.67	±	0.07	0.0025	0.37	±	0.01	0.0251	0.92	±	0.32	0.4543	0.71	±	0.04	0.2636
iso-14:0	<0.09	±	0.00	1.0000	0.29	±	0.04	0.1180	<0.08	±	0.00	1.0000	0.23	±	0.02	0.2445
14:1ω9c	0.90	±	0.09	0.0008	0.37	±	0.03	0.0090	1.38	±	0.07	0.0801	0.27	±	0.01	0.3339
14:1ω3c	<0.09	±	0.00	1.0000	<0.11	±	0.00	1.0000	<0.08	±	0.00	1.0000	<0.08	±	0.00	1.0000
14:0	3.39	±	0.58	0.1638	1.36	±	0.02	0.0012	2.60	±	1.62	0.1942	0.79	±	0.03	0.1220
iso-15:1ω9c	0.21	±	0.02	0.0001	0.21	±	0.03	0.0047	0.62	±	0.03	0.0917	0.26	±	0.03	0.0022
iso-15:1ω3c	<0.09	±	0.00	1.0000	<0.11	±	0.00	1.0000	<0.08	±	0.00	1.0000	<0.08	±	0.00	1.0000
iso-15:0	22.45	±	6.00	0.0188	25.35	±	2.96	0.0489	40.78	±	3.04	0.2380	39.11	±	1.17	0.5731
15:0	1.47	±	0.18	0.0124	0.68	±	0.04	0.0074	0.69	±	0.06	0.2934	0.24	±	0.00	0.6010
15:1ω10c	1.73	±	0.15	0.0092	0.76	±	0.03	0.0003	0.97	±	0.04	0.0592	<0.08	±	0.00	1.0000
15:1ω4c	1.85	±	0.16	0.0015	0.85	±	0.05	0.0009	1.00	±	0.04	0.3707	<0.08	±	0.00	1.0000
iso-16:0	<0.09	±	0.00	1.0000	3.25	±	0.47	0.0827	0.05	±	0.08	0.2863	2.58	±	0.15	0.5445
16:2ω5c,11c	5.33	±	0.62	0.4277	3.63	±	0.06	0.3988	5.11	±	0.15	0.0643	3.26	±	0.11	0.3316
16:1ω11c	1.37	±	0.16	0.0233	0.73	±	0.06	0.0016	0.80	±	0.00	0.0354	<0.08	±	0.00	1.0000
16:1w5c	23.08	±	2.56	0.0060	20.68	±	1.08	0.0009	12.23	±	0.48	0.1300	10.75	±	0.35	0.1050
16:0	2.60	±	0.46	0.0373	2.98	±	0.05	0.0003	1.52	±	0.06	0.6040	0.86	±	0.30	0.0860
iso-17:2ω5c,11c	3.58	±	0.54	0.5278	2.01	±	0.02	0.1453	3.72	±	0.24	0.4366	1.67	±	0.07	0.2059
iso-17:1ω11c	1.68	±	0.23	0.4575	0.85	±	0.03	0.0800	1.60	±	0.07	0.0719	0.44	±	0.05	0.4489
iso-17:1ω5c	3.40	±	0.67	0.4305	3.24	±	0.17	0.2941	3.17	±	0.14	0.4330	3.25	±	0.11	0.2979
iso-17:0	6.46	±	2.84	0.4638	10.29	±	0.40	0.0081	6.86	±	0.51	0.2107	5.73	±	0.20	0.2396
14:0 3-OH	0.74	±	0.11	0.0051	0.56	±	0.08	0.0009	0.28	±	0.08	0.0446	0.18	±	0.03	0.0492
iso-15:0 3-OH	4.25	±	0.56	0.0039	3.56	±	0.10	0.0000	2.49	±	0.56	0.0278	1.98	±	0.16	0.0013
16:0 2-OH	0.79	±	0.05	0.0054	0.65	±	0.07	0.2222	0.42	±	0.07	0.0715	0.17	±	0.10	0.0574
16:0 3-OH	0.21	±	0.10	0.0959	0.22	±	0.12	0.0600	0.18	±	0.06	0.0529	0.10	±	0.02	0.0072
iso-17:0 2-OH	11.90	±	1.57	0.0039	12.12	±	1.48	0.0175	6.21	±	2.36	0.3707	7.23	±	0.90	0.4324
iso-17:0 3-OH	0.15	±	0.15	0.4358	0.50	±	0.42	0.2903	0.50	±	0.22	0.0943	0.64	±	0.14	0.0194
iso-15:0 DMA	0.74	±	0.11	0.0000	1.63	±	0.03	0.0101	3.71	±	0.38	0.0331	8.29	±	0.26	0.1357
iso-15:0 OAG	0.95	±	0.10	0.0009	2.87	±	0.20	0.0269	2.10	±	0.09	0.1938	11.42	±	0.71	0.4973

	elbA⁻/ *elbD*+								*elbB*⁻							
	0h			p-value	72h			p-value	0h			p-value	72h			p-value
12:0	<0.08	±	0.00	0.0173	<0.12	±	0.00	1.0000	0.11	±	0.02	0.2772	<0.08	±	0.00	1.0000
iso-13:0	0.80	±	0.06	0.0109	0.72	±	0.05	0.3001	0.85	±	0.05	0.0222	0.73	±	0.07	0.3417
iso-14:0	<0.08	±	0.00	1.0000	0.33	±	0.01	0.0866	<0.12	±	0.00	1.0000	0.51	±	0.12	0.0152
14:1ω9c	1.26	±	0.08	0.0126	0.33	±	0.02	0.0299	1.60	±	0.07	0.1029	0.46	±	0.04	0.0017
14:1ω3c	<0.08	±	0.00	1.0000	<0.12	±	0.00	1.0000	<0.12	±	0.00	1.0000	<0.08	±	0.00	1.0000
14:0	3.39	±	0.16	0.0495	0.84	±	0.03	0.4383	4.72	±	1.23	0.2747	1.42	±	0.19	0.0183
iso-15:1ω9c	0.49	±	0.01	0.0073	0.30	±	0.05	0.0062	0.48	±	0.03	0.0018	0.18	±	0.16	0.1312
iso-15:1ω3c	<0.08	±	0.00	1.0000	<0.12	±	0.00	1.0000	<0.12	±	0.00	1.0000	<0.08	±	0.00	1.0000
iso-15:0	39.32	±	1.42	0.0245	36.25	±	0.67	0.3723	36.66	±	1.73	0.0121	30.03	±	7.57	0.1529
15:0	1.42	±	0.02	0.0000	0.41	±	0.01	0.0343	2.05	±	0.07	0.0002	0.79	±	0.02	0.0074
15:1ω10c	1.85	±	0.12	0.0045	0.28	±	0.24	0.1288	2.00	±	0.18	0.0076	0.58	±	0.16	0.0167
15:1ω4c	1.92	±	0.27	0.0077	0.62	±	0.06	0.0019	1.99	±	0.34	0.0131	0.89	±	0.08	0.0019
iso-16:0	<0.08	±	0.00	1.0000	3.18	±	0.03	0.0605	<0.12	±	0.00	1.0000	5.17	±	0.77	0.0110
16:2ω5c,11c	5.25	±	0.16	0.1507	2.38	±	0.14	0.0289	5.25	±	0.27	0.2059	3.51	±	0.40	0.5767
16:1ω11c	0.83	±	0.05	0.1265	<0.12	±	0.00	1.0000	1.07	±	0.08	0.0344	0.14	±	0.24	0.2863
16:1w5c	12.83	±	0.76	0.0594	12.26	±	0.37	0.5215	15.77	±	0.38	0.0048	16.19	±	2.72	0.0858
16:0	1.30	±	0.03	0.0031	1.45	±	0.09	0.0912	2.04	±	0.14	0.0103	1.99	±	0.05	0.0022
iso-17:2ω5c,11c	3.93	±	0.28	0.1528	1.78	±	0.13	0.5283	3.03	±	0.12	0.0058	1.64	±	0.02	0.1607
iso-17:1ω11c	1.57	±	0.14	0.1211	0.48	±	0.03	0.3775	1.50	±	0.07	0.0157	0.58	±	0.06	0.2386
iso-17:1ω5c	3.65	±	0.21	0.0472	4.03	±	0.25	0.1474	2.91	±	0.04	0.0019	3.76	±	0.42	0.3805
iso-17:0	4.96	±	2.05	0.4051	7.82	±	0.18	0.0894	6.25	±	0.10	0.3989	11.80	±	0.54	0.0023
14:0 3-OH	0.14	±	0.02	0.2604	0.24	±	0.03	0.0151	0.45	±	0.23	0.0917	0.22	±	0.09	0.0567
iso-15:0 3-OH	1.35	±	0.02	0.1575	2.13	±	0.17	0.0009	2.47	±	0.96	0.0953	1.95	±	0.23	0.0063
16:0 2-OH	0.27	±	0.07	0.4679	0.24	±	0.13	0.0992	0.64	±	0.08	0.0089	0.37	±	0.21	0.3252
16:0 3-OH	0.08	±	0.01	0.2901	0.13	±	0.03	0.0141	0.24	±	0.11	0.0814	0.16	±	0.03	0.0081
iso-17:0 2-OH	6.75	±	0.54	0.1252	5.92	±	0.40	0.0197	6.96	±	1.52	0.1468	8.41	±	1.01	0.0902
iso-17:0 3-OH	0.33	±	0.07	0.1696	1.06	±	0.14	0.0033	0.65	±	0.49	0.1740	0.84	±	0.31	0.0546
iso-15:0 DMA	4.05	±	0.07	0.0105	5.86	±	0.20	0.1468	0.25	±	0.03	0.0002	2.35	±	0.42	0.0079
iso-15:0 OAG	2.25	±	0.09	0.5695	10.96	±	0.48	0.5753	0.08	±	0.01	0.0015	5.32	±	1.02	0.0434

	elbB- / elbD+								*elbE*$^{-}$							
	0h			p-value	72h			p-value	0h			p-value	72h			p-value
12:0	<0.14	±	0.00	0.0173	<0.14	±	0.00	1.0000	0.06	±	0.06	0.3116	<0.06	±	0.00	1.0000
iso-13:0	0.92	±	0.05	0.1122	0.50	±	0.12	0.0231	0.80	±	0.07	0.0194	0.60	±	0.32	0.2726
iso-14:0	<0.14	±	0.00	1.0000	0.34	±	0.01	0.0807	<0.13	±	0.00	1.0000	0.30	±	0.14	0.1631
14:1ω9c	1.00	±	0.03	0.0015	0.30	±	0.03	0.1349	1.30	±	0.14	0.0934	0.42	±	0.09	0.0549
14:1ω3c	<0.14	±	0.00	1.0000	<0.14	±	0.00	1.0000	0.01	±	0.01	0.2863	<0.06	±	0.00	1.0000
14:0	3.33	±	0.33	0.0534	0.97	±	0.02	0.0558	4.63	±	0.20	0.0367	1.14	±	0.13	0.0313
iso-15:1ω9c	0.37	±	0.03	0.0003	0.30	±	0.01	0.0002	0.44	±	0.06	0.0053	0.17	±	0.15	0.1287
iso-15:1ω3c	<0.14	±	0.00	1.0000	<0.14	±	0.00	1.0000	<0.13	±	0.00	1.0000	<0.06	±	0.00	1.0000
iso-15:0	34.64	±	0.85	0.0003	34.59	±	0.36	0.2805	37.69	±	1.10	0.0039	32.52	±	9.15	0.2748
15:0	1.76	±	0.06	0.0002	0.59	±	0.04	0.0114	2.02	±	0.24	0.0075	0.81	±	0.14	0.0021
15:1ω10c	2.03	±	0.14	0.0043	0.65	±	0.03	0.0005	2.04	±	0.14	0.0041	0.70	±	0.15	0.0105
15:1ω4c	2.12	±	0.06	0.0015	0.89	±	0.04	0.0005	2.14	±	0.22	0.0015	0.79	±	0.15	0.0079
iso-16:0	<0.14	±	0.00	1.0000	3.46	±	0.17	0.0162	<0.13	±	0.00	1.0000	3.95	±	0.42	0.0088
16:2ω5c,11c	5.05	±	0.07	0.0507	2.71	±	0.01	0.0684	5.01	±	0.49	0.1484	3.64	±	0.39	0.4370
16:1ω11c	0.94	±	0.03	0.1531	<0.14	±	0.00	1.0000	1.17	±	0.10	0.0193	<0.06	±	0.00	1.0000
16:1w5c	13.93	±	0.25	0.0214	14.27	±	0.08	0.0932	15.67	±	1.22	0.0063	14.84	±	2.33	0.1510
16:0	1.54	±	0.06	0.4484	1.55	±	0.03	0.0337	2.19	±	0.20	0.0171	1.88	±	0.28	0.0341
iso-17:2ω5c,11c	3.94	±	0.32	0.1731	1.97	±	0.08	0.1372	2.92	±	0.28	0.0191	1.81	±	0.28	0.5997
iso-17:1ω11c	1.89	±	0.09	0.0626	0.74	±	0.03	0.1142	1.60	±	0.14	0.1742	0.60	±	0.12	0.2193
iso-17:1ω5c	3.54	±	0.08	0.0112	4.00	±	0.20	0.1932	2.81	±	0.26	0.0841	3.82	±	0.50	0.3472
iso-17:0	6.62	±	0.29	0.2712	7.57	±	0.39	0.0983	6.86	±	0.26	0.2090	9.41	±	1.51	0.0394
14:0 3-OH	0.20	±	0.04	0.0476	0.24	±	0.02	0.0235	0.27	±	0.01	0.0034	0.21	±	0.03	0.0246
iso-15:0 3-OH	1.61	±	0.17	0.0312	1.93	±	0.09	0.0006	1.73	±	0.23	0.0225	1.97	±	0.28	0.0127
16:0 2-OH	0.27	±	0.02	0.4118	0.29	±	0.02	0.1336	0.81	±	0.19	0.0132	0.34	±	0.13	0.2206
16:0 3-OH	0.14	±	0.03	0.0267	0.11	±	0.02	0.0036	0.18	±	0.01	0.0003	0.10	±	0.06	0.0681
iso-17:0 2-OH	6.38	±	0.36	0.1831	6.50	±	0.19	0.0252	4.85	±	3.16	0.5392	8.10	±	1.43	0.2109
iso-17:0 3-OH	0.43	±	0.21	0.1460	0.83	±	0.06	0.0002	0.50	±	0.26	0.1246	0.45	±	0.40	0.3200
iso-15:0 DMA	4.82	±	0.52	0.3114	6.41	±	0.21	0.2556	1.42	±	0.05	0.0002	4.26	±	0.82	0.0224
iso-15:0 OAG	2.55	±	0.06	0.0626	8.29	±	0.09	0.1669	0.89	±	0.02	0.0038	7.15	±	0.30	0.1010

	elbE- / elbD+							
	0h			p-value	72h			p-value
12:0	<0.10	±	0.00	0.0173	<0.09	±	0.00	1.0000
iso-13:0	0.58	±	0.02	0.0018	0.72	±	0.13	0.3368
iso-14:0	<0.10	±	0.00	1.0000	0.49	±	0.05	0.0205
14:1ω9c	1.11	±	0.06	0.0012	0.40	±	0.06	0.0233
14:1ω3c	<0.10	±	0.00	1.0000	<0.09	±	0.00	1.0000
14:0	4.24	±	0.69	0.3801	1.44	±	0.14	0.0071
iso-15:1ω9c	0.24	±	0.02	0.0003	0.19	±	0.17	0.1378
iso-15:1ω3c	<0.10	±	0.00	1.0000	<0.09	±	0.00	1.0000
iso-15:0	35.86	±	2.16	0.0170	32.43	±	6.35	0.2162
15:0	3.15	±	0.01	0.0000	1.19	±	0.15	0.0005
15:1ω10c	2.94	±	0.18	0.0020	1.01	±	0.09	0.0018
15:1ω4c	2.85	±	0.13	0.0001	1.35	±	0.20	0.0053
iso-16:0	<0.10	±	0.00	1.0000	4.26	±	0.53	0.0101
16:2ω5c,11c	5.10	±	0.51	0.2101	2.76	±	0.03	0.0762
16:1ω11c	1.33	±	0.05	0.0003	0.19	±	0.32	0.2863
16:1w5c	16.28	±	2.07	0.0243	16.05	±	1.10	0.0158
16:0	1.98	±	0.01	0.0012	1.82	±	0.11	0.0032
iso-17:2ω5c,11c	2.97	±	0.15	0.0049	1.66	±	0.10	0.2118
iso-17:1ω11c	1.64	±	0.10	0.2218	0.61	±	0.06	0.2108
iso-17:1ω5c	2.95	±	0.06	0.0095	3.97	±	0.45	0.2171
iso-17:0	5.85	±	0.25	0.5568	9.18	±	1.19	0.0280
14:0 3-OH	0.17	±	0.08	0.2984	0.35	±	0.03	0.0035
iso-15:0 3-OH	1.13	±	0.57	0.5593	2.49	±	0.32	0.0061
16:0 2-OH	0.25	±	0.08	0.5351	0.10	±	0.05	0.0446
16:0 3-OH	0.10	±	0.08	0.3807	0.22	±	0.03	0.0051
iso-17:0 2-OH	4.03	±	0.89	0.2476	4.05	±	0.75	0.0113
iso-17:0 3-OH	0.19	±	0.20	0.5845	0.98	±	0.59	0.1183
iso-15:0 DMA	3.48	±	0.20	0.0017	6.05	±	0.69	0.2008
iso-15:0 OAG	1.57	±	0.34	0.0398	6.03	±	1.18	0.0555

Supplementary Data Set 2 | Closest homologues of ElbA-E from *Myxococcus xanthus* and the human alkyl-dihydroxyacetonephosphate synthase found in other sequenced species of the order myxococcales by means of BLAST P search. Description and Pfam numbers from the sanger institute (http://pfam.sanger.ac.uk).

		***Myxococcus xanthus* DK1622**	*Anaeromyxobacter dehalogenans* 2CP-1	*Anaeromyxobacter dehalogenans* 2CP-C	*Anaeromyxobacter sp.* Fw109-5	*Anaeromyxobacter sp.* K	*Corallococcus coralloides* DSM 2259	*Cystobacter fuscus* DSM 2262	*Haliangium ochraceum* DSM14365	*Myxococcus fulvus* HW-1	*Myxococcus stipitatus* DSM 14675	*Plesiocystis pacifica* SIR-1	*Sorangium cellulosum* So ce 56	*Stigmatella aurantiaca* DW4/3-1
ElbA	Accession	YP_629783 (MXAN_1531)	YP_002491739	YP_464379	YP_001378407	YP_002133589	YP_005367544	WP_002629077	-	YP_004663235	YP_007358674	-	YP_001617847	YP_003951936
	Sequence Length	326	329	329	329	329	331	325	-	326	327	-	338	326
	Bit-Score	655.21	255.373	276.944	281.952	256.529	460.685	406.371	-	618.231	526.554	-	164.466	449.129
	Query coverage %	100.00%	100.00%	100.00%	100.00%	100.00%	100.00%	99.69%	-	100.00%	100.00%	-	100.00%	100.00%
	Identical Sites	100.00%	50.50%	52.00%	51.10%	50.80%	72.80%	66.20%	-	92.60%	78.90%	-	35.50%	72.70%
	Description	short chain dehydrogenase/3-beta hydroxysteroid dehydrogenase/isomerase family/NAD dependent epimerase/dehydratase family/male sterility protein	short chain dehydrogenase/3-beta hydroxysteroid dehydrogenase/isomerase family/NAD dependent epimerase/dehydratase family/male sterility protein	short chain dehydrogenase/3-beta hydroxysteroid dehydrogenase/isomerase family/NAD dependent epimerase/dehydratase family/male sterility protein	short chain dehydrogenase/3-beta hydroxysteroid dehydrogenase/isomerase family/NAD dependent epimerase/dehydratase family/male sterility protein	short chain dehydrogenase/3-beta hydroxysteroid dehydrogenase/isomerase family/NAD dependent epimerase/dehydratase family/male sterility protein	NAD dependent epimerase/dehydratase family/short chain dehydrogenase	NAD dependent epimerase/dehydratase family	-	NAD dependent epimerase/dehydratase family	NAD dependent epimerase/dehydratase family	-	NAD dependent epimerase/dehydratase family	NAD dependent epimerase/dehydratase family
	Pfam number	PF00106/PF01073/PF01370/PF07993	PF00106/PF01073/PF01370/PF07993	PF00106/PF01073/PF01370/PF07993	PF00106/PF01073/PF01370/PF07993	PF00106/PF01073/PF01370/PF07993	PF01370/PF00106	PF01370		PF01370	PF01370		PF01370	PF01370
ElbB	Accession	YP_629782 (MXAN_1530)	YP_002491738	YP_464378	YP_001378406	YP_002133588	YP_005367543	WP_020918089.1	YP_003268023	YP_004663236	YP_007358673	WP_006969398	YP_001618944	YP_003951935
	Sequence Length	221	215	215	215	215	221	221	220	221	221	216	216	221
	Bit-Score	457.218	295.049	296.59	315.079	295.049	414.461	416.772	259.61	454.521	440.654	173.326	199.519	400.593
	Query coverage %	100.00%	97.29%	97.29%	97.29%	97.29%	100.00%	100.00%	99.10%	100.00%	100.00%	97.74%	97.74%	100.00%
	Identical Sites	100.00%	63.70%	63.30%	67.90%	63.70%	87.30%	87.30%	54.50%	99.10%	94.60%	38.00%	44.40%	84.20%
	Description	HAD superfamily hydrolase	HAD superfamily hydrolase	HAD superfamily hydrolase	HAD superfamily hydrolase	HAD superfamily hydrolase	HAD superfamily hydrolase	HAD superfamily hydrolase	HAD superfamily hydrolase	HAD superfamily hydrolase	HAD superfamily hydrolase	HAD superfamily hydrolase	HAD superfamily hydrolase	HAD superfamily hydrolase
	Pfam number	PF12710	PF12710	PF12710	PF12710	PF12710	PF12710	PF12710	PF12710	PF12710	PF12710	PF12710	PF12710	PF12710

ElbC	Accession	YP_629781 (MXAN_1529)	YP_002491737	YP_464377	YP_002133587	YP_001378405	YP_005367542	WP_002629079	YP_003268024	YP_004663237	YP_007358672	WP_006969399	YP_001618943	WP_002610269
	Sequence Length	536	532	532	532	532	536	537	521	536	536	520	519	481
	Bit-Score	1105.12	749.584	731.865	749.199	764.607	1031.17	976.467	687.952	1098.58	1059.28	593.964	605.905	918.302
	Query coverage %	100.00%	99.25%	99.25%	99.25%	99.25%	100.00%	100.00%	97.01%	100.00%	100.00%	97.01%	96.83%	89.74%
	Identical Sites	100.00%	65.20%	65.00%	65.00%	67.10%	91.80%	86.40%	61.40%	99.30%	94.20%	52.70%	53.90%	90.40%
	Description	hypothetical protein	hypothetical protein	hypothetical protein	hypothetical protein	hypothetical protein	hypothetical protein	Transcriptional regulator	hypothetical protein	hypothetical protein	hypothetical protein	hypothetical protein	hypothetical protein	hypothetical protein
	Pfam number	DUF2088	DUF2088	DUF2088	DUF2088	DUF2088	DUF2088	DUF2088	DUF2088	DUF2088	DUF2088	DUF2088	DUF2088	DUF2088
ElbD	Accession	YP_629780 (MXAN_1528)	YP_464376	YP_002491736	YP_002133586	YP_001378404	YP_005367541	WP_002629080	YP_003267643	YP_004663238	YP_007358671	WP_006969400	YP_001618662	YP_003951933
	Sequence Length	1470	1492	1472	1472	1466	1476	1448	1515	1470	1450	1479	1130	1451
	Bit-Score	2983.36	1442.17	1449.49	1456.04	1500.72	2434.06	2254.17	1228.39	2831.2	2479.9	1045.8	729.169	2378.21
	Query coverage %	100.00%	98.91%	97.55%	97.55%	97.69%	100.00%	98.23%	97.48%	100.00%	98.44%	98.30%	74.56%	98.50%
	Identical Sites	100.00%	53.60%	54.30%	54.60%	55.90%	81.00%	74.70%	44.90%	95.80%	84.30%	40.90%	38.60%	78.10%
	Description	Male sterility protein /long-chain-fatty-acid-CoA ligase/Phosphopantetheine attachment site/acyltransferase/	Male sterility protein /long-chain-fatty-acid-CoA ligase/Phosphopantetheine attachment site/acyltransferase	Male sterility protein /long-chain-fatty-acid-CoA ligase/Phosphopantetheine attachment site/acyltransferase	Male sterility protein /long-chain-fatty-acid-CoA ligase/Phosphopantetheine attachment site/acyltransferase	Male sterility protein /long-chain-fatty-acid-CoA ligase/Phosphopantetheine attachment site/acyltransferase	Male sterility protein /long-chain-fatty-acid-CoA ligase/Phosphopantetheine attachment site/acyltransferase	Male sterility protein /long-chain-fatty-acid-CoA ligase/Phosphopantetheine attachment site/acyltransferase	Male sterility protein /long-chain-fatty-acid-CoA ligase/Phosphopantetheine attachment site/acyltransferase	Male sterility protein /long-chain-fatty-acid-CoA ligase/Phosphopantetheine attachment site/acyltransferase	Male sterility protein /long-chain-fatty-acid-CoA ligase/Phosphopantetheine attachment site/acyltransferase	Male sterility protein /long-chain-fatty-acid-CoA ligase/Phosphopantetheine attachment site/acyltransferase /SCP-2 sterol transfer family	Male sterility protein /long-chain-fatty-acid-CoA ligase/Phosphopantetheine attachment site/acyltransferase	Male sterility protein /long-chain-fatty-acid-CoA ligase/Phosphopantetheine attachment site/acyltransferase
	Pfam number	PF07993/PF00501/PF00550/PF01553	PF07993/PF00501/PF00550/PF01553	PF07993/PF00501/PF00550/PF01553	PF07993/PF00501/PF00550/PF01553	PF07993/PF00501/PF00550/PF01553	PF07993/PF00501/PF00550/PF01553	PF07993/PF00501/PF00550/PF01553	PF07993/PF00501/PF00550/PF01553	PF07993/PF00501/PF00550/PF01553	PF07993/PF00501/PF00550/PF01553	PF07993/PF00501/PF00550/PF01553/PF02036	PF07993/PF00501/PF00550/PF01553	PF07993/PF00501/PF00550/PF01553
ElbE	Accession	YP_629779 (MXAN_1527)	YP_464375	YP_002491735	YP_001378403	YP_002133585	YP_005367540	WP_002629081	YP_003267644	YP_004663239	YP_007358670	WP_006969401	YP_001618663	YP_003951932
	Sequence Length	342	336	333	337	333	342	342	331	342	342	344	325	342
	Bit-Score	694.115	337.035	332.413	342.813	331.643	564.303	557.37	283.108	662.529	580.482	183.726	256.914	538.11
	Query coverage %	100.00%	97.95%	95.91%	98.25%	95.91%	100.00%	100.00%	93.27%	100.00%	100.00%	93.86%	93.86%	100.00%
	Identical Sites	99.70%	55.70%	55.30%	55.20%	55.00%	79.80%	79.20%	47.40%	95.30%	81.00%	34.60%	44.30%	75.40%

	Description	NAD dependent epimerase/dehydratase	NAD-dependent epimerase/dehydratase	NAD-dependent epimerase/dehydratase	NAD-dependent epimerase/dehydratase	NAD-dependent epimerase/dehydratase	NAD dependent epimerase/dehydratase family protein	NAD dependent epimerase/dehydratase	NAD-dependent epimerase/dehydratase	NAD dependent epimerase/dehydratase family protein	NAD dependent epimerase/dehydratase family protein	NAD-dependent epimerase/dehydratase	NAD-dependent epimerase/dehydratase	NAD dependent epimerase/dehydratase family protein
	Pfam number	PF01370	PF01370	PF01370	PF01370	PF01370	PF01370	PF01370	PF01370	PF01370	PF01370	PF01370	PF01370	PF01370
NP_003650 (human alkyl-DHAP Synthase)	Accession	YP_629928 (MXAN_1676)	-	-	-	-	-	-	-	YP_004663072	YP_007363053	-	YP_001619974	-
	Sequence Length	631	-	-	-	-	-	-	-	614	597	-	614	-
	Bit-Score	532.332	-	-	-	-	-	-	-	510.76	519.62	-	548.895	-
	Query coverage %	91.79%	-	-	-	-	-	-	-	91.79%	90.43%	-	93.01%	-
	Identical Sites	44.20%	-	-	-	-	-	-	-	43.30%	43.60%	-	43.60%	-
	Description	oxidase, FAD binding	-	-	-	-	-	-	-	oxidase, FAD binding	oxidase, FAD binding	-	oxidase, FAD binding	-
	Pfam number	PF02913								PF02913	PF02913		PF02913	

Supplementary Data Set 3 | Result of MAFFT alignment from which the cladogram in Supplementary Figure 9 was calculated. For details see Supplementary Note 3 section.

Sequence Name	Alignment
>PlsC1_M._xanthus 1-acyl-sn-glycerol-3-phosphate acyltransferase [*Myxococcus xanthus* DK 1622]	NHQSTIDIPAHFLAVPIP--------FRYVAKTQL-KW--VPLI-GWYLALAGHVFINRS------------------ NRSKAI---------ASLNA-AAAKIRGGT--S-IFLYPEGTRSTDG-RVLPFKKGPF-ALALKA---------- RVPVCPVTIEGSGDL----------------MPKSTWNITPG-----------------P-IRVKIGKPID--- TTTFAEN-- DREGLARAVRAVIIADSLSLGGKGGDVDD
>PlsC_C._apiculatus 1-acyl-sn-glycerol-3-phosphate acyltransferase [*Chondromyces apiculatus* DSM 436]	NHQSTIDIPAHFMAVPVP--------FRYVAKSQL-KW--VPII-GWYLWIAGHVFINRT------------------ NRRKAI---------ASLDE-AARKIRAGT--S-IFLYPEGTRSEDG-SILPFKKGPF-ALALKA---------- RVPICPVTIEGSGNL----------------MPKSTWNITPG-----------------T-IRVKIGKPID--- TTAFAEN-- DREGLARAVRAVIIADSLALGGKGGDPDD
>PlsC_C._coralloides 1-acyl-sn-glycerol-3-phosphate acyltransferase [*Corallococcus coralloides* DSM 2259]	NHLSTLDIPAHFLAVPVD--------FRFVAKSQL-RF--VPFI-GWYLWLAGHIFIDRG------------------ DRSSAI---------ASLEK-AARKIRAGT--S-IFLYPEGTRSPDG-RVLPFKKGPF-ALALKA---------- RVPICPVTIEGTDNV----------------MPKNSWNITPG-----------------P-VRVKVGRPID--- TSGFADN-- DREGLARAVRAQIIADSLSLGGKGGDPDT
>PlsC_S._cellulosum 1-acylglycerol-3-phosphate O-acyltransferase [*Sorangium cellulosum* So ce56]	NHQSLFDIPVVFRAIPGR--------LRMIAKKEL-FN--VPIF-GQAMKAAGFIRINRS------------------ DHVQAS---------ASLQV-GASMLQDGT--R-VWIAPEGTRSKTG-ALLPFKSGGF-RMAIET---------- NTPILPVAIDGTRHV----------------LRAKDFVVQEH-----------------HRVVVTIMPPID--- PAPYGAG-- GRNRLMRDVRAAIAGALGHDPGLVHRGAG
>PlsC4_M._xanthus 1-acyl-sn-glycerol-3-phosphate acyltransferase [*Myxococcus xanthus* DK 1622]	NHQSAADILAVMGLFRP---------YKFVAKASL-FS--LPLV-GWMMTLLAYVPIVRG------------------ SSTAMN---------QLLDP-CRRWLRRGM--P-VLIFPEGTYSKGG-QLLPFKRGAF-QLALEE---------- HVPVVPVVVEGTPGL----------------LDGDGPWMSPT-----------------ASIRVRVLPALP--- PESFSP--DSQALATQVRALFEQTLAKTG------ --
>PlsC5_M._xanthus acetyltransferase [*Myxococcus xanthus* DK 1622]	NHESLGDILVLFGLYRP---------FKWVSKASN-FK--LPLI-GWNMRLNRYVPLVRG------------------ DRASIT---------KMLAD-CEYWLSRGV--P-ILMFPEGTRSSDG-VVKPFKDGAF-ALALKQ---------- RCPVIPVVLTGTART----------------LPKHGLVLETT-----------------ARCHVQVMPPVD---PSAFT- --DVASLREHVRNLIVSEKARIEALTPGA--
>PlsC_A._dehalogenans 1-acyl-sn-glycerol-3-phosphate acyltransferase [*Anaeromyxobacter dehalogenans* 2CP-C]	NHQSMLDILLLSRMPRE---------MKWVAKEEL-FK--IPWV-GTMLRMTGDIPVRRG------------------ DPESGG---------EALGK-AKGYLARGM--N-VMMFPEGTRSAKG-RMLPFKSGAF-RLAIEA---------- GVPVLPVAVSGTAHG----------------MPKGGPWVRPC-----------------RGTARILAPVS--- VEGMKPE--DAPKLRDVVRARIEEALATLPPA---- --
>PlsC2_M._xanthus 1-acyl-sn-glycerol-3-phosphate acyltransferase [*Myxococcus xanthus* DK 1622]	NHESNADPFLISHLPWE---------MKWLGKASL-FK--IPVV-GWSMWMAGDVPVHRG------------------ DRDSAT---------GAMAK-CRQWLAKGM--P-VMIFPEGTRSKTD-DLLPFKDGAF-RLAIEA---------- QADVLPLAVSGTRRA----------------LPKHSWRFATS-----------------RGLVTVGTPIS--- TKGMTLA-- DVETLKNLAREQILSLRASLMPLTRTEPA

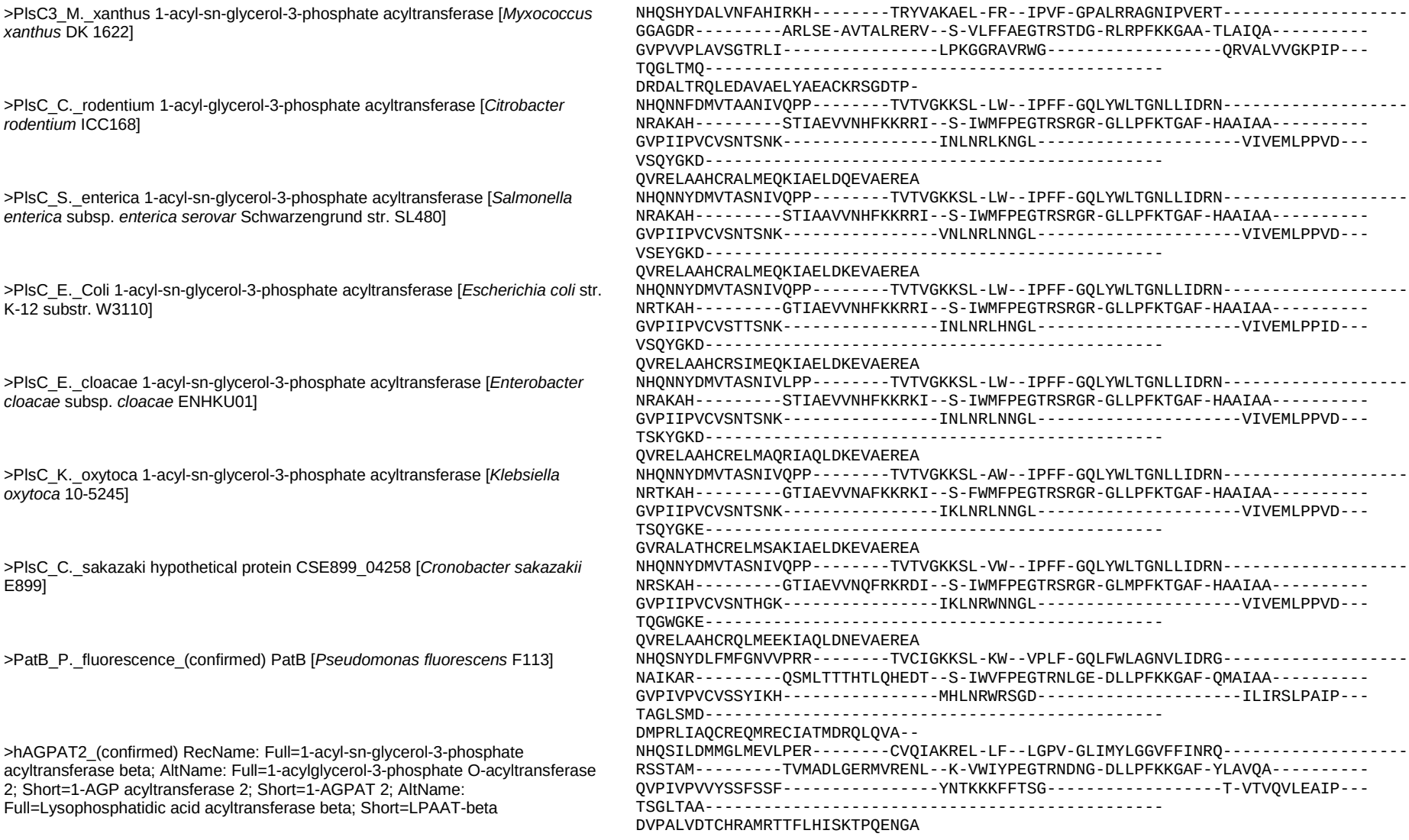
>PlsC3_M._xanthus 1-acyl-sn-glycerol-3-phosphate acyltransferase [*Myxococcus xanthus* DK 1622]
NHQSHYDALVNFAHIRKH--------TRYVAKAEL-FR--IPVF-GPALRRAGNIPVERT------------------
GGAGDR---------ARLSE-AVTALRERV--S-VLFFAEGTRSTDG-RLRPFKKGAA-TLAIQA----------
GVPVVPLAVSGTRLI---------------LPKGGRAVRWG-----------------QRVALVVGKPIP---
TQGLTMQ---
DRDALTRQLEDAVAELYAEACKRSGDTP-
>PlsC_C._rodentium 1-acyl-glycerol-3-phosphate acyltransferase [*Citrobacter rodentium* ICC168]
NHQNNFDMVTAANIVQPP--------TVTVGKKSL-LW--IPFF-GQLYWLTGNLLIDRN------------------
NRAKAH---------STIAEVVNHFKKRRI--S-IWMFPEGTRSRGR-GLLPFKTGAF-HAAIAA----------
GVPIIPVCVSNTSNK---------------INLNRLKNGL--------------------VIVEMLPPVD---
VSQYGKD---
QVRELAAHCRALMEQKIAELDQEVAEREA
>PlsC_S._enterica 1-acyl-sn-glycerol-3-phosphate acyltransferase [*Salmonella enterica* subsp. *enterica serovar* Schwarzengrund str. SL480]
NHQNNYDMVTASNIVQPP--------TVTVGKKSL-LW--IPFF-GQLYWLTGNLLIDRN------------------
NRAKAH---------STIAAVVNHFKKRRI--S-IWMFPEGTRSRGR-GLLPFKTGAF-HAAIAA----------
GVPIIPVCVSNTSNK---------------VNLNRLNNGL--------------------VIVEMLPPVD---
VSEYGKD---
QVRELAAHCRALMEQKIAELDKEVAEREA
>PlsC_E._Coli 1-acyl-sn-glycerol-3-phosphate acyltransferase [*Escherichia coli* str. K-12 substr. W3110]
NHQNNYDMVTASNIVQPP--------TVTVGKKSL-LW--IPFF-GQLYWLTGNLLIDRN------------------
NRTKAH---------GTIAEVVNHFKKRRI--S-IWMFPEGTRSRGR-GLLPFKTGAF-HAAIAA----------
GVPIIPVCVSTTSNK---------------INLNRLHNGL--------------------VIVEMLPPID---
VSQYGKD---
QVRELAAHCRSIMEQKIAELDKEVAEREA
>PlsC_E._cloacae 1-acyl-sn-glycerol-3-phosphate acyltransferase [*Enterobacter cloacae* subsp. *cloacae* ENHKU01]
NHQNNYDMVTASNIVLPP--------TVTVGKKSL-LW--IPFF-GQLYWLTGNLLIDRN------------------
NRAKAH---------STIAEVVNHFKKRKI--S-IWMFPEGTRSRGR-GLLPFKTGAF-HAAIAA----------
GVPIIPVCVSNTSNK---------------INLNRLNNGL--------------------VIVEMLPPVD---
TSKYGKD---
QVRELAAHCRELMAQRIAQLDKEVAEREA
>PlsC_K._oxytoca 1-acyl-sn-glycerol-3-phosphate acyltransferase [*Klebsiella oxytoca* 10-5245]
NHQNNYDMVTASNIVQPP--------TVTVGKKSL-AW--IPFF-GQLYWLTGNLLIDRN------------------
NRTKAH---------GTIAEVVNAFKKRKI--S-FWMFPEGTRSRGR-GLLPFKTGAF-HAAIAA----------
GVPIIPVCVSNTSNK---------------IKLNRLNNGL--------------------VIVEMLPPVD---
TSQYGKE---
GVRALATHCRELMSAKIAELDKEVAEREA
>PlsC_C._sakazaki hypothetical protein CSE899_04258 [*Cronobacter sakazakii* E899]
NHQNNYDMVTASNIVQPP--------TVTVGKKSL-VW--IPFF-GQLYWLTGNLLIDRN------------------
NRSKAH---------GTIAEVVNQFRKRDI--S-IWMFPEGTRSRGR-GLMPFKTGAF-HAAIAA----------
GVPIIPVCVSNTHGK---------------IKLNRWNNGL--------------------VIVEMLPPVD---
TQGWGKE---
QVRELAAHCRQLMEEKIAQLDNEVAEREA
>PatB_P._fluorescence_(confirmed) PatB [*Pseudomonas fluorescens* F113]
NHQSNYDLFMFGNVVPRR--------TVCIGKKSL-KW--VPLF-GQLFWLAGNVLIDRG------------------
NAIKAR---------QSMLTTTHTLQHEDT--S-IWVFPEGTRNLGE-DLLPFKKGAF-QMAIAA----------
GVPIVPVCVSSYIKH---------------MHLNRWRSGD--------------------ILIRSLPAIP---
TAGLSMD---
DMPRLIAQCREQMRECIATMDRQLQVA--
>hAGPAT2_(confirmed) RecName: Full=1-acyl-sn-glycerol-3-phosphate acyltransferase beta; AltName: Full=1-acylglycerol-3-phosphate O-acyltransferase 2; Short=1-AGP acyltransferase 2; Short=1-AGPAT 2; AltName: Full=Lysophosphatidic acid acyltransferase beta; Short=LPAAT-beta
NHQSILDMMGLMEVLPER--------CVQIAKREL-LF--LGPV-GLIMYLGGVFFINRQ------------------
RSSTAM---------TVMADLGERMVRENL--K-VWIYPEGTRNDNG-DLLPFKKGAF-YLAVQA----------
QVPIVPVVYSSFSSF---------------YNTKKKFFTSG-----------------T-VTVQVLEAIP---
TSGLTAA---
DVPALVDTCHRAMRTTFLHISKTPQENGA

>hAGPAT1_(confirmed) RecName: Full=1-acyl-sn-glycerol-3-phosphate acyltransferase alpha; AltName: Full=1-acylglycerol-3-phosphate O-acyltransferase 1; Short=1-AGP acyltransferase 1; Short=1-AGPAT 1; AltName: Full=Lysophosphatidic acid acyltransferase alpha; Short=LPAAT-alpha; AltName: Full=Protein G15	NHQSSLDLLGMMEVLPGR--------CVPIAKREL-LW--AGSA-GLACWLAGVIFIDRK------------------ RTGDAI---------SVMSEVAQTLLTQDV--R-VWVFPEGTRNHNG-SMLPFKRGAF-HLAVQA---------- QVPIVPIVMSSYQDF----------------YCKKERRFTSG------------------Q-CQVRVLPPVP--- TEGLTPD--- DVPALADRVRHSMLTVFREISTDGRGGGD
>NlaB_N._meningitidis_(confirmed) lysophosphatidic acid acyltransferase homolog NlaB [*Neisseria meningitidis* NMB]	KHQSGWETLALQDIFPP---------QVYVAKREL-FK--IPFF-GWGLKLVKTIGIDRN------------------ NRREAN---------EQLIKQGLARKNEGY--W-ITIFPEGTRLAPG-KRGKYKLGGA-RMAKMF---------- EMDIVPVALNSGEF-----------------WPKNSFLKYPG-------------------EITVVICPTIP------ HASG---SEAELMGKCEHLIETQQPLISGAGPFAAK
>HdtS_P._fluorescence_(confirmed) HdtS, LptA [*Pseudomonas fluorescens* F113]	NHQSTWETFFLSAYFEP---------LSQVLKREL-LF--VPFF-GWAMAMLRPIAIDRD------------------ NPKAAL---------KQVAKKGDELLKDNV--W-VLIFPEGTRVPYG-TVGKFSRSGS-ALAVNA---------- DLPVLPIAHNAGKF-----------------WPKAGWIRKPG-------------------VITVVIGAPMY--- AEGTGPR--- AIAELNDRVQAWNEQTQREMGSLPPTPTT
>ElbD_H._ochraceum AMP-dependent synthetase and ligase [*Haliangium ochraceum* DSM 14365]	NHASHLDMGLVKHALGETGDL-----VVALAAKDY-FFE-DPVRRAYFENFTNLVPMERY-------------------- GSLR---------ESLRL-ASDVLRDGH--I-LLIFPEGTRSKDG-VMDAFLPSLG-YLAMQN---------- RCGILPMYLAGTHDA----------------MPKGAFLPKQR------------------E- VSAHIAPFLTYEQVQGLAAG--- KSRSAAYRAISQQVEARVRKLAPAEYEWTL
>Elb_D_C._fuscus_(modified) Long-chain-fatty-acid--CoA ligase [*Cystobacter fuscus*]	NHTSHLDMGLVKLVLGEQGQR-----LTTIAARDY-FFD-TPLKRAYFENFTDLIPMDRH-------------------- GSLR---------ESLRM-AGSALQQGY--N-LLIFPEGTRSVTG-ELLEFKPTLG-YLSLTY---------- NVDVLPIYLKGAYEA----------------LPKGRILPKSR------------------E- LEGHIGPVLTHEMLRAKTHG--- MSRSESYRYATRLAEDAIRALAAGRVLSF-
>ElbD_M.xanthus long-chain-fatty-acid--CoA ligase [*Myxococcus xanthus* DK 1622]	NHSSHLDAGLVRVALGDQGER-----LVSLAARDY-FFN-TPLKRAWFENFTNLIPIERQ-------------------- GSLR---------ESLRM-AGEALRQGF--N-VLIFPEGTRSTTG-ELMEFKSTLG-YLALTF---------- NMDVLPLYIGGAFDA----------------LPKGSVLPKTK------------------ TPLRVNIGPALGHADLRTRVQG--- MARSEGYRYVTRIAEDSMRALRDGRVLNL-
>ElbD_M._fulvus putative long-chain-fatty-acid--CoA ligase [*Myxococcus fulvus* HW-1]	NHSSHLDAGLVRTALGEQGER-----LVSLAARDY-FFN-TPLKRAWFENFTNLVPIERQ-------------------- GSLR---------ESLRM-AGEALRQGF--N-VLIFPEGTRSPTG-ELMEFKSTLG-YLALTY---------- HVDVLPLYIGGAFDA----------------LPKGSVLPRTK------------------ TPLRVNIGPVLGHADLRTRVQG--- MARSEGYRYVTRIAEDSMRALRDGRVLSL-
>ElbD_M._stipitatus AMP-dependent synthetase and ligase [*Myxococcus stipitatus* DSM 14675]	NHASHLDAGLVRVVLEEQGER-----LISLAARDY-FFD-TPLKRAWFENFTNLVPIERH-------------------- GSLR---------ESLRQ-AGEALRQGY--N-VLIFPEGTRSPTG-ELQEFKSTLG-YLALTY---------- RVDVLPLYIHGAFEA----------------LPKGSVFPKSK------------------D- LKVSIGPALGHEALRARTQG--- MARSESYRYATRIAEDAVRELRDGRVLHL-
>ElbD_C._coralloides putative long-chain-fatty-acid--CoA ligase [*Corallococcus coralloides* DSM 2259]	NHASHLDAGLVRVVLGDQGER-----LVSLAARDY-FFD-TPLKRAWFENFTNLIPIDRQ-------------------- GSLR---------ESLRV-AGEALRQGF--N-VLIFPEGTRSKTG-ELMEFKPTLG-YLSLTY---------- GVDVLPLYIHGAYEA----------------LPKGSMFPKTK------------------E- LEVHVGPALEYASLKARAQG--- MARSEGYRYVTHIAEEAVRALRAGKVLDL-
>ElbD_S._aurantiaca AMP-binding enzyme/acyltransferase [*Stigmatella aurantiaca* DW4/3-1]	NHASHLDAGLIRTVLQEQGQK-----LVALAARDY-FFD-TPLKRAYFENFTDLIPMDRH-------------------- GSLR---------ESLRL-AGESLRLGY--N-LLIFPEGTRSPTG-ELLEFKPTLG-YLALSY---------- EVDVLPLYLRGTFEA----------------LPKGTMFPKSK------------------K- LEVHIGPVLKHTDLRTLTQG--- MARSESYRYATRLAEDAVKALRAGRVLNI-

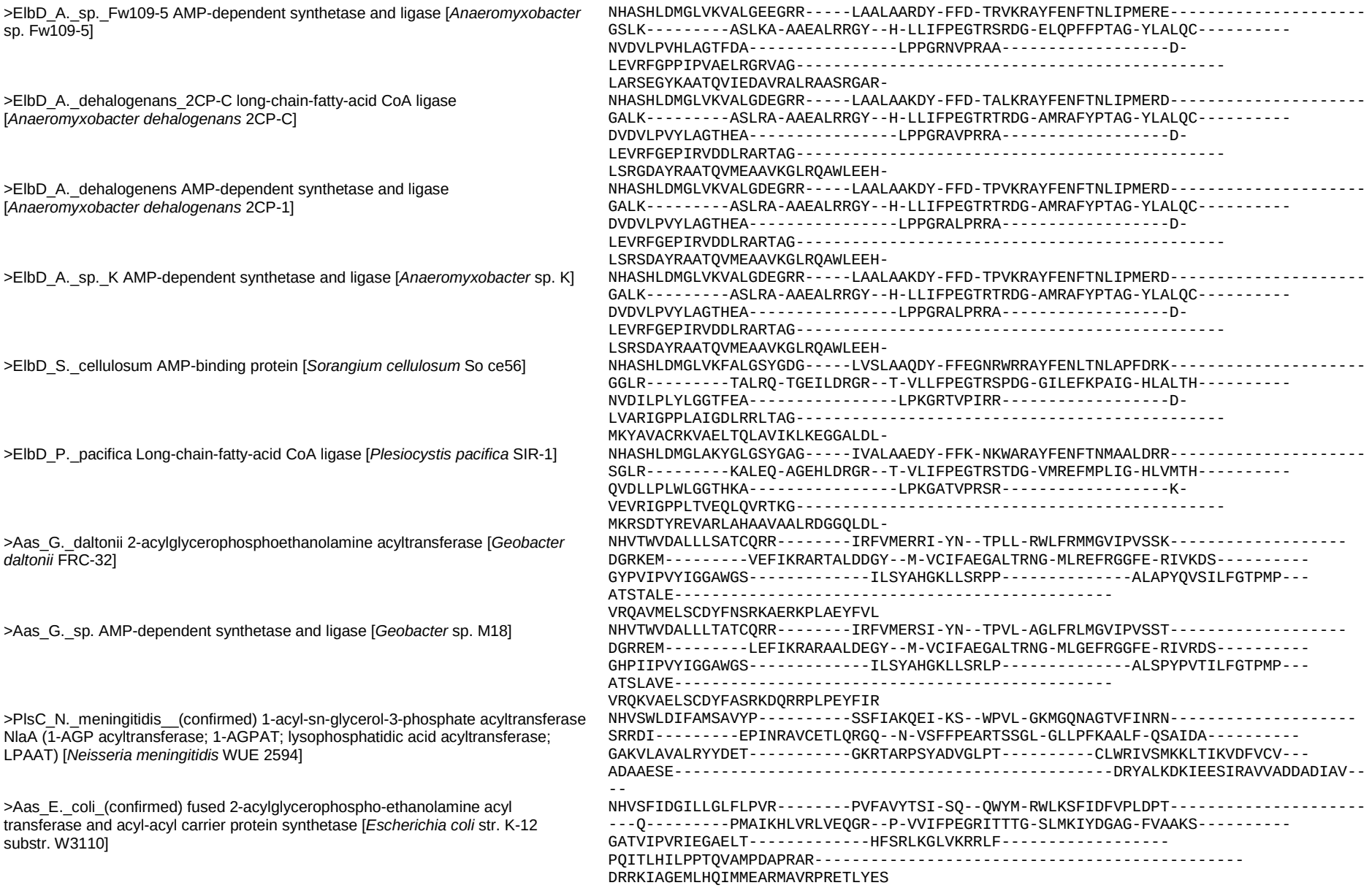
>ElbD_A._sp._Fw109-5 AMP-dependent synthetase and ligase [*Anaeromyxobacter* sp. Fw109-5]
NHASHLDMGLVKVALGEEGRR-----LAALAARDY-FFD-TRVKRAYFENFTNLIPMERE----------
GSLK---------ASLKA-AAEALRRGY--H-LLIFPEGTRSRDG-ELQPFFPTAG-YLALQC----------
NVDVLPVHLAGTFDA---------------LPPGRNVPRAA-----------------D-
LEVRFGPPIPVAELRGRVAG---
LARSEGYKAATQVIEDAVRALRAASRGAR-
>ElbD_A._dehalogenans_2CP-C long-chain-fatty-acid CoA ligase [*Anaeromyxobacter dehalogenans* 2CP-C]
NHASHLDMGLVKVALGDEGRR-----LAALAAKDY-FFD-TALKRAYFENFTNLIPMERD----------
GALK---------ASLRA-AAEALRRGY--H-LLIFPEGTRTRDG-AMRAFYPTAG-YLALQC----------
DVDVLPVYLAGTHEA---------------LPPGRAVPRRA-----------------D-
LEVRFGEPIRVDDLRARTAG---
LSRGDAYRAATQVMEAAVKGLRQAWLEEH-
>ElbD_A._dehalogenens AMP-dependent synthetase and ligase [*Anaeromyxobacter dehalogenans* 2CP-1]
NHASHLDMGLVKVALGDEGRR-----LAALAAKDY-FFD-TPVKRAYFENFTNLIPMERD----------
GALK---------ASLRA-AAEALRRGY--H-LLIFPEGTRTRDG-AMRAFYPTAG-YLALQC----------
DVDVLPVYLAGTHEA---------------LPPGRALPRRA-----------------D-
LEVRFGEPIRVDDLRARTAG---
LSRSDAYRAATQVMEAAVKGLRQAWLEEH-
>ElbD_A._sp._K AMP-dependent synthetase and ligase [*Anaeromyxobacter* sp. K]
NHASHLDMGLVKVALGDEGRR-----LAALAAKDY-FFD-TPVKRAYFENFTNLIPMERD----------
GALK---------ASLRA-AAEALRRGY--H-LLIFPEGTRTRDG-AMRAFYPTAG-YLALQC----------
DVDVLPVYLAGTHEA---------------LPPGRALPRRA-----------------D-
LEVRFGEPIRVDDLRARTAG---
LSRSDAYRAATQVMEAAVKGLRQAWLEEH-
>ElbD_S._cellulosum AMP-binding protein [*Sorangium cellulosum* So ce56]
NHASHLDMGLVKFALGSYGDG-----LVSLAAQDY-FFEGNRWRRAYFENLTNLAPFDRK----------
GGLR---------TALRQ-TGEILDRGR--T-VLLFPEGTRSPDG-GILEFKPAIG-HLALTH----------
NVDILPLYLGGTFEA---------------LPKGRTVPIRR-----------------D-
LVARIGPPLAIGDLRRLTAG---
MKYAVACRKVAELTQLAVIKLKEGGALDL-
>ElbD_P._pacifica Long-chain-fatty-acid CoA ligase [*Plesiocystis pacifica* SIR-1]
NHASHLDMGLAKYGLGSYGAG-----IVALAAEDY-FFK-NKWARAYFENFTNMAALDRR----------
SGLR---------KALEQ-AGEHLDRGR--T-VLIFPEGTRSTDG-VMREFMPLIG-HLVMTH----------
QVDLLPLWLGGTHKA---------------LPKGATVPRSR-----------------K-
VEVRIGPPLTVEQLQVRTKG---
MKRSDTYREVARLAHAAVAALRDGGQLDL-
>Aas_G._daltonii 2-acylglycerophosphoethanolamine acyltransferase [*Geobacter daltonii* FRC-32]
NHVTWVDALLLSATCQRR--------IRFVMERRI-YN--TPLL-RWLFRMMGVIPVSSK----------
DGRKEM---------VEFIKRARTALDDGY--M-VCIFAEGALTRNG-MLREFRGGFE-RIVKDS----------
GYPVIPVYIGGAWGS-------------ILSYAHGKLLSRPP--------------ALAPYQVSILFGTPMP---
ATSTALE---
VRQAVMELSCDYFNSRKAERKPLAEYFVL
>Aas_G._sp. AMP-dependent synthetase and ligase [*Geobacter* sp. M18]
NHVTWVDALLLTATCQRR--------IRFVMERSI-YN--TPVL-AGLFRLMGVIPVSST----------
DGRREM---------LEFIKRARAALDEGY--M-VCIFAEGALTRNG-MLGEFRGGFE-RIVRDS----------
GHPIIPVYIGGAWGS-------------ILSYAHGKLLSRLP--------------ALSPYPVTILFGTPMP---
ATSLAVE---
VRQKVAELSCDYFASRKDQRRPLPEYFIR
>PlsC_N._meningitidis__(confirmed) 1-acyl-sn-glycerol-3-phosphate acyltransferase NlaA (1-AGP acyltransferase; 1-AGPAT; lysophosphatidic acid acyltransferase; LPAAT) [*Neisseria meningitidis* WUE 2594]
NHVSWLDIFAMSAVYP----------SSFIAKQEI-KS--WPVL-GKMGQNAGTVFINRN----------
SRRDI---------EPINRAVCETLQRGQ--N-VSFFPEARTSSGL-GLLPFKAALF-QSAIDA----------
GAKVLAVALRYYDET----------GKRTARPSYADVGLPT----------CLWRIVSMKKLTIKVDFVCV---
ADAAESE---DRYALKDKIEESIRAVVADDADIAV--
--
>Aas_E._coli_(confirmed) fused 2-acylglycerophospho-ethanolamine acyl transferase and acyl-acyl carrier protein synthetase [*Escherichia coli* str. K-12 substr. W3110]
NHVSFIDGILLGLFLPVR--------PVFAVYTSI-SQ--QWYM-RWLKSFIDFVPLDPT----------
---Q---------PMAIKHLVRLVEQGR--P-VVIFPEGRITTTG-SLMKIYDGAG-FVAAKS----------
GATVIPVRIEGAELT-------------HFSRLKGLVKRRLF-----------------
PQITLHILPPTQVAMPDAPRAR---
DRRKIAGEMLHQIMMEARMAVRPRETLYES

>Aas_E._cloacae bifunctional acyl-[acyl carrier protein] synthetase/2-acylglycerophosphoethanolamine acyltransferase [*Enterobacter cloacae* subsp. *dissolvens* SDM]

```
NHVSFIDGILLALFLPVR--------PVFAVYTSI-SQ--QWYM-RWLTPLIDFVPLDPT----------
---K---------PMMIKHLVRLVEQGR--P-VVIFPEGRISVTG-SLMKIYDGAG-FVAAKS----------
KATVVPLRIEGAELT-------------HFSRLKGLVKQRLF------------------
PKITLHILPPTSLPMPDAPRAR-----------------------------------------------
DRRKIAGEMLHQIMMEARMAVRPRETLYES
```

>Aas_C._sp. RecN [*Citrobacter* sp. A1]

```
NHVSFIDGILLALFLPIR--------PVFAVYTSI-SQ--QWYM-RWLTPLIDFVPLDPT----------
---K---------PMSIKHLVRLVEQGR--P-VVIFPEGRISTTG-SLMKIYDGAG-FVAAKS----------
GATVVPVRIEGAELS-------------RFSRLKGLVKQRFF------------------
PRIRLHILPPTQLPMPEAPRAR-----------------------------------------------
DRRKIAGEMLHQIMMEARMAVRPRETLYES
```

>Aas_S._enterica bifunctional acyl-[acyl carrier protein] synthetase/2-acylglycerophosphoethanolamine acyltransferase [*Salmonella enterica* subsp. *enterica serovar Choleraesuis str*. SC-B67]

```
NHVSFIDGMLLALFLPVR--------PVFAVYTSI-SQ--QWYM-RWLTPLIDFVPLDPT----------
---K---------PMSIKHLVRLVEQGR--P-VVIFPEGRISVTG-SLMKIYDGAG-FVAAKS----------
GATVIPLRIDGAELT-------------PFSRLKGLVKRRLF------------------
PRIQLHILPPTQIPMPEAPRAR-----------------------------------------------
DRRKIAGEMLHQIMMEARMAVRPRETLYES
```

>Aas_K._oxytoca aas [*Klebsiella oxytoca* 10-5245]

```
NHVSFIDGVLLALFLPVR--------PVFAVYSSI-SE--RWFM-RALKPLIDFVPLDPT----------
---K---------PMSIKHLVRLIEQGR--P-VVIFPEGRISVSG-SLMKIYDGAA-FVAAKS----------
QATIVPLRIEGAELT-------------HFSRLKGLVRRRLF------------------
PRIQLHLLPPTHLPMPEVPRAR-----------------------------------------------
DRRKIAGEMLHQIMMEARMAVRPRETLYES
```

>Aas_C._sakazakii 2-acylglycerophosphoethanolamine acyltransferase / Acyl-[acyl-carrier-protein] synthetase [*Cronobacter sakazakii* 696]

```
NHVSFLDGALMALFLPVR--------PVFAVYTSI-SQ--QWYM-RALKPLIDFVPLDPT----------
---K---------PMSVKQLVRLVGEGR--P-VVIFPEGRISISG-SLMKIYEGAG-FVAAKS----------
QATVIPVRIEGAELT-------------FFSRLKGLVKRRLF------------------
PRISIHILPPTSIPMPDAPKAR-----------------------------------------------
DRRKMAGEMLHQVMMEARMAARPRETLFEA
```

>Aas_D._propionicus AMP-dependent synthetase and ligase [*Desulfobulbus propionicus* DSM 2032]

```
NHESLLDGLLLGLFIPIN--------PVFVVHTAV-AN--KPFF-RLILSLVDYLAVDPT----------
---N---------PMAMKQVVRLLEAGR--P-VVIFPEGRITTTG-SLMKVYDGPA-FVAART----------
GATILPVRLDGPSRS-------------YFSRLSGKYPKVLF------------------
PRIRLTILPTTTIPLPSAPTAK-----------------------------------------------
LRRRLAGEAMRRLMQEMVFSCRPAQTLFAA
```

>PlsD_C._butyricum sn-glycerol-3-phosphate acyltransferase [*Clostridium butyricum*]

```
NHLSNSDGLVLNKILKEKSD------PYFIAGIKL-SN--DPIT-NIGTKIVKNIAIKPN----------
SADK---------EAITK-VVKALKSGE--D-ILIFPEGTRSRIG-AMIEGKKGIL-LFARMA----------
KAEIIPIGMSGTDKL----------------LPISNDGNMGA-------------EKWQRADVTINIGDKIQ--
FPKREKDE-------------------------------------------------
DKHEYEDRCMDTLMRSIARLLPEHYRGVY
```

>hGPAT3/hAGPAT10_(confirmed) glycerol-3-phosphate acyltransferase 3 [*Homo sapiens*]

```
NHTSPIDVLILTTD------------GCYAMVGQV-HGGLMGIIQRAMVKACPHVWFERS----------
EMKDR---------HLVTKRLKEHIADKKKLP-ILIFPEGTCINNT-SVMMFKKGSF-EI-------------
GGTIHPVAIKYNPQFGDAFWNSSKYNMVSYLLRMMTSWAIV---------------------CDVWYMPPMT-----
REEGE-----------------------------------------------DAVQFANRVKSAIAIQGGLTELPWDGGLK
```

>hAGPAT9_(confirmed) AGPAT9 protein, partial [*Homo sapiens*]

```
D------------------------GCYAMVGQV-HGGLMGIIQRAMVKACPHVWFERS----------
EMKDR---------HLVTKRLKEHIADKKKLP-ILIFPEGTCINNT-SVMMFKKGSF-EI-------------
GGTIHPVAIKYNPQFGDAFWNSSKYNMVSYLLRMMTSWAIV---------------------CDVWYMPPMT-----
REEGE-----------------------------------------------DAVQFANRVKSAIAIQGGLTELPWDGGLK
```

>hGPAT4_(confirmed) RecName: Full=Glycerol-3-phosphate acyltransferase 4; Short=GPAT4; AltName: Full=1-acylglycerol-3-phosphate O-acyltransferase 6; Short=1-AGP acyltransferase 6; Short=1-AGPAT 6; AltName: Full=Acyl-CoA:glycerol-3-phosphate acyltransferase 4; AltName: Full=Lysophosphatidic acid acyltransferase zeta; Short=LPAAT-zeta; Flags: Precursor

```
NHTSPIDVIILASD------------GYYAMVGQV-HGGLMGVIQRAMVKACPHVWFERS----------
EVKDR---------HLVAKRLTEHVQDKSKLP-ILIFPEGTCINNT-SVMMFKKGSF-EI-------------
GATVYPVAIKYDPQFGDAFWNSSKYGMVTYLLRMMTSWAIV---------------------CSVWYLPPMT-----
READE-----------------------------------------------DAVQFANRVKSAIARQGGLVDLLWDGGLK
```


>hAGPAT6_(confirmed) 1-acylglycerol-3-phosphate O-acyltransferase 6 (lysophosphatidic acid acyltransferase, zeta) [Homo sapiens]
NHTSPIDVIILASD----------GYYAMVGQV-HGGLMGVIQRAMVKACPHVWFERS--------------------
EVKDR---------HLVAKRLTEHVQDKSKLP-ILIFPEGTCINNT-SVMMFKKGSF-EI--------------
GATVYPVAIKYDPQFGDAFWNSSKYGMVTYLLRMMTSWAIV---------------------CSVWYLPPMT-----
READE---DAVQFANRVKSAIARQGGLVDLLWDGGLK
>hLPCAT1_(confirmed) lysophosphatidylcholine acyltransferase 1 [Homo sapiens]
PHSSYFDAIPVTMTM----------SSIVMKAES-RD--IPIW-GTLIQYIRPVFVSRS--------------------
DQDSRR---------KTVEEIKRRAQSNGKWPQ-IMIFPEGTCTNRT-CLITFKPGAF--------------
IPGAPVQPVVLRYPNKLDTITWTWQGPGALEILWLTLCQFHNQ---------------------VEIEFLPVYS---
PSEEEKR---
NPALYASNVRRVMAEALGVSVTDYTFEDC
>hLPCAT2_(confirmed) RecName: Full=Lysophosphatidylcholine acyltransferase 2; Short=LPC acyltransferase 2; Short=LPCAT-2; Short=LysoPC acyltransferase 2; AltName: Full=1-acylglycerophosphocholine O-acyltransferase; AltName: Full=1-alkylglycerophosphocholine O-acetyltransferase; AltName: Full=Acetyl-CoA:lyso-platelet-activating factor acetyltransferase; Short=Acetyl-CoA:lyso-PAF acetyltransferase; Short=Lyso-PAF acetyltransferase; Short=LysoPAFAT; AltName: Full=Acyltransferase-like 1
PHSTFFDGIACVVAGL----------PSMVSRNEN-AQ--VPLI-GRLLRAVQPVLVSRV--------------------
DPDSRK---------NTINEIIKRTTSGGEWPQ-ILVFPEGTCTNRS-CLITFKPGAF--------------
IPGVPVQPVLLRYPNKLDTVTWTWQGYTFIQLCMLTFCQLFTK---------------------VEVEFMPVQV---
PNDEEKN---
DPVLFANKVRNLMAEALGIPVTDHTYEDC
>hAGPAT7_(confirmed) lysophospholipid acyltransferase LPCAT4 [Homo sapiens]
PHSTFFDPIVLLPCDL----------PKVVSRAEN-LS--VPVI-GALLRFNQAILVSRH--------------------
DPASRR---------RVVEEVRRRATSGGKWPQ-VLFFPEGTCSNKK-ALLKFKPGAF--------------
IAGVPVQPVLIRYPNSLDTTSWAWRGPGVLKVLWLTASQPCSI---------------------VDVEFLPVYH---
PSPEESR---
DPTLYANNVQRVMAQALGIPATECEFVGS
>PlsB_M._fulvus glycerol-3-phosphate O-acyltransferase [Myxococcus fulvus HW-1]
SHKSHVDYLVMSWVLWNRGYA-----VPLVAAGAN-LS--FWPL-GTFFRRCGAFFLRRS-----------------
FKGDKVYA---------ASFKAYVRKLVHDGI--H-QEFFPEGGRSRTG-KLLLPKLGMF-TWQVESVL---
EGARDDLIFVPVAIDYEKVVESSSYSKELAGGEKKPEDIKALLSAPK------------VLAARYGRIHLGFDEPIS---
LRAFMQA-------------RGINPDEPVS----------------------
DEQKKGLVRALGNRVMYGISKVSTVTPHALV
>PlsB1_M._xanthus acyltransferase [Myxococcus xanthus DK 1622]
SHKSHVDYLVMSWVLWNRGYA-----VPLVAAGAN-LS--FWPL-GTFFRRCGAFFLRRS-----------------
FKGDKVYA---------ASFKAYVRKLVHDGI--H-QEFFPEGGRSRTG-KLLLPKLGMF-TWQVESVL---
EGARDDLIFVPVAIDYEKVVESSSYSKELAGGEKKPEDLKALLSTPK------------VLAARYGRIHLGFDEPIS---
LRAFMQA-------------RGINPDEPVS----------------------
DEQKKGLVRALGNRVMYGISKVSTVTPHALV
>PlsB_C._apiculatus Glycerol-3-phosphate acyltransferase [Chondromyces apiculatus DSM 436]
SHKSHVDYLVMSWVLWNRGYA-----VPLVAAGAN-LS--FWPL-GTFFRRCGAFFLRRS-----------------
FKGDKVYA---------ASFKAYVRKLVHDGI--H-QEFFPEGGRSRTG-KLLLPKLGMF-TWQVESVL---
EGARDDLIFVPVAIDYEKVVESSSYSKELAGGEKKPEDIKALLSAPK------------VLAARYGRIHLGFDEPIS---
LRDFMKA-------------RGINPDEPVS----------------------
DEQKKGLVRALGNRVMYGISKVSTVTPHALV
>PlsB_C._coralloides acyltransferase [Corallococcus coralloides DSM 2259]
SHKSHVDYLVMSWVLWNRGYT-----APLVAAGAN-LS--FWPL-GVLFRRCGAFFLRRS-----------------
FKGDKVYA---------ASFKAYIKKLVHDGI--H-QEFFPEGGRSRTG-KLLTPKLGML-TWQVEAVL---
DGARNDLYFVPVSIDYEKVVESDSYSKELAGGEKKPEDLKALLSAPK------------VLAARYGRIHLTFDEPLS---
LVEFMKA-------------RGLSPQEPVS----------------------
DEQKKGLVRALGNRVMYGISKVSTVTPHALV
>PlsB_S._aurantiaca glycerol-3-phosphate o-acyltransferase [Stigmatella aurantiaca DW4/3-1]
SHKSHVDYLVLSWVLWNRGYA-----VPLVAAGAN-LS--FFPL-GAFLRRCGAFFLRRS-----------------
FKGDPIYS---------ETFQAYVRKLVHDGV--H-QEFFPEGGRSRTG-KLLLPKLGMF-TWQVEAVL---
GGARNDLIFVPVSIDYEKVVESGSYSKELAGGEKKPEDLKALLSTPK------------VLTAQYGRIHLTFDEPLS---
LVELMKS-------------RGIGSGQPVT----------------------
DEQKKGLVRALGNRVMYGISKVSTVTPHALA

>PlsB_A._dehalogenans glycerol-3-phosphate O-acyltransferase [*Anaeromyxobacter dehalogenans* 2CP-1]	SHKSHVDYLVLSWLLYENGMT-----PPHIAAGIN-LA--FWPF-GAIARRGGAFFIRRK---------- VKGDRVYT---------AVLRAYVKHLLRDRF--P-QEFYVEGGRSRTG-KLLFPKTGLV-SMEVDAWL--- DGAADDVLFVPVAIDYERLIEASSYANELAGGEKRKESLRGLLGAAR-----------VLLRRYERLYVQFETPIS--- LRQVAAE-----------
>PlsB_D._autotrophicum protein PlsB [*Desulfobacterium autotrophicum* HRM2]	RLGARAASLAVDEAWGGEAERRAAPGAAGAGDDAEAKRQLVQGLANRIAYGISRAVTITPVGLV CHKSHLDYLLLSYVMFKKSMP-----CPHVAAGNN-LS--FWPL-GPIFRGGGAFFLRRT---------- FKGAVLYS---------RIFSAYIEKLLSEGF--N-LECFIEGGRSRSG-KLLSPRLGFL-SILVKAQQ--- NRACEDLLFVPIYVGYDRVLEEDSYLHEIEGGKKNPENLSQLIKARR-----------FLKKKYGKVYINFDEPIS--- LQRYIQE-----------TISLETVPVKTHDY---- KENSIQGKAPGFRLDEENQRRICQGMGYKLINAINSIAIVTPHGIM
>PlsB_D._toluolica glycerol-3-phosphate acyltransferase PlsB [*Desulfobacula toluolica* Tol2]	CHKSHLDYLLLPYVMFKNNMP-----CPHIAAGKN-LS--FWPL-GPLFRGGGAFFLRRT---------- FKGAPLYA---------KIFAAYLEKLLYEGF--N-IKIFIEGGRSRTG-KLLSPKPGGL-AMLINAYI--- NGACSNLYFVPVFIGYDRVLEEDAYLKEIEGGKKTPETLKGLINARK-----------FLKKKYGKVYMRFDEPIS--- IKEYIQK-----------K-NIDLSKTS---------- SDEYIKFIKSFGYKLINAINTNAVVTPHGII
>PlsB_D._postgatei glycerol-3-phosphate O-acyltransferase [*Desulfobacter postgatei* 2ac9]	CHKSHLDYLLLPYVMYKNNMP-----CPHIAAGKN-LS--FWPL-GPLFRGAGAFFLRRT---------- FKGAELYA---------RIFAAYIEKLLYEGF--N-IKIYIEGGRSRTG-KVLPPKIGGL-SMIIRAFL--- SGACEDLYFVPIYVGYDRVLEEDAYLKEIEGGNKTPENLKGLLNTRK-----------FLKRKYGKVYIRFDTPIS--- MNRYMEE-----------K-GVDLKKFS---------- DPEFSHFVKRFGYKLINHINDNIVATPHGII
>PlsB_D._oleovorans glycerol-3-phosphate O-acyltransferase [*Desulfococcus oleovorans* Hxd3]	THKSHLDYLVLSYVLYYNNIA-----CPHIAAGKN-LS--FWPL-GPIFRGGGAFFMRRT---------- FKGQKLYS---------KVFFEYIYKILQEGF--N-VEFFLEGGRSRTG-KMLSPKTGLL-SIILDAYA--- QGACSDLMFVPVNIGYDRIIEEASYIREIKGGEKKAENLPELIKARK-----------SLKSRYGKVYVNFNEPLS--- LKEFLAH-----------T-GTDLAALD---------- PDARREFIGTLSHILTKRIDNVTTVTPYSIV
>PlsB_E._cloacae glycerol-3-phosphate acyltransferase [*Enterobacter cloacae* subsp. *cloacae* ENHKU01]	CHRSHMDYLLLSYVLYHQGLV-----PPHIAAGIN-LN--FWPA-GPIFRRLGAFFIRRT---------- FKGNKLYS---------TVFREYLGELFSRGY--S-VEYFVEGGRSRTG-RLLDPKTGTL-SMTIQAML--- RGGTRPITLVPIYIGYEHVMEVGTYAKELRGATKEKESLPQMLRGLS-----------KL-RNLGQGYVNFGEPMP--- LMTYLNH-------HVPEWRESIDPIEAVR---------- PAWLTPTVNGIASELMVRINNAGAANAMNLC
>PlsB_S._bongori glycerol-3-phosphate acyltransferase [*Salmonella bongori* NCTC 12419]	CHRSHMDYLLLSYVLYHQGLV-----PPHIAAGIN-LN--FWPA-GPIFRRLGAFFIRRT---------- FKGNKLYS---------TVFREYLGELFSRGY--S-VEYFVEGGRSRTG-RLLDPKTGTL-SMTIQAML--- RGGTRPITLVPIYIGYEHVMEVGTYAKELRGATKEKESLPQMLRGLS-----------KL-RNLGQGYVNFGEPMP--- LMTYLNQ-------HVPEWRESIDPIEAIR---------- PAWLTPTVNGIAAELMVRINNAGAANAMNLC
>PlsB_C._rodentium glycerol-3-phosphate acyltransferase [*Citrobacter rodentium* ICC168]	CHRSHMDYLLLSYVLYHQGLV-----PPHIAAGIN-LN--FWPA-GPIFRRLGAFFIRRT---------- FKGNKLYS---------TVFREYLGELFSRGY--S-VEYFVEGGRSRTG-RLLDPKTGTL-SMTIQAML--- RGGTRPITLVPIYIGYEHVMEVGTYAKELRGATKEKESLPQMLRGLS-----------KL-RNLGQGYVNFGEPMP--- LMTWLNH-------HVPDWRESIDPIEAVR---------- PAWLTPTVNGIAEELMVRINNAGAANAMNLC
>PlsB_E._Coli glycerol-3-phosphate O-acyltransferase [*Escherichia coli* str. K-12 substr. W3110]	CHRSHMDYLLLSYVLYHQGLV-----PPHIAAGIN-LN--FWPA-GPIFRRLGAFFIRRT---------- FKGNKLYS---------TVFREYLGELFSRGY--S-VEYFVEGGRSRTG-RLLDPKTGTL-SMTIQAML--- RGGTRPITLIPIYIGYEHVMEVGTYAKELRGATKEKESLPQMLRGLS-----------KL-RNLGQGYVNFGEPMP--- LMTYLNQ-------HVPDWRESIDPIEAVR---------- PAWLTPTVNNIAADLMVRINNAGAANAMNLC
>PlsB_K._oxytoca glycerol-3-phosphate acyltransferase [*Klebsiella oxytoca* 10-5246]	CHRSHMDYLLLSYVLYHQGLV-----PPHIAAGIN-LN--FWPA-GPIFRRGGAFFIRRT---------- FKGNKLYS---------TVFREYLGELFSRGY--S-VEYFVEGGRSRTG-RLLDPKTGTL-SMTIQAML--- RGGTRPITLVPIYIGYEHVMEVGTYAKELRGATKEKESLPQMLRGLS-----------KL-RNLGQGYVNFGEPLP--- LMTYLNQ-------HVPEWRESIDPIEAVR---------- PSWLTPTVNNIASDLMVRINNAGAANAMNLC

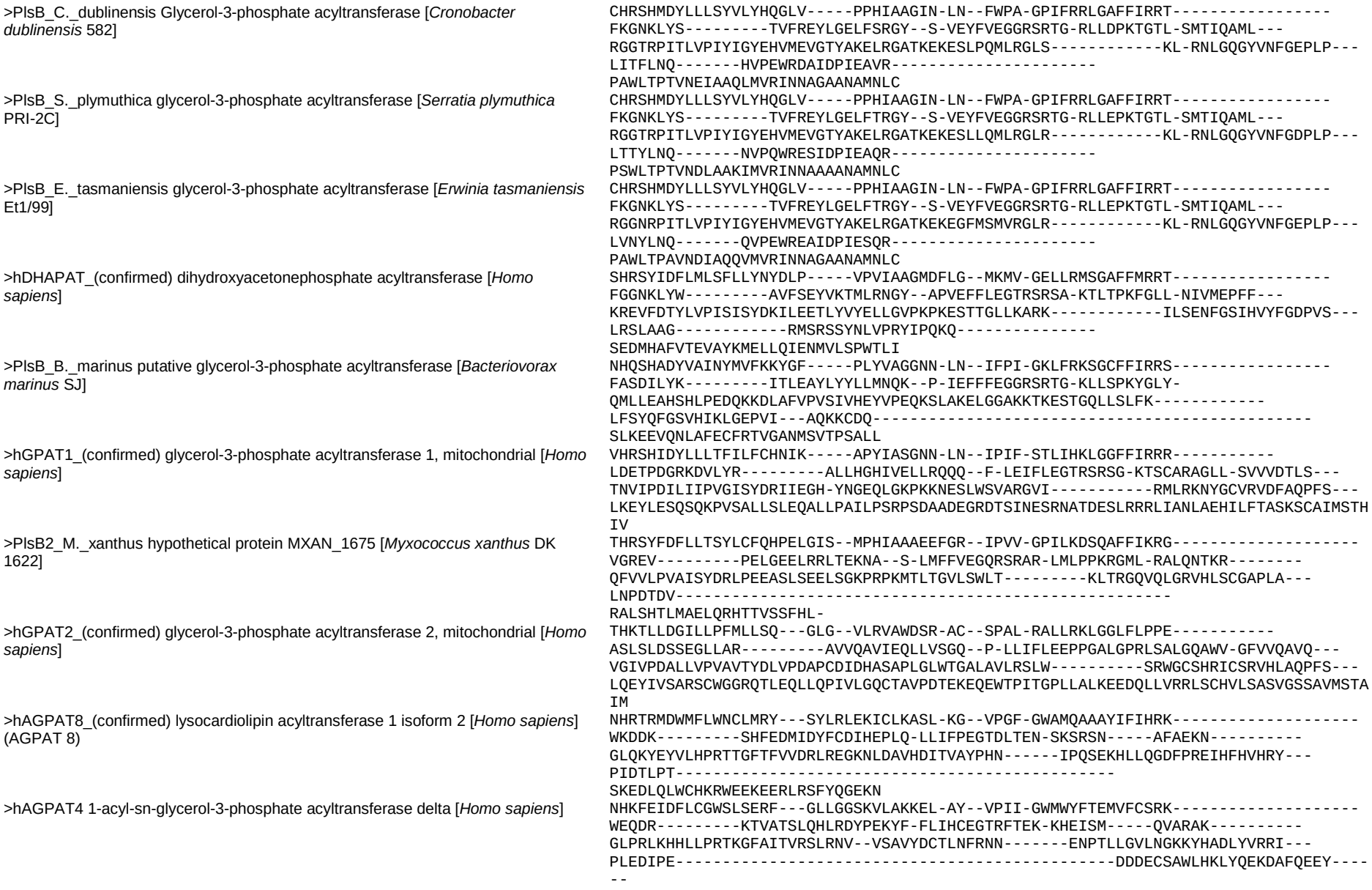
>PlsB_C._dublinensis Glycerol-3-phosphate acyltransferase [*Cronobacter dublinensis* 582]
CHRSHMDYLLLSYVLYHQGLV-----PPHIAAGIN-LN--FWPA-GPIFRRLGAFFIRRT----------
FKGNKLYS---------TVFREYLGELFSRGY--S-VEYFVEGGRSRTG-RLLDPKTGTL-SMTIQAML---
RGGTRPITLVPIYIGYEHVMEVGTYAKELRGATKEKESLPQMLRGLS----------KL-RNLGQGYVNFGEPLP---
LITFLNQ-------HVPEWRDAIDPIEAVR----------
PAWLTPTVNEIAAQLMVRINNAGAANAMNLC
>PlsB_S._plymuthica glycerol-3-phosphate acyltransferase [*Serratia plymuthica* PRI-2C]
CHRSHMDYLLLSYVLYHQGLV-----PPHIAAGIN-LN--FWPA-GPIFRRLGAFFIRRT----------
FKGNKLYS---------TVFREYLGELFTRGY--S-VEYFVEGGRSRTG-RLLEPKTGTL-SMTIQAML---
RGGTRPITLVPIYIGYEHVMEVGTYAKELRGATKEKESLLQMLRGLR----------KL-RNLGQGYVNFGDPLP---
LTTYLNQ-------NVPQWRESIDPIEAQR----------
PSWLTPTVNDLAAKIMVRINNAAAANAMNLC
>PlsB_E._tasmaniensis glycerol-3-phosphate acyltransferase [*Erwinia tasmaniensis* Et1/99]
CHRSHMDYLLLSYVLYHQGLV-----PPHIAAGIN-LN--FWPA-GPIFRRLGAFFIRRT----------
FKGNKLYS---------TVFREYLGELFTRGY--S-VEYFVEGGRSRTG-RLLEPKTGTL-SMTIQAML---
RGGNRPITLVPIYIGYEHVMEVGTYAKELRGATKEKEGFMSMVRGLR----------KL-RNLGQGYVNFGEPLP---
LVNYLNQ-------QVPEWREAIDPIESQR----------
PAWLTPAVNDIAQQVMVRINNAGAANAMNLC
>hDHAPAT_(confirmed) dihydroxyacetonephosphate acyltransferase [*Homo sapiens*]
SHRSYIDFLMLSFLLYNYDLP-----VPVIAAGMDFLG--MKMV-GELLRMSGAFFMRRT----------
FGGNKLYW---------AVFSEYVKTMLRNGY--APVEFFLEGTRSRSA-KTLTPKFGLL-NIVMEPFF---
KREVFDTYLVPISISYDKILEETLYVYELLGVPKPKESTTGLLKARK----------ILSENFGSIHVYFGDPVS---
LRSLAAG----------RMSRSSYNLVPRYIPQKQ----------
SEDMHAFVTEVAYKMELLQIENMVLSPWTLI
>PlsB_B._marinus putative glycerol-3-phosphate acyltransferase [*Bacteriovorax marinus* SJ]
NHQSHADYVAINYMVFKKYGF-----PLYVAGGNN-LN--IFPI-GKLFRKSGCFFIRRS----------
FASDILYK---------ITLEAYLYYLLMNQK--P-IEFFFEGGRSRTG-KLLSPKYGLY-
QMLLEAHSHLPEDQKKDLAFVPVSIVHEYVPEQKSLAKELGGAKKTKESTGQLLSLFK----------
LFSYQFGSVHIKLGEPVI---AQKKCDQ----------
SLKEEVQNLAFECFRTVGANMSVTPSALL
>hGPAT1_(confirmed) glycerol-3-phosphate acyltransferase 1, mitochondrial [*Homo sapiens*]
VHRSHIDYLLLTFILFCHNIK-----APYIASGNN-LN--IPIF-STLIHKLGGFFIRRR----------
LDETPDGRKDVLYR---------ALLHGHIVELLRQQQ--F-LEIFLEGTRSRSG-KTSCARAGLL-SVVVDTLS---
TNVIPDILIIPVGISYDRIIEGH-YNGEQLGKPKKNESLWSVARGVI----------RMLRKNYGCVRVDFAQPFS---
LKEYLESQSQKPVSALLSLEQALLPAILPSRPSDAADEGRDTSINESRNATDESLRRRLIANLAEHILFTASKSCAIMSTH
IV
>PlsB2_M._xanthus hypothetical protein MXAN_1675 [*Myxococcus xanthus* DK 1622]
THRSYFDFLLTSYLCFQHPELGIS--MPHIAAAEEFGR--IPVV-GPILKDSQAFFIKRG----------
VGREV---------PELGEELRRLTEKNA--S-LMFFVEGQRSRAR-LMLPPKRGML-RALQNTKR--------
QFVVLPVAISYDRLPEEASLSEELSGKPRPKMTLTGVLSWLT---------KLTRGQVQLGRVHLSCGAPLA---
LNPDTDV----------
RALSHTLMAELQRHTTVSSFHL-
>hGPAT2_(confirmed) glycerol-3-phosphate acyltransferase 2, mitochondrial [*Homo sapiens*]
THKTLLDGILLPFMLLSQ---GLG--VLRVAWDSR-AC--SPAL-RALLRKLGGLFLPPE----------
ASLSLDSSEGLLAR---------AVVQAVIEQLLVSGQ--P-LLIFLEEPPGALGPRLSALGQAWV-GFVVQAVQ---
VGIVPDALLVPVAVTYDLVPDAPCDIDHASAPLGLWTGALAVLRSLW----------SRWGCSHRICSRVHLAQPFS---
LQEYIVSARSCWGGRQTLEQLLQPIVLGQCTAVPDTEKEQEWTPITGPLLALKEEDQLLVRRLSCHVLSASVGSSAVMSTA
IM
>hAGPAT8_(confirmed) lysocardiolipin acyltransferase 1 isoform 2 [*Homo sapiens*] (AGPAT 8)
NHRTRMDWMFLWNCLMRY---SYLRLEKICLKASL-KG--VPGF-GWAMQAAAYIFIHRK----------
WKDDK---------SHFEDMIDYFCDIHEPLQ-LLIFPEGTDLTEN-SKSRSN-----AFAEKN----------
GLQKYEYVLHPRTTGFTFVVDRLREGKNLDAVHDITVAYPHN------IPQSEKHLLQGDFPREIHFHVHRY---
PIDTLPT----------
SKEDLQLWCHKRWEEKEERLRSFYQGEKN
>hAGPAT4 1-acyl-sn-glycerol-3-phosphate acyltransferase delta [*Homo sapiens*]
NHKFEIDFLCGWSLSERF---GLLGGSKVLAKKEL-AY--VPII-GWMWYFTEMVFCSRK----------
WEQDR---------KTVATSLQHLRDYPEKYF-FLIHCEGTRFTEK-KHEISM-----QVARAK----------
GLPRLKHHLLPRTKGFAITVRSLRNV--VSAVYDCTLNFRNN-------ENPTLLGVLNGKKYHADLYVRRI---
PLEDIPE----------DDDECSAWLHKLYQEKDAFQEEY----
--

>hAGPAT3_(confirmed) AGPAT3 [*Homo sapiens*]	NHNFEIDFLCGWTMCERF---GVLGSSKVLAKKEL-LY--VPLI-GWTWYFLEIVFCKRK---------- WEEDR---------DTVVEGLRRLSDYPEYMW-FLLYCEGTRFTET-KHRVSM-----EVAAAK---------- GLPVLKYHLLPRTKGFTTAVKCLRGT--VAAVYDVTLNFRGN-------KNPSLLGILYGKKYEADMCVRRF--- PLEDIPL---DEKEAAQWLHKLYQEKDALQEIY---- --
>LPAAT_B._napus_(confirmed) lysophosphatidic acid acyltransferase [*Brassica napus*]	NHRSDIDWLVGWILAQRS---GCLGSALAVMKKSS-KF--LPVI-GWSMWFSEYLFLERN---------- WAKDE---------STLKSGLQRLNDFPRPFW-LALFVEGTRFTEA-KLKAAQ-----EYAASS---------- ELPVPRNVLIPRTKGFVSAVSNMRSF--VPAIYDMTVAIPKT------SPPPTMLRLFKGQPSVVHVHIKCH--- SMKDLPE---SDDAIAQWCRDQFVAKDALLDKH---- --
>LPAT2_ARATH_(confirmed) RecName: Full=1-acyl-sn-glycerol-3-phosphate acyltransferase 2; AltName: Full=Lysophosphatidyl acyltransferase 2	NHRSDIDWLVGWILAQRS---GCLGSALAVMKKSS-KF--LPVI-GWSMWFSEYLFLERN---------- WAKDE---------STLKSGLQRLSDFPRPFW-LALFVEGTRFTEA-KLKAAQ-----EYAASS---------- ELPIPRNVLIPRTKGFVSAVSNMRSF--VPAIYDMTVTIPKT------SPPPTMLRLFKGQPSVVHVHIKCH--- SMKDLPE---SDDAIAQWCRDQFVAKDALLDKH---- --
>hAGPAT5_(confirmed) 1-acyl-sn-glycerol-3-phosphate acyltransferase epsilon [*Homo sapiens*]	NHQSTVDWIVADILAIRQ---NALGHVRYVLKEGL-KW--LPLY-GCYFAQHGGIYVKRS---------- AKFNE---------KEMRNKLQSYVDAGTPMY-LVIFPEGTRYNPE-QTKVLSASQ--AFAAQR---------- GLAVLKHVLTPRIKATHVAFDCMKNY--LDAIYDVTVVYEGKDDGGQRRESPTMTEFLCKECPKIHIHIDRI--- DKKDVPE--- EQEHMRRWLHERFEIKDKMLIEFYESPDP
>TAZ_HUMAN RecName: Full=Tafazzin; AltName: Full=Protein G4.5	NHQSCMDDPHLWGILKLRHIWNLKLMRWTPAAADICFT--KELH- SHFFSLGKCVPVCRGAEFFQAENEGKGVLDTGRHMPGAGKRREKGDGVYQKGMDFILEKLNHGD--W- VHIFPEGKVNMSS-EFLRFKWGIG-RLIAECHL--------NPIILPLWHVGMNDV---------- LPNSPPYFPRF----------GQKITVLIGKPFS---ALPVLER---------- -------LRAENKSAVEMRKALTDFIQEEFQHLKTQAEQLHNHLQP
>GPAT_C._moscata_(confirmed,_crystal) Chain A, The 1.55 A Crystal Structure Of Glycerol-3-Phosphate Acyltransferase	NHQTEADPAIISLLLEKT--------NPYIAENTI-FVAGDRVL--- ADPLCKPFSIGRNLICVYSKKHXFDIPELTETKRKANT---------RSLKE-XALLLRGGS-- QLIWIAPSGGRDRPDPSTGEWYPAPFDASSVDNXRRLIQHSDVPGHLFPLALLCHDIXPPPSQVEIEIGEKRVIAFNGAGL SVAP---------EISFEEIAA---THKNPEE---------- ----------VREAYSKALFDSVAXQYNVLKTA------

6.2.6 Supplementary References

35.Plückthun, A. & Dennis, E. A. Acyl and phosphoryl migration in lysophospholipids: importance in phospholipid synthesis and phospholipase specificity. *Biochemistry* **21,** 1743- 50 (1982).

36.Coleman, R. & Lee, D. Enzymes of triacylglycerol synthesis and their regulation. *Prog. Lipid. Res.* **43**, 134-76 (2004).

37.Arand, M. *et al.* Catalytic triad of microsomal epoxide hydrolase: replacement of Glu404 with Asp leads to a strongly increased turnover rate. *Biochem. J.* **337 (Pt 1),** 37-43 (1999).

38.Hagen, P. O. Lipids of *Sphaerophorus ridiculosis*: plasmalogen composition. *J. Bacteriol.* **119,** 643-5 (1974).

39.Adriaans, B. & Garelick, H. Cytotoxicity of *Fusobacterium ulcerans*. *J. Med. Microbiol.* **29,** 177-80 (1989).

40.Siegl, A. *et al.* Single-cell genomics reveals the lifestyle of *Poribacteria*, a candidate phylum symbiotically associated with marine sponges. *ISME J.* **5,** 61-70 (2011).

41.Smith, G. M. & Djerassi, C. Phospholipid studies of marine organisms: 14. Ether lipids of the sponge *Tethya aurantia*. *Lipids* **22,** 236-40 (1987).

42.Sugiura, T., Fukuda, T., Miyamoto, T. & Waku, K. Distribution of alkyl and alkenyl ether linked phospholipids and platelet-activating factor-like lipid in various species of invertebrates. *Biochim. Biophys. Acta.* **1126,** 298-308 (1992).

43.Cullinane, M., Baysse, C., Morrissey, J. P. & O'Gara, F. Identification of two lysophosphatidic acid acyltransferase genes with overlapping function in *Pseudomonas fluorescens*. *Microbiology (Reading, England)* **151,** 3071-80 (2005).

44.Shih, G. C. *et al.* Multiple lysophosphatidic acid acyltransferases in *Neisseria meningitidis*. *Mol. Microbiol.* **32,** 942-52 (1999).

45.Prasad, S. S., Garg, A. & Agarwal, A. K. Enzymatic activities of the human AGPAT isoform 3 and isoform 5: localization of AGPAT5 to mitochondria. *J. Lipid. Res.* **52,** 451-462 (2011).

46.Agarwal, A. K., Barnes, R. I. & Garg, A. Functional characterization of human 1-acylglycerol-3-phosphate acyltransferase isoform 8: Cloning, tissue distribution, gene structure, and enzymatic activity. *Arch. Biochem. Biophys.* **449,** 64-76 (2006).

47.Lu, B. *et al.* Cloning and characterization of murine 1-acyl-sn-glycerol 3-phosphate acyltransferases and their regulation by PPARalpha in murine heart. *Biochem. J.* **385,** 469-77 (2005).

48.Kim, H. U., Li, Y. & Huang, A. H. Ubiquitous and endoplasmic reticulum-located lysophosphatidyl acyltransferase, LPAT2, is essential for female but not male gametophyte development in *Arabidopsis*. *Plant cell* **17,** 1073-89 (2005).

49.Maisonneuve, S., Bessoule, J., Lessire, R., Delseny, M. & Roscoe, T. J. Expression of Rapeseed Microsomal Lysophosphatidic Acid Acyltransferase Isozymes Enhances Seed Oil Content in Arabidopsis. *Plant Physiol.* **152,** 670-84 (2010).

50.Agarwal, A. K. *et al.* Human 1-Acylglycerol-3-phosphate O-Acyltransferase Isoforms 1 and 2: Biochemical Characterization and Inability to Rescue Hepatic Steatosis in Agpat2-/- Gene Lipidystrophic Mice. *J. Biol. Chem.* **286,** 37676-37691 (2011).

51.Cao, J. *et al.* Molecular Identification of a Novel Mammalian Brain Isoform of Acyl-CoA:Lysophospholipid Acyltransferase with Prominent Ethanolamine Lysophospholipid Acylating Activity, LPEAT2. *J. Biol. Chem.* **283,** 19049-19057 (2008).

52.Shindou, H. *et al.* A single enzyme catalyzes both platelet-activating factor production and membrane biogenesis of inflammatory cells. Cloning and characterization of acetyl-CoA:LYSO-PAF acetyltransferase. *J. Biol. Chem.* **282,** 6532-9 (2007).

53.Harayama, T., Shindou, H. & Shimizu, T. Biosynthesis of phosphatidylcholine by human lysophosphatidylcholine acyltransferase 1. *J. Lipid. Res.* **50,** 1824-31 (2009).

54.Li, D. *et al.* Cloning and identification of the human LPAAT-zeta gene, a novel member of the lysophosphatidic acid acyltransferase family. *J. Hum. Genet.* **48,** 438-442 (2003).

55.Shan, D. *et al.* GPAT3 and GPAT4 are regulated by insulin-stimulated phosphorylation and play distinct roles in adipogenesis. *J. Lipid. Res.* **51,** 1971-81 (2010).

56.Sukumaran, S., Barnes, R. I., Garg, A. & Agarwal, A. K. Functional characterization of the human 1-acylglycerol-3-phosphate-O-acyltransferase isoform 10/glycerol-3-phosphate acyltransferase isoform 3. *Mol. Endocrinol.* **42,** 469-478 (2009).

57.Chen, Y. Q. *et al.* AGPAT6 Is a Novel Microsomal Glycerol-3-phosphate Acyltransferase. *J. Biol. Chem.* **283,** 10048-10057 (2008).

58.Lewin, T. M., Schwerbrock, N. M., Lee, D. P. & Coleman, R. A. Identification of a new glycerol-3-phosphate acyltransferase isoenzyme, mtGPAT2, in mitochondria. *J. Biol. Chem.* **279,** 13488-95 (2004).

59.Vancura, A. & Haldar, D. Purification and characterization of glycerophosphate acyltransferase from rat liver mitochondria. *J. Biol. Chem.* **269,** 27209-15 (1994).

60.Coleman, R. & Lee, D. Enzymes of triacylglycerol synthesis and their regulation. *Prog. Lipid. Res.* 1-43 (2004).

61.Heath, R. J., Goldfine, H. & Rock, C. O. A gene (*plsD*) from *Clostridium butyricum* that functionally substitutes for the sn-glycerol-3-phosphate acyltransferase gene (*plsB*) of *Escherichia coli*. *J. Bacteriol.* **179,** 7257-63 (1997).

62.Tamada, T. *et al.* Substrate recognition and selectivity of plant glycerol-3-phosphate acyltransferases (GPATs) from *Cucurbita moscata* and *Spinacea oleracea*. *Acta Crystallogr. D* **60,** 13-21 (2004).

63.Grant, S. G., Jessee, J., Bloom, F. R. & Hanahan, D. Differential plasmid rescue from transgenic mouse DNAs into Escherichia coli methylation-restriction mutants. *P. Natl. Acad. Sci. USA* **87,** 4645-9 (1990).

64.Kalogeraki, V. S. & Winans, S. C. Suicide plasmids containing promoterless reporter genes can simultaneously disrupt and create fusions to target genes of diverse bacteria. *Gene* **188,** 69-75 (1997).

65.Studier, F. W. & Moffatt, B. A. Use of bacteriophage T7 RNA polymerase to direct selective high-level expression of cloned genes. *J. Mol. Biol.* **189,** 113-30 (1986).

66.Kaiser, D. Social gliding is correlated with the presence of pili in *Myxococcus xanthus*. *P. Natl. Acad. Sci. USA* **76,** 5952-6 (1979).

67.Cortina, N. S., Revermann, O., Krug, D. & Müller, R. Identification and characterization of the althiomycin biosynthetic gene cluster in *Myxococcus xanthus* DK897. *ChemBioChem* **12,** 1411-6 (2011).

68.Qualls, G., Stephens, K. & White, D. Light-stimulated morphogenesis in the fruiting myxobacterium *Stigmatella aurantiaca*. *Science (New York, N.Y.)* **201,** 444-5 (1978).

69.Pradella, S. *et al.* Characterisation, genome size and genetic manipulation of the myxobacterium *Sorangium cellulosum* So ce56. *Arch. Microbiol.* **178,** 484-92 (2002).

70.Augustiniak, H., Höfle, G., Irschik, H. & Reichenbach, H. Antibiotics from Gliding Bacteria, LXXVIII. Ripostatin A, B, and C: Isolation and Structure and Structure Elucidation of Novel Metabolites from *Sorangium cellulosum*. *Liebigs Ann.* **1996,** 1657-1663 (1996).

71.Chai, Y. *et al.* Discovery of 23 natural tubulysins from *Angiococcus disciformis* An d48 and Cystobacter SBCb004. *Chem. Biol.* **17,** 296-309 (2010).

72.Ring, M. W., Schwär, G. & Bode, H. B. Biosynthesis of 2-hydroxy and iso-even fatty acids is connected to sphingolipid formation in myxobacteria. *ChemBioChem* **10,** 2003-10 (2009).

73.Kegler, C. *et al.* Rapid determination of the amino acid configuration of xenotetrapeptide. *ChemBioChem*, **15** (2014)

74.Mülhardt, C. *Der Experimentator: Molekularbiologie / Genomics*. (Springer DE, 2008).

75.Shevchenko, A., Tomas, H., Havlis, J., Olsen, J. V. & Mann, M. In-gel digestion for mass spectrometric characterization of proteins and proteomes. *Nat. Protoc.* **1,** 2856-60 (2006).

76.Papasotiriou, D. G. *et al.* Peptide Mass Fingerprinting after Less Specific In-Gel Proteolysis Using MALDI-LTQ-Orbitrap and 4-Chloro-α-cyanocinnamic Acid. *Journal of Proteome Research* **9,** 2619-2629 (2010).

77.Kearse, M. *et al.* Geneious Basic: an integrated and extendable desktop software platform for the organization and analysis of sequence data. *Bioinformatics (Oxford, England)* **28,** 1647-9 (2012).

78.Smits, T. H., Seeger, M. A., Witholt, B. & van Beilen, J. B. New alkane-responsive expression vectors for *Escherichia coli* and *Pseudomonas*. *Plasmid* **46,** 16-24 (2001).

79.Bode, H. B. *et al.* Identification of additional players in the alternative biosynthesis pathway to isovaleryl-CoA in the myxobacterium *Myxococcus xanthus*. *ChemBioChem* **10,** 128-40 (2009).

80.Kuspa, A., Kroos, L. & Kaiser, D. Intercellular signaling is required for developmental gene expression in *Myxococcus xanthus*. *Dev. Biol.* **117,** 267-76 (1986).

81.Silakowski, B., Ehret, H. & Schairer, H. U. fbfB, a gene encoding a putative galactose oxidase, is involved in *Stigmatella aurantiaca* fruiting body formation. *J. Bacteriol.* **180,** 1241-7 (1998).

82.White, T., Bursten, S., Federighi, D., Lewis, R. A. & Nudelman, E. High-resolution separation and quantification of neutral lipid and phospholipid species in mammalian cells and sera by multi-one-dimensional thin-layer chromatography. *Anal. Biochem.* **258,** 109-17 (1998).

83.Bode, H. B. *et al.* 3-Hydroxy-3-methylglutaryl-coenzyme A (CoA) synthase is involved in biosynthesis of isovaleryl-CoA in the myxobacterium *Myxococcus xanthus* during fruiting body formation. *J. Bacteriol.* **188,** 6524-8 (2006).

84.Dickschat, J. S., Bode, H. B., Wenzel, S. C., Müller, R. & Schulz, S. Biosynthesis and identification of volatiles released by the myxobacterium *Stigmatella aurantiaca*. *ChemBioChem* **6,** 2023-33 (2005).

85.Lee, H. *et al. Caenorhabditis elegans mboa*-7, a member of the MBOAT family, is required for selective incorporation of polyunsaturated fatty acids into phosphatidylinositol. *Mol. Biol. Cell* **19,** 1174-84 (2008).

86.Homma, H., Nishijima, M., Kobayashi, T., Okuyama, H. & Nojima, S. Incorporation and metabolism of 2-acyl lysophospholipids by *Escherichia coli*. *Biochim. Biophys. Acta.* **663,** 1-13 (1981).

87.Dickschat, J. S., Bode, H. B., Kroppenstedt, R. M., Müller, R. & Schulz, S. Biosynthesis of iso-fatty acids in myxobacteria. *Org. Biomol. Chem.* **3,** 2824-31 (2005).

88.Dunphy, J. T. *et al.* Differential effects of acyl-CoA binding protein on enzymatic and non-enzymatic thioacylation of protein and peptide substrates. *Biochim. Biophys. Acta.* **1485,** 185-98 (2000).

89.Altschul, S. F., Gish, W., Miller, W., Myers, E. W. & Lipman, D. J. Basic local alignment search tool. *J. Mol. Biol.* **215,** 403-10 (1990).

90.Altschul, S. F. *et al.* Gapped BLAST and PSI-BLAST: a new generation of protein database search programs. *Nucleic Acids Res.* **25,** 3389-402 (1997).

91.Ishikawa, J. & Hotta, K. FramePlot: a new implementation of the frame analysis for predicting protein-coding regions in bacterial DNA with a high G + C content. *FEMS Microbiol. Lett.* **174**, 251-3 (1999).

92.Edgar, R. C. MUSCLE: multiple sequence alignment with high accuracy and high throughput. *Nucleic Acids Res.* **32,** 1792-7 (2004).

93.Untergasser, A. *et al.* Primer3--new capabilities and interfaces. *Nucleic Acids Res.* **40,** e115 (2012).

94.Koressaar, T. & Remm, M. Enhancements and modifications of primer design program Primer3. *Bioinformatics (Oxford, England)* **23,** 1289-91 (2007).

95.Benson, D. A. *et al.* GenBank. *Nucleic Acids Res.* **41,** D36-42 (2013).

96.Guindon, S. & Gascuel, O. A simple, fast, and accurate algorithm to estimate large phylogenies by maximum likelihood. *Syst. Biol.* **52,** 696-704 (2003).

97.Dayhoff, M., Schwartz, R. & Orcutt, B. in *Atlas of Protein Sequence and Structure* **5,** 345-352 (Natl Biomedical Research).

98.Molecular Operating Environment (MOE). *Chemical Computing Group Inc., 1010 Sherbooke St. West, Suite #910, Montreal, QC, Canada*

99.Levitt, M. Accurate modeling of protein conformation by automatic segment matching. *J. Mol. Biol.*, **226** 507-33 (1992).

100.Fechteler, T., Dengler, U. & Schomburg, D. Prediction of protein three-dimensional structures in insertion and deletion regions: a procedure for searching data bases of

representative protein fragments using geometric scoring criteria. *J. Mol. Biol.* **253,** 114-31 (1995).

101.Conti, E., Stachelhaus, T., Marahiel, M. A. & Brick, P. Structural basis for the activation of phenylalanine in the non-ribosomal biosynthesis of gramicidin S. *The EMBO journal* **16,** 4174-83 (1997).

102.Tamada *et al.* Substrate recognition and selectivity of plant glycerol-3-phosphate acyltransferases (GPATs) from *Cucurbita moscata* and *Spinacea oleracea*. *Acta Crystallogr. D* **60,** 13-21 (2004).

103.Jones, G., Willett, P., Glen, R. C., Leach, A. R. & Taylor, R. Development and validation of a genetic algorithm for flexible docking. *J. Mol. Biol.* **267,** 727-48 (1997).

104.Korb, O., Stützle, T. & Exner, T. Empirical scoring functions for advanced protein-ligand docking with PLANTS. *J. Chem. Inf. Model.* **49,** 84-96 (2009).

6.3 Manuscript: "A comprehensive insight into the lipid composition of *Myxococcus xanthus* by UPLC ESI-MS"

Authors: Wolfram Lorenzen*, Kenan A. J. Bozhüyük*, Niña S. Cortina†, Helge B. Bode*

*Merck Stiftungsprofessur für Molekulare Biotechnologie, Fachbereich Biowissenschaften, Johann Wolfgang Goethe-Universität Frankfurt, Max-von-Laue Str. 9, D-60438 Frankfurt am Main, Germany

†Cluster of Excellence Macromolecular Complexes, Johann Wolfgang Goethe-Universität Frankfurt, Campus Riedberg, Buchmann Insitute for Molecular Life Sciences, Max-von-Laue-Str. 15, D-60438 Frankfurt am Main, Germany

Submitted in: The Journal of Lipid Research on the 7th of March 2014

Erklärung über Anteile der Autoren/Autorinnen an den einzelnen Kapiteln der Promotionsarbeit

Titel der Manuskriptes: "A comprehensive insight into the lipid composition of *Myxococcus xanthus* by UPLC ESI-MS"

	Beiträge des Promovierenden und der Co-Autoren/innen
(1) Entwicklung und Planung	WLO: 90%; HBB: 10%
(2) Durchführung der einzelnen Untersuchungen/Experimente	WLO: Kultivierung, Extraktion, Probenvorbereitung, Methodenentwicklung LC und MS, Entwicklung Datenauswertung; NSC: Durchführung HPLC-ESI-hrMS Messungen
(3) Erstellung der Datensammlung und Abbildungen	WLO: Alle Tabellen und Abbildungen außer: KAJB: MathLab Diagramme (3D Scatter Plots)
(4) Analyse/Interpretation der Daten	WLO: hrMS / MS^2 Daten, Integration, relative Quantifizierung
(5) übergeordnete Einleitung/Ergebnisse/Diskussion	WLO: 80%; HBB: 20%

A comprehensive insight into the lipid composition of *Myxococcus xanthus* by UPLC ESI-MS

Wolfram Lorenzen[*], Kenan A. J. Bozhüyük[*], Niña S. Cortina[†], Helge B. Bode*[1]

[*]Merck Stiftungsprofessur für Molekulare Biotechnologie, Fachbereich Biowissenschaften, Johann Wolfgang Goethe-Universität Frankfurt, Max-von-Laue Str. 9, D-60438 Frankfurt am Main, Germany

[†]Cluster of Excellence Macromolecular Complexes, Johann Wolfgang Goethe-Universität Frankfurt, Campus Riedberg, Buchmann Insitute for Molecular Life Sciences, Max-von-Laue-Str. 15, D-60438 Frankfurt am Main, Germany

[1]To whom correspondence should be addressed:

phone: +49(0)69-79829557

fax: +49(0)69-79829527

e-mail: h.bode@bio.uni-frankfurt.de

mail addresses:

Wolfram Lorenzen: lorenzen@bio.uni-frankfurt.de

Kenan Bozhüyük: kenan.bozhueyuek@bio.uni-frankfurt.de

Niña Socorro Cortina: cortina@chemie.uni-frankfurt.de

6.3.1 Abstract

Analysis of whole cell lipid extracts of bacteria by means of UPLC MS allows a comprehensive determination of molecular lipid species present in the respective organism and conclusions on both, its metabolic potential as well as the creation of lipid profiles which can visualize the organism's response to the change of internal and external conditions. We describe (i) a fast reversed phase UPLC ESI-MS method suitable for detection and determination of individual lipids from whole cell lipid extracts of all polarities from monoacylglycerophosphoethanolamines to triacylglycerols, (ii) the first overview of a wide range of lipid molecular species in vegetative *M. xanthus* DK1622 cell and (iii) changes of their relative composition in selected mutants impaired in the biosynthesis of alpha-hydroxylated fatty acids, sphingolipids and ether lipids.

Supplementary keywords

lipidomics, myxobacteria, ceramide phosphoinositols, ether lipids, lipid profiles, ESI-MS, reversed phase, UPLC

6.3.2 Main text

Introduction

Myxobacteria are a globally occurring order of soil-dwelling, Gram-negative, δ-proteobacteria that attract interest due to a wide range of remarkable features including cooperative motility and predation or simple multicellularity, including fungi-like fruiting body formation (1), and as being producers of a wide range of secondary metabolites (2). Additionally, they proved to exhibit a complex pattern of primary metabolites whereas fatty acyl species and associated lipid belong to the best studied ones. Some of these lipids proved to be involved in processes like chemotaxis or the starvation induced fruiting body formation either as biomarkers or chemotactic signals (3-5). However, to date no methodology is described which enables the investigation of the lipid repertoire of these bacteria as a whole in order to compare changes of the lipid composition on the molecular level in dependency on different metabolic conditions or growth stages.

In the recent years progress was made identifying and elucidating the biosynthesis and putative biological importance of fatty acids (FA) including branched-chain (6), straight-chain (7), unsaturated (8) and hydroxylated FA as well as sphingoid species (9) from myxobacteria particularly with regard to the best studied model organism *M. xanthus*. Analysis focused on fatty acid methyl esters by means of GC-MS or selected lipid classes, so that there is limited information on the complete lipidome of these organisms. High temperature GC-MS was applied on unhydrolyzed lipid extracts (10) in order to elucidate the structure and the relative abundance of neutral lipids and HPLC ESI-MS-MS experiments were used to determine changes in the glycerophosphoethanolamines composition of mutant strains with inactivated acyltransferases (11) on the one hand and to determine the ratio of certain ether glycerophosphoethanolamines to acyl glycerophosphoethanolamines during the process of starvation induced fruiting body formation (4) on the other hand. Results from TLC resolved $^{32}PO_4^{3-}$ metabolic labelling studies are available for *Stigmatella aurantiaca* (12), *Myxococcus fulvus* (13) and *Myxococcus xanthus* (14), which give some information about phosphate containing lipid classes and their molar ratio present in those bacteria. However, no comprehensive information of the complete lipidome of myxobacteria are available to date, which is a prerequisite to visualize and evaluate the changes in lipid composition of e.g. mutant strains during vegetative growth or fruiting body formation and can be used as the basis for further investigations for e.g. lipid biomarkers for fruiting body formation.

We sought to find a LC-MS method that (i) is able to resolve as many lipid species as possible ranging from lysophospholipids over glycerophospholipids and glycerolipids; (ii) gives MS and MS/MS spectra from the abundant molecular species in a single run for structure elucidation and identification; (iii) involves the standard setup of UPLC-MS instrumentation used for routine analysis; (iv) solely involves the use of readily available software and (v) needs a very short measuring time.

Many lipidomic methods, which involve the direct measurement of lipid species from lipid extracts, base on direct infusion into ESI sources or ionization by MALDI (15, 16) but ion suppression usually impedes the detection of less abundant molecular species in such a complex mixture which can be circumvented by separation of the analytes using a chromatographic technic (17). The development of a comprehensive LC method for lipids proved to be challenging due their highly divers putative physical properties ranging from partly water soluble (lysophospholipids) over amphiphilic (glycerophospholipids) to highly non-polar (glycerolipids), non-ionic (glycerolipids, ceramides) and strongly pH dependent zwitter, cationic and anionic molecules (glycerophospholipids) so that all chromatographic conditions (different eluents, nature and quantity of additives as well as temperature and pH) have to be controlled over the whole chromatographic process. The use of eluent additives is limited as they have to be compatible with MS-coupling.

Many LC methods have been published till now that involve normal phase (NP), hydrophilic/lipophilic interaction chromatography (HILIC), and reversed phase (RP) chromatography in most cases to address particular analytical challenges (18-20). RP-chromatography, which can be regarded as “the” gold standard in routine small molecule analytics, is ideal for resolving molecules even with small differences in polarity so that it became the method of our choice not least being part of the standard instrumentation of our system.

Results

A binary eluent system consisting of water and acetonitrile in solvent A and acetonitrile and isopropanol in solvent B (for details see experimental section) proved to be useful for the separation and elution of a wide range of lipid standards on a RP-18 column (**Figure 1**). The addition of 10 mM ammonium acetate and the adjustment to pH 5.5, which is (i) the buffer optimum of ammonium ions and (ii) an pH at which all major phospholipids have a equable charge state (21, 22), with formic acid in both solvent mixtures gave an

acceptable separation of the lipid extract of *Myxococcus xanthus* DK1622 (23) as depicted in **Figure 2**, whereas ESI-MS/MS allowed the detection and identification of eluting lipid species (**Figure 3-8**).

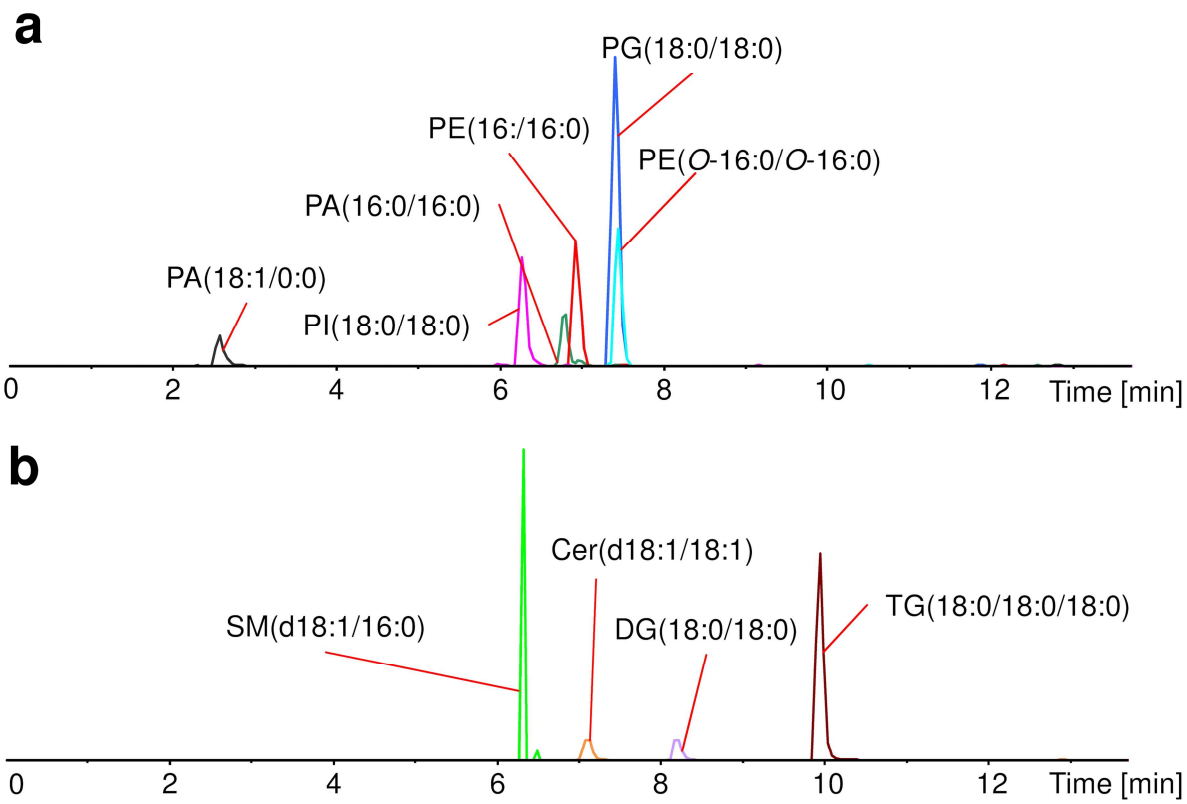

Figure 1 | Extracted ion chromatograms of lipid standards from runs using the described LC method.

a) Data acquired in the negative and b) positive ionization mode with standards mentioned in the materials and method section. All tested lipids could be resolved by the applied eluent system. For details see method section. PA: mono/diacylglycerophosphate; PE(*O*/*O*): dialkylglycerophosphoethanolamine; PG: glycerophosphoglycerol; PI: glycerophosphoinositol; Cer: ceramide; SM: ceramide phosphocholine; DG: diacylglycerols; TG: triacylgylcerols.

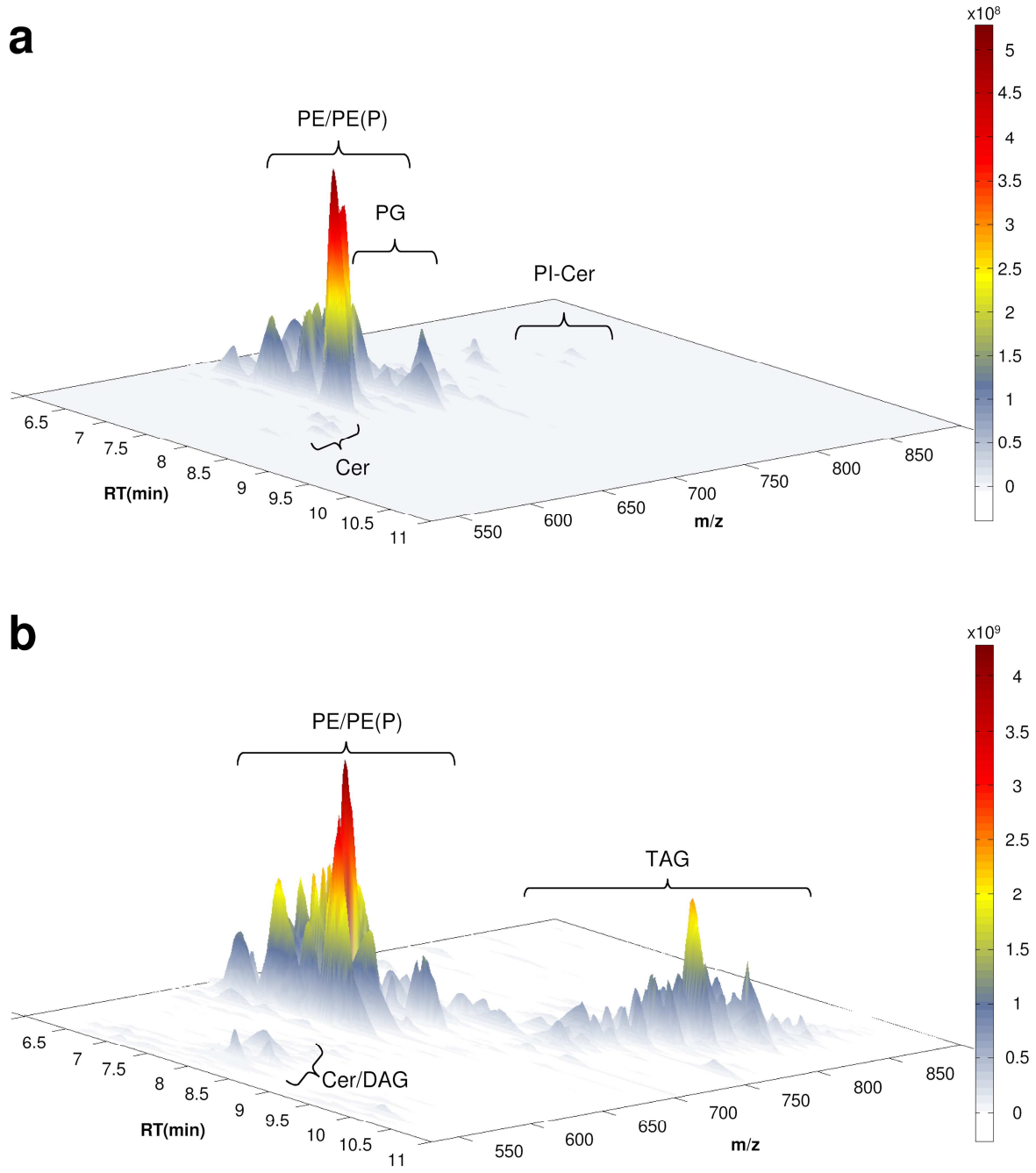

Figure 2 | Base peak UPLC-ESI-MS chromatograms of a wild type DK1622 lipid extract.

a) Data acquired in the negative and b) positive ionization mode. PE(P): (plasmenyl)glycerophosphoethanolamines; PG: glycerophosphoglycerols; Cer: Ceramides; PI-Cer: ceramide phosphoinositols; DG: diacylglycerols; TG: triacylglycerols. Most intense signals are discernable in the region of R_t = 6.0-8.5 minutes and *m/z* of about 550-850 in the negative ion mode and another large group of signals at R_t = 9.0-10.5 and *m/z* of 700-880 in the positive ion mode.

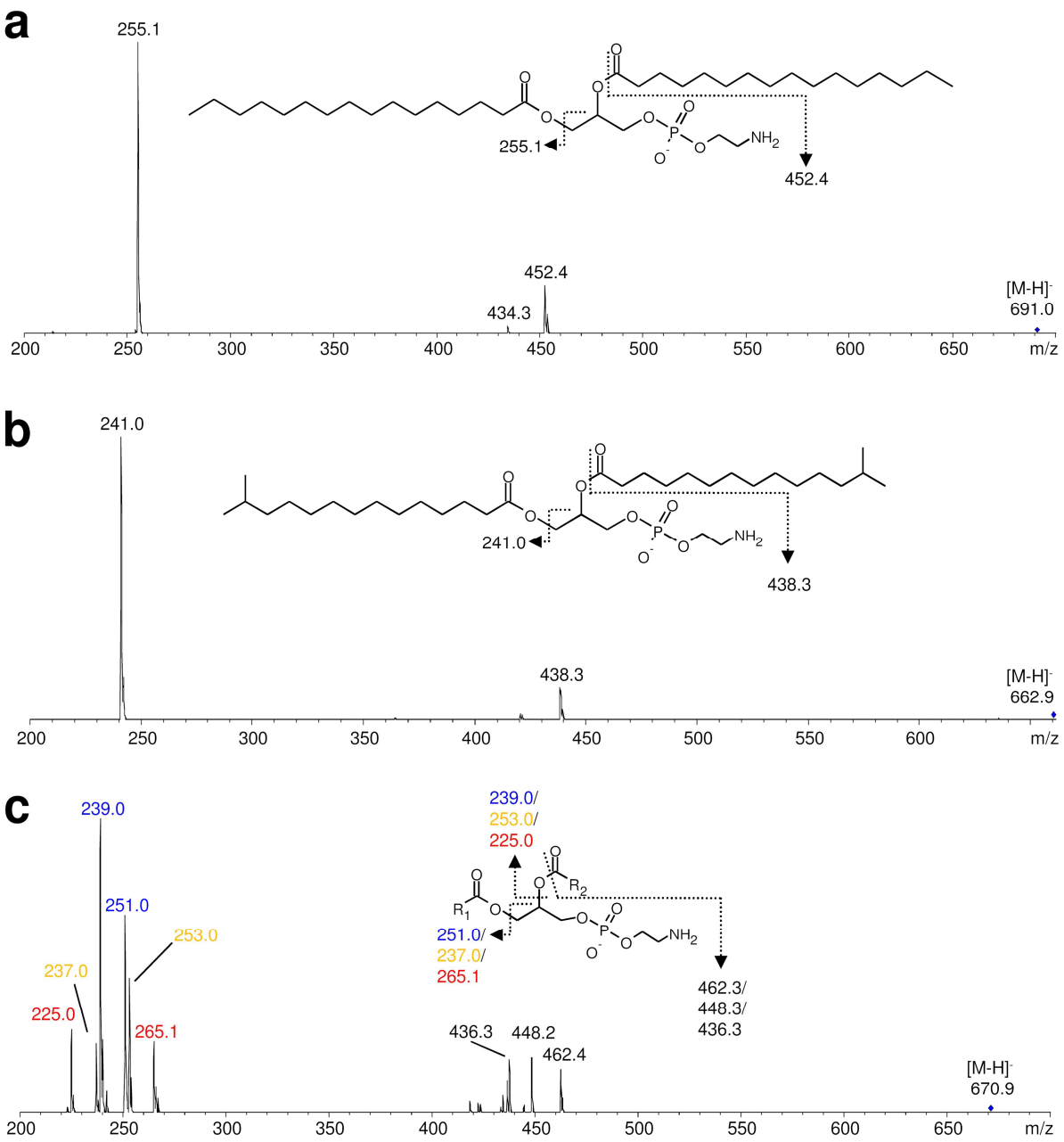

Figure 3 | Example spectra for glycerophosphoethanolamine (PE) identification.

Mass spectra of a) PE(16:0/16:0) lipid standard b) PE(15:0/15:0), the main glycerophosphoethanolamine in *M. xanthus*. and c) combined PE(16:2/15:1); PE(15:2/16:1); PE(17:2/14:1) spectrum. Fragment signals derive from $[RCOO_{sn\text{-}1}]^-$ / $[RCOO_{sn\text{-}2}]^-$ as well as $[M\text{-}H\text{-}RCHO]^-$ and $[M\text{-}H\text{-}RCHO\text{-}H_2O]^-$ (not assigned) ions (25). Carboxylate ions with the higher relative abundance were assigned to the *sn*-2 position of the glycerol backbone (43).

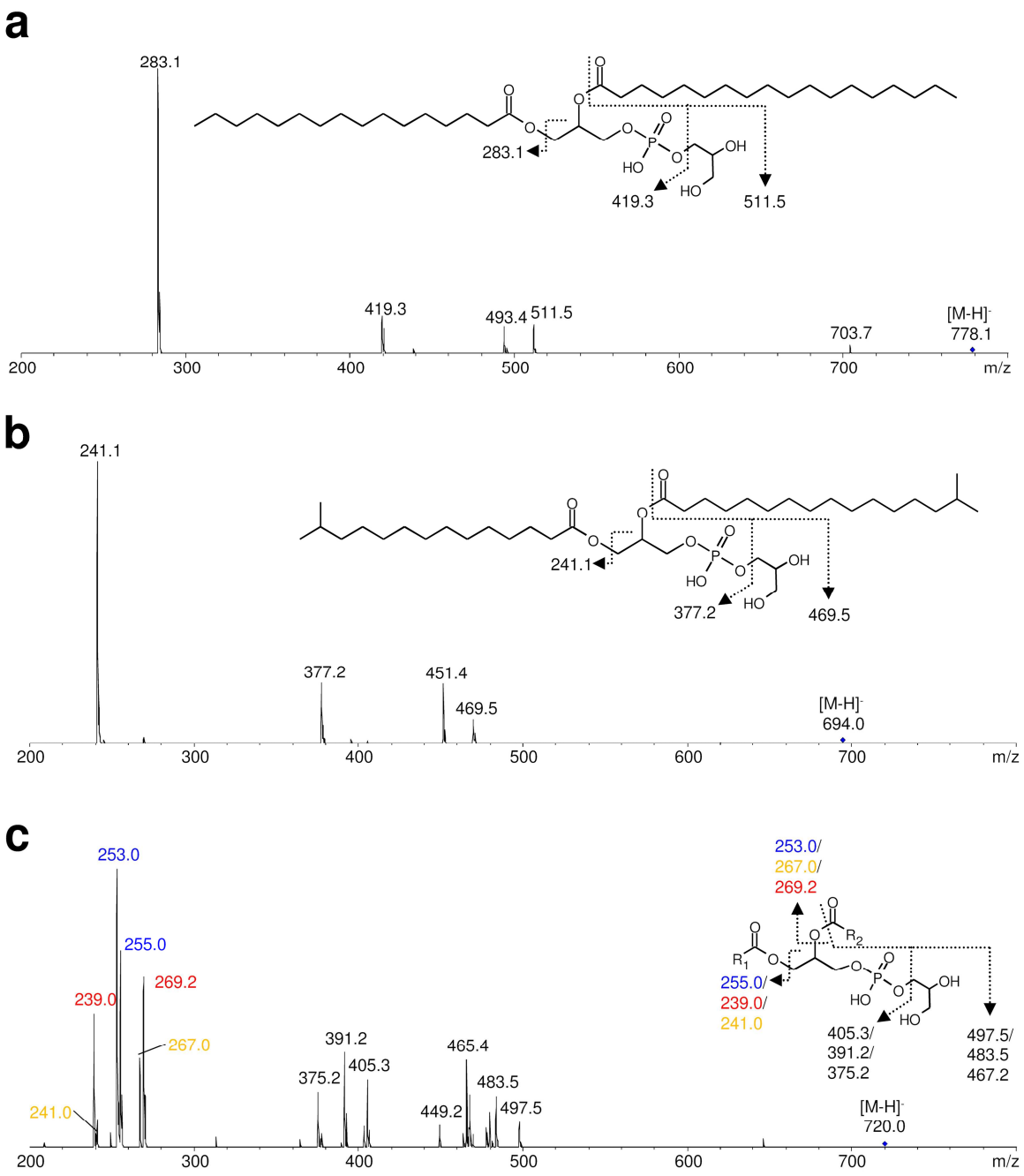

Figure 4 | Example spectra for glycerophosphoglycerol (PG) identification.

Mass spectra of a) PG(18:0/18:0) lipid standard b) PG(15:0/15:0), the main glycerophosphoglycerol in *M. xanthus*. and c) combined PG(16:0/16:1); PG(15:1/17:0); PG(15:0/17:1) spectrum. Signals derive from $[RCOO_{sn\text{-}1}]^-$ / $[RCOO_{sn\text{-}2}]^-$ ions as well as $[M–H–74–RCH_2COOH]^-$, [M-H-RCHO]-/[M-H-RCHO-H_2O]$^-$ (the latter not assigned) (25). Caboxylate ions with the higher relative abundance were assigned to the *sn*-2 position of the glycerol backbone (43).

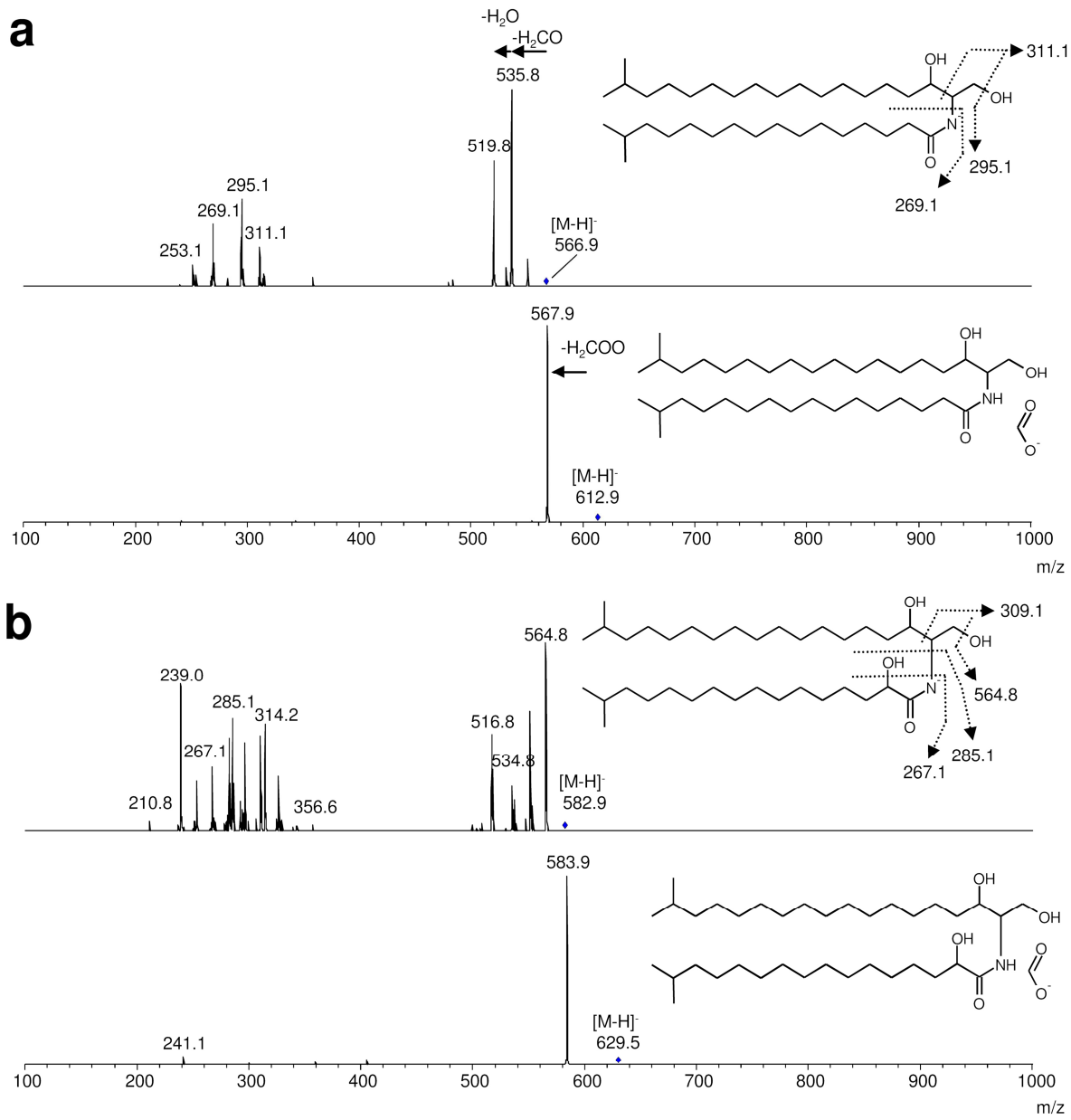

Figure 5 | Example spectra for N-aclsphinganine (Cer) identification.

Mass spectra of a) Cer(d19:0/17:0) and b) Cer(d19:0/17:0 2-OH). Structure elucidation was performed according to (44). Top spectrum was obtained from $[M-H]^-$ bottom spectrum from $[M+HCOO]^-$ molecular ion. Molecular composition was confirmed using hrMS (see **Table 3**).

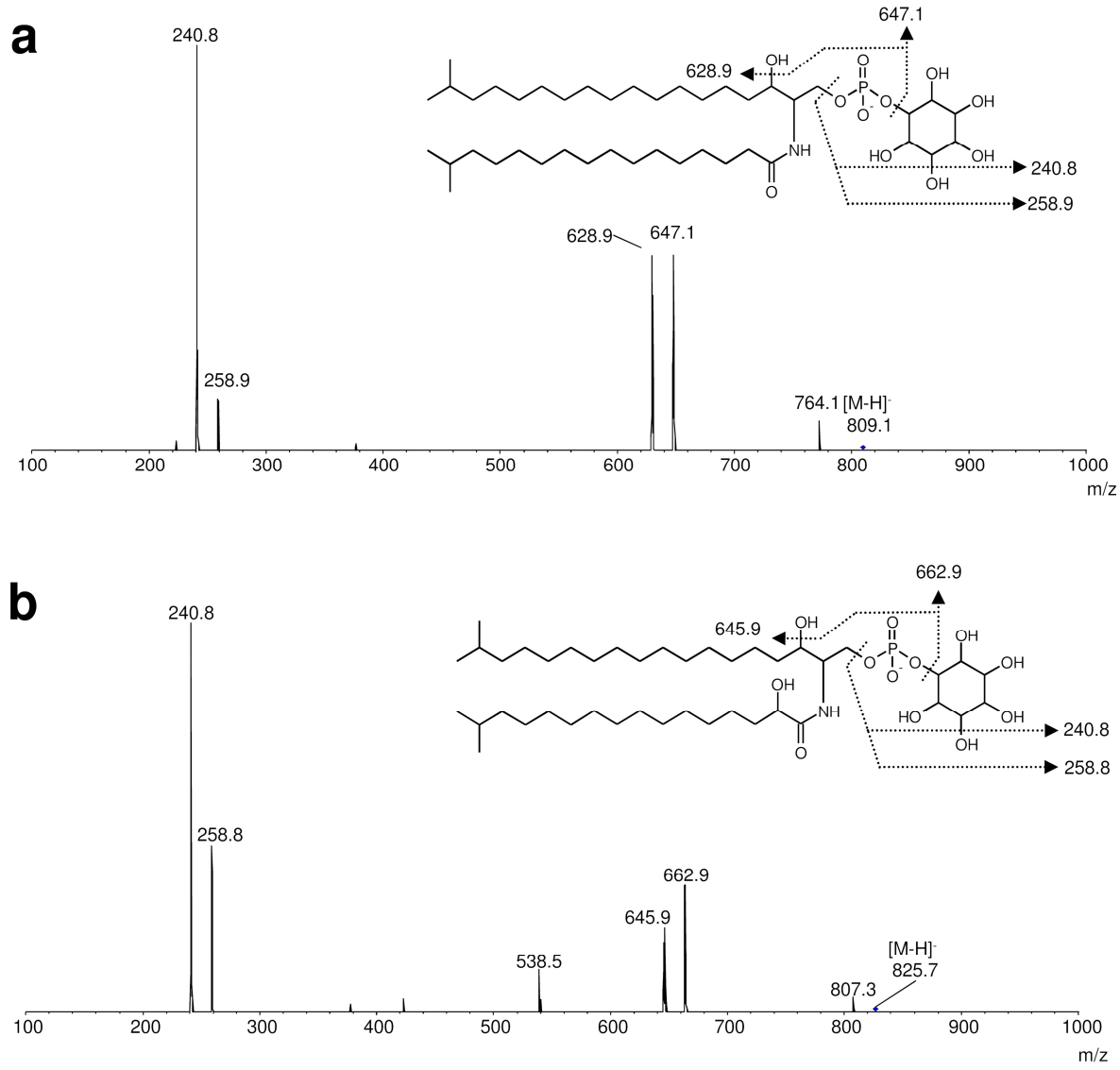

Figure 6 | Example spectra for ceramide phosphoinositol (PI-Cer) identification.

MS^2 fragment spectra of a) PI-Cer(d19:0/17:0) and b) PI-Cer(d19:0/17:0 2-OH). Fragments are $[IP]^-$, $[IP-H_2O]^-$, $[P\text{-}Cer\text{-}H_2O]^-$ and $[P\text{-}Cer]^-$ (41, 42). Molecular composition was confirmed by hrMS (see **Table 3**).

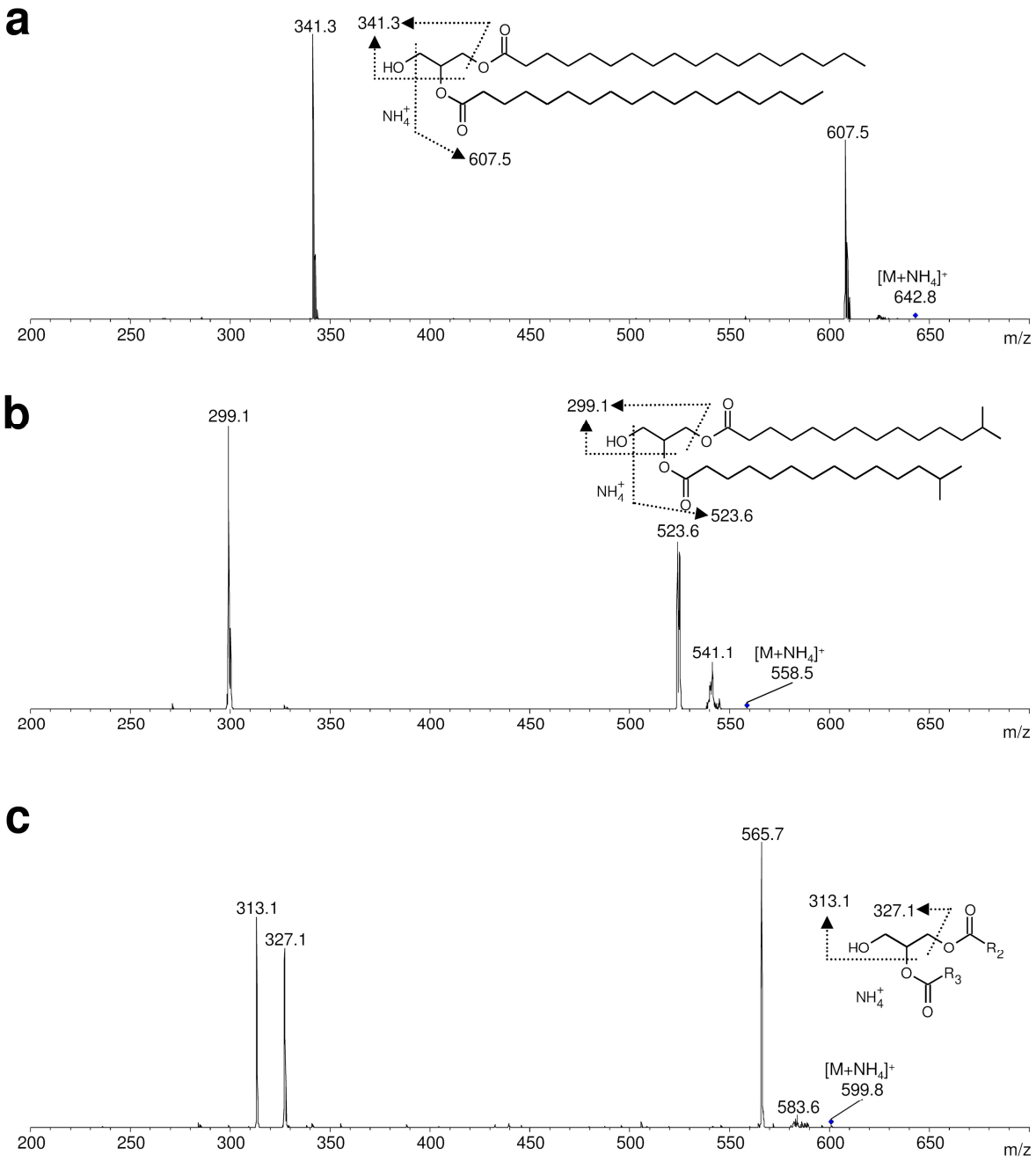

Figure 7 | Example spectra for diacylglycerol (DG) identification.

MS^2 fragment spectra of a) DG(18:0/18:0) standard b) DG(15:0/15:0) and c) DG(33:0) from $[M+NH_4]^+$ molecular ion. Fragment ions derive from neutral loss of fatty acid derived keten moieties and water $[M-NH_3-H_2O-RCHCO]^+$ (24).

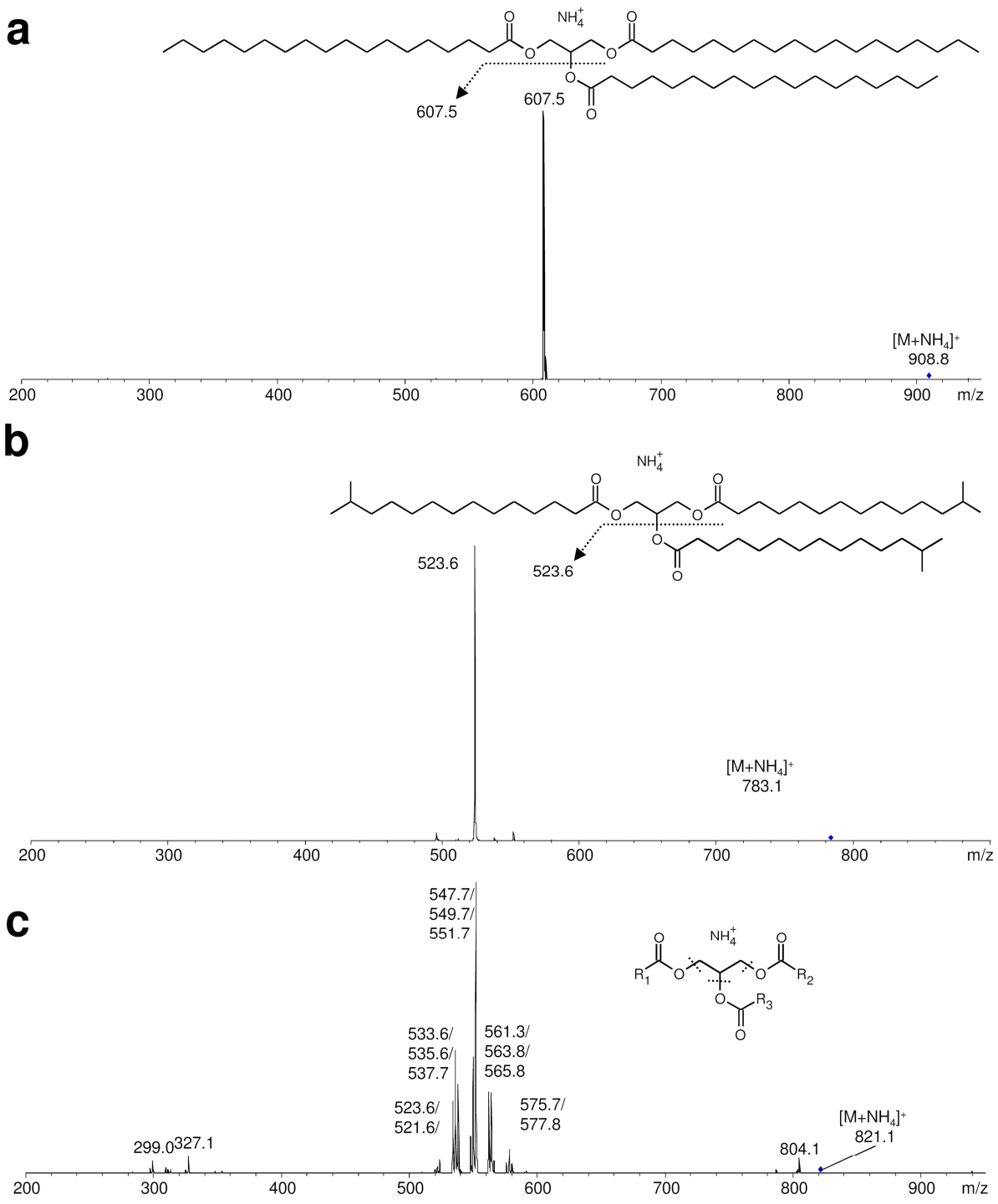

Figure 8 | Example spectra for triacylglycerol (TG) identification.

MS^2 fragment spectra of a) TG(18:0/18:0/18:0) standard b) TG(15:0/15:0/15:0) and c) TG(48:3) from $[M+NH_4]^+$ molecular ion. Fragment ions derive from neutral loss of fatty acids and ammonia ($[M-NH3-R_nCOOH]^+$) (corresponding to fatty acids C14:1 to C18:2) and fatty acid derived $[R_nCO + 74]^+$ ions (24). Exact assignment of fatty acyl residues to glycerol backbone was not possible under these conditions.

Lipid profile of *Myxococcus xanthus*

Applying the described method on normalized lipid extracts resulted in two sets of LC-MS data for each sample: one recorded in the positive ion mode the other one in the negative ion mode. **Figure 2** shows the resulting base peak chromatograms (BPC) of the UPLC-MS runs of lipid extracts from vegetatively grown DK1622 wild type cells recorded in the negative (**Figure 1 a**) and the positive (**Figure 1 b**) ion mode respectively.

Evaluation of the autoMS^2 Data of these signals resulted in the identification of a large number of PE and PG species as well as the previously identified 1-(1*Z*-alkenyl),2-acylglycerophosphoethanolamines (PE(P)) (4) (**Figures 3-4**). Hydroxylated and non-hydroxylated N-acylsphinganines (Cer) (**Figures 5**) and interestingly, for the first time in myxobacteria, ceramide phosphoinositols (PI-Cer) (**Figures 6**; for a summary see **Supplemental Table 1 and 2** the full data set obtained from Data Analysis) are detectable as less abundant compounds, which is consistent with the relative small abundance and limited diversity of sphingoid bases determined by GC-MS analysis of lipid methanolysed cell extracts (**Table 1**).

Fragmentation spectra of the late eluting molecules in the positive ionization mode are consistent with ammonium adducts of diacylglycerols (DG) and triacylglycerols (TG) (24) (**Figure 7-8**) as well as protonated ceramides. PEs are the only detectable glycerophospholipids species as distinguishable by the $[M-141+H]^+$ MS^2 fragment resulting from the neutral loss of the polar headgroup. They were not further evaluated as these fragment spectra do not contain additional information.

None of the evaluated MS^2 spectra gave evidence for other glycerophospholipids, glycerolipids or precursors of identified lipids like, lysophospholipids, diacylglycerophosphoserines or CDP-diacylglycerols.

Concerning the elution pattern of these lipid species, under our conditions the following regularities can be observed (**Figure 2, Supplemental Table 1** and **2**):

1. As expected, with increasing length of the acyl chains attached to the glycerophospholipids, retention time increases as non-polar interaction with the RP-18 stationary phase increase.

2. Elution order for glycerophospholipids is PGs → PEs → pPEs when the number of carbon atoms and the degree of saturation in the acyl side chains are identical.
3. PI-Cers elute earlier than Cers whereas α-hydroxylation in the acyl side chain further decreases the retention time.
4. For DGs and TGs, analogously to the glycerophospholipids, retention time increases with acyl chain length and degree of saturation.
5. Lipids from the same class with an identical overall carbon and double bond number generally co-elute. Still, data from MS^2 fragmentation of glycerophospholipids in the negative ion mode allows the assignment of fatty acyl residues to *sn*-1 or *sn*-2 positions of the glycerol backbone of those lipid species (**Figure 3-4).**

In total 3 ceramide, 4 ceramide phosphoinositols, 52 glycerophosphoethanolamines, two 1-(1*Z*-alkenyl),2-acylglycerophosphoethanolamines, 20 glycerophosphoglycerols, 7 diacylglycerols could be identified. 46 triacylglycerol molecular species were identified as well. The exact assignment of all three fatty acyl moieties to the three hydroxyl functions of the glycerol backbone was not possible. Fragment spectra of triacylglycerols indicated a high variance of those molecules with almost all saturated and unsaturated fatty acyls present in *M. xanthus* so that each molecular ion consists of several isobaric triacylglycerol species. (**Figure 8c**).

<u>UPLC-MS analysis allows the assignment of a particular polar headgroup to ceramides and detects loss of lipid species</u>

We applied the method and data evaluation procedure on lipid extracts of vegetatively grown cells from various strains with mutations in various genes involved in lipid biosynthesis. Strain Δ0191 lacks a fatty acid hydroxylase, which is responsible for the formation of 2-OH fatty acids (**Table 1**). Strain ¯MXAN_3748 bears a mutation in a serine-palmitoyl-CoA acyltransferase homologue and is known to be incapable of sphingoid base formation (9) (**Table 1**). **Figure 9 a-c** shows EICs of various ceramide

species from wt, Δ0191 and ¯MXAN_3748 extracts. Δ0191 shows the selective loss of hydroxylated ceramides,¯MXAN_3748 does form neither Cers nor PI-Cers anymore as determined by both low resolution MS and confirmative high resolution MS experiments (**Table 3**).

Analogously, in strain ¯MXAN_1528, that bears a mutation in *elbD,* a multidomain enzyme involved in ether lipid biosynthesis (4), the relative abundance of vinyl ether species is strongly reduced (**Supplemental Table 2, Figure 9 d**).

Lipid profiles of various mutants deficient in lipid biosynthesis

Integration of the EIC peak areas of the monoisotopic masses of the respective lipid molecular species allows the construction of lipid profiles. If only the relative proportion of all lipid species are being compared among the various strains investigated, no major differences are observable apart from the afore mentioned loss of certain lipid species and the expected relative increase of the remaining molecular species (**Figure 10**).

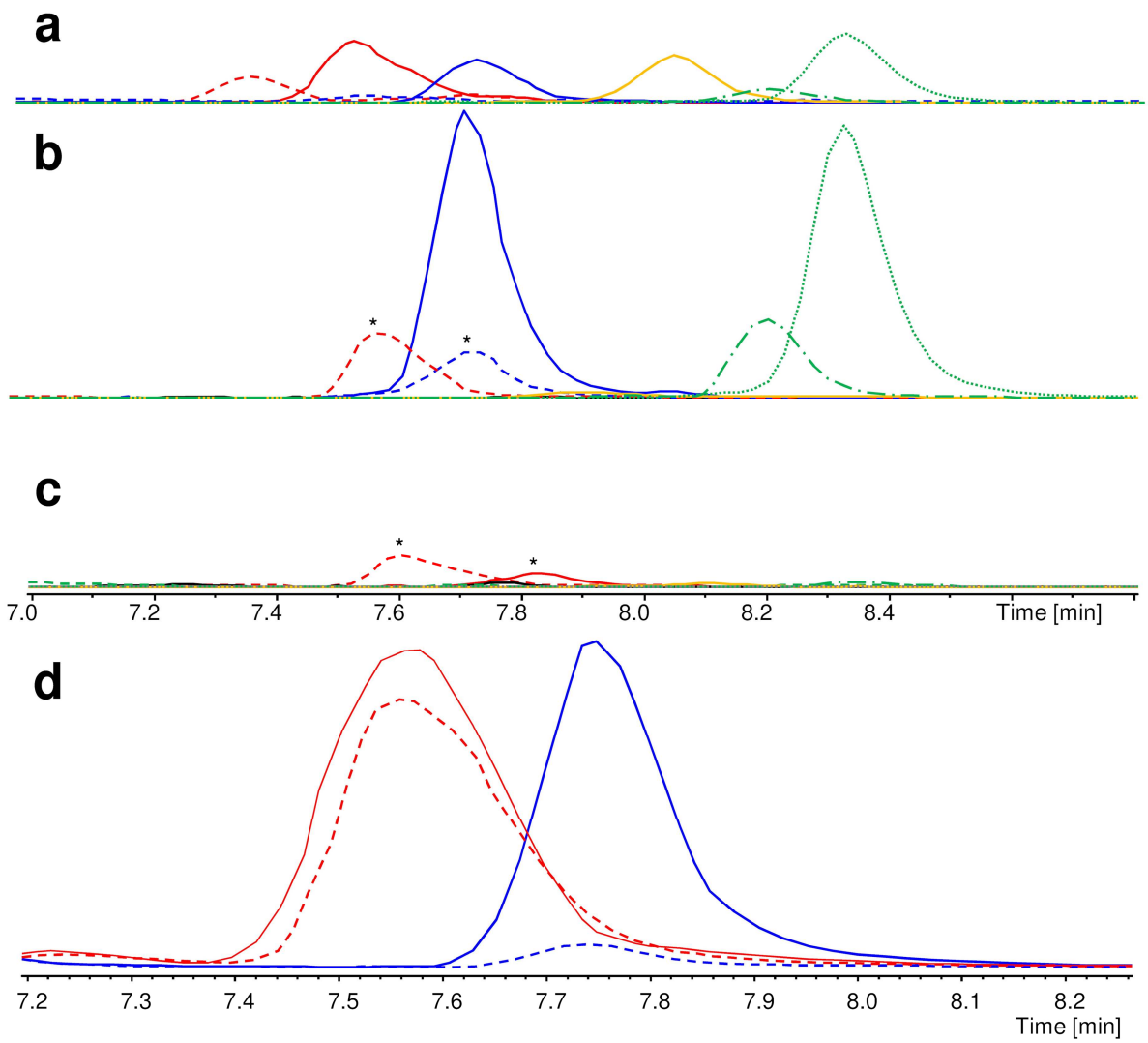

Figure 9 | Extracted Ion chromatograms of identified N-acylsphinganines and ceramide phosphoinositols.

Chromatograms are from *M. xanthus* a) wild type b) Δ0191 c) ⁻MXAN_3748. Intensity scale is normalized to 10^8 counts. Red lines: hydroxylated ceramide phosphoinositols; blue: non-hydroxylated ceramide phosphoinositols; orange: hydroxylated N-acylsphinganines; green: non-hydroxylated N-acylsphinganines. Asterisks indicate signals due to overlapping isotopic peaks from other molecular species unrelated to sphingolipids. d) Superimposed chromatograms of PE(15:0/15:0) (red), PE(P-15:0/15:0) (blue) of wild type (solid) and ⁻MXAN_1528 (dashed) reflecting the reduction of vinyl ether production as also visible in **Table 1**.

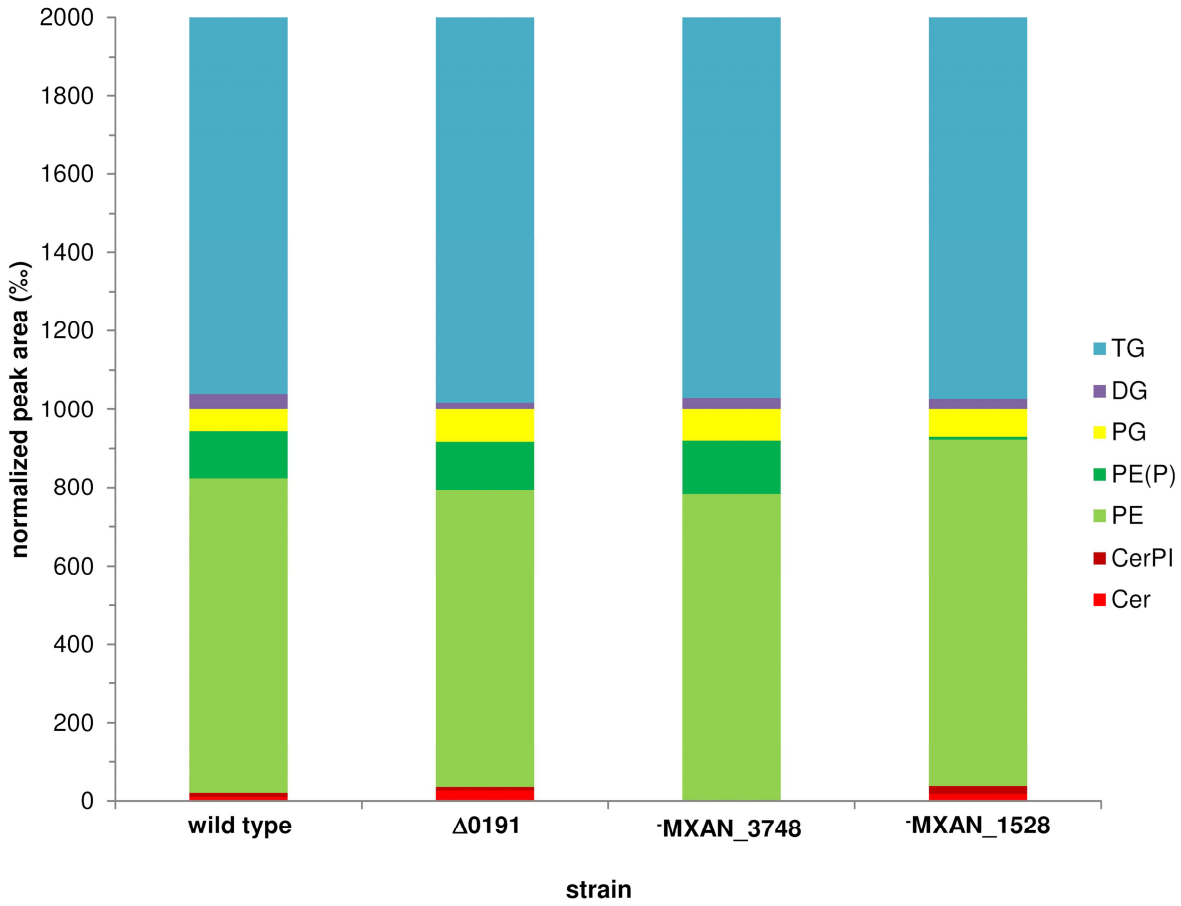

Figure 10 | Ratio of lipid species present in lipid extracts.

Ratios of lipid species present in various strains of *M. xanthus* given in per mil of total lipid AUC determined for the DG and TG in the positive and all other lipid species in the negative ionisation mode. TG: triacylglycerols; DG: diacylglycerols; PG: glycerophosphoglycerols; PE(P): 1-(1Z-alkenyl)-2-acylglycerophosphoethanolamines; PE: glycerophosphoethanolamines; PI-Cer: ceramide phosphoinositols; Cer: N-acylsphinganines.

To get further insights into the lipid profile of *M. xanthus* we constructed a scatter plot comprising mass, retention time and relative abundances of all analyzed lipid molecular species given as per mil of the sum of all peak areas (**Figure 11**). The observed pattern reflects previous results from GC-MS analysis of fatty acid methyl esters and neutral lipids with a high proportion of lipid molecular species containing 15:0 and 16:1 (**Table 1** and **2**). It seems that the occurring fatty acids are somewhat equally distributed among the various lipid classes with almost “Gaussian” like distribution among the triacylglycerols. Like *Curtis et al.*(11) we identified many PE and also PG molecular species with unsaturated fatty acids attached to the *sn*-1 position of the glycerol backbone, indicating a less specific glycerol-3-phosphate 1-*O*-acyltransferases activity compared to e.g. *E. coli* where those lipids are less prevalent (25). Vinyl ether containing phospholipids were exclusively detected within the glycerophosphoethanolamine molecules with a high overall proportion

whereas *O*-alkylglycerols could not be detected under these conditions, which is consistent with previous results (4).

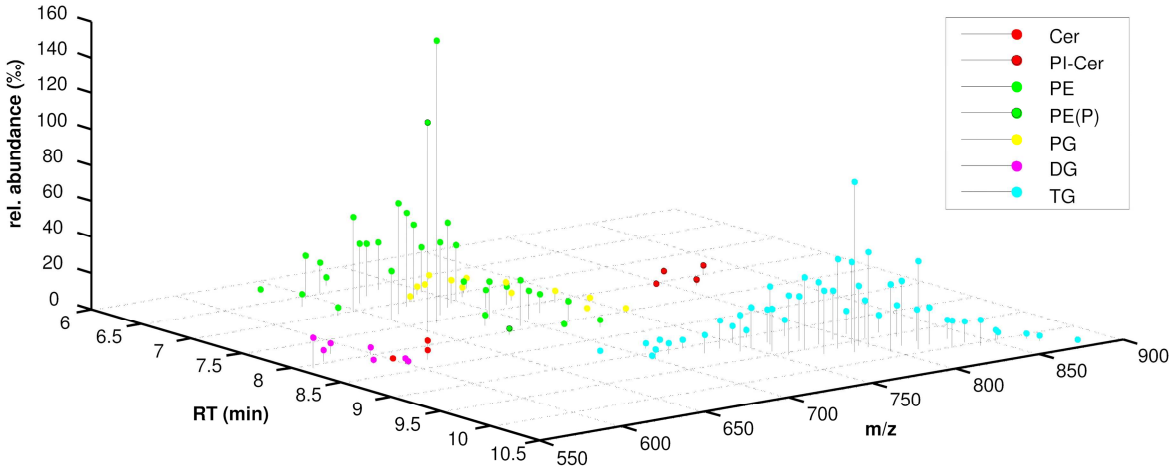

Figure 11 | Lipid profile of *M. xanthus* DK1622 wild type.

Data from Table 2 visualized in a scatter plot with relative abundance of individual lipid molecular species given as per mil of the total abundance of all lipid species separately determined for the positive and negative ionization mode. PE(P): (plasmenyl)glycerophosphoethanolamines; PG: glycerophosphoglycerols; Cer: Ceramides; PI-Cer: ceramide phosphoinositols; DG: diacylglycerols; TG: triacylglycerols.

In an additional step, we created scatter plots, comparing the relative changes in the abundance of the individual lipid species of the mutant lipid profiles compared to the wild types profiles. This reflects the changes in the abundance of individual molecular species in the analyzed mutant strains compared to the wild type, displayed as a whole in a three-dimensional way in order to visualize changes in their profile (**Figure 12 a-c**).

The fairly low proportion of glycerophosphoglycerols is consistent with results from *Orndorff et al.* (14) who specified the amount of glycerophosphoglycerols 9 % of total $^{32}PO_4^{3-}$ labelled *M. xanthus* membranes. Neutral lipids, especially triacylglycerols gave strong signals as ammonium adducts although they are less prevalent in vegetative cells (10). Their molecular diversity seems to be even higher than that of the polar lipids.

Lipid profile of strain Δ0191 vs. wild type shows that, apart from the afore mentioned loss of hydroxylated ceramide molecular species and the expected relative increase of non-hydroxylated ceramides (**Figure 12, Table 2**), there is a general increase in the abundance of PG molecular species and (**Figure 12 a**). Within the PE species, there is a conspicuous increase in PE(15:0/17:0) with PE(15:0/15:0) and PE(15:1/15:0) strongest decreased in abundance. This matches well with the FAME pattern of strain Δ0191, which shows a

higher proportion of i17:0 fatty acid than the wild type. The changes in abundance within the triacylglycerol molecular species seem to be rather random however might also be attributed to more i17:0 and less i15:0.

Figure 12 b visualizes the changes in the lipid profile of ¯MXAN_3748 compared to the wild type. A general increase in higher molecular weight lipid species within the PE, PG, TG molecular species as well as a greater proportion of PE(P) can be observed which means that there is a general increase in longer and/or less saturated fatty acids that could compensate for the loss of the lipophilic ceramide species.

The scatter plot in **Figure 12 c** shows the expected decrease of PE(P-15:0/15:0) in the ¯ MXAN_1528 mutant. Rather surprising is the synchronous relative drop in PE(15:0/15:0) and TG(15:0/15:0/15:0) suggesting a common precursor of all these lipid species.

Discussion

Such comprehensive data sets about molecular lipid species in myxobacteria has not been published before. *Curtis et al.* (26) reported the analysis of lipid molecular species from the PE fraction of *M. xanthus* by HPLC ESI-MS resulting in the identification of 26 PE molecular species whereas for four of them no assignment of the fatty acyl residues to the *sn*-1 and *sn*-2 position of the glycerol backbone was achieved.

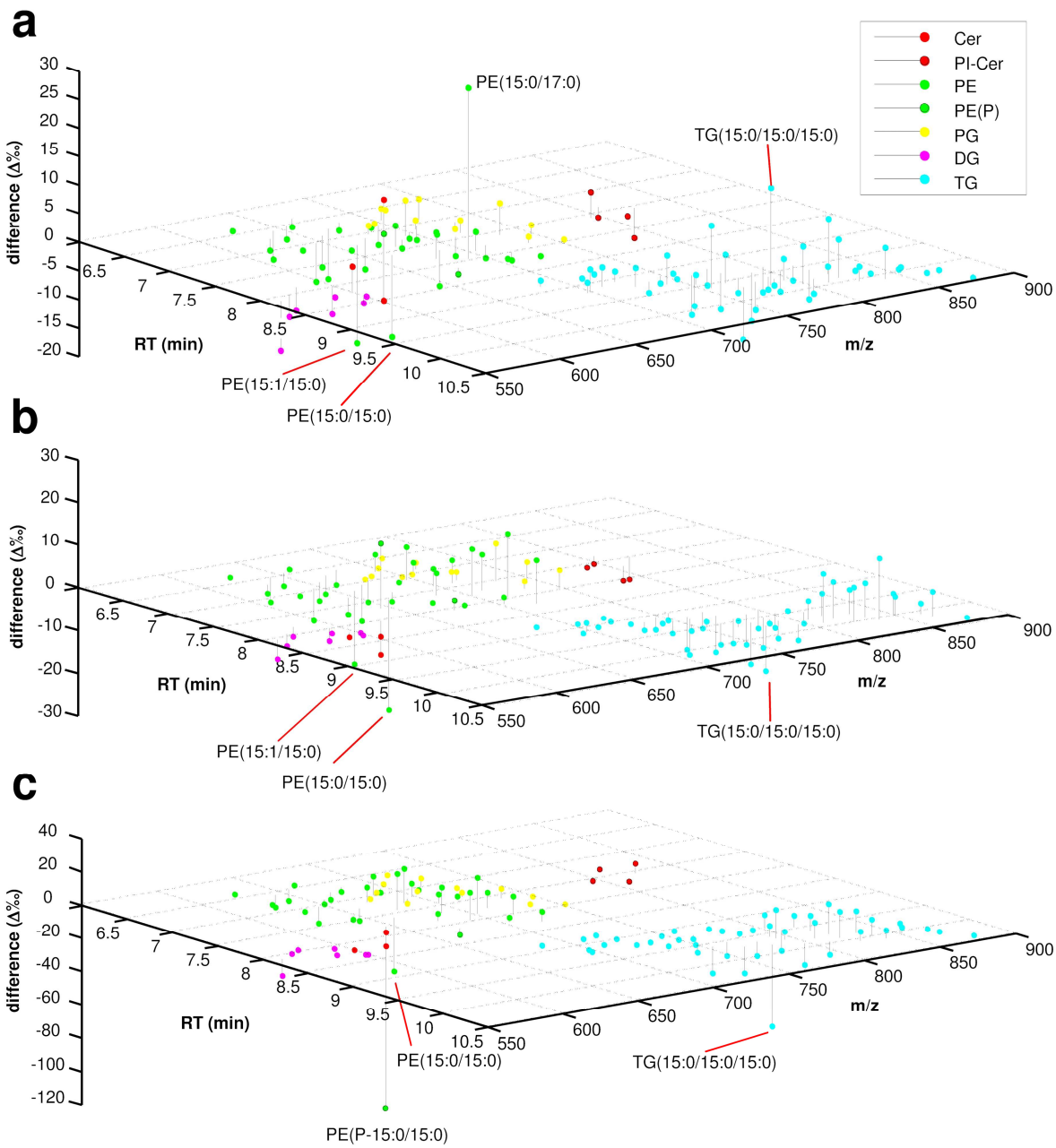

Figure 12 | Relative changes in the lipid profile of Δ0191 (a), ¯MXAN_3748 (b) and ¯MXAN_1528 (c) vs. wild type.

For details see text and Supplemental **Table 1**. PE(P): (plasmenyl)glycerophosphoethanolamines; PG: glycerophosphoglycerols; Cer: Ceramides; PI-Cer: ceramide phosphoinositols; DG: diacylglycerols; TG: triacylglycerols.

Our UPLC-MS analysis confirmed that α-hydroxylation of fatty acids and sphingolipids are indeed metabolically linked in such a way that the lipid extract of the α-hydroxylase deletion mutant Δ0191 lacks the hydroxylated sphingolipids and the *spt*-disruption mutant ¯MXAN_3748 is devoid of any detectable sphingolipids with nor further molecules bearing a α-hydroxylated fatty acid. When the results concerning the abundance of neutral

lipids are compared to those obtained by high temperature GC-MS analysis (10) it seems that the latter method overestimates the presences of mono- and diacylglycerols very likely due to the derivatisation with MSTFA, which converts them in easily ionizable molecules. We conclude from this observation that the neutral lipid pattern by ESI-MS is more representative than the data obtained by high temperature GC-MS. Interestingly, though not further evaluated, triacylglycerol molecular species seem to contain also fatty acyl species that are not detectable in FAME-GC-MS analysis as e.g. the $[M\text{-}NH3\text{-}R_nCOOH]^+$ fragment at *m/z* 521.6 in the mass spectrum shown in **Figure 8 c** indicates neutral loss of a 18:1 fatty acid.

The presence of ceramide phosphoinositol is an interesting finding of this study as this is a lipid known to be present in fungi like *Saccharomyces cerevisiae* (27) and *Aspergillus niger* (28) but were also found in protozoan pathogens like *Trichomonas brucei* (29) and plants (30), however to our knowledge not described before in bacteria. In general, ceramides seem to be rather common as they were found in all myxobacteria investigated for this lipid class with ceramides detected in *Cystobacter fuscus* (31), ceramide phosphoethanolamines in *Myxococcus stipitatus* (32), ceramide phosphoethanolamines, β-D-Glucosylsphingenines and even phosphonosphingolipids in *Sorangium cellulosum* So ce56 (33), where they serve together with ornithine containing lipids and glycerol etherlipids as substitutes for missing lipopolysaccharides in the outer membrane (33).

In *Saccharomyces cerevisiae* ceramide phosphoinositols are synthesized by the inositol phosphorylceramide synthase catalytic subunit (AUR1), an enzyme that transfers a phosphoinositol headgroup to α-hydroxyceramides from diacylglycerophosphoinositol moiety(34). Protein MXAN_0451 (annotated as PAP2 family protein) is 29% homologous to AUR1 (E-Value = 2^{-20}) a further indication for *M. xanthus* capability to synthesize this lipid species. Interestingly no diacylphosphoinositols were detected in the lipid extracts though it was noted before that a *myo*-inositol-1-phosphate synthase homologue (MXAN_0452) as well as a CDP-alcohol phosphatidyltransferase homologue (MXAN_0450) are encoded next to MXAN_0451 (35). This may be due to a fast conversion of diacylglycerophosphoinositols to ceramide phosphoinositols as the occurrence of diacylglycerophosphoinositols are indeed described for *M. fulvus* and *Stigmatella aurantiaca* (12).

Glycosylated ceramides in general are important signaling molecules in multicellular organisms (36) but no specific function for PI-Cers are known in lower eukaryotes except that inhibition of AUR1 is lethal to *Saccharomyces cerevisiae* (37) and that PI-Cer is at least indirectly associated with pathogenicity of *Cryptococcus neoformans* (38). A possible signaling function in e.g. fruiting body formation or sporulation of PI-Cers and ceramides in general in *M. xanthus* remains to be investigated. Although no systematic investigations on putative signaling functions of ceramides are available in bacteria it was noted that sphingolipids (as determined by the hydrolysis derived sphingobases) accumulate in developing *M. xanthus* cells but are dispensable for fruiting body formation (9).

We are aware that final statements concerning the changes of the lipid profiles are not possible without statistically analyzable data but some observable changes, like the previously established decrease or loss of selected molecular species and the easily explainable general increase in degree of saturation and chain length of fatty acids within the lipids suggest that this is generally a valid approach whereat the visualization of the data using scatter plots resolved by the lipid class strongly facilitates data inspection and interpretation. This facet will become even more important the higher the number of analytes becomes. We envision that after refinement of this method utilizing appropriate internal standards and statistics the obtained lipid profiles can be linked to other properties like transition profiles or diffusibility of membranes, activities of selected membrane proteins and membrane proteomes in order to unravel the multifactorial links between those properties

6.3.3 Tables

Table 1 | Complete FAME-GC-MS data from DK1622 wild type and mutants in per cent of all Fatty Acid Methyl Esters. DMA: Vinyl ether derived dimethylacetales; OAG: ether derived *O*-alkylglycerols; d: sphingoid bases.

	wild type	Δ0191(9)	-MXAN_3748 (9)	-MXAN_1528 (4)
12:0	0.09	<0.17	0.05	0.08
iso-13:0	0.33	0.33	0.25	0.59
iso-14:0	0.16	0.00	<0.05	<0.08
14:1ω9c	1.23	0.49	0.57	0.20
14:1ω3c	0.04	<0.17	0.05	<0.08
14:0	5.85	2.65	3.43	3.05
iso-15:1ω9c	0.32	0.16	0.11	0.29
iso-15:0	38.93	40.67	33.62	33.86
15:0	2.78	0.74	4.06	2.07
15:1ω10c	3.54	1.03	2.89	2.21
15:1ω4c	3.04	0.69	2.92	2.11
iso-16:0	<0.09	<0.17	3.31	<0.08
16:2ω5c,11c	4.92	4.61	4.53	5.33
16:1ω11c	0.97	0.85	1.15	1.17
16:1ω5c	11.48	13.03	14.08	17.45
16:0	1.88	3.29	2.65	1.99
iso-17:2ω5c,11c	1.67	2.84	3.12	2.94
iso-17:1ω11c	0.74	1.00	1.79	1.33
iso-17:1ω5c	1.39	1.80	3.57	2.34
iso-17:0	3.35	9.38	7.88	4.99
14:0 3-OH	0.53	0.13	0.55	0.55
iso-15:0 3-OH	2.88	2.06	3.21	3.32
16:0 2-OH	0.79	<0.17	<0.05	0.87
16:0 3-OH	0.47	<0.17	0.51	0.23
iso-17:0 2-OH	4.67	<0.17	<0.05	10.28
iso-17:0 3-OH	1.16	0.25	1.69	0.13
iso-15:0 DMA	2.42	8.99	4.19	0.08
iso-15:0 OAG	0.87	3.39	3.06	0.15
d18:0	0.68	0.17	<0.05	0.45
iso-d19:0	2.92	1.46	<0.05	1.96

Table 2 | Identified molecular species with relative AUCs given as per mil of the total AUC of all identified lipid molecular species determined separately for the positive and negative ionization mode. Lib. MW is calculated molecular weight of monoisotopic mass of respective lipid species. Abs.: absolute; Rel.: relative. See Supplemental Table 1 and 2 for details.

Compound Name	**Lib. MW**	Chemical Formula	Molecular species	m/z (calculated)	**Rel. abundance wt**	**Rel. abundance Δ0191**	**Rel. abundance $^{-}$MXAN_3748**	**Rel. abundance $^{-}$MXAN_1528**
Cer(D19:0/16:0)	**553.5**	C35H71NO3	$[M+HCOO]^-$	598.5	**1.1**	**5.7**	**0.0**	**2.0**
Cer(D19:0/i17:0 2-OH)	**583.6**	C36H73NO4	$[M+HCOO]^-$	628.6	**3.6**	**0.0**	**0.0**	**8.0**
Cer(D19:0/i17:0)	**567.6**	C36H73NO3	$[M+HCOO]^-$	612.6	**5.3**	**21.5**	**0.0**	**8.2**
CerPI(D19:0/16:0 2-OH)	**811.6**	C41H82NO12P	$[M-H]^-$	811.0	**1.8**	**0.0**	**0.0**	**3.8**
CerPI(D19:0/16:0)	**795.6**	C41H82NO11P	$[M-H]^-$	795.0	**0.5**	**4.9**	**0.0**	**0.9**
CerPI(D19:0/i17:0 2-OH)	**825.6**	C42H84NO12P	$[M-H]^-$	825.0	**5.3**	**0.0**	**0.0**	**10.9**
CerPI(D19:0/i17:0)	**809.6**	C42H84NO11P	$[M-H]^-$	809.0	**3.3**	**3.8**	**0.0**	**4.1**
PE(12:1/17:1);PE(13:1/16:1); PE(16:2/13:0);PE(14:1/15:1)	**645.4**	C34H64NO8P	$[M-H]^-$	644.8	**23.5**	**18.5**	**17.8**	**16.1**
PE(14:0/14:0);PE(13:0/15:0)	**635.5**	C33H66NO8P	$[M-H]^-$	634.8	**4.8**	**4.4**	**4.2**	**4.1**
PE(14:0/15:0)	**649.5**	C34H68NO8P	$[M-H]^-$	648.9	**27.6**	**28.0**	**23.5**	**25.0**
PE(14:1/14:1);PE(16:1/12:1)PE(15:1/13:1)	**631.4**	C33H62NO8P	$[M-H]^-$	630.8	**3.6**	**3.3**	**3.2**	**2.4**
PE(14:1/15:0);PE(16:1/13:0)	**647.5**	C34H66NO8P	$[M-H]^-$	646.8	**51.9**	**45.3**	**44.5**	**41.7**
PE(15:0/15:0)	**663.5**	C35H70NO8P	$[M-H]^-$	662.9	**157.0**	**142.8**	**131.3**	**124.8**
PE(15:0/17:0)	**691.5**	C37H74NO8P	$[M-H]^-$	690.9	**25.2**	**55.0**	**24.5**	**41.7**
PE(15:1/13:0)	**633.4**	C33H64NO8P	$[M-H]^-$	632.8	**7.1**	**5.3**	**5.2**	**5.7**
PE(15:1/15:0)	**661.5**	C35H68NO8P	$[M-H]^-$	660.9	**61.0**	**44.0**	**43.9**	**53.5**
PE(16:0/15:0);PE(14:0/17:0)	**677.5**	C36H72NO8P	$[M-H]^-$	676.9	**6.2**	**10.8**	**6.1**	**10.3**
PE(16:0/17:0)	**705.5**	C38H76NO8P	$[M-H]^-$	704.9	**1.9**	**2.2**	**3.4**	**4.6**
PE(16:1/15:0)	**675.5**	C36H70NO8P	$[M-H]^-$	674.9	**39.9**	**43.7**	**37.8**	**61.5**
PE(16:1/15:1);PE(17:1/14:1)	**673.5**	C36H68NO8P	$[M-H]^-$	672.9	**52.1**	**46.8**	**43.5**	**61.0**

PE(16:1/16:1);PE(17:2/15:0)	**687.5**	C37H70NO8P	$[M-H]^-$	686.9	**47.1**	**45.6**	**47.9**	**67.7**
PE(16:1/17:0)	**703.5**	C38H74NO8P	$[M-H]^-$	702.9	**15.8**	**19.2**	**26.7**	**37.2**
PE(16:2/14:1);PE(15:2/15:1)	**657.4**	C35H64NO8P	$[M-H]^-$	656.8	**16.8**	**14.5**	**13.8**	**10.5**
PE(16:2/15:1);PE(15:2/16:1);PE(17:2/14:1)	**671.5**	C36H66NO8P	$[M-H]^-$	670.8	**29.0**	**20.3**	**24.7**	**24.7**
PE(16:2/15:2);PE(17:2/14:2)	**669.4**	C36H64NO8P	$[M-H]^-$	668.8	**4.6**	**3.2**	**3.9**	**3.3**
PE(16:2/16:1); PE(17:2/15:1)	**685.5**	C37H68NO8P	$[M-H]^-$	684.9	**41.3**	**42.0**	**35.8**	**52.7**
PE(17:0/17:0)	**719.5**	C39H78NO8P	$[M-H]^-$	718.9	**4.4**	**5.2**	**14.5**	**10.2**
PE(17:1/15:0);PE(16:1/16:0);PE(15:1/17:0)	**689.5**	C37H72NO8P	$[M-H]^-$	688.9	**20.3**	**14.2**	**25.4**	**35.7**
PE(17:1/16:1)	**701.5**	C38H72NO8P	$[M-H]^-$	700.9	**9.9**	**10.9**	**14.0**	**15.1**
PE(17:1/17:0)	**717.5**	C39H76NO8P	$[M-H]^-$	716.9	**10.3**	**8.9**	**25.0**	**21.2**
PE(17:2/13:0);PE(16:1/14:1);PE(15:1/15:1)	**659.5**	C35H66NO8P	$[M-H]^-$	658.8	**32.8**	**27.4**	**28.4**	**29.9**
PE(17:2/15:2);PE(16:2/16:2)	**683.5**	C37H66NO8P	$[M-H]^-$	682.8	**26.4**	**25.0**	**22.9**	**23.7**
PE(17:2/16:1);PE(16:2/17:1)	**699.5**	C38H70NO8P	$[M-H]^-$	698.9	**30.6**	**29.6**	**38.1**	**38.4**
PE(17:2/16:2)	**697.5**	C38H68NO8P	$[M-H]^-$	696.9	**24.7**	**21.2**	**28.7**	**22.7**
PE(17:2/17:0); PE(17:1/17:1)	**715.5**	C39H74NO8P	$[M-H]^-$	714.9	**10.4**	**8.2**	**18.8**	**19.8**
PE(17:2/17:1)	**713.5**	C39H72NO8P	$[M-H]^-$	712.9	**10.0**	**6.7**	**15.4**	**12.3**
PE(17:2/17:2)	**711.5**	C39H70NO8P	$[M-H]^-$	710.9	**6.5**	**4.2**	**9.0**	**6.5**
PE(P-15:0/15:0)	**647.5**	C35H70NO7P	$[M-H]^-$	646.9	**117.0**	**122.5**	**132.1**	**8.0**
PE(P-15:0/17:0)	**675.5**	C37H74NO7P	$[M-H]^-$	674.9	**3.6**	**2.5**	**6.0**	**0.0**
PG(14:0/15:0)	**680.5**	C35H69O10P	$[M-H]^-$	679.9	**3.2**	**4.7**	**3.6**	**2.5**
PG(15:0/15:0)	**694.5**	C36H71O10P	$[M-H]^-$	693.9	**12.8**	**19.0**	**13.9**	**10.1**
PG(15:0/15:1);PG(16:1/14:0)	**692.5**	C36H69O10P	$[M-H]^-$	691.9	**4.4**	**5.1**	**3.9**	**3.8**
PG(15:0/16:1);PG(14:1/17:0)	**706.5**	C37H71O10P	$[M-H]^-$	705.9	**5.4**	**7.1**	**5.8**	**6.7**
PG(15:1/16:1;PG(15:0/16:2);PG(14:1/17:1);PG(14:0/17:2)	**704.5**	C37H69O10P	$[M-H]^-$	703.9	**1.7**	**3.8**	**1.7**	**2.2**
PG(16:0/16:1);PG(15:1/17:0);PG(15:0/17:1)	**720.5**	C38H73O10P	$[M-H]^-$	719.9	**4.3**	**6.6**	**6.0**	**6.9**
PG(16:0/17:0)	**736.5**	C39H77O10P	$[M-H]^-$	735.9	**1.2**	**2.2**	**2.8**	**2.1**

PG(16:1/16:1)	**718.5**	C38H71O10P	$[M-H]^-$	717.9	**6.1**	**10.0**	**7.5**	**10.5**
PG(16:1/16:2)	**716.5**	C38H69O10P	$[M-H]^-$	715.9	**2.2**	**2.6**	**2.8**	**3.3**
PG(17:0/16:1)	**734.5**	C39H75O10P	$[M-H]^-$	733.9	**6.4**	**12.1**	**15.3**	**12.3**
PG(17:0/17:0)	**750.5**	C40H79O10P	$[M-H]^-$	749.9	**1.8**	**2.5**	**6.1**	**3.0**
PG(17:0/17:1)	**748.5**	C40H77O10P	$[M-H]^-$	747.9	**2.3**	**4.0**	**6.7**	**3.4**
PG(17:1/16:1)	**732.5**	C39H73O10P	$[M-H]^-$	731.9	**4.2**	**3.0**	**3.7**	**3.2**
DG(15:0/15:0/0:0)	**540.5**	C33H64O5	$[M+NH_4]^+$	558.5	**16.9**	**8.2**	**12.4**	**6.8**
DG(31:1)	**552.5**	C34H64O5	$[M+NH_4]^+$	570.5	**6.4**	**2.5**	**3.7**	**6.1**
DG(32:0)	**568.5**	C35H68O5	$[M+NH_4]^+$	586.5	**2.4**	**2.3**	**3.0**	**2.2**
DG(32:2)	**564.5**	C35H64O5	$[M+NH_4]^+$	582.5	**6.3**	**2.3**	**4.2**	**4.0**
DG(33:0)	**582.5**	C36H70O5	$[M+NH_4]^+$	600.6	**1.0**	**0.9**	**1.0**	**0.9**
DG(33:1)	**580.5**	C36H68O5	$[M+NH_4]^+$	598.5	**3.2**	**2.1**	**3.9**	**3.7**
DG(33:2)	**578.5**	C36H66O5	$[M+NH_4]^+$	596.5	**4.5**	**0.0**	**1.6**	**3.8**
TG(15:0/15:0/15:0)	**764.7**	C48H92O6	$[M+NH_4]^+$	782.7	**94.8**	**111.8**	**84.4**	**46.0**
TG(38:1)	**666.6**	C41H78O6	$[M+NH_4]^+$	684.6	**1.7**	**2.9**	**1.7**	**2.2**
TG(39:0)	**680.6**	C42H80O6	$[M+NH_4]^+$	698.6	**5.5**	**9.5**	**7.6**	**4.9**
TG(39:1)	**678.6**	C42H78O6	$[M+NH_4]^+$	696.6	**2.5**	**4.3**	**2.4**	**3.4**
TG(40:1)	**692.6**	C43H80O6	$[M+NH_4]^+$	710.6	**6.0**	**9.4**	**5.9**	**6.8**
TG(40:2)	**690.6**	C43H78O6	$[M+NH_4]^+$	708.6	**3.2**	**3.9**	**2.8**	**4.4**
TG(41:1)	**706.6**	C44H82O6	$[M+NH_4]^+$	724.6	**10.4**	**13.7**	**11.1**	**10.9**
TG(41:2)	**704.6**	C44H80O6	$[M+NH_4]^+$	722.6	**5.0**	**6.8**	**5.1**	**6.1**
TG(41:3)	**702.6**	C44H78O6	$[M+NH_4]^+$	720.6	**2.1**	**2.5**	**1.9**	**2.6**
TG(42:1)	**722.6**	C45H86O6	$[M+NH_4]^+$	740.7	**20.3**	**25.3**	**20.6**	**18.9**
TG(42:2)	**718.6**	C45H82O6	$[M+NH_4]^+$	736.6	**15.7**	**13.7**	**13.8**	**15.2**
TG(43:0)	**736.7**	C46H88O6	$[M+NH_4]^+$	754.7	**33.3**	**44.1**	**34.7**	**17.6**
TG(43:1)	**734.6**	C46H86O6	$[M+NH_4]^+$	752.7	**23.9**	**25.5**	**22.5**	**18.7**

TG(43:2)	**732.6**	C46H84O6	$[M+NH_4]^+$	750.7	**22.2**	**22.3**	**19.2**	**22.2**
TG(43:3)	**730.6**	C46H82O6	$[M+NH_4]^+$	748.6	**9.4**	**8.1**	**6.5**	**9.3**
TG(44:0)	**750.7**	C47H90O6	$[M+NH_4]^+$	768.7	**35.6**	**25.0**	**37.2**	**19.5**
TG(44:1)	**748.7**	C47H88O6	$[M+NH_4]^+$	766.7	**40.6**	**45.5**	**35.8**	**32.8**
TG(44:2)	**746.6**	C47H86O6	$[M+NH_4]^+$	764.7	**32.4**	**27.4**	**24.0**	**28.1**
TG(44:3)	**744.6**	C47H84O6	$[M+NH_4]^+$	762.7	**18.4**	**11.5**	**10.8**	**16.2**
TG(44:4)	**742.6**	C47H82O6	$[M+NH_4]^+$	760.6	**4.2**	**3.8**	**2.4**	**4.4**
TG(45:1)	**762.7**	C48H90O6	$[M+NH_4]^+$	780.7	**49.9**	**45.0**	**40.4**	**41.2**
TG(45:2)	**760.7**	C48H88O6	$[M+NH_4]^+$	778.7	**34.7**	**32.1**	**29.0**	**37.4**
TG(45:3)	**758.6**	C48H86O6	$[M+NH_4]^+$	776.7	**25.0**	**18.8**	**16.5**	**27.1**
TG(45:4)	**758.6**	C48H86O6	$[M+NH_4]^+$	776.7	**9.3**	**6.6**	**5.4**	**10.0**
TG(46:0)	**779.7**	C49H95O6	$[M+NH_4]^+$	797.7	**37.3**	**43.9**	**33.7**	**24.7**
TG(46:1)	**776.7**	C49H92O6	$[M+NH_4]^+$	794.7	**52.6**	**56.3**	**48.6**	**57.7**
TG(46:2)	**774.7**	C49H90O6	$[M+NH_4]^+$	792.7	**45.4**	**43.2**	**38.5**	**51.9**
TG(46:3)	**772.7**	C49H88O6	$[M+NH_4]^+$	790.7	**27.3**	**18.9**	**20.3**	**29.2**
TG(47:0)	**792.7**	C50H96O6	$[M+NH_4]^+$	810.8	**48.8**	**59.8**	**60.4**	**41.1**
TG(47:1)	**790.7**	C50H94O6	$[M+NH_4]^+$	808.7	**36.2**	**33.6**	**40.7**	**46.0**
TG(47:2)	**774.7**	C49H90O6	$[M+NH_4]^+$	792.7	**33.4**	**32.2**	**32.5**	**50.9**
TG(47:3)	**786.7**	C50H90O6	$[M+NH_4]^+$	804.7	**21.0**	**17.5**	**17.5**	**9.7**
TG(47:4)	**784.7**	C50H88O6	$[M+NH_4]^+$	802.7	**13.1**	**8.7**	**8.7**	**21.0**
TG(48:0)	**806.7**	C51H98O6	$[M+NH_4]^+$	824.8	**15.7**	**18.2**	**23.8**	**21.4**
TG(48:1)	**802.7**	C51H94O6	$[M+NH_4]^+$	820.7	**21.0**	**27.6**	**29.7**	**36.8**
TG(48:2)	**802.7**	C51H94O6	$[M+NH_4]^+$	820.7	**17.9**	**19.2**	**23.1**	**36.0**
TG(48:3)	**800.7**	C51H92O6	$[M+NH_4]^+$	818.7	**17.8**	**12.7**	**15.0**	**26.5**
TG(48:4)	**798.7**	C51H90O6	$[M+NH_4]^+$	816.7	**10.1**	**7.6**	**9.6**	**17.0**
TG(49:0)	**820.8**	C52H100O6	$[M+NH_4]^+$	838.8	**14.8**	**20.1**	**29.2**	**19.7**

TG(49:1)	**818.7**	C52H98O6	$[M+NH_4]^+$	836.8	**12.0**	**12.4**	**20.1**	**21.7**
TG(49:2)	**816.7**	C52H96O6	$[M+NH_4]^+$	834.8	**11.1**	**11.2**	**16.8**	**24.0**
TG(50:0)	**834.8**	C53H102O6	$[M+NH_4]^+$	852.8	**4.5**	**5.5**	**8.7**	**8.2**
TG(50:1)	**832.8**	C53H100O6	$[M+NH_4]^+$	850.8	**6.0**	**6.8**	**11.2**	**12.6**
TG(51:0)	**848.8**	C54H104O6	$[M+NH_4]^+$	866.8	**3.0**	**3.8**	**8.8**	**4.9**
TG(51:1)	**846.8**	C54H102O6	$[M+NH_4]^+$	864.8	**3.0**	**2.8**	**5.4**	**5.1**
TG(52:0)	**862.8**	C55H106O6	$[M+NH_4]^+$	880.8	**1.1**	**0.5**	**0.8**	**0.9**

Table 3 | High resolution MS data of molecular sphingolipid species in lipid extracts of investigated strains. Lib.: library; RT: retention time; meas.: measured; calc.: calculated; err.: error.

Strain	Compound Name	Lib. RT [min]	Lib. MW	Chemical Formula	Chemical Formula Ion	Meas. m/z	Calc. m/z	err [ppm]
wt	**Cer(d19:0/16:0)**	8.215	553.5434	C35H71NO3	C36H72NO5	598.5454	598.54160	-6.3
	Cer(d19:0/i17:0 2-OH)	8.034	583.554	C36H73NO4	C37H74NO6	628.5564	628.5522	-6.7
	Cer(d19:0/i17:0)	8.305	567.559	C36H73NO3	C37H74NO5	612.5618	612.5572	-7.4
	PI-Cer(d19:0/16:0 2-OH)	7.425	811.5575	C41H82NO12P	C41H81NO12P	810.5457	810.5502	5.5
	PI-Cer(d19:0/16:0)	7.614	795.5625	C41H82NO11P	C41H81NO11P	794.56106	794.55527	-7.3
	PI-Cer(d19:0/i17:0 2-OH)	7.549	**825.5731**	C42H84NO12P	C42H83NO12P	824.5644	824.5658	1.7
	PI-Cer(d19:0/i17:0)	7.729	809.5782	C42H84NO11P	C42H83NO11P	808.5691	808.5709	2.2
Δ0191	**Cer(d19:0/16:0)**	8.215	553.5434	C35H71NO3	C36H72NO5	598.5415	598.5416	0.1
	Cer(d19:0/i17:0)	8.305	567.559	C36H73NO3	C36H74NO5	612.5579	612.5572	-1.1
	PI-Cer(d19:0/16:0)	7.614	795.5625	C41H82NO11P	C41H81NO11P	794.5525	794.5553	3.5
	PI-Cer(d19:0/i17:0)	7.729	809.5782	C42H84NO11P	C42H83NO11P	808.5714	808.5709	-0.6
ΔMXAN_1528	**Cer(d19:0/16:0)**	8.215	553.5434	C35H71NO3	C36H72NO3	598.5434	598.5416	-3.1
	Cer(d19:0/i17:0 2-OH)	8.034	583.554	C36H73NO4	C37H74NO4	628.5552	628.5522	-4.9
	Cer(d19:0/i17:0)	8.305	567.559	C36H73NO3	C37H74NO3	612.5608	612.5572	-5.7
	PI-Cer(d19:0/16:0 2-OH)	7.425	811.5575	C41H82NO12P	C41H81NO12P	810.5503	810.5502	-0.1
	PI-Cer(d19:0/16:0)	7.614	795.5625	C41H82NO11P	C41H81NO11P	794.556	794.5553	-0.9
	PI-Cer(d19:0/i17:0 2-OH)	7.549	**825.5731**	C42H84NO12P	C42H83NO12P	824.5661	824.5658	-0.4
	PI-Cer(d19:0/i17:0)	7.729	809.5782	C42H84NO11P	C42H83NO11P	808.5714	808.5709	-0.6

6.3.4 Experimental section

Materials, chemicals and analytical standards

Water (H_2O), methanol (MeOH), acetonitrile (ACN) and dichloromethane (DCM) (all Carl Roth) used as solvents and eluents were of LC-MS grade. HPLC grade ammonia (Sigma) was used as a 10% aqueous solution and formic and acetic acid (both Carl Roth) were of analytical grade. Glyceryl tristearate ~99% (TG(18:0/18:0/18:0); $[M+NH_4]^+$ = 908), rac-1,2-distearoylglycerol ~99% (GC) (DG(18:0/18:0/0:0); $[M+NH_4]^+$ = 642), 1,2-dipalmitoyl-*sn*-glycero-3-phosphoethanolamine, syn. >97% (PE(16:0/16:0); $[M-H]^-$ = 690), 1,2-distearoyl-*sn*-glycero-3-phospho-*rac*-(1-glycerol) sodium salt (PG(18:0/18:0); $[M-H]^-$ = 777), 1,2-dihexadecyl-*sn*-glycero-3-phosphoethanolamine ≥ 99.0% (TLC) (PE(*O*-16:0/*O*-16:0); $[M-H]^-$ = 663), 1,2-dipalmitoyl-*sn*-glycero-3-phosphate sodium salt ≥99% (Sigma) ((PA(16:0/16:0); $[M-H]^-$ = 648), oleoyl-L-α-lysophosphatidic acid (PA(18:1/0:0); $[M-H]^-$ = 436), ceramide from bovine brain >98% (TLC) (mainly Cer(d18:1/18:1)), L-α-phosphatidylinositol from *Glycine max* (mainly PI(18:0/18:0); $[M-H]^-$ = 833), sphingomyelin from chicken egg yolk, ~99% (mainly SM(d18:1/16:0); $[M+H]^+$ = 703) were obtained from Sigma as analytical standards for the development of the optimal eluent system and to produce reference spectra. Stock solutions with a concentration of 1 mg/ml were prepared of each standard in either DCM:MeOH:H_2O 65:35:8 (V/V/V) for the ceramides and phospholipids and ACN:DCM 1:1 (V/V) for the neutral lipids and diluted to a final concentration of 50 µM in MeOH:DCM:H_2O 70:35:5 (V/V/V) prior to HPLC-MS analysis.

Strains and growth conditions

Myxococcus xanthus DK1622 wild type and mutant strains were grown in 150 ml CTT media (10 g Casitone (Difco), 8 mM $MgSO_4$, 1mM K_2HPO_4, 10 mM Tris-HCl, pH 7.6) supplemented with 40 µg/ml Kanamycin when appropriate at 30 °C and 230 rpm on a rotary shaker in 1l conical flasks to an optical density of OD_{600} ~1.6. Strains Δ0191 and $^-$MXAN_3748 are published elsewhere (9). Strain $^-$MXAN_1528 bears a mutation in *elbD*, a multidomain enzyme involved in ether lipid biosynthesis (4).

Extraction procedures

Cells were harvested by centrifugation at 15,000 x g for 15 minutes at room temperature and washed ones with the same amount of distilled water.

A modified method of Bligh and Dyer (39) was applied to extract all lipids. The cell pellets were thoroughly resuspended in 2 ml of distilled water and 7.5 ml of a mixture of MeOH/DCM 2:1 (V/V) was added. After incubation for 20 minutes under agitation, phase separation was induced by the addition of 2.5 ml of DCM and water respectively. The lower phase was removed after centrifugation at 750 x g for 20 minutes and the cells and upper phase was reextracted twice with 2 ml DCM. The combined lower phases were filtered through solvent resistant 0.22 µM PTFE membrane filters and dried under a stream of nitrogen at 40 °C in weighted vials for exact determination of the extracts mass. For analysis the lipid extracts were dissolved in mixture of MeOH:DCM:H_2O (70:35:5 V/V/V) to a final concentration of 10 mg/ml.

GC-MS fatty acid methyl ester (FAME) analysis

Derivatization procedures and GC-MS conditions are described somewhere else (40).

HPLC-MS Conditions

For every data set 5 µl of lipid extract was separated on a ACQUITY UPLC^{TM} BEH C18 column (Waters) with a length of 50 mm an inner diameter of 2.1 mm and a mean particle size of 1.7 µM connected to a UltiMate 3000 (Thermo) HPLC system coupled to an amaZonX (Bruker) mass spectrometer at a constant flow rate of 0.6 ml/min a temperature of 50 °C and a binary gradient. Eluent A consisted of water/acetonitrile 50/50 (V/V) and solvent system B of acetonitrile/isopropanol 10/90 (V/V). Both eluents contained 10 mM NH_4AcO as a buffering additive and were set to a pH of 5.5 using formic acid in order to maintain the analytes in the same charge state during the separation process. The gradient was programmed as follows: Start at 1% B, increased to 95% within 10 minutes in a linear manner, hold at 95% for 2 minutes and reequilibration was performed for 2 minutes at 1% B.

The ESI parameters were: capillary voltage: +4.5 kV (negative mode); -4.5kV (positive mode); end plate offset: -500.0 V; capillary exit: -140.0 V (negative mode) +140.0 V (positive mode); nitrogen flow: 11.83 l/min; drying gas temperature: 300 °C; nebulizing gas pressure: 44.00 psi.

Both, UPLC-MS and UPLC-MS/MS were recorded in the same run using the “ultra” scan mode with a trap drive of 64.3 (negative mode) and 53.3 (positive mode) respectively, a scan speed of 25,000 *m/z* per second and the mass resolution was 0.6 *m/z* over a range of

100-1000 *m/z* whereas one spectrum was an average of 7 scans in the MS mode and 3 scans in the MS^2 mode. For autoMS/MS fragmentation an absolute threshold of 25000 cts was chosen and already fragmented precursor ions were excluded for further fragmentation after two spectra for 0.5 minutes. The isolation width was 1.5 *m/z*.

Data Processing

For the visualization, processing and analysis of the HPLC-MS data the programs DataAnalysis Version 4.0 SP 2 (Build 274, Bruker) was used in combination with LibraryEditor Version 4.0 SP 2 (Build 274, Bruker) and Excel 2010 (Version 14.0.7106.5003 (32-Bit).

In a first step a LibraryEditor library was established to enable automatic identification of lipid species from the lipid extracts. MS^2 spectra that were acquired during the runs automatically were extracted from the dataset using the "Compound-autoMS(n)" algorithm with the following settings: intensity threshold positive: 1,000,000; intensity threshold negative 10,000; Maximum number of compounds: 350; retention time window (min): 0.25; spectrum type: line spectra only; background subtraction: none. Lipid species were identified from the MS^2 spectra and added to the library together with their retention times. This library was applied to all HPLC-MS runs using the "Identify Mass Spectra" function of Data Analysis with the following settings: Desired score: 900; Minimum score: 600; minimum parameter matching score: 250: maximum number of spectra: 1; accepted retention time deviation: 0.1 minutes; maximum retention time deviation: 0.2 minutes.

For the calculation of the relative % of lipid species Extracted Ion Chromatograms (EICs) were created for every single precursor ion of the identified lipid species. For better peak detection all chromatographic traces were smoothed using a Gaussian algorithm (1 pt width, 2 cycles). Those EICs from the identified lipid species were integrated by applying the "Compounds-Chromatograms" algorithm with the following settings: S/N threshold: 5; Area threshold: 10%; Intensity threshold: 10000 for the negative ion mode and 1000000 for the positive ion mode; skim ratio: 0; smoothing width: 1. Charts containing the identified autoMSn compounds and the AUCs of the EICs were exported into Excel charts. Those charts were manually inspected for false identifications and missing EIC peak integrations.

Peak areas of PEs, PGs, PI-Cers, the formate adducts of Cers and pPEs from the HPLC-MS runs in the negative ion mode and the DGs and TGs in the positive ion mode were separately summed up and normalized to 1000, and the peak area of each individual EIC peak was calculated as per mil of the total integral of all peak (see **Supplemental Table 2** and **3** for the complete data set and **Table 2** for a summary).

For the visualization of the base peak full scan UPLC-ESI-MS chromatograms and plotting the lipid profiles MATLAB Release 2013b (**The MathWorks, Inc., Natick, Massachusetts, United States**) was used. The base peak full scan UPLC-ESI-MS chromatograms were created by using the functions "meshgrid" and" surf". The "stem3" function was applied to create the 3D lipid profiles.

Identification of lipids by MS

The experiments of the positive ionization and the negative ionization mode were combined in order to identify a maximal possible number of lipids. The above mentioned standards were used in order to evaluate the chromatographic and fragmentation behavior of those lipid species. Those information plus the reference spectra and software tools from www.lipidmaps.org were used as the bases for the MS based structure elucidation of the lipid species. The fragmentation behavior of ceramide phosphoinositols (PI-Cers) have been described previously (41, 42). HPLC-ESI-MS data for the identification of structure elucidation of glycerophosphoglycerols (PGs), glycerophosphoethanolamines (PEs) are already available as well (25, 43). The presence of PGs, PEs, N-acylsphinganines (Cers) as well as the presence of distinctive α-hydroxylated fatty acids together with the complete fatty acid profiles of the investigated strains have been published (9, 11, 13, 14).

In the negative ion mode, PGs and PEs were detected as $[M-H]^-$ ions and Cers, both hydroxylated and non-hydroxylated, as $[M+HCOO]^-$ ions respectively.

PEs, Cers (dihydroceramides), diacylglycerols (DAGs) and triacylglycerols (TAGs) were detected in the positive ion mode, the former two as $[M+H]^+$ ions and the latter two as $[M+NH_4]^+$ Ions.

In general, isobaric molecular species could not be resolved by HPLC so that they yielded one MS^2 spectra (see **Supplemental Table 2** and **3, Figure 3-8**)

For the creation of the lipid profiles only the integrals from the negative ion mode for the PEs, PGs, PI-Cers and Cers and from the positive ion mode for the DGs and TGs were used. PE and Cer ions were also clearly detectable in the positive ion mode but not used for the creation of lipid profiles.

High resolution MS readings

Determination of the exact mass of ceramide molecular species from lipid extracts was carried out using a Dionex Ultimate 3000 RSLC coupled to a Bruker micrOTOF-Q II equipped with an electrospray ionization source set to negative ionization mode. HPLC settings were identical to those described above though the column bed was 100 mm in length and the gradient length was doubled to 20 min accordingly. The mass spectrometer was calibrated using a sodium formate calibrant solution (10 mM). MS data were acquired within the mass range of 200-2000 *m/z*.

Nomenclature

For the sake of uniformity and comprehensibility we used the nomenclature of the LIPID MAPS Lipid Classification System (see www.lipidmaps.org/data/classification/LM_classification_exp.php) for the names and abbreviations.

6.3.5 Supplemental data

Supplemental Table 1 | Identified molecular species with relative AUCs given as per mil of the total AUC of all identified lipid molecular species determined separately for the positive and negative ionization mode. “Difference” is relative AUC differences in per mil between the mutant and wild type strain and basis for the plots in **Figure 12**. Lib. MW is calculated molecular weight of monoisotopic mass of respective lipid species. Retention times are those determined by the softwares peak detection algorithm. Abs.: absolute; Rel.: relative.

Compound Name	Lib. MW	Chemical Formula	Molecular species	m/z (calculated)	RT [min] wt	RT [min] Δ0191	RT [min] - MXAN_3748	RT [min] - MXAN_1528	Abs. abundance wt	Abs. abundance Δ0191	Abs. abundance - MXAN_3748	Abs. abundance -MXAN_1528	Rel. abundance wt	Rel. abundance Δ0191	Rel. abundance - MXAN_3748	Rel. abundance - MXAN_1528	Difference Δ0191 vs. wt	Difference - MXAN_3748 vs. wt	Difference MXAN_1528 vs. wt
Cer(D19:0/16:0)	**553.5434**	C35H71NO3	$[M+HCOO]^-$	598.541603	**8.211**	**8.212**	-	**8.213**	38573964	204217681	0	71442906	**1.1**	**5.7**	**0.0**	**2.0**	**4.6**	**-1.1**	**0.9**
Cer(D19:0/i17:0 2-OH)	**583.554**	C36H73NO4	$[M+HCOO]^-$	628.552203	**8.058**	-	-	**8.052**	125260931	0	0	282171289	**3.6**	**0.0**	**0.0**	**8.0**	**-3.6**	**-3.6**	**4.4**
Cer(D19:0/i17:0)	**567.559**	C36H73NO3	$[M+HCOO]^-$	612.557203	**8.329**	**8.341**	-	**8.341**	181968237	770054191	0	288097431	**5.3**	**21.5**	**0.0**	**8.2**	**16.2**	**-5.3**	**2.9**
CerPI(D19:0/16:0 2-OH)	**811.5575**	C41H82NO12P	$[M-H]^-$	810.950224	**7.377**	-	-	**7.383**	62927020	0	0	135656829	**1.8**	**0.0**	**0.0**	**3.8**	**-1.8**	**-1.8**	**2.0**
CerPI(D19:0/16:0)	**795.5625**	C41H82NO11P	$[M-H]^-$	794.955224	**7.566**	**7.596**	-	**7.62**	17139969	176243578	0	32531918	**0.5**	**4.9**	**0.0**	**0.9**	**4.4**	**-0.5**	**0.4**
CerPI(D19:0/i17:0 2-OH)	**825.5731**	C42H84NO12P	$[M-H]^-$	824.965824	**7.541**	-	-	**7.533**	182535791	0	0	386420605	**5.3**	**0.0**	**0.0**	**10.9**	**-5.3**	**-5.3**	**5.7**
CerPI(D19:0/i17:0)	**809.5782**	C42H84NO11P	$[M-H]^-$	808.970924	**7.738**	**7.739**	-	**7.714**	115192371	135047884	0	143494765	**3.3**	**3.8**	**0.0**	**4.1**	**0.4**	**-3.3**	**0.7**
PE(12:1/17:1);PE(13:1/16:1); PE(16:2/13:0);PE(14:1/15:1)	**645.437**	C34H64NO8P	$[M-H]^-$	644.829724	**6.56**	**6.559**	**6.578**	**6.564**	810396868	664715107	631044316	569010734	**23.5**	**18.5**	**17.8**	**16.1**	**-5.0**	**-5.7**	**-7.4**
PE(14:0/14:0);PE(13:0/15:0)	**635.4526**	C33H66NO8P	$[M-H]^-$	634.845324	**7.054**	**7.061**	**7.061**	**7.059**	164325035	159112512	147459117	144067971	**4.8**	**4.4**	**4.2**	**4.1**	**-0.3**	**-0.6**	**-0.7**
PE(14:0/15:0)	**649.4683**	C34H68NO8P	$[M-H]^-$	648.861024	**7.359**	**7.361**	**7.369**	**7.371**	950674061	1006002189	835126931	884067144	**27.6**	**28.0**	**23.5**	**25.0**	**0.5**	**-4.0**	**-2.5**
PE(14:1/14:1);PE(16:1/12:1) PE(15:1/13:1)	**631.4213**	C33H62NO8P	$[M-H]^-$	630.814024	**6.341**	**6.352**	**6.345**	**6.275**	124381724	116914252	114531371	83575005	**3.6**	**3.3**	**3.2**	**2.4**	**-0.3**	**-0.4**	**-1.2**
PE(14:1/15:0);PE(16:1/13:0)	**647.4526**	C34H66NO8P	$[M-H]^-$	646.845324	**7.005**	**7.013**	**7.013**	**7.015**	1791131504	1626740279	1579244971	1470401803	**51.9**	**45.3**	**44.5**	**41.7**	**-6.6**	**-7.4**	**-10.3**
PE(15:0/15:0)	**663.4839**	C35H70NO8P	$[M-H]^-$	662.876624	**7.573**	**7.553**	**7.562**	**7.567**	5414894594	5125094213	4659376458	4403140441	**157.0**	**142.8**	**131.3**	**124.8**	**-14.2**	**-25.7**	**-32.3**
PE(15:0/17:0)	**691.5152**	C37H74NO8P	$[M-H]^-$	690.907924	**7.95**	**8.066**	**7.937**	**8.033**	868124953	1974453996	867708251	1470416292	**25.2**	**55.0**	**24.5**	**41.7**	**29.9**	**-0.7**	**16.5**
PE(15:1/13:0)	**633.437**	C33H64NO8P	$[M-H]^-$	632.829724	**6.726**	**6.749**	**6.743**	**6.73**	246197897	189210000	185423979	202489533	**7.1**	**5.3**	**5.2**	**5.7**	**-1.9**	**-1.9**	**-1.4**
PE(15:1/15:0)	**661.4683**	C35H68NO8P	$[M-H]^-$	660.861024	**7.222**	**7.222**	**7.229**	**7.241**	2102735263	1580347044	1556018154	1887907909	**61.0**	**44.0**	**43.9**	**53.5**	**-16.9**	**-17.1**	**-7.5**
PE(16:0/15:0);PE(14:0/17:0)	**677.4996**	C36H72NO8P	$[M-H]^-$	676.892324	**7.824**	**7.905**	**7.812**	**7.816**	212375183	386268599	216935819	363275766	**6.2**	**10.8**	**6.1**	**10.3**	**4.6**	**0.0**	**4.1**
PE(16:0/17:0)	**705.5309**	C38H76NO8P	$[M-H]^-$	704.923624	**8.149**	**8.14**	**8.167**	**8.162**	65380218	79529515	119361108	162972795	**1.9**	**2.2**	**3.4**	**4.6**	**0.3**	**1.5**	**2.7**
PE(16:1/15:0)	**675.4839**	C36H70NO8P	$[M-H]^-$	674.876624	**7.406**	**7.414**	**7.416**	**7.434**	1377180076	1569337791	1340973228	2169500686	**39.9**	**43.7**	**37.8**	**61.5**	**3.8**	**-2.1**	**21.5**
PE(16:1/15:1);PE(17:1/14:1)	**673.4683**	C36H68NO8P	$[M-H]^-$	672.861024	**7.107**	**7.111**	**7.118**	**7.117**	1794938789	1678724801	1541423855	2154360414	**52.1**	**46.8**	**43.5**	**61.0**	**-5.3**	**-8.6**	**9.0**
PE(16:1/16:1);PE(17:2/15:0)	**687.4839**	C37H70NO8P	$[M-H]^-$	686.876624	**7.28**	**7.282**	**7.281**	**7.297**	1623140234	1636361875	1698284066	2390970569	**47.1**	**45.6**	**47.9**	**67.7**	**-1.5**	**0.8**	**20.7**
PE(16:1/17:0)	**703.5152**	C38H74NO8P	$[M-H]^-$	702.907924	**7.828**	**7.841**	**7.831**	**7.855**	545370894	689927540	947633173	1314275214	**15.8**	**19.2**	**26.7**	**37.2**	**3.4**	**10.9**	**21.4**
PE(16:2/14:1);PE(15:2/15:1)	**657.437**	C35H64NO8P	$[M-H]^-$	656.829724	**6.507**	**6.52**	**6.52**	**6.528**	578937509	519176277	488156001	370032503	**16.8**	**14.5**	**13.8**	**10.5**	**-2.3**	**-3.0**	**-6.3**

PE(16:2/15:1);PE(15:2/16:1); PE(17:2/14:1)	**671.4526**	C36H66NO8P	$[M-H]^-$	670.845324	**6.735**	**6.736**	**6.743**	**6.75**	999731203	728609751	876593798	871968010	**29.0**	**20.3**	**24.7**	**24.7**	**-8.7**	**-4.3**	**-4.3**
PE(16:2/15:2);PE(17:2/14:2)	**669.437**	C36H64NO8P	$[M-H]^-$	668.829724	**6.369**	**6.381**	**6.377**	**6.382**	158186419	113487112	136907428	117189061	**4.6**	**3.2**	**3.9**	**3.3**	**-1.4**	**-0.7**	**-1.3**
PE(16:2/16:1); PE(17:2/15:1)	**685.4683**	C37H68NO8P	$[M-H]^-$	684.861024	**6.976**	**6.983**	**6.986**	**6.987**	1424895926	1507045387	1269109284	1859425447	**41.3**	**42.0**	**35.8**	**52.7**	**0.7**	**-5.5**	**11.4**
PE(17:0/17:0)	**719.5465**	C39H78NO8P	$[M-H]^-$	718.939224	**8.278**	**8.28**	**8.285**	**8.279**	152306862	184944136	514979986	359363966	**4.4**	**5.2**	**14.5**	**10.2**	**0.7**	**10.1**	**5.8**
PE(17:1/15:0);PE(16:1/16:0); PE(15:1/17:0)	**689.4996**	C37H72NO8P	$[M-H]^-$	688.892324	**7.664**	**7.659**	**7.668**	**7.686**	700696438	509217301	902071627	1261116444	**20.3**	**14.2**	**25.4**	**35.7**	**-6.1**	**5.1**	**15.4**
PE(17:1/16:1)	**701.4996**	C38H72NO8P	$[M-H]^-$	700.892324	**7.432**	**7.441**	**7.442**	**7.456**	340535300	392061495	495101376	533363234	**9.9**	**10.9**	**14.0**	**15.1**	**1.1**	**4.1**	**5.2**
PE(17:1/17:0)	**717.5309**	C39H76NO8P	$[M-H]^-$	716.923624	**7.993**	**7.964**	**8.021**	**8.029**	353982545	317777803	886639475	748981748	**10.3**	**8.9**	**25.0**	**21.2**	**-1.4**	**14.7**	**11.0**
PE(17:2/13:0);PE(16:1/14:1); PE(15:1/15:1)	**659.4526**	C35H66NO8P	$[M-H]^-$	658.845324	**6.865**	**6.87**	**6.873**	**6.877**	1130534586	982907560	1005818351	1053637274	**32.8**	**27.4**	**28.4**	**29.9**	**-5.4**	**-4.4**	**-2.9**
PE(17:2/15:2);PE(16:2/16:2)	**683.4526**	C37H66NO8P	$[M-H]^-$	682.845324	**6.651**	**6.656**	**6.661**	**6.66**	909436000	897681601	814084054	835921475	**26.4**	**25.0**	**22.9**	**23.7**	**-1.4**	**-3.4**	**-2.7**
PE(17:2/16:1);PE(16:2/17:1)	**699.4839**	C38H70NO8P	$[M-H]^-$	698.876624	**7.165**	**7.163**	**7.175**	**7.179**	1053628563	1063820821	1352393140	1355662772	**30.6**	**29.6**	**38.1**	**38.4**	**-0.9**	**7.6**	**7.9**
PE(17:2/16:2)	**697.4683**	C38H68NO8P	$[M-H]^-$	696.861024	**6.854**	**6.857**	**6.864**	**6.864**	851518593	761456859	1018784117	799408501	**24.7**	**21.2**	**28.7**	**22.7**	**-3.5**	**4.0**	**-2.0**
PE(17:2/17:0); PE(17:1/17:1)	**715.5152**	C39H74NO8P	$[M-H]^-$	714.907924	**7.737**	**7.772**	**7.776**	**7.734**	359852616	293071420	667362870	698308325	**10.4**	**8.2**	**18.8**	**19.8**	**-2.3**	**8.4**	**9.4**
PE(17:2/17:1)	**713.4996**	C39H72NO8P	$[M-H]^-$	712.892324	**7.44**	**7.448**	**7.451**	**7.46**	346337222	241616370	545866676	434789338	**10.0**	**6.7**	**15.4**	**12.3**	**-3.3**	**5.3**	**2.3**
PE(17:2/17:2)	**711.4839**	C39H70NO8P	$[M-H]^-$	710.876624	**7.039**	**7.047**	**7.052**	**7.053**	225294688	148984048	320258022	227673540	**6.5**	**4.2**	**9.0**	**6.5**	**-2.4**	**2.5**	**-0.1**
PE(P-15:0/15:0)	**647.489**	C35H70NO7P	$[M-H]^-$	646.881724	**7.75**	**7.765**	**7.777**	**7.745**	4034959183	4393949158	4687887430	284038480	**117.0**	**122.5**	**132.1**	**8.0**	**5.4**	**15.1**	**-109.0**
PE(P-15:0/17:0)	**675.5203**	C37H74NO7P	$[M-H]^-$	674.913024	**8.105**	**8.109**	**8.118**	-	124233827	89441967	211950113	0	**3.6**	**2.5**	**6.0**	**0.0**	**-1.1**	**2.4**	**-3.6**
PG(14:0/15:0)	**680.4628**	C35H69O10P	$[M-H]^-$	679.855524	**7.026**	**7.024**	**7.025**	**7.037**	108895211	168209440	126235411	87901696	**3.2**	**4.7**	**3.6**	**2.5**	**1.5**	**0.4**	**-0.7**
PG(15:0/15:0)	**694.4785**	C36H71O10P	$[M-H]^-$	693.871224	**7.204**	**7.206**	**7.204**	**7.218**	440727551	682355973	494120026	355797884	**12.8**	**19.0**	**13.9**	**10.1**	**6.2**	**1.1**	**-2.7**
PG(15:0/15:1);PG(16:1/14:0)	**692.4628**	C36H69O10P	$[M-H]^-$	691.855524	**6.895**	**6.889**	**6.887**	**6.9**	150686728	181951876	139439791	134647300	**4.4**	**5.1**	**3.9**	**3.8**	**0.7**	**-0.4**	**-0.6**
PG(15:0/16:1);PG(14:1/17:0)	**706.4785**	C37H71O10P	$[M-H]^-$	705.871224	**7.112**	**7.101**	**7.098**	**7.131**	185823105	254478885	206620577	237053139	**5.4**	**7.1**	**5.8**	**6.7**	**1.7**	**0.4**	**1.3**
PG(15:1/16:1;PG(15:0/16:2); PG(14:1/17:1);PG(14:0/17:2)	**704.4628**	C37H69O10P	$[M-H]^-$	703.855524	**6.769**	**6.79**	**6.785**	**6.763**	59143503	137009336	60397212	77462640	**1.7**	**3.8**	**1.7**	**2.2**	**2.1**	**0.0**	**0.5**
PG(16:0/16:1);PG(15:1/17:0); PG(15:0/17:1)	**720.4941**	C38H73O10P	$[M-H]^-$	719.886824	**7.374**	**7.379**	**7.375**	**7.404**	147531945	237785930	214396558	243734339	**4.3**	**6.6**	**6.0**	**6.9**	**2.3**	**1.8**	**2.6**
PG(16:0/17:0)	**736.5254**	C39H77O10P	$[M-H]^-$	735.918124	**7.864**	**7.884**	**7.892**	**7.9**	39778700	79225045	100975182	75649268	**1.2**	**2.2**	**2.8**	**2.1**	**1.1**	**1.7**	**1.0**
PG(16:1/16:1)	**718.4785**	C38H71O10P	$[M-H]^-$	717.871224	**6.951**	**6.953**	**6.952**	**6.954**	209390448	359991181	267747214	370007117	**6.1**	**10.0**	**7.5**	**10.5**	**4.0**	**1.5**	**4.4**
PG(16:1/16:2)	**716.4628**	C38H69O10P	$[M-H]^-$	715.855524	**6.612**	**6.653**	**6.637**	**6.613**	75745121	92949097	100852772	117061862	**2.2**	**2.6**	**2.8**	**3.3**	**0.4**	**0.6**	**1.1**
PG(17:0/16:1)	**734.5098**	C39H75O10P	$[M-H]^-$	733.902524	**7.576**	**7.571**	**7.574**	**7.565**	222150012	432997682	541628129	435815295	**6.4**	**12.1**	**15.3**	**12.3**	**5.6**	**8.8**	**5.9**
PG(17:0/17:0)	**750.5411**	C40H79O10P	$[M-H]^-$	749.933824	**8.019**	**8.028**	**8.025**	**8.024**	61232182	90111776	216890413	107052343	**1.8**	**2.5**	**6.1**	**3.0**	**0.7**	**4.3**	**1.3**
PG(17:0/17:1)	**748.5254**	C40H77O10P	$[M-H]^-$	747.918124	**7.691**	**7.694**	**7.723**	**7.686**	79632676	144109298	238252735	118792876	**2.3**	**4.0**	**6.7**	**3.4**	**1.7**	**4.4**	**1.1**
PG(17:1/16:1)	**732.4941**	C39H73O10P	$[M-H]^-$	731.886824	**7.116**	**7.116**	**7.106**	**7.132**	143469064	108067120	132045509	111332416	**4.2**	**3.0**	**3.7**	**3.2**	**-1.1**	**-0.4**	**-1.0**
DG(15:0/15:0/0:0)	**540.4754**	C33H64O5	$[M+NH_4]^+$	558.509226	**8.086**	**8.097**	**8.084**	**8.091**	4121220545	4017667278	4423957409	2203147261	**16.9**	**8.2**	**12.4**	**6.8**	**-8.7**	**-4.5**	**-10.1**
DG(31:1)	**552.4754**	C34H64O5	$[M+NH_4]^+$	570.509226	**7.987**	**7.976**	**7.972**	**7.949**	1570472455	1226915558	1301125173	1970133440	**6.4**	**2.5**	**3.7**	**6.1**	**-3.9**	**-2.8**	**-0.4**
DG(32:0)	**568.5067**	C35H68O5	$[M+NH_4]^+$	586.540526	**8.442**	**8.446**	**8.447**	**8.441**	575571455	1116232799	1054715297	723446245	**2.4**	**2.3**	**3.0**	**2.2**	**-0.1**	**0.6**	**-0.1**
DG(32:2)	**564.4754**	C35H64O5	$[M+NH_4]^+$	582.509226	**7.857**	**7.849**	**7.876**	**7.852**	1538850492	1114034211	1478714210	1305559855	**6.3**	**2.3**	**4.2**	**4.0**	**-4.0**	**-2.2**	**-2.3**
DG(33:0)	**582.5223**	C36H70O5	$[M+NH_4]^+$	600.556126	**8.651**	**8.644**	**8.648**	**8.648**	233105253	423982286	347126229	279435072	**1.0**	**0.9**	**1.0**	**0.9**	**-0.1**	**0.0**	**-0.1**
DG(33:1)	**580.5067**	C36H68O5	$[M+NH_4]^+$	598.540526	**8.341**	**8.338**	**8.33**	**8.336**	773036816	1012754882	1392989382	1194113584	**3.2**	**2.1**	**3.9**	**3.7**	**-1.1**	**0.7**	**0.5**
DG(33:2)	**578.491**	C36H66O5	$[M+NH_4]^+$	596.524826	**8.024**	-	**8.018**	**8.109**	1105621336	0	572214408	1226079075	**4.5**	**0.0**	**1.6**	**3.8**	**-4.5**	**-2.9**	**-0.8**
TG(15:0/15:0/15:0)	**764.6894**	C48H92O6	$[M+NH_4]^+$	782.723226	**9.766**	**9.753**	**9.758**	**9.762**	23094843874	54792088912	30039602740	14940467524	**94.8**	**111.8**	**84.4**	**46.0**	**17.0**	**-10.4**	**-48.9**
TG(38:1)	**666.5798**	C41H78O6	$[M+NH_4]^+$	684.613626	**8.853**	**8.847**	**8.829**	**8.853**	426152868	1429599181	610804520	716972943	**1.7**	**2.9**	**1.7**	**2.2**	**1.2**	**0.0**	**0.5**

TG(39:0)	**680.5955**	C42H80O6	$[M+NH_4]^+$	698.629326	**9.174**	**9.156**	**9.168**	**9.17**	1351552037	4650697044	2709149396	1582903124	**5.5**	**9.5**	**7.6**	**4.9**	**3.9**	**2.1**	**-0.7**
TG(39:1)	**678.5798**	C42H78O6	$[M+NH_4]^+$	696.613626	**8.997**	**8.986**	**8.988**	**8.998**	617477839	2110955429	838467610	1089411962	**2.5**	**4.3**	**2.4**	**3.4**	**1.8**	**-0.2**	**0.8**
TG(40:1)	**692.5955**	C43H80O6	$[M+NH_4]^+$	710.629326	**9.107**	**9.092**	**9.1**	**9.096**	1464559396	4617695265	2105829344	2196280232	**6.0**	**9.4**	**5.9**	**6.8**	**3.4**	**-0.1**	**0.7**
TG(40:2)	**690.5798**	C43H78O6	$[M+NH_4]^+$	708.613626	**8.914**	**8.907**	**8.909**	**8.903**	780164182	1886370294	1003825444	1421183627	**3.2**	**3.9**	**2.8**	**4.4**	**0.6**	**-0.4**	**1.2**
TG(41:1)	**706.61114**	C44H82O6	$[M+NH_4]^+$	724.644966	**9.236**	**9.223**	**9.229**	**9.234**	2543241843	6690435497	3955530120	3530263770	**10.4**	**13.7**	**11.1**	**10.9**	**3.2**	**0.7**	**0.4**
TG(41:2)	**704.5955**	C44H80O6	$[M+NH_4]^+$	722.629326	**9.047**	**9.044**	**9.043**	**9.038**	1218786468	3318902410	1823721061	1991542027	**5.0**	**6.8**	**5.1**	**6.1**	**1.8**	**0.1**	**1.1**
TG(41:3)	**702.5798**	C44H78O6	$[M+NH_4]^+$	720.613626	**8.85**	**8.839**	**8.838**	**8.839**	512817239	1242992803	661133147	855411274	**2.1**	**2.5**	**1.9**	**2.6**	**0.4**	**-0.2**	**0.5**
TG(42:1)	**722.6424**	C45H86O6	$[M+NH_4]^+$	740.676226	**9.32**	**9.304**	**9.311**	**9.304**	4935623974	12393472902	7325580217	6137497600	**20.3**	**25.3**	**20.6**	**18.9**	**5.0**	**0.3**	**-1.4**
TG(42:2)	**718.6111**	C45H82O6	$[M+NH_4]^+$	736.644926	**9.189**	**9.16**	**9.208**	**9.168**	3812841732	6725958949	4900134854	4934695094	**15.7**	**13.7**	**13.8**	**15.2**	**-1.9**	**-1.9**	**-0.5**
TG(43:0)	**736.6581**	C46H88O6	$[M+NH_4]^+$	754.691926	**9.576**	**9.567**	**9.569**	**9.582**	8101377876	21581166153	12360541086	5710029151	**33.3**	**44.1**	**34.7**	**17.6**	**10.8**	**1.5**	**-15.7**
TG(43:1)	**734.6424**	C46H86O6	$[M+NH_4]^+$	752.676226	**9.438**	**9.427**	**9.423**	**9.423**	5809590103	12482769381	8005897829	6090055112	**23.9**	**25.5**	**22.5**	**18.7**	**1.6**	**-1.4**	**-5.1**
TG(43:2)	**732.6268**	C46H84O6	$[M+NH_4]^+$	750.660626	**9.265**	**9.255**	**9.258**	**9.26**	5401867195	10947414707	6830093388	7224112185	**22.2**	**22.3**	**19.2**	**22.2**	**0.2**	**-3.0**	**0.0**
TG(43:3)	**730.6111**	C46H82O6	$[M+NH_4]^+$	748.644926	**9.109**	**9.091**	**9.101**	**9.099**	2294365269	3968696972	2313365326	3012429665	**9.4**	**8.1**	**6.5**	**9.3**	**-1.3**	**-2.9**	**-0.2**
TG(44:0)	**750.6737**	C47H90O6	$[M+NH_4]^+$	768.707526	**9.696**	**9.684**	**9.687**	**9.694**	8682156958	12242499864	13244908539	6342002478	**35.6**	**25.0**	**37.2**	**19.5**	**-10.7**	**1.6**	**-16.1**
TG(44:1)	**748.6581**	C47H88O6	$[M+NH_4]^+$	766.691926	**9.532**	**9.516**	**9.514**	**9.521**	9881382140		12726099355	10672106327	**40.6**	**45.5**	**35.8**	**32.8**	**4.9**	**-4.8**	**-7.7**
TG(44:2)	**746.6424**	C47H86O6	$[M+NH_4]^+$	764.676226	**9.377**	**9.361**	**9.366**	**9.363**	7888909386	13446682082	8557753672	9128781266	**32.4**	**27.4**	**24.0**	**28.1**	**-4.9**	**-8.3**	**-4.3**
TG(44:3)	**744.6268**	C47H84O6	$[M+NH_4]^+$	762.660626	**9.223**	**9.213**	**9.214**	**9.214**	4484202070	5620922973	3840680531	5263571742	**18.4**	**11.5**	**10.8**	**16.2**	**-6.9**	**-7.6**	**-2.2**
TG(44:4)	**742.6111**	C47H82O6	$[M+NH_4]^+$	760.644926	**9.052**	**9.025**	**9.04**	**9.044**	1025121431	1857081487	851164205	1424167992	**4.2**	**3.8**	**2.4**	**4.4**	**-0.4**	**-1.8**	**0.2**
TG(45:1)	**762.6737**	C48H90O6	$[M+NH_4]^+$	780.707526	**9.63**	**9.62**	**9.615**	**9.627**	12154841933	22048528241	14365241109	13405805736	**49.9**	**45.0**	**40.4**	**41.2**	**-4.9**	**-9.5**	**-8.7**
TG(45:2)	**760.6581**	C48H88O6	$[M+NH_4]^+$	778.691926	**9.47**	**9.457**	**9.462**	**9.465**	8452882941	15710861847	10327580708	12157425984	**34.7**	**32.1**	**29.0**	**37.4**	**-2.6**	**-5.7**	**2.7**
TG(45:3)	**758.6424**	C48H86O6	$[M+NH_4]^+$	776.676226	**9.311**	**9.295**	**9.299**	**9.299**	6096598003	9218368560	5875184648	8797723300	**25.0**	**18.8**	**16.5**	**27.1**	**-6.2**	**-8.5**	**2.0**
TG(45:4)	**758.6424**	C48H86O6	$[M+NH_4]^+$	776.676226	**9.165**	**9.147**	**9.149**	**9.153**	2269739943	3210820468	1907284518	3246704461	**9.3**	**6.6**	**5.4**	**10.0**	**-2.8**	**-4.0**	**0.7**
TG(46:0)	**779.7129**	C49H95O6	$[M+NH_4]^+$	797.746726	**9.873**	**9.864**	**9.868**	**9.869**	9095900078	21494945137	12011742066	8035661933	**37.3**	**43.9**	**33.7**	**24.7**	**6.5**	**-3.6**	**-12.6**
TG(46:1)	**776.6894**	C49H92O6	$[M+NH_4]^+$	794.723226	**9.705**	**9.689**	**9.691**	**9.701**	12823185520	27577357781	17281322876	18757500274	**52.6**	**56.3**	**48.6**	**57.7**	**3.6**	**-4.1**	**5.1**
TG(46:2)	**774.6737**	C49H90O6	$[M+NH_4]^+$	792.707526	**9.568**	**9.556**	**9.56**	**9.56**	11059338111	21168793221	13713516585	16859739481	**45.4**	**43.2**	**38.5**	**51.9**	**-2.2**	**-6.9**	**6.5**
TG(46:3)	**772.6581**	C49H88O6	$[M+NH_4]^+$	790.691926	**9.417**	**9.399**	**9.399**	**9.413**	6649487792	9256418531	7220124613	9502264898	**27.3**	**18.9**	**20.3**	**29.2**	**-8.4**	**-7.0**	**1.9**
TG(47:0)	**792.7207**	C50H96O6	$[M+NH_4]^+$	810.754526	**9.936**	**9.925**	**9.931**	**9.932**	11877311458	29279806732	21492505444	13365936262	**48.8**	**59.8**	**60.4**	**41.1**	**11.0**	**11.6**	**-7.6**
TG(47:1)	**790.705**	C50H94O6	$[M+NH_4]^+$	808.738826	**9.802**	**9.8**	**9.792**	**9.8**	8804780209	16462638369	14472111483	14948279252	**36.2**	**33.6**	**40.7**	**46.0**	**-2.5**	**4.5**	**9.8**
TG(47:2)	**774.6737**	C49H90O6	$[M+NH_4]^+$	792.707526	**9.638**	**9.629**	**9.634**	**9.645**	8143597233	15792107652	11577849876	16555643551	**33.4**	**32.2**	**32.5**	**50.9**	**-1.2**	**-0.9**	**17.5**
TG(47:3)	**786.6737**	C50H90O6	$[M+NH_4]^+$	804.707526	**9.502**	**9.491**	**9.49**	**9.337**	5110134289	8552338415	6239402945	3149039857	**21.0**	**17.5**	**17.5**	**9.7**	**-3.5**	**-3.5**	**-11.3**
TG(47:4)	**784.6581**	C50H88O6	$[M+NH_4]^+$	802.691926	**9.346**	**9.346**	**9.344**	**9.348**	3180042958	4271167167	3091964011	6824347077	**13.1**	**8.7**	**8.7**	**21.0**	**-4.3**	**-4.4**	**7.9**
TG(48:0)	**806.7363**	C51H98O6	$[M+NH_4]^+$	824.770126	**10.043**	**10.022**	**10.032**	**10.031**	3819241015	8908110989	8478690533	6956406832	**15.7**	**18.2**	**23.8**	**21.4**	**2.5**	**8.1**	**5.7**
TG(48:1)	**802.705**	C51H94O6	$[M+NH_4]^+$	820.738826	**9.878**	**9.87**	**9.865**	**9.88**	5118217473	13516164988	10577183508	11948487078	**21.0**	**27.6**	**29.7**	**36.8**	**6.6**	**8.7**	**15.7**
TG(48:2)	**802.705**	C51H94O6	$[M+NH_4]^+$	820.738826	**9.757**	**9.738**	**9.75**	**9.749**	4359981832	9388179522	8232200446	11689068311	**17.9**	**19.2**	**23.1**	**36.0**	**1.3**	**5.2**	**18.1**
TG(48:3)	**800.6894**	C51H92O6	$[M+NH_4]^+$	818.723226	**9.588**	**9.576**	**9.576**	**9.581**	4323725089	6207506885	5355755378	8621023530	**17.8**	**12.7**	**15.0**	**26.5**	**-5.1**	**-2.7**	**8.8**
TG(48:4)	**798.6737**	C51H90O6	$[M+NH_4]^+$	816.707526	**9.44**	**9.422**	**9.429**	**9.423**	2452247747	3723045468	3408336074	5527446014	**10.1**	**7.6**	**9.6**	**17.0**	**-2.5**	**-0.5**	**6.9**
TG(49:0)	**820.752**	C52H100O6	$[M+NH_4]^+$	838.785826	**10.097**	**10.078**	**10.083**	**10.09**	3596716797	9841584231	10410458309	6403648592	**14.8**	**20.1**	**29.2**	**19.7**	**5.3**	**14.5**	**4.9**
TG(49:1)	**818.7363**	C52H98O6	$[M+NH_4]^+$	836.770126	**9.967**	**9.954**	**9.946**	**9.959**	2934843234	6083654389	7164933704	7062692213	**12.0**	**12.4**	**20.1**	**21.7**	**0.4**	**8.1**	**9.7**
TG(49:2)	**816.7207**	C52H96O6	$[M+NH_4]^+$	834.754526	**9.828**	**9.823**	**9.818**	**9.827**	2692190149	5508630067	5983087892	7810404999	**11.1**	**11.2**	**16.8**	**24.0**	**0.2**	**5.8**	**13.0**

TG(50:0)	**834.7676**	C53H102O6	$[M+NH_4]^+$	852.801426	**10.193**	**10.175**	**10.183**	**10.184**	1099956183	2684632396	3103663093	2665874081	**4.5**	**5.5**	**8.7**	**8.2**	**1.0**	**4.2**	**3.7**
TG(50:1)	**832.752**	C53H100O6	$[M+NH_4]^+$	850.785826	**10.045**	**10.018**	**10.028**	**10.035**	1459086708	3313958273	3989569458	4092361152	**6.0**	**6.8**	**11.2**	**12.6**	**0.8**	**5.2**	**6.6**
TG(51:0)	**848.7833**	C54H104O6	$[M+NH_4]^+$	866.817126	**10.219**	**10.216**	**10.218**	**10.223**	742768019	1861834182	3118211406	1581967188	**3.0**	**3.8**	**8.8**	**4.9**	**0.8**	**5.7**	**1.8**
TG(51:1)	**846.7676**	C54H102O6	$[M+NH_4]^+$	864.801426	**10.119**	**10.1**	**10.103**	**10.093**	719272646	1362833913	1930895114	1645928887	**3.0**	**2.8**	**5.4**	**5.1**	**-0.2**	**2.5**	**2.1**
TG(52:0)	**862.7989**	C55H106O6	$[M+NH_4]^+$	880.832726	**10.363**	**10.353**	**10.335**	**10.334**	276044215	259282825	287957860	287574362	**1.1**	**0.5**	**0.8**	**0.9**	**-0.6**	**-0.3**	**-0.2**

Supplemental Table 2 | Complete table of lipid species identified by the procedure described in the method section. Lipid species highlighted in red were not fragmented in the respective run, but the peaks were detected at the given retention time in the extracted ion chromatogram.

Strain	Chromatogram	RT [min]	Range [min]	Compound Name	MS(n) Isol. m/z	I (precursor)	Lib. RT [min]	Lib. MW	Chemical Formula	Int. %	Chromatogram	RT [min]	Range [min]	Area	Rel. Quant
wt	AutoMS(n): TIC -All MS FullScan	8.204	8.181 - 8.228	Cer(D19:0/16:0)	599.9162	2026798	8.215	553.5434	C35H71NO3	1	EIC 598.9416 -All MS, Smoothed (1.60,2,GA)	8.211	8.056 - 8.639	38573964	1.1
wt	AutoMS(n): TIC -All MS FullScan	8.077	8.056 - 8.097	Cer(D19:0/i17:0 2-OH)	629.8589	9665441	8.086	583.554	C36H73NO4	3	EIC 628.9522 -All MS, Smoothed (1.60,2,GA)	8.058	7.740 - 8.611	125260931	3.6
wt	AutoMS(n): TIC -All MS FullScan	8.3	8.284 - 8.317	Cer(D19:0/i17:0)	612.9431	19170392	8.305	567.559	C36H73NO3	5	EIC 612.9572 -All MS, Smoothed (1.60,2,GA)	8.329	8.154 - 9.292	181968237	5.3
wt			7.159 - 7.528	CerPI(D19:0/16:0 2-OH)				811.5575			EIC 810.9502 -All MS, Smoothed (1.60,2,GA)	7.377	7.159 - 7.528	62927020	1.8
wt			7.328 - 7.791	CerPI(D19:0/16:0)				795.5625			EIC 794.9552 -All MS, Smoothed (1.60,2,GA)	7.566	7.328 - 7.791	17139969	0.5
wt	AutoMS(n): TIC -All MS FullScan	7.544	7.528 - 7.561	CerPI(D19:0/i17:0 2-OH)	826.1826	16123966	7.549	825.5731	C42H84NO12P	4	EIC 824.9658 -All MS, Smoothed (1.60,2,GA)	7.541	7.328 - 7.960	182535791	5.3
wt			7.581 - 8.259	CerPI(D19:0/i17:0)				809.5782			EIC 808.9709 -All MS, Smoothed (1.60,2,GA)	7.738	7.581 - 8.259	115192371	3.3
wt	AutoMS(n): TIC -All MS FullScan	6.532	6.414 - 6.650	PE(12:1/17:1);PE(13:1/16:1); PE(16:2/13:0);PE(14:1/15:1)	644.8546	22563106	6.512	645.437	C34H64NO8P	15	EIC 644.8297 -All MS, Smoothed (1.60,2,GA)	6.56	6.309 - 6.957	810396868	23.5
wt	AutoMS(n): TIC -All MS FullScan	7.18	7.159 - 7.201	PE(14:0/14:0);PE(13:0/15:0)	635.1603	8802562	7.212	635.4526	C33H66NO8P	2	EIC 634.8453 -All MS, Smoothed (1.60,2,GA)	7.054	6.885 - 7.528	164325035	4.8
wt	AutoMS(n): TIC -All MS FullScan	7.321	7.305 - 7.337	PE(14:0/15:0)	649.2268	86542536	7.325	649.4683	C34H68NO8P	26	EIC 648.8610 -All MS, Smoothed (1.60,2,GA)	7.359	7.206 - 7.595	950674061	27.6
wt	AutoMS(n): TIC -All MS FullScan	6.162	6.143 - 6.181	PE(14:1/14:1);PE(16:1/12:1) PE(15:1/13:1)	631.1887	3127864	6.168	631.4213	C33H62NO8P	1	EIC 630.8140 -All MS, Smoothed (1.60,2,GA)	6.341	5.582 - 6.728	124381724	3.6
wt	AutoMS(n): TIC -All MS FullScan	6.842	6.814 - 6.871	PE(14:1/15:0);PE(16:1/13:0)	646.8777	31675826	6.851	647.4526	C34H66NO8P1	31	EIC 646.8453 -All MS, Smoothed (1.60,2,GA)	7.005	6.728 - 7.505	1791131504	51.9
wt	AutoMS(n): TIC -All MS FullScan	7.554	7.445 - 7.664	PE(15:0/15:0)	662.9193	249337104	7.477	663.4839	C35H70NO8P	82	EIC 662.8766 -All MS, Smoothed (1.60,2,GA)	7.573	7.374 - 8.804	5414894594	157.0
wt	AutoMS(n): TIC -All MS FullScan	7.965	7.864 - 8.065	PE(15:0/17:0)	690.9802	47392664	7.897	691.5152	C37H74NO8P	18	EIC 690.9079 -All MS, Smoothed (1.60,2,GA)	7.95	7.776 - 8.723	868124953	25.2
wt	AutoMS(n): TIC -All MS FullScan	6.555	6.533 - 6.577	PE(15:1/13:0)	632.8768	5620089	6.565	633.437	C33H64NO8P	3	EIC 632.8297 -All MS, Smoothed (1.60,2,GA)	6.726	6.440 - 7.041	246197897	7.1
wt	AutoMS(n): TIC -All MS FullScan	7.194	7.112 - 7.275	PE(15:1/15:0)	660.9041	112707864	7.26	661.4683	C35H68NO8P	35	EIC 660.8610 -All MS, Smoothed (1.60,2,GA)	7.222	6.980 - 7.543	2102735263	61.0
wt	AutoMS(n): TIC -All MS FullScan	7.88	7.805 - 7.955	PE(16:0/15:0);PE(14:0/17:0)	676.959	12896000	7.822	677.4996	C36H72NO8P	3	EIC 676.8923 -All MS, Smoothed (1.60,2,GA)	7.824	7.566 - 8.056	212375183	6.2
wt	AutoMS(n): TIC -All MS FullScan	8.146	8.128 - 8.164	PE(16:0/17:0)	705.2944	7202785	8.151	705.5309	C38H76NO8P	29	EIC 704.9236 -All MS, Smoothed (1.60,2,GA)	8.149	8.009 - 8.778	65380218	1.9
wt	AutoMS(n): TIC -All MS FullScan	7.425	7.328 - 7.523	PE(16:1/15:0)	674.9265	72182416	7.36	675.4839	C36H70NO8P	31	EIC 674.8766 -All MS, Smoothed (1.60,2,GA)	7.406	7.235 - 7.960	1377180076	39.9
wt	AutoMS(n): TIC -All MS FullScan	6.98	6.957 - 7.003	PE(16:1/15:1);PE(17:1/14:1)	672.9109	23134710	6.989	673.4683	C36H68NO8P	35	EIC 672.8610 -All MS, Smoothed (1.60,2,GA)	7.107	6.885 - 7.566	1794938789	52.1
wt	AutoMS(n): TIC -All MS FullScan	7.224	7.182 - 7.267	PE(16:1/16:1);PE(17:2/15:0)	686.3376		7.26	687.4839	C37H70NO8P	35	EIC 686.8766 -All MS, Smoothed (1.60,2,GA)	7.28	7.089 - 7.595	1623140234	47.1
wt	AutoMS(n): TIC -All MS FullScan	7.788	7.776 - 7.800	PE(16:1/17:0)	703.0039	37544968	7.793	703.5152	C38H74NO8P	12	EIC 702.9079 -All MS, Smoothed (1.60,2,GA)	7.828	7.702 - 8.723	545370894	15.8

wt	AutoMS(n): TIC -All MS FullScan	6.419	6.335 - 6.503	**PE(16:2/14:1);PE(15:2/15:1)**	656.8661	18232844	6.363	**657.437**	C35H64NO8P	9	EIC 656.8297 -All MS, Smoothed (1.60,2,GA)	**6.507**	5.892 - 7.089	578937509	**16.8**
wt	AutoMS(n): TIC -All MS FullScan	6.672	6.583 - 6.761	**PE(16:2/15:1);PE(15:2/16:1); PE(17:2/14:1)**	670.883	40502396	6.677	**671.4526**	C36H66NO8P	16	EIC 670.8453 -All MS, Smoothed (1.60,2,GA)	**6.735**	6.466 - 7.281	999731203	**29.0**
wt	AutoMS(n): TIC -All MS FullScan	6.285	6.226 - 6.345	**PE(16:2/15:2);PE(17:2/14:2)**	668.8861	5787369	6.332	**669.437**	C36H64NO8P	3	EIC 668.8297 -All MS, Smoothed (1.60,2,GA)	**6.369**	6.089 - 7.041	158186419	**4.6**
wt	AutoMS(n): TIC -All MS FullScan	6.914	6.862 - 6.965	**PE(16:2/16:1); PE(17:2/15:1)**	684.9336	79979200	6.954	**685.4683**	C37H68NO8P	30	EIC 684.8610 -All MS, Smoothed (1.60,2,GA)	**6.976**	6.790 - 7.581	1424895926	**41.3**
wt	AutoMS(n): TIC -All MS FullScan	8.251	8.233 - 8.268	**PE(17:0/17:0)**	719.0575	16768209	8.256	**719.5465**	C39H78NO8P	4	EIC 718.9392 -All MS, Smoothed (1.60,2,GA)	**8.278**	8.128 - 8.611	152306862	**4.4**
wt	AutoMS(n): TIC -All MS FullScan	7.627	7.581 - 7.673	**PE(17:1/15:0);PE(16:1/16:0); PE(15:1/17:0)**	689.2277	42773376	7.608	**689.4996**	C37H72NO8P	12	EIC 688.8923 -All MS, Smoothed (1.60,2,GA)	**7.664**	7.482 - 8.695	700696438	**20.3**
wt	AutoMS(n): TIC -All MS FullScan	7.402	7.374 - 7.430	**PE(17:1/16:1)**	700.4775		7.411	**701.4996**	C38H72NO8P	10	EIC 700.8923 -All MS, Smoothed (1.60,2,GA)	**7.432**	7.281 - 7.528	340535300	**9.9**
wt	AutoMS(n): TIC -All MS FullScan	7.941	7.889 - 7.993	**PE(17:1/17:0)**	717.0081	21224440	7.914	**717.5309**	C39H76NO8P	5	EIC 716.9236 -All MS, Smoothed (1.60,2,GA)	**7.993**	7.820 - 8.557	353982545	**10.3**
wt	AutoMS(n): TIC -All MS FullScan	6.725	6.680 - 6.769	**PE(17:2/13:0);PE(16:1/14:1) ;PE(15:1/15:1)**	658.875	39822700	6.717	**659.4526**	C35H66NO8P	16	EIC 658.8453 -All MS, Smoothed (1.60,2,GA)	**6.865**	6.608 - 7.505	1130534586	**32.8**
wt	AutoMS(n): TIC -All MS FullScan	6.6	6.558 - 6.642	**PE(17:2/15:2);PE(16:2/16:2)**	683.2143	64389888	6.48	**683.4526**	C37H66NO8P	22	EIC 682.8453 -All MS, Smoothed (1.60,2,GA)	**6.651**	6.440 - 7.258	909436000	**26.4**
wt	AutoMS(n): TIC -All MS FullScan	7.105	7.089 - 7.121	**PE(17:2/16:1);PE(16:2/17:1)**	698.9474	32384504	7.114	**699.4839**	C38H70NO8P	21	EIC 698.8766 -All MS, Smoothed (1.60,2,GA)	**7.165**	6.995 - 7.835	1053628563	**30.6**
wt	AutoMS(n): TIC -All MS FullScan	6.787	6.775 - 6.798	**PE(17:2/16:2)**	696.9426	20398304	6.791	**697.4683**	C38H68NO8P	22	EIC 696.8610 -All MS, Smoothed (1.60,2,GA)	**6.854**	6.656 - 7.374	851518593	**24.7**
wt	AutoMS(n): TIC -All MS FullScan	7.699	7.678 - 7.719	**PE(17:2/17:0); PE(17:1/17:1)**	714.9958	17790864	7.708	**715.5152**	C39H74NO8P	6	EIC 714.9079 -All MS, Smoothed (1.60,2,GA)	**7.737**	7.543 - 8.501	359852616	**10.4**
wt	AutoMS(n): TIC -All MS FullScan	7.302	7.281 - 7.322	**PE(17:2/17:1)**	712.9589	17608080	7.311	**713.4996**	C39H72NO8P	6	EIC 712.8923 -All MS, Smoothed (1.60,2,GA)	**7.44**	7.182 - 7.754	346337222	**10.0**
wt	AutoMS(n): TIC -All MS FullScan	7.011	6.995 - 7.027	**PE(17:2/17:2)**	711.3594		7.02	**711.4839**	C39H70NO8P	6	EIC 710.8766 -All MS, Smoothed (1.60,2,GA)	**7.039**	6.862 - 7.543	225294688	**6.5**
wt	AutoMS(n): TIC -All MS FullScan	7.72	7.678 - 7.762	**PE(P-15:0/15:0)**	647.3196		7.699	**647.489**	C35H70NO7P	100	EIC 646.8817 -All MS, Smoothed (1.60,2,GA)	**7.75**	7.505 - 8.804	4034959183	**117.0**
wt	AutoMS(n): TIC -All MS FullScan	8.096	8.079 - 8.112	**PE(P-15:0/17:0)**	675.3153	15994563	8.071	**675.5203**	C37H74NO7P	3	EIC 674.9130 -All MS, Smoothed (1.60,2,GA)	**8.105**	7.960 - 8.839	124233827	**3.6**
wt	AutoMS(n): TIC -All MS FullScan	7.034	7.018 - 7.051	**PG(14:0/15:0)**	680.2349	13424238	7.043	**680.4628**	C35H69O10P	3	EIC 679.8555 -All MS, Smoothed (1.60,2,GA)	**7.026**	6.838 - 7.258	108895211	**3.2**
wt	AutoMS(n): TIC -All MS FullScan	7.152	7.136 - 7.167	**PG(15:0/15:0)**	694.2623	27967290	7.16	**694.4785**	C36H71O10P	9	EIC 693.8712 -All MS, Smoothed (1.60,2,GA)	**7.204**	7.018 - 7.543	440727551	**12.8**
wt	AutoMS(n): TIC -All MS FullScan	6.835	6.814 - 6.856	**PG(15:0/15:1);PG(16:1/14:0)**	692.2932	9093056	6.84	**692.4628**	C36H69O10P	3	EIC 691.8555 -All MS, Smoothed (1.60,2,GA)	**6.895**	6.656 - 7.221	150686728	**4.4**
wt	AutoMS(n): TIC -All MS FullScan	7.082	7.065 - 7.098	**PG(15:0/16:1);PG(14:1/17:0)**	706.3936		7.091	**706.4785**	C37H71O10P	4	EIC 705.8712 -All MS, Smoothed (1.60,2,GA)	**7.112**	6.909 - 7.421	185823105	**5.4**
wt	AutoMS(n): TIC -All MS FullScan	6.725	6.703 - 6.746	**PG(15:1/16:1;PG(15:0/16:2); PG(14:1/17:1);PG(14:0/17:2)**	704.2032	7754940	6.734	**704.4628**	C37H69O10P	2	EIC 704.9236 -All MS, Smoothed (1.60,2,GA)	**6.769**	6.533 - 7.041	59143503	**1.7**
wt	AutoMS(n): TIC -All MS FullScan	7.383	7.351 - 7.416	**PG(16:0/16:1);PG(15:1/17:0); PG(15:0/17:1)**	720.2877	13674252	7.392	**720.4941**	C38H73O10P	3	EIC 719.8868 -All MS, Smoothed (1.60,2,GA)	**7.374**	7.136 - 7.595	147531945	**4.3**
wt	AutoMS(n): TIC -All MS FullScan	7.874	7.864 - 7.883	**PG(16:0/17:0)**	736.3972	5686417	7.883	**736.5254**	C39H77O10P	1	EIC 735.9181 -All MS, Smoothed (1.60,2,GA)	**7.864**	7.754 - 8.079	39778700	**1.2**
wt	AutoMS(n): TIC -All MS FullScan	6.93	6.909 - 6.951	**PG(16:1/16:1)**	718.2595	20512012	6.935	**718.4785**	C38H71O10P 1	5	EIC 717.8712 -All MS, Smoothed (1.60,2,GA)	**6.951**	6.775 - 7.281	209390448	**6.1**
wt	AutoMS(n): TIC -All MS FullScan	6.507	6.387 - 6.627	**PG(16:1/16:2)**	716.9708	2803138	6.627	**716.4628**	C38H69O10P	1	EIC 716.9236 -All MS, Smoothed (1.60,2,GA)	**6.612**	6.171 - 6.862	75745121	**2.2**

wt	AutoMS(n): TIC -All MS FullScan	7.559	7.543 - 7.575	**PG(17:0/16:1)**	734.3436	27082224	7.563	**734.5098**	C39H75O10P	6	EIC 733.9025 -All MS, Smoothed (1.60,2,GA)	**7.576**	7.421 - 8.079	222150012	**6.4**
wt			7.835 - 8.723	**PG(17:0/17:0)**				**750.5411**			EIC 749.9338 -All MS, Smoothed (1.60,2,GA)	**8.019**	7.835 - 8.723	61232182	**1.8**
wt			7.566 - 7.960	**PG(17:0/17:1)**				**748.5254**			EIC 747.9181 -All MS, Smoothed (1.60,2,GA)	**7.691**	7.566 - 7.960	79632676	**2.3**
wt			6.957 - 7.581	**PG(17:1/16:1)**				**732.4941**			EIC 731.8868 -All MS, Smoothed (1.60,2,GA)	**7.116**	6.957 - 7.581	143469064	**4.2**
Sum negative														**3.448E+10**	**1000.0**
wt	AutoMS(n): TIC +All MS FullScan	8.067	8.051 - 8.083	**DG(15:0/15:0/0:0)**	559.012		8.071	**540.4754**	C33H64O5	13	EIC 558.9092 +All MS, Smoothed (1.39,2,GA)	**8.086**	7.913 - 8.628	4121220545	**16.9**
wt	AutoMS(n): TIC +All MS FullScan	7.998	7.982 - 8.014	**DG(31:1)**	570.5684	141392848	8.007	**552.4754**	C34H64O5	4	EIC 570.9092 +All MS, Smoothed (1.39,2,GA)	**7.987**	7.801 - 8.212	1570472455	**6.4**
wt	AutoMS(n): TIC +All MS FullScan	8.447	8.442 - 8.451	**DG(32:0)**	586.55	63817100	8.451	**568.5067**	C35H68O5	2	EIC 586.9405 +All MS, Smoothed (1.39,2,GA)	**8.442**	8.281 - 8.721	575571455	**2.4**
wt	AutoMS(n): TIC +All MS FullScan	7.853	7.844 - 7.862	**DG(32:2)**	582.6011	129591328	7.862	**564.4754**	C35H64O5	3	EIC 582.9092 +All MS, Smoothed (1.39,2,GA)	**7.857**	7.574 - 8.304	1538850492	**6.3**
wt	AutoMS(n): TIC +All MS FullScan	8.672	8.651 - 8.692	**DG(33:0)**	600.7368	28945252	8.669	**582.5223**	C36H70O5	1	EIC 600.9561 +All MS, Smoothed (1.39,2,GA)	**8.651**	8.212 - 8.489	233105253	**1.0**
wt	AutoMS(n): TIC +All MS FullScan	8.343	8.327 - 8.359	**DG(33:1)**	599.0021	108448288	8.336	**580.5067**	C36H68O5	3	EIC 598.9405 +All MS, Smoothed (1.39,2,GA)	**8.341**	8.189 - 8.791	773036816	**3.2**
wt			7.844 - 8.304	**DG(33:2)**				**578.491**			EIC 596.9248 +All MS, Smoothed (1.39,2,GA)	**8.024**	7.844 - 8.304	1105621336	**4.5**
wt	AutoMS(n): TIC +All MS FullScan	9.722	9.694 - 9.749	**TG(15:0/15:0/15:0)**	783.072	1646782976	9.73	**764.6894**	C48H92O6	60	EIC 783.1232 +All MS, Smoothed (1.39,2,GA)	**9.766**	9.440 - 10.505	23094843874	**94.8**
wt	AutoMS(n): TIC +All MS FullScan	8.854	8.838 - 8.870	**TG(38:1)**	683.2786		8.862	**666.5798**	C41H78O6	1	EIC 682.7169 +All MS, Smoothed (1.39,2,GA)	**8.853**	8.698 - 9.140	426152868	**1.7**
wt	AutoMS(n): TIC +All MS FullScan	9.16	9.140 - 9.180	**TG(39:0)**	699.9623	112496064	9.169	**680.5955**	C42H80O6	4	EIC 699.0293 +All MS, Smoothed (1.39,2,GA)	**9.174**	8.745 - 9.463	1351552037	**5.5**
wt	AutoMS(n): TIC +All MS FullScan	8.986	8.977 - 8.995	**TG(39:1)**	697.2049	51166844	8.995	**678.5798**	C42H78O6	1	EIC 697.0136 +All MS, Smoothed (1.39,2,GA)	**8.997**	8.512 - 9.348	617477839	**2.5**
wt	AutoMS(n): TIC +All MS FullScan	9.063	9.047 - 9.079	**TG(40:1)**	711.194	96139680	9.072	**692.5955**	C43H80O6	4	EIC 711.0293 +All MS, Smoothed (1.39,2,GA)	**9.107**	8.814 - 9.394	1464559396	**6.0**
wt	AutoMS(n): TIC +All MS FullScan	8.905	8.884 - 8.925	**TG(40:2)**	708.9641	61583288	8.913	**690.5798**	C43H78O6	2	EIC 709.0136 +All MS, Smoothed (1.39,2,GA)	**8.914**	8.559 - 9.279	780164182	**3.2**
wt	AutoMS(n): TIC +All MS FullScan	9.195	9.186 - 9.204	**TG(41:1)**	725.2581	253989472	9.149	**706.61114**	C44H82O6	9	EIC 725.0450 +All MS, Smoothed (1.39,2,GA)	**9.236**	8.768 - 9.579	2543241843	**10.4**
wt	AutoMS(n): TIC +All MS FullScan	8.993	8.977 - 9.009	**TG(41:2)**	722.9436	73380712	8.998	**704.5955**	C44H80O6	3	EIC 723.0293 +All MS, Smoothed (1.39,2,GA)	**9.047**	8.861 - 9.510	1218786468	**5.0**
wt	AutoMS(n): TIC +All MS FullScan	8.87	8.861 - 8.878	**TG(41:3)**	720.9323	47982264	8.878	**702.5798**	C44H78O6	3	EIC 720.9538 +All MS, Smoothed (1.39,2,GA)	**8.85**	8.628 - 9.047	512817239	**2.1**
wt	AutoMS(n): TIC +All MS FullScan	9.322	9.302 - 9.342	**TG(42:1)**	738.9904	507773696	9.331	**722.6424**	C45H86O6	13	EIC 739.0606 +All MS, Smoothed (1.39,2,GA)	**9.32**	8.931 - 9.671	4935623974	**20.3**
wt	AutoMS(n): TIC +All MS FullScan	9.144	9.093 - 9.195	**TG(42:2)**	736.9882	208150448	9.149	**718.6111**	C45H82O6	8	EIC 737.0449 +All MS, Smoothed (1.39,2,GA)	**9.189**	8.977 - 9.648	3812841732	**15.7**
wt	AutoMS(n): TIC +All MS FullScan	9.549	9.533 - 9.565	**TG(43:0)**	755.0398	762359040	9.557	**736.6581**	C46H88O6	21	EIC 755.0919 +All MS, Smoothed (1.39,2,GA)	**9.576**	9.255 - 10.272	8101377876	**33.3**

wt	AutoMS(n): TIC +All MS FullScan	9.41	9.394 - 9.426	**TG(43:1)**	753.0186	475619328	9.419	**734.6424**	C46H86O6	15	EIC 753.0762 +All MS, Smoothed (1.39,2,GA)	**9.438**	9.047 - 9.902	5809590103	**23.9**
wt	AutoMS(n): TIC +All MS FullScan	9.276	9.255 - 9.296	**TG(43:2)**	751.3641	552601408	9.28	**732.6268**	C46H84O6	14	EIC 751.0606 +All MS, Smoothed (1.39,2,GA)	**9.265**	8.838 - 9.556	5401867195	**22.2**
wt	AutoMS(n): TIC +All MS FullScan	9.04	9.024 - 9.056	**TG(43:3)**	748.9678	106044672	9.049	**730.6111**	C46H82O6	5	EIC 749.0449 +All MS, Smoothed (1.39,2,GA)	**9.109**	8.768 - 9.325	2294365269	**9.4**
wt	AutoMS(n): TIC +All MS FullScan	9.668	9.648 - 9.689	**TG(44:0)**	769.0368	707531136	9.677	**750.6737**	C47H90O6	27	EIC 769.1075 +All MS, Smoothed (1.39,2,GA)	**9.696**	9.302 - 9.902	8682156958	**35.6**
wt	AutoMS(n): TIC +All MS FullScan	9.491	9.463 - 9.518	**TG(44:1)**	767.0149	713742592	9.495	**748.6581**	C47H88O6	28	EIC 767.0919 +All MS, Smoothed (1.39,2,GA)	**9.532**	9.163 - 9.763	9881382140	**40.6**
wt	AutoMS(n): TIC +All MS FullScan	9.341	9.325 - 9.357	**TG(44:2)**	765.0325	637574400	9.345	**746.6424**	C47H86O6	21	EIC 765.1127 +All MS, Smoothed (1.39,2,GA)	**9.377**	9.047 - 9.671	7888909386	**32.4**
wt	AutoMS(n): TIC +All MS FullScan	9.195	9.140 - 9.250	**TG(44:3)**	762.9928	365546432	9.238	**744.6268**	C47H84O6	13	EIC 763.0606 +All MS, Smoothed (1.39,2,GA)	**9.223**	8.861 - 9.579	4484202070	**18.4**
wt	AutoMS(n): TIC +All MS FullScan	9.017	9.001 - 9.033	**TG(44:4)**	761.3501	87352192	9.025	**742.6111**	C47H82O6	3	EIC 761.0449 +All MS, Smoothed (1.39,2,GA)	**9.052**	8.721 - 9.232	1025121431	**4.2**
wt	AutoMS(n): TIC +All MS FullScan	9.583	9.556 - 9.611	**TG(45:1)**	781.0839	812946112	9.592	**762.6737**	C48H90O6	28	EIC 781.1075 +All MS, Smoothed (1.39,2,GA)	**9.63**	9.279 - 10.133	12154841933	**49.9**
wt	AutoMS(n): TIC +All MS FullScan	9.433	9.417 - 9.449	**TG(45:2)**	779.056	640189376	9.442	**760.6581**	C48H88O6	21	EIC 779.0919 +All MS, Smoothed (1.39,2,GA)	**9.47**	9.047 - 9.740	8452882941	**34.7**
wt	AutoMS(n): TIC +All MS FullScan	9.295	9.279 - 9.311	**TG(45:3)**	777.4838		9.299	**758.6424**	C48H86O6	14	EIC 777.0762 +All MS, Smoothed (1.39,2,GA)	**9.311**	8.931 - 9.602	6096598003	**25.0**
wt	AutoMS(n): TIC +All MS FullScan	9.114	9.093 - 9.134	**TG(45:4)**	775.4032	139503680	9.123	**758.6424**	C48H86O6	6	EIC 775.0606 +All MS, Smoothed (1.39,2,GA)	**9.165**	8.931 - 9.348	2269739943	**9.3**
wt	AutoMS(n): TIC +All MS FullScan	9.849	9.833 - 9.865	**TG(46:0)**	797.0966	763003904	9.853	**779.7129**	C49H95O6	22	EIC 797.1389 +All MS, Smoothed (1.39,2,GA)	**9.873**	9.440 - 10.365	9095900078	**37.3**
wt	AutoMS(n): TIC +All MS FullScan	9.676	9.648 - 9.703	**TG(46:1)**	795.1099	1004698816	9.68	**776.6894**	C49H92O6	31	EIC 795.1232 +All MS, Smoothed (1.39,2,GA)	**9.705**	9.348 - 10.179	12823185520	**52.6**
wt	AutoMS(n): TIC +All MS FullScan	9.576	9.510 - 9.642	**TG(46:2)**	793.0814	765620416	9.543	**774.6737**	C49H90O6	30	EIC 793.1075 +All MS, Smoothed (1.39,2,GA)	**9.568**	9.209 - 9.994	11059338111	**45.4**
wt	AutoMS(n): TIC +All MS FullScan	9.387	9.371 - 9.403	**TG(46:3)**	791.3792	505469408	9.391	**772.6581**	C49H88O6	15	EIC 791.0919 +All MS, Smoothed (1.39,2,GA)	**9.417**	9.001 - 9.879	6649487792	**27.3**
wt	AutoMS(n): TIC +All MS FullScan	9.906	9.879 - 9.934	**TG(47:0)**	811.1313	1021741184	9.911	**792.7207**	C50H96O6	32	EIC 811.1545 +All MS, Smoothed (1.39,2,GA)	**9.936**	9.486 - 10.599	11877311458	**48.8**
wt	AutoMS(n): TIC +All MS FullScan	9.768	9.740 - 9.795	**TG(47:1)**	809.1141	613415680	9.784	**790.705**	C50H94O6	19	EIC 809.1388 +All MS, Smoothed (1.39,2,GA)	**9.802**	9.440 - 10.295	8804780209	**36.2**
wt	AutoMS(n): TIC +All MS FullScan	9.668	9.602 - 9.735	**TG(47:2)**	807.1022	700378560	9.543	**774.6737**	C49H90O6	24	EIC 807.1232 +All MS, Smoothed (1.39,2,GA)	**9.638**	9.325 - 9.994	8143597233	**33.4**
wt	AutoMS(n): TIC +All MS FullScan	9.484	9.463 - 9.504	**TG(47:3)**	805.0908	479058560	9.492	**786.6737**	C50H90O6	15	EIC 805.1075 +All MS, Smoothed (1.39,2,GA)	**9.502**	9.140 - 9.694	5110134289	**21.0**
wt	AutoMS(n): TIC +All MS FullScan	9.368	9.348 - 9.388	**TG(47:4)**	803.5576		9.377	**784.6581**	C50H88O6	8	EIC 803.0919 +All MS, Smoothed (1.39,2,GA)	**9.346**	9.093 - 9.533	3180042958	**13.1**
wt	AutoMS(n): TIC +All MS FullScan	10.061	9.994 - 10.127	**TG(48:0)**	825.1717	303215808	10.073	**806.7363**	C51H98O6	10	EIC 825.1701 +All MS, Smoothed (1.39,2,GA)	**10.043**	9.902 - 10.575	3819241015	**15.7**
wt	AutoMS(n): TIC +All MS FullScan	9.864	9.833 - 9.896	**TG(48:1)**	823.1522	481779872	9.759	**802.705**	C51H94O6	14	EIC 823.1545 +All MS, Smoothed (1.39,2,GA)	**9.878**	9.533 - 10.481	5118217473	**21.0**
wt	AutoMS(n): TIC +All MS FullScan	9.784	9.763 - 9.804	**TG(48:2)**	821.438	354241280	9.759	**802.705**	C51H94O6	9	EIC 821.1388 +All MS, Smoothed (1.39,2,GA)	**9.757**	9.440 - 10.064	4359981832	**17.9**
wt	AutoMS(n): TIC +All MS FullScan	9.588	9.579 - 9.596	**TG(48:3)**	819.477	375711872	9.596	**800.6894**	C51H92O6	9	EIC 819.1232 +All MS, Smoothed (1.39,2,GA)	**9.588**	9.209 - 10.017	4323725089	**17.8**
wt			9.163 - 9.625	**TG(48:4)**				**798.6737**			EIC 817.1075 +All MS, Smoothed (1.39,2,GA)	**9.44**	9.163 - 9.625	2452247747	**10.1**

wt	AutoMS(n): TIC +All MS FullScan	10.072	10.041 - 10.104	**TG(49:0)**	839.1955	307190240	10.065	**820.752**	C52H100O6	10	EIC 839.1858 +All MS, Smoothed (1.39,2,GA)	**10.097**	9.671 - 10.732	3596716797	**14.8**
wt	AutoMS(n): TIC +All MS FullScan	9.968	9.902 - 10.035	**TG(49:1)**	837.4661	183432032	9.931	**818.7363**	C52H98O6	7	EIC 837.1701 +All MS, Smoothed (1.39,2,GA)	**9.967**	9.648 - 10.575	2934843234	**12.0**
wt	AutoMS(n): TIC +All MS FullScan	9.818	9.810 - 9.827	**TG(49:2)**	835.5793		9.827	**816.7207**	C52H96O6	8	EIC 835.1545 +All MS, Smoothed (1.39,2,GA)	**9.828**	9.533 - 10.179	2692190149	**11.1**
wt	AutoMS(n): TIC +All MS FullScan	10.223	10.156 - 10.289	**TG(50:0)**	853.1992	80432688	10.278	**834.7676**	C53H102O6	3	EIC 853.2014 +All MS, Smoothed (1.39,2,GA)	**10.193**	10.064 - 10.756	1099956183	**4.5**
wt	AutoMS(n): TIC +All MS FullScan	10.049	10.041 - 10.058	**TG(50:1)**	851.2251	152118240	10.058	**832.752**	C53H100O6	4	EIC 851.1858 +All MS, Smoothed (1.39,2,GA)	**10.045**	9.763 - 10.341	1459086708	**6.0**
wt	AutoMS(n): TIC +All MS FullScan	10.223	10.202 - 10.243	**TG(51:0)**	867.253	77592160	10.231	**848.7833**	C54H104O6	2	EIC 867.2171 +All MS, Smoothed (1.39,2,GA)	**10.219**	9.902 - 10.552	742768019	**3.0**
wt			9.833 - 10.637	**TG(51:1)**				**846.7676**			EIC 865.2014 +All MS, Smoothed (1.39,2,GA)	**10.119**	9.833 - 10.637	719272646	**3.0**
wt			9.879 - 10.660	**TG(52:0)**				**862.7989**			EIC 881.2327 +All MS, Smoothed (1.39,2,GA)	**10.363**	9.879 - 10.660	276044215	**1.1**
Sum positive														**2.436E+11**	**1000.0**
Δ0191	AutoMS(n): TIC -All MS FullScan	8.185	8.169 - 8.201	**Cer(D19:0/16:0)**	599.872	12429500	8.215	**553.5434**	C35H71NO3	6	EIC 598.9416 -All MS, Smoothed (1.58,2,GA)	**8.212**	8.085 - 8.810	204217681	**5.7**
				Cer(D19:0/i17:0 2-OH)											**0.0**
Δ0191	AutoMS(n): TIC -All MS FullScan	8.337	8.267 - 8.407	**Cer(D19:0/i17:0)**	612.9475	55418892	8.305	**567.559**	C36H73NO3	19	EIC 612.9572 -All MS, Smoothed (1.58,2,GA)	**8.341**	8.005 - 9.525	770054191	**21.5**
				CerPI(D19:0/16:0 2-OH)											**0.0**
Δ0191	AutoMS(n): TIC -All MS FullScan	7.605	7.585 - 7.626	**CerPI(D19:0/16:0)**	795.6332		7.614	**795.5625**	C41H82NO11P	5	EIC 794.9552 -All MS, Smoothed (1.58,2,GA)	**7.596**	7.452 - 8.057	176243578	**4.9**
				CerPI(D19:0/i17:0 2-OH)											**0.0**
Δ0191	AutoMS(n): TIC -All MS FullScan	7.72	7.670 - 7.771	**CerPI(D19:0/i17:0)**	810.1511	36768012	7.729	**809.5782**	C42H84NO11P	20	EIC 810.9502 -All MS, Smoothed (1.58,2,GA)	**7.739**	7.467 - 8.057	135047884	**3.8**
Δ0191	AutoMS(n): TIC -All MS FullScan	6.484	6.416 - 6.552	**PE(12:1/17:1);PE(13:1/16:1); PE(16:2/13:0);PE(14:1/15:1)**	644.8557	19926974	6.512	**645.437**	C34H64NO8P	11	EIC 644.8297 -All MS, Smoothed (1.58,2,GA)	**6.559**	6.309 - 7.049	664715107	**18.5**
Δ0191	AutoMS(n): TIC -All MS FullScan	7.07	7.049 - 7.091	**PE(14:0/14:0);PE(13:0/15:0)**	635.2366	10194018	7.079	**635.4526**	C33H66NO8P	2	EIC 634.8453 -All MS, Smoothed (1.58,2,GA)	**7.061**	6.884 - 7.452	159112512	**4.4**
Δ0191	AutoMS(n): TIC -All MS FullScan	7.314	7.297 - 7.330	**PE(14:0/15:0)**	649.2209	68976864	7.325	**649.4683**	C34H68NO8P	27	EIC 648.8610 -All MS, Smoothed (1.58,2,GA)	**7.361**	7.190 - 7.585	1006002189	**28.0**
Δ0191	AutoMS(n): TIC -All MS FullScan	6.161	6.142 - 6.180	**PE(14:1/14:1);PE(16:1/12:1) PE(15:1/13:1)**	630.839	2058271	6.168	**631.4213**	C33H62NO8P	1	EIC 630.8140 -All MS, Smoothed (1.58,2,GA)	**6.352**	5.918 - 6.718	116914252	**3.3**
Δ0191	AutoMS(n): TIC -All MS FullScan	6.893	6.813 - 6.972	**PE(14:1/15:0);PE(16:1/13:0)**	646.8829	40856648	6.851	**647.4526**	C34H66NO8P1	28	EIC 646.8453 -All MS, Smoothed (1.58,2,GA)	**7.013**	6.743 - 7.452	1626740279	**45.3**
Δ0191	AutoMS(n): TIC -All MS FullScan	7.504	7.437 - 7.570	**PE(15:0/15:0)**	662.423		7.477	**663.4839**	C35H70NO8P	91	EIC 662.8766 -All MS, Smoothed (1.58,2,GA)	**7.553**	7.367 - 8.129	5125094213	**142.8**
Δ0191	AutoMS(n): TIC -All MS FullScan	8.009	7.909 - 8.109	**PE(15:0/17:0)**	690.9906	144883552	8.013	**691.5152**	C37H74NO8P	78	EIC 690.9079 -All MS, Smoothed (1.58,2,GA)	**8.066**	7.776 - 8.844	1974453996	**55.0**
Δ0191	AutoMS(n): TIC -All MS FullScan	6.608	6.566 - 6.650	**PE(15:1/13:0)**	632.8467	5428030	6.565	**633.437**	C33H64NO8P	2	EIC 632.8297 -All MS, Smoothed (1.58,2,GA)	**6.749**	6.469 - 7.120	189210000	**5.3**

Δ0191	AutoMS(n): TIC -All MS FullScan	7.206	7.120 - 7.292	**PE(15:1/15:0)**	660.9063	81889520	7.26	**661.4683**	C35H68NO8P	27	EIC 660.8610 -All MS, Smoothed (1.58,2,GA)	**7.222**	6.978 - 7.547	1580347044	**44.0**
Δ0191	AutoMS(n): TIC -All MS FullScan	7.87	7.814 - 7.927	**PE(16:0/15:0);PE(14:0/17:0)**	676.9642	27995564	7.822	**677.4996**	C36H72NO8P	12	EIC 676.8923 -All MS, Smoothed (1.58,2,GA)	**7.905**	7.693 - 8.085	386268599	**10.8**
Δ0191	AutoMS(n): TIC -All MS FullScan	8.149	8.144 - 8.154	**PE(16:0/17:0)**	704.9882	9739544	8.151	**705.5309**	C38H76NO8P	2	EIC 704.9236 -All MS, Smoothed (1.58,2,GA)	**8.14**	8.020 - 8.729	79529515	**2.2**
Δ0191	AutoMS(n): TIC -All MS FullScan	7.421	7.344 - 7.498	**PE(16:1/15:0)**	674.9334	88227768	7.36	**675.4839**	C36H70NO8P	34	EIC 674.8766 -All MS, Smoothed (1.58,2,GA)	**7.414**	7.251 - 8.005	1569337791	**43.7**
Δ0191	AutoMS(n): TIC -All MS FullScan	6.994	6.978 - 7.011	**PE(16:1/15:1);PE(17:1/14:1)**	672.8843	23997848	6.989	**673.4683**	C36H68NO8P	34	EIC 672.8610 -All MS, Smoothed (1.58,2,GA)	**7.111**	6.884 - 7.547	1678724801	**46.8**
Δ0191	AutoMS(n): TIC -All MS FullScan	7.248	7.213 - 7.283	**PE(16:1/16:1);PE(17:2/15:0)**	686.9492	117332808	7.26	**687.4839**	C37H70NO8P	38	EIC 686.8766 -All MS, Smoothed (1.58,2,GA)	**7.282**	7.120 - 7.585	1636361875	**45.6**
Δ0191	AutoMS(n): TIC -All MS FullScan	7.788	7.776 - 7.800	**PE(16:1/17:0)**	702.9748	41053180	7.793	**703.5152**	C38H74NO8P	15	EIC 702.9079 -All MS, Smoothed (1.58,2,GA)	**7.841**	7.693 - 8.844	689927540	**19.2**
Δ0191	AutoMS(n): TIC -All MS FullScan	6.463	6.365 - 6.561	**PE(16:2/14:1);PE(15:2/15:1)**	657.1898	21819300	6.363	**657.437**	C35H64NO8P	8	EIC 656.8297 -All MS, Smoothed (1.58,2,GA)	**6.52**	6.253 - 7.120	519176277	**14.5**
Δ0191	AutoMS(n): TIC -All MS FullScan	6.683	6.591 - 6.775	**PE(16:2/15:1);PE(15:2/16:1) ;PE(17:2/14:1)**	670.8973	33067080	6.677	**671.4526**	C36H66NO8P	12	EIC 670.8453 -All MS, Smoothed (1.58,2,GA)	**6.736**	6.511 - 7.251	728609751	**20.3**
Δ0191	AutoMS(n): TIC -All MS FullScan	6.379	6.253 - 6.505	**PE(16:2/15:2);PE(17:2/14:2)**	668.8638	2135341	6.283	**669.437**	C36H64NO8P	2	EIC 668.8297 -All MS, Smoothed (1.58,2,GA)	**6.381**	6.114 - 6.766	113487112	**3.2**
Δ0191	AutoMS(n): TIC -All MS FullScan	6.924	6.884 - 6.964	**PE(16:2/16:1); PE(17:2/15:1)**	684.9392	72989888	6.954	**685.4683**	C37H68NO8P	33	EIC 684.8610 -All MS, Smoothed (1.58,2,GA)	**6.983**	6.789 - 7.562	1507045387	**42.0**
Δ0191	AutoMS(n): TIC -All MS FullScan	8.233	8.216 - 8.250	**PE(17:0/17:0)**	719.0568	13274137	8.256	**719.5465**	C39H78NO8P	5	EIC 718.9392 -All MS, Smoothed (1.58,2,GA)	**8.28**	8.129 - 8.644	184944136	**5.2**
Δ0191	AutoMS(n): TIC -All MS FullScan	7.704	7.585 - 7.823	**PE(17:1/15:0);PE(16:1/16:0) ;PE(15:1/17:0)**	688.9562	31251632	7.608	**689.4996**	C37H72NO8P	9	EIC 688.8923 -All MS, Smoothed (1.58,2,GA)	**7.659**	7.481 - 7.776	509217301	**14.2**
Δ0191	AutoMS(n): TIC -All MS FullScan	7.325	7.251 - 7.399	**PE(17:1/16:1)**	699.9344	14526030	7.411	**701.4996**	C38H72NO8P	11	EIC 700.8923 -All MS, Smoothed (1.58,2,GA)	**7.441**	7.297 - 7.533	392061495	**10.9**
Δ0191	AutoMS(n): TIC -All MS FullScan	7.985	7.932 - 8.037	**PE(17:1/17:0)**	717.0205	24469504	7.914	**717.5309**	C39H76NO8P	5	EIC 716.9236 -All MS, Smoothed (1.58,2,GA)	**7.964**	7.753 - 8.399	317777803	**8.9**
Δ0191	AutoMS(n): TIC -All MS FullScan	6.744	6.703 - 6.784	**PE(17:2/13:0);PE(16:1/14:1); PE(15:1/15:1)**	658.8864	37071588	6.717	**659.4526**	C35H66NO8P	14	EIC 658.8453 -All MS, Smoothed (1.58,2,GA)	**6.87**	6.615 - 7.437	982907560	**27.4**
Δ0191	AutoMS(n): TIC -All MS FullScan	6.596	6.591 - 6.600	**PE(17:2/15:2);PE(16:2/16:2)**	683.2897	66420144	6.48	**683.4526**	C37H66NO8P	21	EIC 682.8453 -All MS, Smoothed (1.58,2,GA)	**6.656**	6.469 - 7.120	897681601	**25.0**
Δ0191	AutoMS(n): TIC -All MS FullScan	7.152	7.096 - 7.207	**PE(17:2/16:1);PE(16:2/17:1)**	698.9434	58310992	7.114	**699.4839**	C38H70NO8P	20	EIC 698.8766 -All MS, Smoothed (1.58,2,GA)	**7.163**	7.002 - 7.547	1063820821	**29.6**
Δ0191	AutoMS(n): TIC -All MS FullScan	6.806	6.789 - 6.822	**PE(17:2/16:2)**	697.2109	37240160	6.791	**697.4683**	C38H68NO8P	19	EIC 696.8610 -All MS, Smoothed (1.58,2,GA)	**6.857**	6.655 - 7.532	761456859	**21.2**
Δ0191	AutoMS(n): TIC -All MS FullScan	7.793	7.716 - 7.870	**PE(17:2/17:0); PE(17:1/17:1)**	715.4308		7.708	**715.5152**	C39H74NO8P	4	EIC 714.9079 -All MS, Smoothed (1.58,2,GA)	**7.772**	7.533 - 8.129	293071420	**8.2**
Δ0191	AutoMS(n): TIC -All MS FullScan	7.318	7.297 - 7.339	**PE(17:2/17:1)**	712.9663	13966728	7.311	**713.4996**	C39H72NO8P	4	EIC 712.8923 -All MS, Smoothed (1.58,2,GA)	**7.448**	7.190 - 7.585	241616370	**6.7**
Δ0191	AutoMS(n): TIC -All MS FullScan	7.029	7.025 - 7.034	**PE(17:2/17:2)**	711.3262	19540330	7.02	**711.4839**	C39H70NO8P	4	EIC 710.8766 -All MS, Smoothed (1.58,2,GA)	**7.047**	6.884 - 7.518	148984048	**4.2**
Δ0191	AutoMS(n): TIC -All MS FullScan	7.716	7.670 - 7.762	**PE(P-15:0/15:0)**	646.925	291322496	7.699	**647.489**	C35H70NO7P	100	EIC 646.8817 -All MS, Smoothed (1.58,2,GA)	**7.765**	7.562 - 8.757	4393949158	**122.5**
Δ0191	AutoMS(n): TIC -All MS FullScan	8.126	8.114 - 8.139	**PE(P-15:0/17:0)**	676.0035	8490969	8.071	**675.5203**	C37H74NO7P	12	EIC 674.8766 -All MS, Smoothed (1.58,2,GA)	**8.109**	8.005 - 8.701	89441967	**2.5**
Δ0191	AutoMS(n): TIC -All MS FullScan	6.999	6.978 - 7.019	**PG(14:0/15:0)**	680.1836	17656712	7.008	**680.4628**	C35H69O10P	4	EIC 679.8555 -All MS, Smoothed (1.58,2,GA)	**7.024**	6.837 - 7.297	168209440	**4.7**
Δ0191	AutoMS(n): TIC -All MS FullScan	7.159	7.143 - 7.175	**PG(15:0/15:0)**	694.2935	50463200	7.16	**694.4785**	C36H71O10P	15	EIC 693.8712 -All MS, Smoothed (1.58,2,GA)	**7.206**	7.025 - 7.585	682355973	**19.0**

Δ0191	AutoMS(n): TIC -All MS FullScan	6.834	6.789 - 6.878	**PG(15:0/15:1);PG(16:1/14:0)**	691.935	10644100	6.874	**692.4628**	C36H69O10P	3	EIC 691.8555 -All MS, Smoothed (1.58,2,GA)	**6.889**	6.640 - 7.227	181951876	**5.1**
Δ0191	AutoMS(n): TIC -All MS FullScan	7.041	7.025 - 7.058	**PG(15:0/16:1);PG(14:1/17:0)**	706.2571	16617700	7.091	**706.4785**	C37H71O10P	4	EIC 705.8712 -All MS, Smoothed (1.58,2,GA)	**7.101**	6.908 - 7.452	254478885	**7.1**
Δ0191	AutoMS(n): TIC -All MS FullScan	6.676	6.655 - 6.698	**PG(15:1/16:1;PG(15:0/16:2); PG(14:1/17:1);PG(14:0/17:2)**	704.2932	6353644	6.734	**704.4628**	C37H69O10P	2	EIC 703.8555 -All MS, Smoothed (1.58,2,GA)	**6.79**	6.543 - 7.120	137009336	**3.8**
Δ0191	AutoMS(n): TIC -All MS FullScan	7.411	7.390 - 7.432	**PG(16:0/16:1);PG(15:1/17:0); PG(15:0/17:1)**	720.4208		7.392	**720.4941**	C38H73O10P	6	EIC 719.8868 -All MS, Smoothed (1.58,2,GA)	**7.379**	7.120 - 7.693	237785930	**6.6**
Δ0191	AutoMS(n): TIC -All MS FullScan	7.882	7.861 - 7.903	**PG(16:0/17:0)**	736.3864	10673636	7.883	**736.5254**	C39H77O10P	2	EIC 735.9181 -All MS, Smoothed (1.58,2,GA)	**7.884**	7.730 - 8.114	79225045	**2.2**
Δ0191	AutoMS(n): TIC -All MS FullScan	6.905	6.884 - 6.925	**PG(16:1/16:1)**	717.9615	18296536	6.935	**718.4785**	C38H71O10P 1	8	EIC 717.8712 -All MS, Smoothed (1.58,2,GA)	**6.953**	6.743 - 7.390	359991181	**10.0**
Δ0191	AutoMS(n): TIC -All MS FullScan	6.728	6.718 - 6.737	**PG(16:1/16:2)**	715.9663	4541968	6.627	**716.4628**	C38H69O10P	2	EIC 715.8555 -All MS, Smoothed (1.58,2,GA)	**6.653**	6.511 - 7.166	92949097	**2.6**
Δ0191	AutoMS(n): TIC -All MS FullScan	7.556	7.533 - 7.579	**PG(17:0/16:1)**	734.3182	49140256	7.563	**734.5098**	C39H75O10P	11	EIC 733.9025 -All MS, Smoothed (1.58,2,GA)	**7.571**	7.437 - 7.885	432997682	**12.1**
Δ0191	AutoMS(n): TIC -All MS FullScan	7.997	7.980 - 8.014	**PG(17:0/17:0)**	750.3843	9315645	7.993	**750.5411**	C40H79O10P	3	EIC 749.9338 -All MS, Smoothed (1.58,2,GA)	**8.028**	7.861 - 8.352	90111776	**2.5**
Δ0191			7.533 - 8.005	**PG(17:0/17:1)**				**748.5254**			EIC 747.9181 -All MS, Smoothed (1.58,2,GA)	**7.694**	7.533 - 8.005	144109298	**4.0**
Δ0191	AutoMS(n): TIC -All MS FullScan	7.217	7.166 - 7.269	**PG(17:1/16:1)**	732.3124	9393053	7.215	**732.4941**	C39H73O10P	3	EIC 731.8868 -All MS, Smoothed (1.58,2,GA)	**7.116**	6.931 - 7.190	108067120	**3.0**
Sum negative														**3.588E+10**	**1000.0**
Δ0191	AutoMS(n): TIC +All MS FullScan	8.034	8.014 - 8.054	**DG(15:0/15:0/0:0)**	558.8811	285600672	8.071	**540.4754**	C33H64O5	7	EIC 558.9092 +All MS, Smoothed (1.40,2,GA)	**8.097**	7.792 - 8.335	4017667278	**8.2**
Δ0191	AutoMS(n): TIC +All MS FullScan	7.972	7.968 - 7.976	**DG(31:1)**	570.9417	129756992	8.007	**552.4754**	C34H64O5	4	EIC 570.9092 +All MS, Smoothed (1.40,2,GA)	**7.976**	7.807 - 8.197	1226915558	**2.5**
Δ0191	AutoMS(n): TIC +All MS FullScan	8.42	8.404 - 8.435	**DG(32:0)**	586.5668	109506352	8.451	**568.5067**	C35H68O5	2	EIC 586.9405 +All MS, Smoothed (1.40,2,GA)	**8.446**	8.289 - 8.913	1116232799	**2.3**
Δ0191	AutoMS(n): TIC +All MS FullScan	7.861	7.853 - 7.870	**DG(32:2)**	582.9741	113926352	7.862	**564.4754**	C35H64O5	2	EIC 582.9092 +All MS, Smoothed (1.40,2,GA)	**7.849**	7.709 - 8.105	1114034211	**2.3**
Δ0191			8.496 - 8.959	**DG(33:0)**				**582.5223**			EIC 600.9561 +All MS, Smoothed (1.40,2,GA)	**8.644**	8.496 - 8.959	423982286	**0.9**
Δ0191	AutoMS(n): TIC +All MS FullScan	8.328	8.312 - 8.343	**DG(33:1)**	599.5544	62732936	8.332	**580.5067**	C36H68O5	2	EIC 598.9405 +All MS, Smoothed (1.40,2,GA)	**8.338**	8.174 - 8.635	1012754882	**2.1**
				DG(33:2)										0	**0.0**
Δ0191	AutoMS(n): TIC +All MS FullScan	9.824	9.698 - 9.949	**TG(15:0/15:0/15:0)**	783.0929	3201516544	9.73	**764.6894**	C48H92O6	100	EIC 783.1232 +All MS, Smoothed (1.40,2,GA)	**9.753**	9.421 - 10.567	54792088912	**111.8**
Δ0191	AutoMS(n): TIC +All MS FullScan	8.837	8.821 - 8.853	**TG(38:1)**	683.2763		8.862	**666.5798**	C41H78O6	3	EIC 682.7169 +All MS, Smoothed (1.40,2,GA)	**8.847**	8.658 - 9.168	1429599181	**2.9**
Δ0191	AutoMS(n): TIC +All MS FullScan	9.114	9.098 - 9.130	**TG(39:0)**	699.2564	387571456	9.169	**680.5955**	C42H80O6	7	EIC 699.0293 +All MS, Smoothed (1.40,2,GA)	**9.156**	8.821 - 9.421	4650697044	**9.5**
Δ0191	AutoMS(n): TIC +All MS FullScan	8.952	8.936 - 8.968	**TG(39:1)**	696.9078	176704912	8.995	**678.5798**	C42H78O6	4	EIC 697.0136 +All MS, Smoothed (1.40,2,GA)	**8.986**	8.682 - 9.398	2110955429	**4.3**
Δ0191	AutoMS(n): TIC +All MS FullScan	9.045	9.029 - 9.061	**TG(40:1)**	710.9408	309019808	9.072	**692.5955**	C43H80O6	7	EIC 711.0293 +All MS, Smoothed (1.40,2,GA)	**9.092**	8.566 - 9.581	4617695265	**9.4**

Δ0191	AutoMS(n): TIC +All MS FullScan	8.883	8.867 - 8.899	**TG(40:2)**	709.2954	167736416	8.913	**690.5798**	C43H78O6	3	EIC 709.0136 +All MS, Smoothed (1.40,2,GA)	**8.907**	8.542 - 9.352	1886370294	**3.9**
Δ0191			8.821 - 9.721	**TG(41:1)**				**706.61114**			EIC 725.0450 +All MS, Smoothed (1.40,2,GA)	**9.223**	8.821 - 9.721	6690435497	**13.7**
Δ0191	AutoMS(n): TIC +All MS FullScan	8.999	8.983 - 9.015	**TG(41:2)**	723.2427	204851904	8.998	**704.5955**	C44H80O6	5	EIC 723.0293 +All MS, Smoothed (1.40,2,GA)	**9.044**	8.589 - 9.421	3318902410	**6.8**
Δ0191	AutoMS(n): TIC +All MS FullScan	8.841	8.797 - 8.884	**TG(41:3)**	720.9038	121418096	8.878	**702.5798**	C44H78O6	2	EIC 720.9538 +All MS, Smoothed (1.40,2,GA)	**8.839**	8.658 - 9.029	1242992803	**2.5**
Δ0191	AutoMS(n): TIC +All MS FullScan	9.276	9.260 - 9.292	**TG(42:1)**	738.9726	1197755520	9.331	**722.6424**	C45H86O6	24	EIC 739.0606 +All MS, Smoothed (1.40,2,GA)	**9.304**	8.983 - 9.629	12393472902	**25.3**
Δ0191	AutoMS(n): TIC +All MS FullScan	9.142	9.075 - 9.208	**TG(42:2)**	736.9742	393436672	9.149	**718.6111**	C45H82O6	10	EIC 737.0449 +All MS, Smoothed (1.40,2,GA)	**9.16**	8.589 - 9.629	6725958949	**13.7**
Δ0191	AutoMS(n): TIC +All MS FullScan	9.534	9.514 - 9.554	**TG(43:0)**	755.0378	1871826688	9.557	**736.6581**	C46H88O6	41	EIC 755.0919 +All MS, Smoothed (1.40,2,GA)	**9.567**	9.237 - 9.848	21581166153	**44.1**
Δ0191	AutoMS(n): TIC +All MS FullScan	9.391	9.375 - 9.407	**TG(43:1)**	753.0243	943389440	9.419	**734.6424**	C46H86O6	21	EIC 753.0762 +All MS, Smoothed (1.40,2,GA)	**9.427**	8.983 - 9.848	12482769381	**25.5**
Δ0191	AutoMS(n): TIC +All MS FullScan	9.23	9.214 - 9.246	**TG(43:2)**	751.3078	1071040832	9.28	**732.6268**	C46H84O6	22	EIC 751.0606 +All MS, Smoothed (1.40,2,GA)	**9.255**	8.936 - 9.652	10947414707	**22.3**
Δ0191	AutoMS(n): TIC +All MS FullScan	9.068	9.052 - 9.084	**TG(43:3)**	749.3679	346536416	9.049	**730.6111**	C46H82O6	6	EIC 749.0449 +All MS, Smoothed (1.40,2,GA)	**9.091**	8.751 - 9.652	3968696972	**8.1**
Δ0191	AutoMS(n): TIC +All MS FullScan	9.645	9.629 - 9.661	**TG(44:0)**	769.0687	2067022080	9.677	**750.6737**	C47H90O6	52	EIC 769.9820 +All MS, Smoothed (1.40,2,GA)	**9.684**	9.306 - 9.894	12242499864	**25.0**
Δ0191	AutoMS(n): TIC +All MS FullScan	9.472	9.445 - 9.500	**TG(44:1)**	767.0495	1607156352	9.485	**748.6581**	C47H88O6	39	EIC 767.0919 +All MS, Smoothed (1.40,2,GA)	**9.516**	9.144 - 9.802	22269648080	**45.5**
Δ0191	AutoMS(n): TIC +All MS FullScan	9.373	9.306 - 9.439	**TG(44:2)**	765.0177	988270912	9.345	**746.6424**	C47H86O6	24	EIC 765.1127 +All MS, Smoothed (1.40,2,GA)	**9.361**	8.983 - 9.776	13446682082	**27.4**
Δ0191	AutoMS(n): TIC +All MS FullScan	9.16	9.144 - 9.176	**TG(44:3)**	763.3187	389996544	9.238	**744.6268**	C47H84O6	10	EIC 763.0606 +All MS, Smoothed (1.40,2,GA)	**9.213**	8.890 - 9.421	5620922973	**11.5**
Δ0191	AutoMS(n): TIC +All MS FullScan	8.991	8.983 - 9.000	**TG(44:4)**	761.3045	149899776	9.025	**742.6111**	C47H82O6	2	EIC 761.0449 +All MS, Smoothed (1.40,2,GA)	**9.025**	8.797 - 9.468	1857081487	**3.8**
Δ0191	AutoMS(n): TIC +All MS FullScan	9.626	9.560 - 9.693	**TG(45:1)**	781.0809	1718205184	9.592	**762.6737**	C48H90O6	39	EIC 781.1075 +All MS, Smoothed (1.40,2,GA)	**9.62**	9.283 - 9.871	22048528241	**45.0**
Δ0191	AutoMS(n): TIC +All MS FullScan	9.426	9.398 - 9.453	**TG(45:2)**	779.0534	1301368192	9.442	**760.6581**	C48H88O6	26	EIC 779.0919 +All MS, Smoothed (1.40,2,GA)	**9.457**	9.121 - 9.721	15710861847	**32.1**
Δ0191	AutoMS(n): TIC +All MS FullScan	9.303	9.283 - 9.324	**TG(45:3)**	777.4882		9.299	**758.6424**	C48H86O6	16	EIC 777.0762 +All MS, Smoothed (1.40,2,GA)	**9.295**	8.890 - 9.802	9218368560	**18.8**
Δ0191	AutoMS(n): TIC +All MS FullScan	9.142	9.121 - 9.162	**TG(45:4)**	775.3878	300068864	9.123	**758.6424**	C48H86O6	5	EIC 775.0606 +All MS, Smoothed (1.40,2,GA)	**9.147**	8.913 - 9.583	3210820468	**6.6**
Δ0191	AutoMS(n): TIC +All MS FullScan	9.841	9.825 - 9.857	**TG(46:0)**	797.1096	1896510720	9.853	**779.7129**	C49H95O6	36	EIC 797.1389 +All MS, Smoothed (1.40,2,GA)	**9.864**	9.491 - 10.590	21494945137	**43.9**
Δ0191	AutoMS(n): TIC +All MS FullScan	9.657	9.629 - 9.684	**TG(46:1)**	795.1166	2225703168	9.68	**776.6894**	C49H92O6	47	EIC 795.1232 +All MS, Smoothed (1.40,2,GA)	**9.689**	9.398 - 10.056	27577357781	**56.3**
Δ0191	AutoMS(n): TIC +All MS FullScan	9.53	9.514 - 9.546	**TG(46:2)**	793.3588	2006646528	9.543	**774.6737**	C49H90O6	41	EIC 793.1075 +All MS, Smoothed (1.40,2,GA)	**9.556**	9.191 - 9.986	21168793221	**43.2**
Δ0191	AutoMS(n): TIC +All MS FullScan	9.368	9.352 - 9.384	**TG(46:3)**	791.0742	741538048	9.391	**772.6581**	C49H88O6	15	EIC 791.0919 +All MS, Smoothed (1.40,2,GA)	**9.399**	9.075 - 9.894	9256418531	**18.9**
Δ0191	AutoMS(n): TIC +All MS FullScan	9.887	9.871 - 9.903	**TG(47:0)**	811.1758	2333168640	9.911	**792.7207**	C50H96O6	55	EIC 811.1545 +All MS, Smoothed (1.40,2,GA)	**9.925**	9.629 - 10.638	29279806732	**59.8**
Δ0191	AutoMS(n): TIC +All MS FullScan	9.767	9.747 - 9.787	**TG(47:1)**	809.1361	1231299584	9.784	**790.705**	C50H94O6	26	EIC 809.1388 +All MS, Smoothed (1.40,2,GA)	**9.8**	9.398 - 10.427	16462638369	**33.6**
Δ0191	AutoMS(n): TIC +All MS FullScan	9.592	9.560 - 9.624	**TG(47:2)**	807.1119	1113617920	9.616	**788.6894**	C50H92O6	27	EIC 807.1232 +All MS, Smoothed (1.40,2,GA)	**9.629**	9.329 - 10.032	15792107652	**32.2**

Δ0191			9.098 - 9.675	**TG(47:3)**				**786.6737**			EIC 805.1075 +All MS, Smoothed (1.40,2,GA)	**9.491**	9.098 - 9.675	8552338415	**17.5**
Δ0191			9.052 - 9.537	**TG(47:4)**				**784.6581**			EIC 803.0919 +All MS, Smoothed (1.40,2,GA)	**9.346**	9.052 - 9.537	4271167167	**8.7**
Δ0191	AutoMS(n): TIC +All MS FullScan	10.002	9.986 - 10.018	**TG(48:0)**	825.1728	977887616	10.073	**806.7363**	C51H98O6	19	EIC 825.1701 +All MS, Smoothed (1.40,2,GA)	**10.022**	9.894 - 10.567	8908110989	**18.2**
Δ0191	AutoMS(n): TIC +All MS FullScan	9.834	9.802 - 9.865	**TG(48:1)**	822.5439	213472592	9.759	**802.705**	C51H94O6	21	EIC 823.1545 +All MS, Smoothed (1.40,2,GA)	**9.87**	9.537 - 10.427	13516164988	**27.6**
Δ0191	AutoMS(n): TIC +All MS FullScan	9.746	9.721 - 9.770	**TG(48:2)**	821.52	840556416	9.759	**802.705**	C51H94O6	14	EIC 821.1388 +All MS, Smoothed (1.40,2,GA)	**9.738**	9.398 - 10.125	9388179522	**19.2**
Δ0191			9.191 - 9.825	**TG(48:3)**				**800.6894**			EIC 819.1232 +All MS, Smoothed (1.40,2,GA)	**9.576**	9.191 - 9.825	6207506885	**12.7**
Δ0191	AutoMS(n): TIC +All MS FullScan	9.449	9.121 - 9.606	**TG(48:4)**	818.1275	184542128	9.458	**798.6737**	C51H90O6	7	EIC 817.1075 +All MS, Smoothed (1.40,2,GA)	**9.422**	9.121 - 9.606	3723045468	**7.6**
Δ0191	AutoMS(n): TIC +All MS FullScan	10.048	10.032 - 10.064	**TG(49:0)**	839.1981	920468800	10.065	**820.752**	C52H100O6	18	EIC 839.1858 +All MS, Smoothed (1.40,2,GA)	**10.078**	9.747 - 10.590	9841584231	**20.1**
Δ0191	AutoMS(n): TIC +All MS FullScan	9.949	9.894 - 10.004	**TG(49:1)**	837.1941	455091040	9.931	**818.7363**	C52H98O6	9	EIC 837.1701 +All MS, Smoothed (1.40,2,GA)	**9.954**	9.583 - 10.544	6083654389	**12.4**
Δ0191	AutoMS(n): TIC +All MS FullScan	9.832	9.776 - 9.888	**TG(49:2)**	835.1757	372421120	9.827	**816.7207**	C52H96O6	10	EIC 835.1545 +All MS, Smoothed (1.40,2,GA)	**9.823**	9.537 - 10.125	5508630067	**11.2**
Δ0191	AutoMS(n): TIC +All MS FullScan	10.268	10.264 - 10.273	**TG(50:0)**	854.1713	85396608	10.278	**834.7676**	C53H102O6	5	EIC 853.2014 +All MS, Smoothed (1.40,2,GA)	**10.175**	9.825 - 10.758	2684632396	**5.5**
Δ0191	AutoMS(n): TIC +All MS FullScan	10.03	10.009 - 10.050	**TG(50:1)**	851.2346	329314944	10.058	**832.752**	C53H100O6	6	EIC 851.1858 +All MS, Smoothed (1.40,2,GA)	**10.018**	9.747 - 10.638	3313958273	**6.8**
Δ0191	AutoMS(n): TIC +All MS FullScan	10.21	10.194 - 10.226	**TG(51:0)**	867.5423	240854672	10.231	**848.7833**	C54H104O6	4	EIC 867.2171 +All MS, Smoothed (1.40,2,GA)	**10.216**	9.894 - 10.711	1861834182	**3.8**
Δ0191	AutoMS(n): TIC +All MS FullScan	10.099	10.079 - 10.119	**TG(51:1)**	865.3401	120854448	10.108	**846.7676**	C54H102O6	2	EIC 865.2014 +All MS, Smoothed (1.40,2,GA)	**10.1**	9.825 - 10.567	1362833913	**2.8**
Δ0191			10.217 - 10.686	**TG(52:0)**				**862.7989**			EIC 881.2327 +All MS, Smoothed (1.40,2,GA)	**10.353**	10.217 - 10.686	259282825	**0.5**
Sum positive														**4.899E+11**	**1000**
MXAN_3748	AutoMS(n): TIC -All MS FullScan	6.466	6.448 - 6.484	**PE(12:1/17:1);PE(13:1/16:1); PE(16:2/13:0);PE(14:1/15:1)**	645.1494	9582117	6.442	**645.437**	C34H64NO8P	11	EIC 644.8297 -All MS, Smoothed (1.58,2,GA)	**6.578**	6.313 - 7.100	631044316	**17.8**
MXAN_3748	AutoMS(n): TIC -All MS FullScan	7.203	7.193 - 7.212	**PE(14:0/14:0);PE(13:0/15:0)**	635.1627	6685988	7.212	**635.4526**	C33H66NO8P	2	EIC 634.8453 -All MS, Smoothed (1.58,2,GA)	**7.061**	6.888 - 7.502	147459117	**4.2**
MXAN_3748	AutoMS(n): TIC -All MS FullScan	7.308	7.292 - 7.325	**PE(14:0/15:0)**	648.8766	34066372	7.325	**649.4683**	C34H68NO8P	22	EIC 648.8610 -All MS, Smoothed (1.58,2,GA)	**7.369**	7.218 - 7.583	835126931	**23.5**
MXAN_3748	AutoMS(n): TIC -All MS FullScan	6.167	6.148 - 6.186	**PE(14:1/14:1);PE(16:1/12:1)PE(15:1/13:1)**	630.8482	2345461	6.168	**631.4213**	C33H62NO8P	1	EIC 630.8140 -All MS, Smoothed (1.58,2,GA)	**6.345**	5.728 - 6.683	114531371	**3.2**
MXAN_3748	AutoMS(n): TIC -All MS FullScan	6.857	6.841 - 6.873	**PE(14:1/15:0);PE(16:1/13:0)**	646.88	32999208	6.851	**647.4526**	C34H66NO8P1	30	EIC 646.8453 -All MS, Smoothed (1.58,2,GA)	**7.013**	6.732 - 7.539	1579244971	**44.5**
MXAN_3748	AutoMS(n): TIC -All MS FullScan	7.523	7.455 - 7.591	**PE(15:0/15:0)**	662.9268	187241520	7.477	**663.4839**	C35H70NO8P	80	EIC 662.8766 -All MS, Smoothed (1.58,2,GA)	**7.562**	7.362 - 8.260	4659376458	**131.3**
MXAN_3748	AutoMS(n): TIC -All MS FullScan	7.865	7.855 - 7.874	**PE(15:0/17:0)**	689.9581	4310535	7.897	**691.5152**	C37H74NO8P	17	EIC 690.9079 -All MS, Smoothed (1.58,2,GA)	**7.937**	7.789 - 8.763	867708251	**24.5**
MXAN_3748	AutoMS(n): TIC -All MS FullScan	6.6	6.578 - 6.622	**PE(15:1/13:0)**	632.8305	5139937	6.565	**633.437**	C33H64NO8P	2	EIC 632.8297 -All MS, Smoothed (1.58,2,GA)	**6.743**	6.474 - 7.053	185423979	**5.2**

MXAN_3748	AutoMS(n): TIC -All MS FullScan	7.205	7.124 - 7.287	**PE(15:1/15:0)**	660.9162	83045192	7.26	**661.4683**	C35H68NO8P	27	EIC 660.8610 -All MS, Smoothed (1.58,2,GA)	**7.229**	6.958 - 7.568	1556018154	**43.9**
MXAN_3748	AutoMS(n): TIC -All MS FullScan	7.815	7.803 - 7.827	**PE(16:0/15:0);PE(14:0/17:0)**	676.9522	26270604	7.822	**677.4996**	C36H72NO8P	5	EIC 676.8923 -All MS, Smoothed (1.58,2,GA)	**7.812**	7.568 - 8.023	216935819	**6.1**
MXAN_3748	AutoMS(n): TIC -All MS FullScan	8.145	8.114 - 8.176	**PE(16:0/17:0)**	705.0287	12388290	8.151	**705.5309**	C38H76NO8P	10	EIC 704.9236 -All MS, Smoothed (1.58,2,GA)	**8.167**	8.023 - 8.735	119361108	**3.4**
MXAN_3748	AutoMS(n): TIC -All MS FullScan	7.429	7.339 - 7.519	**PE(16:1/15:0)**	674.9307	53978188	7.36	**675.4839**	C36H70NO8P	32	EIC 674.8766 -All MS, Smoothed (1.58,2,GA)	**7.416**	7.247 - 7.832	1340973228	**37.8**
MXAN_3748	AutoMS(n): TIC -All MS FullScan	6.987	6.958 - 7.015	**PE(16:1/15:1);PE(17:1/14:1)**	672.4053		6.989	**673.4683**	C36H68NO8P	32	EIC 672.8610 -All MS, Smoothed (1.58,2,GA)	**7.118**	6.888 - 7.554	1541423855	**43.5**
MXAN_3748	AutoMS(n): TIC -All MS FullScan	7.186	7.170 - 7.203	**PE(16:1/16:1);PE(17:2/15:0)**	685.9182	6481096	7.195	**687.4839**	C37H70NO8P	29	EIC 686.8766 -All MS, Smoothed (1.58,2,GA)	**7.281**	7.100 - 7.818	1698284066	**47.9**
MXAN_3748	AutoMS(n): TIC -All MS FullScan	7.812	7.774 - 7.850	**PE(16:1/17:0)**	702.9643	67091320	7.793	**703.5152**	C38H74NO8P	22	EIC 702.9079 -All MS, Smoothed (1.58,2,GA)	**7.831**	7.690 - 8.814	947633173	**26.7**
MXAN_3748	AutoMS(n): TIC -All MS FullScan	6.373	6.341 - 6.404	**PE(16:2/14:1);PE(15:2/15:1)**	656.8871	8386795	6.363	**657.437**	C35H64NO8P	8	EIC 656.8297 -All MS, Smoothed (1.58,2,GA)	**6.52**	5.783 - 6.983	488156001	**13.8**
MXAN_3748	AutoMS(n): TIC -All MS FullScan	6.691	6.603 - 6.778	**PE(16:2/15:1);PE(15:2/16:1); PE(17:2/14:1)**	670.8878	42669940	6.695	**671.4526**	C36H66NO8P	14	EIC 670.8453 -All MS, Smoothed (1.58,2,GA)	**6.743**	6.500 - 7.193	876593798	**24.7**
MXAN_3748	AutoMS(n): TIC -All MS FullScan	6.278	6.259 - 6.297	**PE(16:2/15:2);PE(17:2/14:2)**	669.1815	2787012	6.283	**669.437**	C36H64NO8P	3	EIC 668.8297 -All MS, Smoothed (1.58,2,GA)	**6.377**	6.092 - 7.076	136907428	**3.9**
MXAN_3748	AutoMS(n): TIC -All MS FullScan	6.904	6.888 - 6.920	**PE(16:2/16:1); PE(17:2/15:1)**	684.922	29903068	6.954	**685.4683**	C37H68NO8P	29	EIC 684.8610 -All MS, Smoothed (1.58,2,GA)	**6.986**	6.793 - 7.568	1269109284	**35.8**
MXAN_3748	AutoMS(n): TIC -All MS FullScan	8.266	8.220 - 8.313	**PE(17:0/17:0)**	719.0441	49635156	8.256	**719.5465**	C39H78NO8P	12	EIC 718.9392 -All MS, Smoothed (1.58,2,GA)	**8.285**	8.140 - 8.679	514979986	**14.5**
MXAN_3748	AutoMS(n): TIC -All MS FullScan	7.565	7.554 - 7.577	**PE(17:1/15:0);PE(16:1/16:0); PE(15:1/17:0)**	688.9095	26602752	7.608	**689.4996**	C37H72NO8P	17	EIC 688.8923 -All MS, Smoothed (1.58,2,GA)	**7.668**	7.455 - 8.246	902071627	**25.4**
MXAN_3748	AutoMS(n): TIC -All MS FullScan	7.5	7.386 - 7.614	**PE(17:1/16:1)**	700.9668	54134520	7.411	**701.4996**	C38H72NO8P	15	EIC 700.8923 -All MS, Smoothed (1.58,2,GA)	**7.442**	7.316 - 7.539	495101376	**14.0**
MXAN_3748	AutoMS(n): TIC -All MS FullScan	7.968	7.903 - 8.032	**PE(17:1/17:0)**	717.0283	52720592	7.914	**717.5309**	C39H76NO8P	13	EIC 716.9236 -All MS, Smoothed (1.58,2,GA)	**8.021**	7.818 - 8.790	886639475	**25.0**
MXAN_3748	AutoMS(n): TIC -All MS FullScan	6.68	6.667 - 6.693	**PE(17:2/13:0);PE(16:1/14:1); PE(15:1/15:1)**	657.7933	2370370	6.717	**659.4526**	C35H66NO8P	8	EIC 658.8453 -All MS, Smoothed (1.58,2,GA)	**6.873**	6.628 - 7.386	1005818351	**28.4**
MXAN_3748	AutoMS(n): TIC -All MS FullScan	6.438	6.313 - 6.563	**PE(17:2/15:2);PE(16:2/16:2)**	682.8928	4280578	6.543	**683.4526**	C37H66NO8P	20	EIC 682.8453 -All MS, Smoothed (1.58,2,GA)	**6.661**	6.448 - 7.231	814084054	**22.9**
MXAN_3748	AutoMS(n): TIC -All MS FullScan	7.116	7.100 - 7.132	**PE(17:2/16:1);PE(16:2/17:1)**	698.9415	50014316	7.114	**699.4839**	C38H70NO8P	26	EIC 698.8766 -All MS, Smoothed (1.58,2,GA)	**7.175**	7.006 - 7.690	1352393140	**38.1**
MXAN_3748	AutoMS(n): TIC -All MS FullScan	6.809	6.793 - 6.826	**PE(17:2/16:2)**	697.2904	43761224	6.791	**697.4683**	C38H68NO8P	27	EIC 696.8610 -All MS, Smoothed (1.58,2,GA)	**6.864**	6.683 - 7.362	1018784117	**28.7**
MXAN_3748	AutoMS(n): TIC -All MS FullScan	7.73	7.690 - 7.769	**PE(17:2/17:0); PE(17:1/17:1)**	715.2953	43304008	7.708	**715.5152**	C39H74NO8P	11	EIC 714.9079 -All MS, Smoothed (1.58,2,GA)	**7.776**	7.539 - 8.289	667362870	**18.8**
MXAN_3748	AutoMS(n): TIC -All MS FullScan	7.313	7.292 - 7.333	**PE(17:2/17:1)**	713.253	27120128	7.311	**713.4996**	C39H72NO8P	10	EIC 712.8923 -All MS, Smoothed (1.58,2,GA)	**7.451**	7.193 - 7.789	545866676	**15.4**
MXAN_3748	AutoMS(n): TIC -All MS FullScan	7.023	7.006 - 7.039	**PE(17:2/17:2)**	711.3853		7.02	**711.4839**	C39H70NO8P	8	EIC 710.8766 -All MS, Smoothed (1.58,2,GA)	**7.052**	6.888 - 7.432	320258022	**9.0**
MXAN_3748	AutoMS(n): TIC -All MS FullScan	7.754	7.667 - 7.841	**PE(P-15:0/15:0)**	647.2	228051936	7.699	**647.489**	C35H70NO7P	100	EIC 646.8817 -All MS, Smoothed (1.58,2,GA)	**7.777**	7.539 - 9.247	4687887430	**132.1**
MXAN_3748	AutoMS(n): TIC -All MS FullScan	8.059	8.047 - 8.071	**PE(P-15:0/17:0)**	675.9549	4499801	8.071	**675.5203**	C37H74NO7P	6	EIC 674.9130 -All MS, Smoothed (1.58,2,GA)	**8.118**	7.975 - 8.707	211950113	**6.0**
MXAN_3748	AutoMS(n): TIC -All MS FullScan	6.992	6.983 - 7.001	**PG(14:0/15:0)**	680.2952	19729438	7.008	**680.4628**	C35H69O10P	4	EIC 679.8555 -All MS, Smoothed (1.58,2,GA)	**7.025**	6.770 - 7.232	126235411	**3.6**
MXAN_3748	AutoMS(n): TIC -All MS FullScan	7.163	7.147 - 7.179	**PG(15:0/15:0)**	694.3254	41480812	7.16	**694.4785**	C36H71O10P	12	EIC 693.8712 -All MS, Smoothed (1.58,2,GA)	**7.204**	7.030 - 7.643	494120026	**13.9**

MXAN_3748	AutoMS(n): TIC -All MS FullScan	6.885	6.793 - 6.977	**PG(15:0/15:1);PG(16:1/14:0)**	691.9441	7460626	6.894	**692.4628**	C36H69O10P	3	EIC 691.8555 -All MS, Smoothed (1.58,2,GA)	**6.887**	6.603 - 7.147	139439791	**3.9**
MXAN_3748	AutoMS(n): TIC -All MS FullScan	7.069	7.053 - 7.086	**PG(15:0/16:1);PG(14:1/17:0)**	706.2852	18279664	7.091	**706.4785**	C37H71O10P	4	EIC 705.8712 -All MS, Smoothed (1.58,2,GA)	**7.098**	6.911 - 7.386	206620577	**5.8**
MXAN_3748	AutoMS(n): TIC -All MS FullScan	6.705	6.683 - 6.726	**PG(15:1/16:1;PG(15:0/16:2); PG(14:1/17:1);PG(14:0/17:2)**	704.233	6790435	6.734	**704.4628**	C37H69O10P	2	EIC 704.9236 -All MS, Smoothed (1.58,2,GA)	**6.785**	6.554 - 7.124	60397212	**1.7**
MXAN_3748	AutoMS(n): TIC -All MS FullScan	7.348	7.339 - 7.357	**PG(16:0/16:1);PG(15:1/17:0); PG(15:0/17:1)**	720.3273	20787600	7.392	**720.4941**	C38H73O10P	4	EIC 719.8868 -All MS, Smoothed (1.58,2,GA)	**7.375**	7.124 - 7.667	214396558	**6.0**
MXAN_3748	AutoMS(n): TIC -All MS FullScan	7.876	7.855 - 7.898	**PG(16:0/17:0)**	736.0376	12730603	7.883	**736.5254**	C39H77O10P	3	EIC 735.9181 -All MS, Smoothed (1.58,2,GA)	**7.892**	7.774 - 8.345	100975182	**2.8**
MXAN_3748	AutoMS(n): TIC -All MS FullScan	6.927	6.911 - 6.944	**PG(16:1/16:1)**	718.2856	25286012	6.935	**718.4785**	C38H71O10P 1	5	EIC 717.8712 -All MS, Smoothed (1.58,2,GA)	**6.952**	6.770 - 7.539	267747214	**7.5**
MXAN_3748			5.839 - 7.006	**PG(16:1/16:2)**				**716.4628**			EIC 716.9236 -All MS, Smoothed (1.58,2,GA)	**6.637**	5.839 - 7.006	100852772	**2.8**
MXAN_3748	AutoMS(n): TIC -All MS FullScan	7.562	7.525 - 7.600	**PG(17:0/16:1)**	734.2773	47584172	7.563	**734.5098**	C39H75O10P	14	EIC 733.9025 -All MS, Smoothed (1.58,2,GA)	**7.574**	7.386 - 8.047	541628129	**15.3**
MXAN_3748	AutoMS(n): TIC -All MS FullScan	7.991	7.975 - 8.008	**PG(17:0/17:0)**	750.4648	22524744	7.993	**750.5411**	C40H79O10P	6	EIC 749.9338 -All MS, Smoothed (1.58,2,GA)	**8.025**	7.880 - 8.275	216890413	**6.1**
MXAN_3748	AutoMS(n): TIC -All MS FullScan	7.707	7.667 - 7.746	**PG(17:0/17:1)**	748.3705	23150438	7.715	**748.5254**	C40H77O10P	5	EIC 747.9181 -All MS, Smoothed (1.58,2,GA)	**7.723**	7.502 - 8.062	238252735	**6.7**
MXAN_3748	AutoMS(n): TIC -All MS FullScan	7.097	7.076 - 7.118	**PG(17:1/16:1)**	732.3453	17980452	7.215	**732.4941**	C39H73O10P	4	EIC 731.8868 -All MS, Smoothed (1.58,2,GA)	**7.106**	6.935 - 7.218	132045509	**3.7**
Sum negative														**3.547E+10**	**1000.0**
MXAN_3748	AutoMS(n): TIC +All MS FullScan	8.036	8.020 - 8.052	**DG(15:0/15:0/0:0)**	559.0586		8.071	**540.4754**	C33H64O5	14	EIC 558.9092 +All MS, Smoothed (1.40,2,GA)	**8.084**	7.595 - 8.504	4423957409	**12.8**
MXAN_3748	AutoMS(n): TIC +All MS FullScan	7.949	7.928 - 7.969	**DG(31:1)**	570.6583	129381168	8.007	**552.4754**	C34H64O5	3	EIC 570.9092 +All MS, Smoothed (1.40,2,GA)	**7.972**	7.762 - 8.227	1301125173	**3.8**
MXAN_3748	AutoMS(n): TIC +All MS FullScan	8.427	8.411 - 8.443	**DG(32:0)**	586.9369	109471312	8.451	**568.5067**	C35H68O5	3	EIC 586.9405 +All MS, Smoothed (1.40,2,GA)	**8.447**	8.158 - 8.944	1054715297	**3.0**
MXAN_3748	AutoMS(n): TIC +All MS FullScan	7.88	7.837 - 7.923	**DG(32:2)**	582.9771	150735440	7.862	**564.4754**	C35H64O5	4	EIC 582.9092 +All MS, Smoothed (1.40,2,GA)	**7.876**	7.655 - 8.020	1478714210	**4.3**
MXAN_3748	AutoMS(n): TIC +All MS FullScan	8.64	8.620 - 8.660	**DG(33:0)**	600.9788	50767800	8.669	**582.5223**	C36H70O5	1	EIC 600.9561 +All MS, Smoothed (1.40,2,GA)	**8.648**	8.504 - 8.851	347126229	**1.0**
MXAN_3748	AutoMS(n): TIC +All MS FullScan	8.312	8.296 - 8.328	**DG(33:1)**	598.6971	188528576	8.336	**580.5067**	C36H68O5	5	EIC 598.9405 +All MS, Smoothed (1.40,2,GA)	**8.33**	8.135 - 8.596	1392989382	**4.0**
MXAN_3748	AutoMS(n): TIC +All MS FullScan	8.017	7.997 - 8.038	**DG(33:2)**	596.9762	85371024	8.026	**578.491**	C36H66O5	2	EIC 596.9248 +All MS, Smoothed (1.40,2,GA)	**8.018**	7.837 - 8.020	572214408	**1.6**
MXAN_3748	AutoMS(n): TIC +All MS FullScan	9.711	9.684 - 9.739	**TG(15:0/15:0/15:0)**	782.5694		9.73	**764.6894**	C48H92O6	83	EIC 783.1232 +All MS, Smoothed (1.40,2,GA)	**9.758**	9.430 - 10.238	30039602740	**86.6**
MXAN_3748	AutoMS(n): TIC +All MS FullScan	8.814	8.805 - 8.823	**TG(38:1)**	682.8636	65986044	8.862	**666.5798**	C41H78O6	2	EIC 682.7169 +All MS, Smoothed (1.40,2,GA)	**8.829**	8.643 - 9.130	610804520	**1.8**
MXAN_3748	AutoMS(n): TIC +All MS FullScan	9.123	9.106 - 9.139	**TG(39:0)**	699.3033	226497792	9.169	**680.5955**	C42H80O6	6	EIC 699.0293 +All MS, Smoothed (1.40,2,GA)	**9.168**	8.828 - 9.545	2709149396	**7.8**
MXAN_3748	AutoMS(n): TIC +All MS FullScan	8.988	8.967 - 9.008	**TG(39:1)**	697.3301		8.995	**678.5798**	C42H78O6	3	EIC 697.0136 +All MS, Smoothed (1.40,2,GA)	**8.988**	8.759 - 9.153	838467610	**2.4**
MXAN_3748	AutoMS(n): TIC +All MS FullScan	9.053	9.037 - 9.069	**TG(40:1)**	710.9272	133654288	9.072	**692.5955**	C43H80O6	5	EIC 711.0293 +All MS, Smoothed (1.40,2,GA)	**9.1**	8.689 - 9.384	2105829344	**6.1**

MXAN_3748	AutoMS(n): TIC +All MS FullScan	8.891	8.875 - 8.907	TG(40:2)	709.3381		8.913	690.5798	C43H78O6	2	EIC 709.0136 +All MS, Smoothed (1.40,2,GA)	8.909	8.504 - 9.199	1003825444	2.9
MXAN_3748			8.851 - 9.453	TG(41:1)				706.61114			EIC 725.0450 +All MS, Smoothed (1.40,2,GA)	9.229	8.851 - 9.453	3955530120	11.4
MXAN_3748	AutoMS(n): TIC +All MS FullScan	9.007	8.991 - 9.023	TG(41:2)	722.9503	133169856	8.998	704.5955	C44H80O6	4	EIC 723.0293 +All MS, Smoothed (1.40,2,GA)	9.043	8.713 - 9.361	1823721061	5.3
MXAN_3748	AutoMS(n): TIC +All MS FullScan	8.86	8.851 - 8.869	TG(41:3)	720.9155	62450500	8.878	702.5798	C44H78O6	1	EIC 720.9538 +All MS, Smoothed (1.40,2,GA)	8.838	8.689 - 9.014	661133147	1.9
MXAN_3748	AutoMS(n): TIC +All MS FullScan	9.307	9.291 - 9.323	TG(42:1)	738.9778	884013952	9.331	722.6424	C45H86O6	22	EIC 739.0606 +All MS, Smoothed (1.40,2,GA)	9.311	8.991 - 9.568	7325580217	21.1
MXAN_3748	AutoMS(n): TIC +All MS FullScan	9.099	9.083 - 9.115	TG(42:2)	736.9563	200405248	9.149	718.6111	C45H82O6	10	EIC 737.0449 +All MS, Smoothed (1.40,2,GA)	9.208	8.759 - 9.568	4900134854	14.1
MXAN_3748	AutoMS(n): TIC +All MS FullScan	9.543	9.522 - 9.563	TG(43:0)	755.0491	1163755264	9.557	736.6581	C46H88O6	33	EIC 755.0919 +All MS, Smoothed (1.40,2,GA)	9.569	9.268 - 9.868	12360541086	35.6
MXAN_3748	AutoMS(n): TIC +All MS FullScan	9.4	9.384 - 9.416	TG(43:1)	753.0388	692778176	9.419	734.6424	C46H86O6	20	EIC 753.0762 +All MS, Smoothed (1.40,2,GA)	9.423	9.083 - 9.799	8005897829	23.1
MXAN_3748	AutoMS(n): TIC +All MS FullScan	9.219	9.199 - 9.240	TG(43:2)	751.0234	561510144	9.28	732.6268	C46H84O6	17	EIC 751.0606 +All MS, Smoothed (1.40,2,GA)	9.258	8.921 - 9.568	6830093388	19.7
MXAN_3748	AutoMS(n): TIC +All MS FullScan	9.057	9.037 - 9.078	TG(43:3)	749.3179	125517976	9.049	730.6111	C46H82O6	5	EIC 749.0449 +All MS, Smoothed (1.40,2,GA)	9.101	8.759 - 9.661	2313365326	6.7
MXAN_3748	AutoMS(n): TIC +All MS FullScan	9.658	9.638 - 9.678	TG(44:0)	769.0679	1169291008	9.677	750.6737	C47H90O6	39	EIC 769.1075 +All MS, Smoothed (1.40,2,GA)	9.687	9.315 - 9.891	13244908539	38.2
MXAN_3748	AutoMS(n): TIC +All MS FullScan	9.481	9.453 - 9.508	TG(44:1)	767.0422	1032677760	9.485	748.6581	C47H88O6	33	EIC 767.0919 +All MS, Smoothed (1.40,2,GA)	9.514	9.153 - 9.776	12726099355	36.7
MXAN_3748	AutoMS(n): TIC +All MS FullScan	9.331	9.315 - 9.347	TG(44:2)	765.4554		9.345	746.6424	C47H86O6	23	EIC 765.1127 +All MS, Smoothed (1.40,2,GA)	9.366	8.967 - 9.638	8557753672	24.7
MXAN_3748	AutoMS(n): TIC +All MS FullScan	9.169	9.153 - 9.185	TG(44:3)	763.395	241817920	9.238	744.6268	C47H84O6	9	EIC 763.0606 +All MS, Smoothed (1.40,2,GA)	9.214	8.736 - 9.730	3840680531	11.1
MXAN_3748	AutoMS(n): TIC +All MS FullScan	9.023	9.014 - 9.031	TG(44:4)	761.4149		9.025	742.6111	C47H82O6	2	EIC 761.0449 +All MS, Smoothed (1.40,2,GA)	9.04	8.828 - 9.222	851164205	2.5
MXAN_3748	AutoMS(n): TIC +All MS FullScan	9.584	9.568 - 9.600	TG(45:1)	781.0558	1218281984	9.592	762.6737	C48H90O6	35	EIC 781.1075 +All MS, Smoothed (1.40,2,GA)	9.615	9.291 - 9.891	14365241109	41.4
MXAN_3748	AutoMS(n): TIC +All MS FullScan	9.423	9.407 - 9.439	TG(45:2)	779.0515	786417664	9.442	760.6581	C48H88O6	24	EIC 779.0919 +All MS, Smoothed (1.40,2,GA)	9.462	9.083 - 9.707	10327580708	29.8
MXAN_3748	AutoMS(n): TIC +All MS FullScan	9.289	9.268 - 9.309	TG(45:3)	777.4559		9.299	758.6424	C48H86O6	16	EIC 777.0762 +All MS, Smoothed (1.40,2,GA)	9.299	8.851 - 9.476	5875184648	16.9
MXAN_3748	AutoMS(n): TIC +All MS FullScan	9.15	9.130 - 9.170	TG(45:4)	775.4718		9.123	758.6424	C48H86O6	4	EIC 775.0606 +All MS, Smoothed (1.40,2,GA)	9.149	8.851 - 9.361	1907284518	5.5
MXAN_3748	AutoMS(n): TIC +All MS FullScan	9.838	9.822 - 9.854	TG(46:0)	797.1242	1082978944	9.853	779.7129	C49H95O6	33	EIC 797.1389 +All MS, Smoothed (1.40,2,GA)	9.868	9.753 - 10.731	12011742066	34.6
MXAN_3748	AutoMS(n): TIC +All MS FullScan	9.665	9.638 - 9.693	TG(46:1)	795.0975	1498688512	9.68	776.6894	C49H92O6	42	EIC 795.1232 +All MS, Smoothed (1.40,2,GA)	9.691	9.361 - 10.564	17281322876	49.8
MXAN_3748	AutoMS(n): TIC +All MS FullScan	9.538	9.522 - 9.554	TG(46:2)	793.4266	1297904768	9.543	774.6737	C49H90O6	34	EIC 793.1075 +All MS, Smoothed (1.40,2,GA)	9.56	9.130 - 9.984	13713516585	39.5
MXAN_3748	AutoMS(n): TIC +All MS FullScan	9.377	9.361 - 9.393	TG(46:3)	791.3301	661233408	9.391	772.6581	C49H88O6	18	EIC 791.0919 +All MS, Smoothed (1.40,2,GA)	9.399	8.944 - 9.638	7220124613	20.8
MXAN_3748	AutoMS(n): TIC +All MS FullScan	9.896	9.868 - 9.923	TG(47:0)	811.1498	1708301440	9.911	792.7207	C50H96O6	60	EIC 811.1545 +All MS, Smoothed (1.40,2,GA)	9.931	9.592 - 10.541	21492505444	62.0
MXAN_3748	AutoMS(n): TIC +All MS FullScan	9.758	9.730 - 9.785	TG(47:1)	809.0922	1018990016	9.784	790.705	C50H94O6	35	EIC 809.1388 +All MS, Smoothed (1.40,2,GA)	9.792	9.453 - 10.494	14472111483	41.7
MXAN_3748	AutoMS(n): TIC +All MS FullScan	9.608	9.592 - 9.624	TG(47:2)	807.393	1070148864	9.543	774.6737	C49H90O6	28	EIC 807.1232 +All MS, Smoothed (1.40,2,GA)	9.634	9.153 - 10.007	11577849876	33.4

MXAN_3748	AutoMS(n): TIC +All MS FullScan	9.462	9.453 - 9.471	TG(47:3)	805.3995	666960448	9.492	786.6737	C50H90O6	16	EIC 805.1075 +All MS, Smoothed (1.40,2,GA)	9.49	9.106 - 9.707	6239402945	18.0
MXAN_3748			9.060 - 9.545	TG(47:4)				784.6581			EIC 803.0919 +All MS, Smoothed (1.40,2,GA)	9.344	9.060 - 9.545	3091964011	8.9
MXAN_3748	AutoMS(n): TIC +All MS FullScan	10	9.984 - 10.016	TG(48:0)	825.1764	676444928	10.073	806.7363	C51H98O6	23	EIC 825.1701 +All MS, Smoothed (1.40,2,GA)	10.032	9.568 - 10.611	8478690533	24.4
MXAN_3748	AutoMS(n): TIC +All MS FullScan	9.889	9.822 - 9.955	TG(48:1)	823.171	774507392	9.759	802.705	C51H94O6	26	EIC 823.1545 +All MS, Smoothed (1.40,2,GA)	9.865	9.568 - 10.707	10577183508	30.5
MXAN_3748	AutoMS(n): TIC +All MS FullScan	9.75	9.707 - 9.794	TG(48:2)	821.4897	686618944	9.759	802.705	C51H94O6	18	EIC 821.1388 +All MS, Smoothed (1.40,2,GA)	9.75	9.361 - 10.099	8232200446	23.7
MXAN_3748	AutoMS(n): TIC +All MS FullScan	9.6	9.568 - 9.632	TG(48:3)	819.4847	476293760	9.596	800.6894	C51H92O6	13	EIC 819.1232 +All MS, Smoothed (1.40,2,GA)	9.576	9.199 - 9.776	5355755378	15.4
MXAN_3748	AutoMS(n): TIC +All MS FullScan	9.439	9.430 - 9.448	TG(48:4)	817.5135		9.458	798.6737	C51H90O6	9	EIC 817.1075 +All MS, Smoothed (1.40,2,GA)	9.429	9.130 - 9.615	3408336074	9.8
MXAN_3748	AutoMS(n): TIC +All MS FullScan	10.12	10.030 - 10.209	TG(49:0)	839.1864	596098816	10.065	820.752	C52H100O6	28	EIC 839.1858 +All MS, Smoothed (1.40,2,GA)	10.083	9.753 - 10.779	10410458309	30.0
MXAN_3748	AutoMS(n): TIC +All MS FullScan	9.93	9.891 - 9.970	TG(49:1)	837.197	563437440	9.931	818.7363	C52H98O6	15	EIC 837.1701 +All MS, Smoothed (1.40,2,GA)	9.946	9.592 - 10.541	7164933704	20.7
MXAN_3748	AutoMS(n): TIC +All MS FullScan	9.843	9.799 - 9.886	TG(49:2)	835.5363	525295456	9.847	816.7207	C52H96O6	16	EIC 835.1545 +All MS, Smoothed (1.40,2,GA)	9.818	9.430 - 10.145	5983087892	17.2
MXAN_3748	AutoMS(n): TIC +All MS FullScan	10.231	10.145 - 10.316	TG(50:0)	853.2351	175882512	10.278	834.7676	C53H102O6	7	EIC 853.2014 +All MS, Smoothed (1.40,2,GA)	10.183	9.845 - 10.587	3103663093	8.9
MXAN_3748	AutoMS(n): TIC +All MS FullScan	9.969	9.961 - 9.978	TG(50:1)	850.1692	149499200	10.058	832.752	C53H100O6	7	EIC 851.1858 +All MS, Smoothed (1.40,2,GA)	10.028	9.730 - 10.731	3989569458	11.5
MXAN_3748	AutoMS(n): TIC +All MS FullScan	10.208	10.192 - 10.224	TG(51:0)	867.5198	383955456	10.231	848.7833	C54H104O6	10	EIC 867.2171 +All MS, Smoothed (1.40,2,GA)	10.218	9.938 - 10.635	3118211406	9.0
MXAN_3748	AutoMS(n): TIC +All MS FullScan	10.108	10.053 - 10.163	TG(51:1)	865.2303	148637392	10.108	846.7676	C54H102O6	4	EIC 865.2014 +All MS, Smoothed (1.40,2,GA)	10.103	9.868 - 10.683	1930895114	5.6
MXAN_3748			10.099 - 10.587	TG(52:0)				862.7989			EIC 881.2327 +All MS, Smoothed (1.40,2,GA)	10.335	10.099 - 10.587	287957860	0.8
Sum positive														3.469E+11	1000
MXAN_1528	AutoMS(n): TIC -All MS FullScan	8.195	8.178 - 8.213	Cer(D19:0/16:0)	599.9295	3185424	8.215	553.5434	C35H71NO3	3	EIC 598.9416 -All MS, Smoothed (1.60,2,GA)	8.213	7.830 - 8.810	71442906	2.0
MXAN_1528	AutoMS(n): TIC -All MS FullScan	8.019	7.999 - 8.039	Cer(D19:0/i17:0 2-OH)	629.3584		8.034	583.554	C36H73NO4	10	EIC 628.9522 -All MS, Smoothed (1.60,2,GA)	8.052	7.852 - 8.645	282171289	8.0
MXAN_1528	AutoMS(n): TIC -All MS FullScan	8.323	8.268 - 8.379	Cer(D19:0/i17:0)	613.2098	19436126	8.305	567.559	C36H73NO3	10	EIC 612.9572 -All MS, Smoothed (1.60,2,GA)	8.341	8.022 - 9.059	288097431	8.2
MXAN_1528	AutoMS(n): TIC -All MS FullScan	7.416	7.395 - 7.437	CerPI(D19:0/16:0 2-OH)	811.4937	15634816	7.425	811.5575	C41H82NO12P	5	EIC 810.9502 -All MS, Smoothed (1.60,2,GA)	7.383	7.209 - 7.576	135656829	3.8
MXAN_1528			7.471 - 7.867	CerPI(D19:0/16:0)				795.5625			EIC 794.9552 -All MS, Smoothed (1.60,2,GA)	7.62	7.471 - 7.867	32531918	0.9
MXAN_1528	AutoMS(n): TIC -All MS FullScan	7.487	7.471 - 7.504	CerPI(D19:0/i17:0 2-OH)	825.5364	19455924	7.549	825.5731	C42H84NO12P	12	EIC 824.9658 -All MS, Smoothed (1.60,2,GA)	7.533	7.372 - 8.114	386420605	10.9
MXAN_1528	AutoMS(n): TIC -All MS FullScan	7.695	7.674 - 7.716	CerPI(D19:0/i17:0)	809.5417	14585614	7.729	809.5782	C42H84NO11P	4	EIC 808.9709 -All MS, Smoothed (1.60,2,GA)	7.714	7.538 - 7.999	143494765	4.1
MXAN_1528	AutoMS(n): TIC -All MS FullScan	6.455	6.437 - 6.473	PE(12:1/17:1);PE(13:1/16:1); PE(16:2/13:0);PE(14:1/15:1)	645.1517	6698363	6.442	645.437	C34H64NO8P	13	EIC 644.8297 -All MS, Smoothed (1.60,2,GA)	6.564	6.303 - 6.997	569010734	16.1

MXAN_1528	AutoMS(n): TIC -All MS FullScan	7.053	7.044 - 7.063	**PE(14:0/14:0);PE(13:0/15:0)**	635.2319	11709715	7.063	**635.4526**	C33H66NO8P	3	EIC 634.8453 -All MS, Smoothed (1.60,2,GA)	**7.059**	6.889 - 7.509	144067971	**4.1**
MXAN_1528	AutoMS(n): TIC -All MS FullScan	7.318	7.302 - 7.334	**PE(14:0/15:0)**	649.2584	45737724	7.325	**649.4683**	C34H68NO8P	31	EIC 648.8610 -All MS, Smoothed (1.60,2,GA)	**7.371**	7.209 - 7.651	884067144	**25.0**
MXAN_1528	AutoMS(n): TIC -All MS FullScan	6.184	6.166 - 6.203	**PE(14:1/14:1);PE(16:1/12:1)PE(15:1/13:1)**	631.2324	3165845	6.195	**631.4213**	C33H62NO8P	1	EIC 630.8140 -All MS, Smoothed (1.60,2,GA)	**6.275**	5.913 - 6.731	83575005	**2.4**
MXAN_1528	AutoMS(n): TIC -All MS FullScan	6.897	6.817 - 6.977	**PE(14:1/15:0);PE(16:1/13:0)**	646.8708	36731484	6.851	**647.4526**	C34H66NO8P1	32	EIC 646.8817 -All MS, Smoothed (1.60,2,GA)	**7.015**	6.731 - 7.471	1470401803	**41.7**
MXAN_1528	AutoMS(n): TIC -All MS FullScan	7.539	7.457 - 7.622	**PE(15:0/15:0)**	662.9215	232457088	7.477	**663.4839**	C35H70NO8P	98	EIC 662.8766 -All MS, Smoothed (1.60,2,GA)	**7.567**	7.395 - 8.784	4403140441	**124.8**
MXAN_1528	AutoMS(n): TIC -All MS FullScan	8.002	7.881 - 8.123	**PE(15:0/17:0)**	690.9883	80008552	7.897	**691.5152**	C37H74NO8P	47	EIC 690.9079 -All MS, Smoothed (1.60,2,GA)	**8.033**	7.815 - 8.810	1470416292	**41.7**
MXAN_1528	AutoMS(n): TIC -All MS FullScan	6.586	6.569 - 6.603	**PE(15:1/13:0)**	633.1572	6276767	6.565	**633.437**	C33H64NO8P	4	EIC 632.8297 -All MS, Smoothed (1.60,2,GA)	**6.73**	6.437 - 7.021	202489533	**5.7**
MXAN_1528	AutoMS(n): TIC -All MS FullScan	7.194	7.092 - 7.297	**PE(15:1/15:0)**	660.9154	76203000	7.26	**661.4683**	C35H68NO8P	41	EIC 660.8610 -All MS, Smoothed (1.60,2,GA)	**7.241**	6.983 - 7.636	1887907909	**53.5**
MXAN_1528	AutoMS(n): TIC -All MS FullScan	7.784	7.745 - 7.824	**PE(16:0/15:0);PE(14:0/17:0)**	676.9504	21050924	7.822	**677.4996**	C36H72NO8P	27	EIC 676.8923 -All MS, Smoothed (1.60,2,GA)	**7.816**	7.613 - 8.342	363275766	**10.3**
MXAN_1528	AutoMS(n): TIC -All MS FullScan	8.15	8.138 - 8.162	**PE(16:0/17:0)**	705.4613		8.151	**705.5309**	C38H76NO8P	100	EIC 704.9236 -All MS, Smoothed (1.60,2,GA)	**8.162**	8.045 - 8.784	162972795	**4.6**
MXAN_1528	AutoMS(n): TIC -All MS FullScan	7.365	7.349 - 7.381	**PE(16:1/15:0)**	674.9288	90196872	7.36	**675.4839**	C36H70NO8P	62	EIC 674.8766 -All MS, Smoothed (1.60,2,GA)	**7.434**	7.256 - 8.045	2169500686	**61.5**
MXAN_1528	AutoMS(n): TIC -All MS FullScan	6.994	6.983 - 7.006	**PE(16:1/15:1);PE(17:1/14:1)**	672.8893	29990484	6.989	**673.4683**	C36H68NO8P	61	EIC 672.8610 -All MS, Smoothed (1.60,2,GA)	**7.117**	6.889 - 7.576	2154360414	**61.0**
MXAN_1528	AutoMS(n): TIC -All MS FullScan	7.248	7.209 - 7.288	**PE(16:1/16:1);PE(17:2/15:0)**	686.9426	149806496	7.26	**687.4839**	C37H70NO8P	70	EIC 686.8766 -All MS, Smoothed (1.60,2,GA)	**7.297**	7.116 - 7.613	2390970569	**67.7**
MXAN_1528	AutoMS(n): TIC -All MS FullScan	7.815	7.769 - 7.861	**PE(16:1/17:0)**	703.0288	93406464	7.793	**703.5152**	C38H74NO8P	39	EIC 702.9079 -All MS, Smoothed (1.60,2,GA)	**7.855**	7.674 - 8.872	1314275214	**37.2**
MXAN_1528	AutoMS(n): TIC -All MS FullScan	6.374	6.356 - 6.392	**PE(16:2/14:1);PE(15:2/15:1)**	656.8807	6094153	6.363	**657.437**	C35H64NO8P	8	EIC 656.8297 -All MS, Smoothed (1.60,2,GA)	**6.528**	6.219 - 6.936	370032503	**10.5**
MXAN_1528	AutoMS(n): TIC -All MS FullScan	6.678	6.594 - 6.763	**PE(16:2/15:1);PE(15:2/16:1); PE(17:2/14:1)**	670.8939	34027948	6.677	**671.4526**	C36H66NO8P	18	EIC 670.8453 -All MS, Smoothed (1.60,2,GA)	**6.75**	6.490 - 7.302	871968010	**24.7**
MXAN_1528	AutoMS(n): TIC -All MS FullScan	6.294	6.275 - 6.313	**PE(16:2/15:2);PE(17:2/14:2)**	668.8779	1858732	6.332	**669.437**	C36H64NO8P	3	EIC 668.8297 -All MS, Smoothed (1.60,2,GA)	**6.382**	6.081 - 6.912	117189061	**3.3**
MXAN_1528	AutoMS(n): TIC -All MS FullScan	6.929	6.889 - 6.968	**PE(16:2/16:1); PE(17:2/15:1)**	684.925	87178976	6.954	**685.4683**	C37H68NO8P	55	EIC 684.8610 -All MS, Smoothed (1.60,2,GA)	**6.987**	6.792 - 7.524	1859425447	**52.7**
MXAN_1528	AutoMS(n): TIC -All MS FullScan	8.245	8.228 - 8.262	**PE(17:0/17:0)**	719.0378	29562118	8.256	**719.5465**	C39H78NO8P	13	EIC 718.9392 -All MS, Smoothed (1.60,2,GA)	**8.279**	8.138 - 8.645	359363966	**10.2**
MXAN_1528	AutoMS(n): TIC -All MS FullScan	7.573	7.561 - 7.584	**PE(17:1/15:0);PE(16:1/16:0); PE(15:1/17:0)**	688.9454	32825824	7.608	**689.4996**	C37H72NO8P	27	EIC 688.8923 -All MS, Smoothed (1.60,2,GA)	**7.686**	7.495 - 8.292	1261116444	**35.7**
MXAN_1528	AutoMS(n): TIC -All MS FullScan	7.513	7.395 - 7.630	**PE(17:1/16:1)**	700.9627	55794664	7.411	**701.4996**	C38H72NO8P	23	EIC 700.8923 -All MS, Smoothed (1.60,2,GA)	**7.456**	7.302 - 7.538	533363234	**15.1**
MXAN_1528	AutoMS(n): TIC -All MS FullScan	8.018	7.905 - 8.132	**PE(17:1/17:0)**	717.0106	37406344	7.914	**717.5309**	C39H76NO8P	15	EIC 716.9236 -All MS, Smoothed (1.60,2,GA)	**8.029**	7.830 - 8.758	748981748	**21.2**
MXAN_1528	AutoMS(n): TIC -All MS FullScan	6.732	6.693 - 6.772	**PE(17:2/13:0);PE(16:1/14:1); PE(15:1/15:1)**	658.8935	40696236	6.717	**659.4526**	C35H66NO8P	19	EIC 658.8453 -All MS, Smoothed (1.60,2,GA)	**6.877**	6.594 - 7.349	1053637274	**29.9**
MXAN_1528	AutoMS(n): TIC -All MS FullScan	6.561	6.543 - 6.579	**PE(17:2/15:2);PE(16:2/16:2)**	682.8731	8095617	6.48	**683.4526**	C37H66NO8P	27	EIC 682.8453 -All MS, Smoothed (1.60,2,GA)	**6.66**	6.437 - 7.232	835921475	**23.7**
MXAN_1528	AutoMS(n): TIC -All MS FullScan	7.132	7.116 - 7.148	**PE(17:2/16:1);PE(16:2/17:1)**	699.2417	76670992	7.114	**699.4839**	C38H70NO8P	36	EIC 698.8766 -All MS, Smoothed (1.60,2,GA)	**7.179**	6.997 - 7.975	1355662772	**38.4**
MXAN_1528	AutoMS(n): TIC -All MS FullScan	6.789	6.777 - 6.801	**PE(17:2/16:2)**	696.9107	11638632	6.791	**697.4683**	C38H68NO8P	29	EIC 696.8610 -All MS, Smoothed (1.60,2,GA)	**6.864**	6.693 - 7.457	799408501	**22.7**

MXAN_1528	AutoMS(n): TIC -All MS FullScan	7.667	7.651 - 7.683	PE(17:2/17:0); PE(17:1/17:1)	714.9904	25846262	7.708	715.5152	C39H74NO8P	19	EIC 714.9079 -All MS, Smoothed (1.60,2,GA)	7.734	7.524 - 8.342	698308325	19.8
MXAN_1528	AutoMS(n): TIC -All MS FullScan	7.323	7.302 - 7.343	PE(17:2/17:1)	712.9726	20545132	7.311	713.4996	C39H72NO8P	12	EIC 712.8923 -All MS, Smoothed (1.60,2,GA)	7.46	7.186 - 7.905	434789338	12.3
MXAN_1528	AutoMS(n): TIC -All MS FullScan	7.013	6.997 - 7.030	PE(17:2/17:2)	711.3162	17939524	7.02	711.4839	C39H70NO8P	9	EIC 710.8766 -All MS, Smoothed (1.60,2,GA)	7.053	6.889 - 7.442	227673540	6.5
MXAN_1528	AutoMS(n): TIC -All MS FullScan	7.714	7.698 - 7.731	PE(P-15:0/15:0)	647.4189		7.699	647.489	C35H70NO7P	10	EIC 646.8817 -All MS, Smoothed (1.60,2,GA)	7.745	7.576 - 8.292	284038480	8.0
MXAN_1528				PE(P-15:0/17:0)										0.0	0.0
MXAN_1528	AutoMS(n): TIC -All MS FullScan	7.03	7.021 - 7.039	PG(14:0/15:0)	680.2456	11476004	7.043	680.4628	C35H69O10P	3	EIC 679.8555 -All MS, Smoothed (1.60,2,GA)	7.037	6.889 - 7.256	87901696	2.5
MXAN_1528	AutoMS(n): TIC -All MS FullScan	7.202	7.186 - 7.218	PG(15:0/15:0)	694.3578		7.16	694.4785	C36H71O10P	10	EIC 693.8712 -All MS, Smoothed (1.60,2,GA)	7.218	7.044 - 7.561	355797884	10.1
MXAN_1528	AutoMS(n): TIC -All MS FullScan	6.886	6.865 - 6.907	PG(15:0/15:1);PG(16:1/14:0)	692.2601	12238273	6.874	692.4628	C36H69O10P	3	EIC 691.8555 -All MS, Smoothed (1.60,2,GA)	6.9	6.619 - 7.256	134647300	3.8
MXAN_1528	AutoMS(n): TIC -All MS FullScan	7.061	7.044 - 7.077	PG(15:0/16:1);PG(14:1/17:0)	706.2328	15168050	7.091	706.4785	C37H71O10P	6	EIC 705.8712 -All MS, Smoothed (1.60,2,GA)	7.131	6.936 - 7.495	237053139	6.7
MXAN_1528	AutoMS(n): TIC -All MS FullScan	6.69	6.668 - 6.711	PG(15:1/16:1;PG(15:0/16:2); PG(14:1/17:1);PG(14:0/17:2)	704.3519		6.734	704.4628	C37H69O10P	4	EIC 704.9236 -All MS, Smoothed (1.60,2,GA)	6.763	6.543 - 7.139	77462640	2.2
MXAN_1528	AutoMS(n): TIC -All MS FullScan	7.369	7.349 - 7.390	PG(16:0/16:1);PG(15:1/17:0); PG(15:0/17:1)	720.3566		7.392	720.4941	C38H73O10P	8	EIC 719.8868 -All MS, Smoothed (1.60,2,GA)	7.404	7.162 - 7.745	243734339	6.9
MXAN_1528			7.769 - 8.292	PG(16:0/17:0)				736.5254			EIC 735.9181 -All MS, Smoothed (1.60,2,GA)	7.9	7.769 - 8.292	75649268	2.1
MXAN_1528	AutoMS(n): TIC -All MS FullScan	6.928	6.912 - 6.944	PG(16:1/16:1)	718.3334	37567624	6.935	718.4785	C38H71O10P 1	11	EIC 717.8712 -All MS, Smoothed (1.60,2,GA)	6.954	6.777 - 7.325	370007117	10.5
MXAN_1528	AutoMS(n): TIC -All MS FullScan	6.543	6.409 - 6.677	PG(16:1/16:2)	716.9466	3790492	6.627	716.4628	C38H69O10P	3	EIC 716.9236 -All MS, Smoothed (1.60,2,GA)	6.613	5.687 - 7.139	117061862	3.3
MXAN_1528	AutoMS(n): TIC -All MS FullScan	7.532	7.509 - 7.556	PG(17:0/16:1)	734.3244	36852204	7.563	734.5098	C39H75O10P	15	EIC 733.9025 -All MS, Smoothed (1.60,2,GA)	7.565	7.419 - 7.999	435815295	12.3
MXAN_1528	AutoMS(n): TIC -All MS FullScan	7.984	7.975 - 7.993	PG(17:0/17:0)	750.0587	14101253	7.993	750.5411	C40H79O10P	4	EIC 749.9338 -All MS, Smoothed (1.60,2,GA)	8.024	7.881 - 8.855	107052343	3.0
MXAN_1528			7.209 - 8.022	PG(17:0/17:1)				748.5254			EIC 747.9181 -All MS, Smoothed (1.60,2,GA)	7.686	7.209 - 8.022	118792876	3.4
MXAN_1528	AutoMS(n): TIC -All MS FullScan	7.206	7.139 - 7.274	PG(17:1/16:1)	732.4402		7.215	732.4941	C39H73O10P	4	EIC 731.8868 -All MS, Smoothed (1.60,2,GA)	7.132	6.960 - 7.209	111332416	3.2
Sum negative														3.529E+10	1000
MXAN_1528	AutoMS(n): TIC +All MS FullScan	8.083	8.067 - 8.099	DG(15:0/15:0/0:0)	558.9095	256541392	8.071	540.4754	C33H64O5	9	EIC 558.9092 +All MS, Smoothed (1.42,2,GA)	8.091	7.907 - 8.481	2203147261	6.8
MXAN_1528			7.763 - 8.205	DG(31:1)				552.4754			EIC 570.9092 +All MS, Smoothed (1.42,2,GA)	7.949	7.763 - 8.205	1970133440	6.1
MXAN_1528	AutoMS(n): TIC +All MS FullScan	8.409	8.389 - 8.429	DG(32:0)	586.5786	58282088	8.451	568.5067	C35H68O5	6	EIC 586.9405 +All MS, Smoothed (1.42,2,GA)	8.441	8.297 - 8.923	723446245	2.2
MXAN_1528	AutoMS(n): TIC +All MS FullScan	7.843	7.832 - 7.855	DG(32:2)	582.9772	120714496	7.862	564.4754	C35H64O5	4	EIC 582.9092 +All MS, Smoothed (1.42,2,GA)	7.852	7.581 - 8.067	1305559855	4.0
MXAN_1528			8.481 - 8.899	DG(33:0)				582.5223			EIC 600.9561 +All MS, Smoothed (1.42,2,GA)	8.648	8.481 - 8.899	279435072	0.9

MXAN_1528	AutoMS(n): TIC +All MS FullScan	8.335	8.320 - 8.351	DG(33:1)	599.1042		8.332	580.5067	C36H68O5	5	EIC 598.9405 +All MS, Smoothed (1.42,2,GA)	8.336	8.159 - 8.737	1194113584	3.7
MXAN_1528			7.832 - 8.274	DG(33:2)				578.491			EIC 596.9248 +All MS, Smoothed (1.42,2,GA)	8.109	7.832 - 8.274	1226079075	3.8
MXAN_1528	AutoMS(n): TIC +All MS FullScan	9.763	9.708 - 9.818	TG(15:0/15:0/15:0)	783.087	1228123008	9.73	764.6894	C48H92O6	44	EIC 783.1232 +All MS, Smoothed (1.42,2,GA)	9.762	9.409 - 10.591	14940467524	46.0
MXAN_1528			8.620 - 9.154	TG(38:1)				666.5798			EIC 682.7169 +All MS, Smoothed (1.42,2,GA)	8.853	8.620 - 9.154	716972943	2.2
MXAN_1528	AutoMS(n): TIC +All MS FullScan	9.152	9.131 - 9.172	TG(39:0)	699.3714		9.169	680.5955	C42H80O6	5	EIC 699.0293 +All MS, Smoothed (1.42,2,GA)	9.17	8.783 - 9.478	1582903124	4.9
MXAN_1528	AutoMS(n): TIC +All MS FullScan	8.966	8.946 - 8.987	TG(39:1)	697.1906	86629936	8.995	678.5798	C42H78O6	3	EIC 697.0136 +All MS, Smoothed (1.42,2,GA)	8.998	8.620 - 9.201	1089411962	3.4
MXAN_1528	AutoMS(n): TIC +All MS FullScan	9.059	9.039 - 9.079	TG(40:1)	710.9506	165941504	9.072	692.5955	C43H80O6	7	EIC 711.0293 +All MS, Smoothed (1.42,2,GA)	9.096	8.737 - 9.478	2196280232	6.8
MXAN_1528	AutoMS(n): TIC +All MS FullScan	8.869	8.853 - 8.885	TG(40:2)	708.8647	95777680	8.913	690.5798	C43H78O6	4	EIC 709.0136 +All MS, Smoothed (1.42,2,GA)	8.903	8.643 - 9.201	1421183627	4.4
MXAN_1528			8.830 - 9.639	TG(41:1)				706.61114			EIC 725.0450 +All MS, Smoothed (1.42,2,GA)	9.234	8.830 - 9.639	3530263770	10.9
MXAN_1528	AutoMS(n): TIC +All MS FullScan	8.985	8.946 - 9.024	TG(41:2)	722.949	125432256	8.998	704.5955	C44H80O6	5	EIC 723.0293 +All MS, Smoothed (1.42,2,GA)	9.038	8.643 - 9.357	1991542027	6.1
MXAN_1528	AutoMS(n): TIC +All MS FullScan	8.804	8.783 - 8.824	TG(41:3)	720.9522	66126272	8.878	702.5798	C44H78O6	4	EIC 720.9538 +All MS, Smoothed (1.42,2,GA)	8.839	8.667 - 9.062	855411274	2.6
MXAN_1528	AutoMS(n): TIC +All MS FullScan	9.29	9.270 - 9.311	TG(42:1)	738.9667	631795840	9.331	722.6424	C45H86O6	20	EIC 739.0606 +All MS, Smoothed (1.42,2,GA)	9.304	9.015 - 9.639	6137497600	18.9
MXAN_1528	AutoMS(n): TIC +All MS FullScan	9.147	9.085 - 9.210	TG(42:2)	736.9527	335375360	9.149	718.6111	C45H82O6	13	EIC 737.0449 +All MS, Smoothed (1.42,2,GA)	9.168	8.969 - 9.501	4934695094	15.2
MXAN_1528			9.270 - 9.870	TG(43:0)				736.6581			EIC 755.0919 +All MS, Smoothed (1.42,2,GA)	9.582	9.270 - 9.870	5710029151	17.6
MXAN_1528	AutoMS(n): TIC +All MS FullScan	9.394	9.362 - 9.426	TG(43:1)	753.0291	472113728	9.419	734.6424	C46H86O6	17	EIC 753.0762 +All MS, Smoothed (1.42,2,GA)	9.423	9.062 - 9.731	6090055112	18.7
MXAN_1528	AutoMS(n): TIC +All MS FullScan	9.217	9.177 - 9.256	TG(43:2)	751.0174	477601024	9.28	732.6268	C46H84O6	24	EIC 751.0606 +All MS, Smoothed (1.42,2,GA)	9.26	8.946 - 9.708	7224112185	22.2
MXAN_1528	AutoMS(n): TIC +All MS FullScan	9.055	9.039 - 9.071	TG(43:3)	749.3124	207493632	9.049	730.6111	C46H82O6	8	EIC 749.0449 +All MS, Smoothed (1.42,2,GA)	9.099	8.783 - 9.455	3012429665	9.3
MXAN_1528	AutoMS(n): TIC +All MS FullScan	9.683	9.662 - 9.703	TG(44:0)	769.0969	602832896	9.677	750.6737	C47H90O6	19	EIC 769.1075 +All MS, Smoothed (1.42,2,GA)	9.694	9.547 - 10.286	6342002478	19.5
MXAN_1528	AutoMS(n): TIC +All MS FullScan	9.475	9.455 - 9.495	TG(44:1)	767.0576	670766720	9.485	748.6581	C47H88O6	28	EIC 767.0919 +All MS, Smoothed (1.42,2,GA)	9.521	9.108 - 9.870	10672106327	32.8
MXAN_1528	AutoMS(n): TIC +All MS FullScan	9.332	9.316 - 9.348	TG(44:2)	765.0566	789322240	9.345	746.6424	C47H86O6	28	EIC 765.1127 +All MS, Smoothed (1.42,2,GA)	9.363	8.992 - 9.662	9128781266	28.1
MXAN_1528	AutoMS(n): TIC +All MS FullScan	9.147	9.131 - 9.163	TG(44:3)	763.0154	256213632	9.238	744.6268	C47H84O6	17	EIC 763.0606 +All MS, Smoothed (1.42,2,GA)	9.214	8.853 - 9.570	5263571742	16.2
MXAN_1528	AutoMS(n): TIC +All MS FullScan	9.013	8.992 - 9.033	TG(44:4)	760.9777	105668992	9.025	742.6111	C47H82O6	4	EIC 761.0449 +All MS, Smoothed (1.42,2,GA)	9.044	8.737 - 9.247	1424167992	4.4
MXAN_1528	AutoMS(n): TIC +All MS FullScan	9.602	9.570 - 9.634	TG(45:1)	781.0683	1013824960	9.592	762.6737	C48H90O6	39	EIC 781.1075 +All MS, Smoothed (1.42,2,GA)	9.627	9.270 - 10.332	13405805736	41.2
MXAN_1528	AutoMS(n): TIC +All MS FullScan	9.475	9.409 - 9.541	TG(45:2)	779.0555	793395328	9.442	760.6581	C48H88O6	36	EIC 779.0919 +All MS, Smoothed (1.42,2,GA)	9.465	9.108 - 9.870	12157425984	37.4
MXAN_1528	AutoMS(n): TIC +All MS FullScan	9.286	9.270 - 9.302	TG(45:3)	777.4645		9.299	758.6424	C48H86O6	30	EIC 777.0762 +All MS, Smoothed (1.42,2,GA)	9.299	8.876 - 9.685	8797723300	27.1
MXAN_1528	AutoMS(n): TIC +All MS FullScan	9.105	9.085 - 9.126	TG(45:4)	775.3733	189520304	9.123	758.6424	C48H86O6	10	EIC 775.0606 +All MS, Smoothed (1.42,2,GA)	9.153	8.830 - 9.593	3246704461	10.0

MXAN_1528	AutoMS(n): TIC +All MS FullScan	9.863	9.847 - 9.879	**TG(46:0)**	797.1186	976071040	9.853	**779.7129**	C49H95O6	31	EIC 797.1389 +All MS, Smoothed (1.42,2,GA)	**9.869**	9.755 - 10.520	8035661933	**24.7**
MXAN_1528	AutoMS(n): TIC +All MS FullScan	9.667	9.639 - 9.694	**TG(46:1)**	795.1138	1453336320	9.68	**776.6894**	C49H92O6	54	EIC 795.1232 +All MS, Smoothed (1.42,2,GA)	**9.701**	9.385 - 10.032	18757500274	**57.7**
MXAN_1528	AutoMS(n): TIC +All MS FullScan	9.528	9.501 - 9.556	**TG(46:2)**	793.0828	1408969984	9.543	**774.6737**	C49H90O6	58	EIC 793.1075 +All MS, Smoothed (1.42,2,GA)	**9.56**	9.177 - 9.893	16859739481	**51.9**
MXAN_1528	AutoMS(n): TIC +All MS FullScan	9.378	9.362 - 9.394	**TG(46:3)**	791.4354	709996032	9.391	**772.6581**	C49H88O6	29	EIC 791.0919 +All MS, Smoothed (1.42,2,GA)	**9.413**	9.015 - 9.824	9502264898	**29.2**
MXAN_1528	AutoMS(n): TIC +All MS FullScan	9.92	9.893 - 9.948	**TG(47:0)**	811.1422	1273215232	9.911	**792.7207**	C50H96O6	41	EIC 811.1545 +All MS, Smoothed (1.42,2,GA)	**9.932**	9.616 - 10.472	13365936262	**41.1**
MXAN_1528	AutoMS(n): TIC +All MS FullScan	9.821	9.755 - 9.887	**TG(47:1)**	809.1483	1044991232	9.784	**790.705**	C50H94O6	39	EIC 809.1388 +All MS, Smoothed (1.42,2,GA)	**9.8**	9.432 - 10.309	14948279252	**46.0**
MXAN_1528	AutoMS(n): TIC +All MS FullScan	9.659	9.593 - 9.726	**TG(47:2)**	807.1105	1213410176	9.616	**788.6894**	C50H92O6	47	EIC 807.1232 +All MS, Smoothed (1.42,2,GA)	**9.645**	9.339 - 10.032	16555643551	**50.9**
MXAN_1528	AutoMS(n): TIC +All MS FullScan	9.459	9.432 - 9.487	**TG(47:3)**	805.0638	857626432	9.468	**786.6737**	C50H90O6	34	EIC 804.3049 +All MS, Smoothed (1.42,2,GA)	**9.337**	9.154 - 9.524	3149039857	**9.7**
MXAN_1528	AutoMS(n): TIC +All MS FullScan	9.336	9.316 - 9.357	**TG(47:4)**	803.4519	676626560	9.377	**784.6581**	C50H88O6	23	EIC 803.0919 +All MS, Smoothed (1.42,2,GA)	**9.348**	9.062 - 9.778	6824347077	**21.0**
MXAN_1528	AutoMS(n): TIC +All MS FullScan	10.013	9.985 - 10.040	**TG(48:0)**	824.6582		10.073	**806.7363**	C51H98O6	22	EIC 825.1701 +All MS, Smoothed (1.42,2,GA)	**10.031**	9.662 - 10.711	6956406832	**21.4**
MXAN_1528	AutoMS(n): TIC +All MS FullScan	9.879	9.824 - 9.934	**TG(48:1)**	823.1589	1006394496	9.759	**802.705**	C51H94O6	36	EIC 823.1545 +All MS, Smoothed (1.42,2,GA)	**9.88**	9.570 - 10.615	11948487078	**36.8**
MXAN_1528	AutoMS(n): TIC +All MS FullScan	9.747	9.731 - 9.763	**TG(48:2)**	821.4935	1150134528	9.792	**802.705**	C51H94O6	36	EIC 821.1388 +All MS, Smoothed (1.42,2,GA)	**9.749**	9.339 - 10.124	11689068311	**36.0**
MXAN_1528	AutoMS(n): TIC +All MS FullScan	9.54	9.501 - 9.579	**TG(48:3)**	819.1184	637246656	9.596	**800.6894**	C51H92O6	28	EIC 819.1232 +All MS, Smoothed (1.42,2,GA)	**9.581**	9.201 - 9.824	8621023530	**26.5**
MXAN_1528			9.131 - 9.870	**TG(48:4)**				**798.6737**			EIC 817.1075 +All MS, Smoothed (1.42,2,GA)	**9.423**	9.131 - 9.870	5527446014	**17.0**
MXAN_1528	AutoMS(n): TIC +All MS FullScan	10.071	10.055 - 10.087	**TG(49:0)**	839.1974	616242816	10.065	**820.752**	C52H100O6	20	EIC 839.1858 +All MS, Smoothed (1.42,2,GA)	**10.09**	9.755 - 10.663	6403648592	**19.7**
MXAN_1528	AutoMS(n): TIC +All MS FullScan	9.983	9.939 - 10.026	**TG(49:1)**	837.1802	590999552	9.931	**818.7363**	C52H98O6	20	EIC 837.1701 +All MS, Smoothed (1.42,2,GA)	**9.959**	9.593 - 10.402	7062692213	**21.7**
MXAN_1528	AutoMS(n): TIC +All MS FullScan	9.828	9.824 - 9.833	**TG(49:2)**	835.5882		9.827	**816.7207**	C52H96O6	24	EIC 835.1545 +All MS, Smoothed (1.42,2,GA)	**9.827**	9.432 - 10.170	7810404999	**24.0**
MXAN_1528	AutoMS(n): TIC +All MS FullScan	10.221	10.147 - 10.295	**TG(50:0)**	853.2231	142514960	10.278	**834.7676**	C53H102O6	8	EIC 853.2014 +All MS, Smoothed (1.42,2,GA)	**10.184**	9.847 - 10.903	2665874081	**8.2**
MXAN_1528	AutoMS(n): TIC +All MS FullScan	10.052	10.032 - 10.072	**TG(50:1)**	851.2351	390687040	10.058	**832.752**	C53H100O6	12	EIC 851.1858 +All MS, Smoothed (1.42,2,GA)	**10.035**	9.755 - 10.663	4092361152	**12.6**
MXAN_1528	AutoMS(n): TIC +All MS FullScan	10.198	10.170 - 10.225	**TG(51:0)**	867.2859	142236160	10.231	**848.7833**	C54H104O6	6	EIC 867.2171 +All MS, Smoothed (1.42,2,GA)	**10.223**	9.962 - 10.663	1581967188	**4.9**
MXAN_1528	AutoMS(n): TIC +All MS FullScan	10.117	10.101 - 10.133	**TG(51:1)**	865.2471	148559856	10.108	**846.7676**	C54H102O6	5	EIC 865.2014 +All MS, Smoothed (1.42,2,GA)	**10.093**	9.755 - 10.591	1645928887	**5.1**
MXAN_1528	AutoMS(n): TIC +All MS FullScan	10.353	10.332 - 10.373	**TG(52:0)**	881.1964	26872484	10.362	**862.7989**	C55H106O6	1	EIC 881.2327 +All MS, Smoothed (1.42,2,GA)	**10.334**	9.939 - 10.687	287574362	**0.9**
Sum positive														**3.251E+11**	**1000**

6.3.6 References

1. Kaiser, D 2008. *Myxococcus*-from Single-Cell Polarity to Complex Multicellular Patterns *Annu. Rev. Genet.* **42**: 109-30.

2. Weissman, K. J., and R. Müller. 2010. Myxobacterial secondary metabolites: bioactivities and modes-of-action *Nat. Prod. Rep.* **27**: 1276-95.

3. Kearns, D. B., and L. J. Shimkets. 2001. Lipid chemotaxis and signal transduction in *Myxococcus xanthus Trends Microbiol.* **9**: 126-9.

4. Ring, M. W., G. Schwär, V. Thiel, J. S. Dickschat, R. M. Kroppenstedt, S. Schulz, and H. B. Bode. 2006. Novel iso-branched ether lipids as specific markers of developmental sporulation in the myxobacterium *Myxococcus xanthus Biol. Chem.* **281**: 36691-700.

5. Bhat, S., T. Ahrendt, C. Dauth, H. B. Bode, and L. J. Shimkets. 2014. Two lipid signals guide fruiting body development of *Myxococcus xanthus mBio*. **5**.

6. Fautz, E., G. Rosenfelder, and L. Grotjahn. 1979. Iso-branched 2- and 3-hydroxy fatty acids as characteristic lipid constituents of some gliding bacteria *J. Bacteriol.* **140**: 852-8.

7. Bode, H. B., M. W. Ring, D. Kaiser, A. C. David, R. M. Kroppenstedt, and G. Schwär. 2006. Straight-chain fatty acids are dispensable in the myxobacterium *Myxococcus xanthus* for vegetative growth and fruiting body formation *J. Bacteriol.* **188**: 5632-4.

8. Ring, M. W., E. Bode, G. Schwär, and H. B. Bode. 2009. Functional analysis of desaturases from the myxobacterium *Myxococcus xanthus FEMS Microbiol. Lett.* **296**: 124-30.

9. Ring, M. W., G. Schwär, and H. B. Bode. 2009. Biosynthesis of 2-hydroxy and iso-even fatty acids is connected to sphingolipid formation in myxobacteria *ChemBioChem* **10**: 2003-10.

10. Hoiczyk, E., M. W. Ring, C. A. McHugh, G. Schwär, E. Bode, D. Krug, M. O. Altmeyer, J. Z. Lu, and H. B. Bode. 2009. Lipid body formation plays a central role in cell fate determination during developmental differentiation of *Myxococcus xanthus Mol. Microbiol.* **74**: 497-517.

11. Curtis, P. D., R. Geyer, D. C. White, and L. J. Shimkets. 2006. Novel lipids in *Myxococcus xanthus* and their role in chemotaxis *Environm. Microbiol*. **8**: 1935-49.

12. Caillon, E., B. Lubochinsky, and D. Rigomier. 1983. Occurrence of dialkyl ether phospholipids in *Stigmatella aurantiaca* DW4 *J. Bacteriol.* **153**: 1348-51.

13. Kleinig, H 1972. Membranes from *Myxococcus fulvus* (Myxobacterales) containing carotenoid glucosides. I. Isolation and composition *Biochim. Biophys. Acta*. **274**: 489-98.

14. Orndorff, P. E., and M. Dworkin. 1980. Separation and properties of the cytoplasmic and outer membranes of vegetative cells *of Myxococcus xanthus J. Bacteriol.* **141**: 914-27.

15. Fuchs, B., and J. Schiller. 2009. Application of MALDI-TOF mass spectrometry in lipidomics. *Eur. J. Lipid Sci. Technol.* **111**: 83-98.

16. Han, X., K. Yang, and R. W. Gross. 2012. Multi-dimensional mass spectrometry-based shotgun lipidomics and novel strategies for lipidomic analyses. *Mass. Spectrom. Rev.* **31**: 134-178.

17. Furey, A., M. Moriarty, V. Bane, B. Kinsella, and M. Lehane. 2013. Ion suppression; a critical review on causes, evaluation, prevention and applications *Talanta*. **115**: 104-22.

18. Shan, L., K. Jaffe, S. Li, and L. Davis. 2008. Quantitative determination of lysophosphatidic acid by LC/ESI/MS/MS employing a reversed phase HPLC column. *J. Chromatogr. B* **864**: 22-28.

19. Hutchins, P. M., R. M. Barkley, and R. C. Murphy. 2008. Separation of cellular nonpolar neutral lipids by normal-phase chromatography and analysis by electrospray ionization mass spectrometry *J. Lipid Res.* **49**: 804-13.

20. Rütters, H., H. Sass, H. Cypionka, and J. Rullkötter. 2001. Monoalkylether phospholipids in the sulfate-reducing bacteria *Desulfosarcina variabilis* and *Desulforhabdus amnigenus Arch. Microbiol.* **176**: 435-42.

21. Tsui, F. C., D. M. Ojcius, and W. L. Hubbell. 1986. The intrinsic pKa values for phosphatidylserine and phosphatidylethanolamine in phosphatidylcholine host bilayers *Biophys. J.* **49**: 459-68.

22. Marsh, D 1990. CRC handbook of lipid bilayers. CRC Press.

23. Kaiser, D 1979. Social gliding is correlated with the presence of pili in *Myxococcus xanthus Proc. Natl. Acad. Sci. USA* **76**: 5952-6.

24. Murphy, R. C., and P. H. Axelsen. 2011. Mass spectrometric analysis of long-chain lipids. *Mass. Spectrom. Rev.* **30**: 579-599.

25. Oursel, D., C. Loutelier-Bourhis, N. Orange, S. Chevalier, V. Norris, and C. M. Lange. 2007. Lipid composition of membranes of *Escherichia coli* by liquid chromatography/tandem mass spectrometry using negative electrospray ionization. *Rapid Commun. Mass. Spectrom.* **21**: 1721-1728.

26. B, P. D. Curtis, R. Geyer, D. C. White, and L. J. Shimkets. 2006. Novel lipids in *Myxococcus xanthus* and their role in chemotaxis. *Environm. Microbiol.* **8**: 1935-1949.

27. Becker, G. W., and R. L. Lester. 1980. Biosynthesis of phosphoinositol-containing sphingolipids from phosphatidylinositol by a membrane preparation from *Saccharomyces cerevisiae J. Bacteriol.* **142**: 747-54.

28. Hackett, J. A., and P. J. Brennan. 1977. The isolation and biosynthesis of the ceramide-phosphoinositol of *Aspergillus niger FEBS Letters*. **74**: 259-63.

29. Smith, T. K., and P. Bütikofer. 2010. Lipid metabolism in *Trypanosoma brucei*. *Mol. Biochem. Parasit.* **172**: 66-79.

30. Kaul, K., and R. L. Lester. 1975. Characterization of Inositol-containing Phosphosphingolipids from Tobacco Leaves: Isolation and Identification of Two Novel, Major Lipids: N-Acetylglucosamidoglucuronidoinositol Phosphorylceramide and Glucosamidoglucuronidoinositol Phosphorylceramide *Plant Physiol.* **55**: 120-9.

31. Eckau, H., D. Dill, and H. Budzikiewicz. 2014. Neuartige Ceramide aus *Cystobacter fuscus* (Myxobacterales). *Z. Naturforsch. C*. **39**: 1-9.

32. Stein, J., and H. Budzikiewicz. 1988. Ceramid-1-phosphoethanolamine aus *Myxococcus stipitatus*. *Z. Naturforsch. B.* **43**: 1063-1067.

33. Keck, M., N. Gisch, H. Moll, F. Vorhölter, K. Gerth, U. Kahmann, M. Lissel, B. Lindner, K. Niehaus, and O. Holst. 2011. Unusual outer membrane lipid composition of the gram-negative, lipopolysaccharide-lacking myxobacterium Sorangium cellulosum So ce56 *Biol. Chem.* **286**: 12850-9.

34. Levine, T. P., C. A. Wiggins, and S. Munro. 2000. Inositol phosphorylceramide synthase is located in the Golgi apparatus of *Saccharomyces cerevisiae Mol. Biol. Cell*. **11**: 2267-81.

35. Whitworth, D. E 2007. Myxobacteria. ASM Press, Herndon.

36. Buré, C., J. Cacas, S. Mongrand, and J. Schmitter. 2014. Characterization of glycosyl inositol phosphoryl ceramides from plants and fungi by mass spectrometry *Anal. Bioanal. Chem.* **406**: 995-1010.

37. Zhong, W., M. W. Jeffries, and N. H. Georgopapadakou. 2000. Inhibition of inositol phosphorylceramide synthase by aureobasidin A in Candida and Aspergillus species *Antimicrob. Agents Chemother.* **44**: 651-3.

38. Rhome, R., M. D. del Poeta, and M. del Poeta. 2009. Lipid Signaling in Pathogenic Fungi. *Annu. Rev. Microbiol.* **63**: 119-131.

39. Bligh, E. G., and W. J. Dyer. 1959. A rapid method of total lipid extraction and purification *Can. J. Biochem. Physiol.* **37**: 911-7.

40. Bode, H. B., M. W. Ring, G. Schwär, R. M. Kroppenstedt, D. Kaiser, and R. Müller. 2006. 3-Hydroxy-3-methylglutaryl-coenzyme A (CoA) synthase is involved in biosynthesis of isovaleryl-CoA in the myxobacterium *Myxococcus xanthus* during fruiting body formation *J. Bacteriol.* **188**: 6524-8.

41. Ejsing, C. S 2007. Molecular characterization of the lipidome by mass spectrometry. (Simons, K., ed.). Dresden.

42. Blaas, N., and H. Humpf. 2013. Structural profiling and quantitation of glycosyl inositol phosphoceramides in plants with Fourier transform mass spectrometry *J. Agric. Food Chem.* **61**: 4257-69.

43. Smith, P. B., A. P. Snyder, and C. S. Harden. 1995. Characterization of bacterial phospholipids by electrospray ionization tandem mass spectrometry *Anal. Chem.* **67**: 1824-30.

44. Elkhayat, E., and G. Mohamed. 2012. Activity and structure elucidation of ceramides. *Curr. Bioact. Compd.* **8**: 370-409.

7 Curriculum vitae

Personal information

Date of birth:	31.10.1981
Birthplace:	Berlin
Nationality:	German

Professional experience

04/2009 – 03/2014	Scientific assistant and doctoral candidate / Merck-Endowed Professorship Molecular Biotechnology (Prof. Dr. Helge B. Bode) / Goethe University Frankfurt (Germany)
03/2008 – 03/2009	Scientific assistant and doctoral candidate / Emmy-Noether junior research group (Dr. Helge B. Bode) / Department of Pharmaceutical Biotechnology Saarland University (Saarbrucken, Germany)
11/2007 – 01/2008	Pharmacist / Syringen Pharmacy (Berlin, Germany)

Academic and college education

02/2007 – 08/2007	Postgraduate student / School of Pharmacy (Prof. Dr. Thomas Rades) / University of Otago (Dunedin / New Zealand); title PGCert report: “Influence of Various Excipients on the Dehydration of Carbamazepine Dihydrate in a Solid Dispersion”
	Postgraduate Certificate in Pharmacy
01/2007	Completion of the third part of the pharmaceutical examination
	License to work as a pharmacist
	Diploma in pharmaceutical sciences
07/2006 – 12/2006	Internship for pharmacists, second part and diploma student / ProBioGen AG (Berlin, Germany) and Ernst-Moritz-Arndt University (Greifswald, Germany) Supervisors: Prof. Dr. Ulrike Lindequist and Dr. Stefan Zietze; title diploma thesis: “Der Einfluss verschiedener Hilfsstoffkombinationen auf die Stabilität von rekombinant hergestelltem α_1-Antitrypsin”

01/2006 – 06/2006	Internship for pharmacists, first part / Gorki Pharmacy (owner: Dr. Sabine Knoll) (Berlin-Tegel, Germany)
10/2001 – 12/2005	Pharmaceutical studies / Free University Berlin (Germany), second part of the pharmaceutical examination
06/2001	General qualification for university entrance
01/1999 – 06/1999	Guest student Morrinsville College (Morrinsville, New Zealand)
08/1994 – 06/2001	Lutheran School Frohnau (grammar school) (Berlin, Germany)
08/1988 – 07/1994	Primary School “Am Fließtal” (Berlin, Germany)

Further professional engagements:

2008 / 2010	Replacement services pharmacy / Charlotten Pharmacy (Berlin-Spandau, Germany)
2011 – 2012	Replacement services pharmacy / Delphin Pharmacy (Frankfurt/Main, Germany)
	Member / German Pharmaceutical Society (DPhG e.V.)
	Training certificate Regional Chamber of Pharmacists for Hessen
	Certificate of the Goethe Graduate Academy (GRADE)

8 Publications

Lorenzen, W., Ahrendt, T., Bozhüyük, K. A. J., Bode, H. B. (2014) A multifunctional enzyme is involved in a novel bacterial ether lipid biosynthesis pathway. *Nature Chemical Biology*
DOI: 10.1038/NCHEMBIO:1526

Brat, D., Weber, C., **Lorenzen, W.**, Bode, H. B., and Boles, E. (2012) Cytosolic re-localization and optimization of valine synthesis and catabolism enables increased isobutanol production with the yeast *Saccharomyces cerevisiae*. *Biotechnology for biofuels 5*, 65.
DOI:10.1186/1754-6834-5-65

Brachmann, A. O., Reimer, D., **Lorenzen, W.**, Alonso, E. A., Kopp, Y., Piel, J., and Bode, H. B. (2012) Reciprocal cross talk between fatty acid and antibiotic biosynthesis in a nematode symbiont. *Angewandte Chemie (International ed. in English) 51*, 12086-9.
DOI: 10.1002/anie.201205384

Bode, H. B., Reimer, D., Fuchs, S. W., Kirchner, F., Dauth, C., Kegler, C., **Lorenzen, W.**, Brachmann, A. O., and Grün, P. (2012) Determination of the absolute configuration of peptide natural products by using stable isotope labeling and mass spectrometry. *Chemistry (Weinheim an der Bergstrasse, Germany) 18*, 2342-8
DOI: 10.1002/chem.201103479

Lorenzen, W., Ring, M. W., Schwär, G., and Bode, H. B. (2009) Isoprenoids Are Essential for Fruiting Body Formation in *Myxococcus xanthus*. *Journal of Bacteriology 191*, 5849-53.
DOI: 10.1128/JB.00539-09

Ohlendorf, B., **Lorenzen, W.**, Kehraus, S., Krick, A., Bode, H. B., and König, G. M. (2009) Myxotyrosides A and B, Unusual rhamnosides from *Myxococcus sp. Journal of Natural Products 72*, 82-6.
DOI: 10.1021/np8005875

Lorenzen, W., Bozhüyük K. A. J., Cortina, N. S., Bode, H. B. (2014) A comprehensive insight into the lipid composition of *Myxococcus xanthus* by UPLC ESI-MS *The Journal of Lipid Research* (currently in revision)

9 Record of conferences

Joint Meeting of the Austrian and German Pharmaceutical Societies 2011 „Shaping the future – Trends and Perspectives in Pharmaceutical Sciences“
20.9.-23.9.2011
Innsbruck, Austria
Contribution: poster

DPhG Annual Meeting 2010 “Personalisierte Therapeutika – Traum oder Wirklichkeit? (Personalised Therapy – Dream or Reality?)”
4.10.-7.10.2010
Brunswick, Germany
Contribution: None

37th International Conference on the Biology of Myxobacteria 2010
29.8.-01.09.2010
Nonnweiler-Otzenhausen/Saarland, Germany
Contribution: poster + oral poster presentation

3rd European Conference on Chemistry for Life Sciences
2.9.-5.9.2009
Frankfurt/Main, Germany
Contribution: poster + oral poster presentation

DPhG Annual Meeting 2009 „Biotechnologisch erzeugte Wirkstoffe: Konzepte, Erfolge, Erwartungen (Bioengineered Active Ingredients: Concepts, Achievements, Expectations)“
28.9.-1.10.2009
Jena, Germany
Contribution: short lecture

VAAM International Workshop 2008 „Biology and Chemistry of Antibiotic-Producing Bacteria“
29.9.-01.10.2008
Berlin, Germany
Contribution: short lecture

10 Declaration on oath

Herewith I confirm that I wrote the present thesis personally and independently and did not use any unnamed sources or aid.

I furthermore declare that I have not drawn up a previous PhD-thesis.

Frankfurt am Main, July 2014 Wolfram Lorenzen

Erklärung

Ich erkläre hiermit, dass ich mich bisher keiner Doktorprüfung im Mathematisch-Naturwissenschaftlichen Bereich unterzogen habe.

Frankfurt am Main, den 09.07.2014 Wolfram Lorenzen

Eidesstattliche Versicherung

Ich erkläre hiermit an Eides Statt, dass ich die vorgelegte Dissertation über

"IDENTIFICATION OF BIOMARKERS FOR THE FRUITING BODY FORMATION IN *MYXOCOCCUS XANTHUS*"

selbständig angefertigt und mich anderer Hilfsmittel als der in ihr angegebenen nicht bedient habe, insbesondere, dass alle Entlehnungen aus anderen Schriften mit Angabe der betreffenden Schrift gekennzeichnet sind.

Ich versichere, die Grundsätze der guten wissenschaftlichen Praxis beachtet, und nicht die Hilfe einer kommerziellen Promotionsvermittlung in Anspruch genommen zu haben.

Frankfurt am Main, den 09.07.2014 Wolfram Lorenzen